GLOBAL CHANGE: A COMPLEX CHALLENGE

Conference Proceedings

Otmar Urban, Mirka Šprtová, Karel Klem

Global Change Research Centre, The Czech Academy of Sciences, v.v.i.
Brno 2015

The conference was organised under the Education for Competitiveness Operational Programme „ENVIMET – Building a scientific team focused on environmental metabolomics and ecophysiology and its integration into international networks“ (CZ.1.07/2.3.00/20.0246).

Published by: Global Change Research Centre AS CR, v.v.i., Bělidla 986/4a, 60300 Brno, Czech Republic
ISBN: 978-80-87902-10-3

Contents

PREFACE

The 4th annual "Global Change: A Complex Challenge" conference was held in Brno, Czech Republic from 23 to 24 March 2015. The conference was organized by the Global Change Research Centre, Czech Academy of Sciences, in cooperation with Mendel University in Brno with financial support from the project "ENVIMET – Building a scientific team focused on environmental metabolomics and ecophysiology and its integration into international networks" (registration number CZ.1.07/2.3.00/20.0246; Ministry of Education, Youth and Sports of the Czech Republic).

The aim of this conference was to provide opportunity for early-stage researchers to present their findings while facilitating the identification of that work's place within worldwide research on global change. The conference programme was structured around invited lectures from leading scientists (John Grace, University of Edinburgh, Scotland; Michel Déqué, Météo-France National Centre for Meteorological Research, France; Miina Rautiainen, University of Helsinki, Finland; Wolfram Weckwerth, University of Vienna, Austria; and Tatiana Kluvánková, Slovak University of Technology & Slovak Academy of Sciences, Slovakia). Accordingly, the four sessions reflected the main research interests at the Global Change Research Centre, which encompass new advances in atmospheric sciences, biosphere sciences, impact studies and molecular adaptations, and societal challenges.

Twenty-four special reports selected from the submitted abstracts covered the full range of conference topics from climate modelling, analysis of climate variability and change, atmospheric chemistry, applications of remote sensing, eddy-covariance and statistical approaches in investigating ecosystems, measurement of greenhouse gases fluxes, applications of omics techniques in ecological and impact studies, ecological and biophysical plant physiology through changes in socio-economic relationships, land use, and ecosystem services induced by global change. Junior investigators presented their best ongoing research at a poster session as well as in the form of 3-minute flash talks (62 in total).

The proceedings cover almost equally the four main conference areas mentioned above and reflect the growing interconnectedness between different areas of research on global change. Each contribution included in the proceedings was peer reviewed by two independent reviewers to enhance the conference's quality and impact. Therefore, our special thanks go to all reviewers. The editors acknowledge Ms Eva Jurková for technical assistance in preparing the Conference Proceedings.

Otmar Urban
Mirka Šprtová
Karel Klem

Reviewers (in alphabetical order):

Ač, Alexander	Global Change Research Centre, CAS, Czech Republic
Blujdea, Viorel	Forest Research and Management Institute, Romania
Calfapietra, Carlo	Institute of Agro-Environmental and Forest Biology, National Research Council, Italy
	Global Change Research Centre, CAS, Czech Republic
Červený, Jan	Global Change Research Centre, CAS, Czech Republic
Ceulemans, Reinhart	University of Antwerp, Belgium
Cudlín, Pavel	Global Change Research Centre, CAS, Czech Republic
DeAngelis, Paolo	University of Tuscia, Italy
Déqué, Michel	Météo-France National Centre for Meteorological Research, France
Ditmarová, Ľubica	Institute of Forest Ecology, Slovak Academy of Sciences, Slovakia
Dubrovský, Martin	Institute of Atmospheric Physics, CAS, Czech Republic
	Global Change Research Centre, CAS, Czech Republic
Dušek, Jiří	Global Change Research Centre, CAS, Czech Republic
Dvorská, Alice	Global Change Research Centre, CAS, Czech Republic
Eitzinger, Josef	University of Natural Resources and Life Sciences (BOKU), Austria
Farda, Aleš	Global Change Research Centre, CAS, Czech Republic
Gaberščik, Alenka	University of Ljubljana, Slovenia
Guidolotti, Gabriele	Institute of Agro-Environmental and Forest Biology, National Research Council, Italy
Hayes, Michael	National Drought Mitigation Centre, USA
Hideg, Éva	University of Pécs, Hungary
Holub, Petr	Global Change Research Centre, CAS, Czech Republic
Hrstka, Miroslav	Brno University of Technology, Czech Republic
Jodha Khalsa, Siri	University of Colorado, USA
Klem, Karel	Global Change Research Centre, CAS, Czech Republic
Kluvánková, Tatiana	Centre for Transdisciplinary Studies of Institutions, Evolution and Policies, Slovak Academy of Sciences, Slovakia
Křen Jan	Mendel University in Brno, Czech Republic
Křůmal, Kamil	Institute of Analytical Chemistry, CAS, Czech Republic
Lhotáková, Zuzana	Charles University in Prague, Czech Republic
Linder, Sune	Swedish University of Agricultural Sciences, Sweden
Malenovský, Zbyněk	University of Tasmania, Australia
Marek, Michal V.	Global Change Research Centre, CAS, Czech Republic
Marková, Irena	Mendel University in Brno, Czech Republic
Olejníčková, Julie	Global Change Research Centre, CAS, Czech Republic
Olejnik, Janusz	University of Poznaň, Poland
	Global Change Research Centre, CAS, Czech Republic
Pallozzi, Emanuele	Institute of Agro-Environmental and Forest Biology, National Research Council, Italy

Pavelka, Marian	Global Change Research Centre, CAS, Czech Republic
Pokorný, Radek	Global Change Research Centre, CAS, Czech Republic
	Mendel University in Brno, Czech Republic
Rivas-Ubach, Albert	Centre for Ecological Research and Forestry (CREAF), Spain
Robson, Matthew T.	University of Helsinki, Finland
Sinetova, Maria	Timiryazev Institute of Plant Physiology, Russian Academy of Sciences, Russia
Šprtová, Mirka	Global Change Research Centre, CAS, Czech Republic
Špunda, Vladimír	University in Ostrava, Czech Republic
	Global Change Research Centre, CAS, Czech Republic
Štěpánek, Petr	Global Change Research Centre, CAS, Czech Republic
Střelcová, Katarína	Technical University in Zvolen, Slovakia
Štroch, Michal	University in Ostrava, Czech Republic
	Global Change Research Centre, CAS, Czech Republic
Sun, Xiaoliang	University of Liverpool, UK
	Global Change Research Centre, CAS, Czech Republic
Tomášková, Ivana	Czech University of Life Sciences in Prague, Czech Republic
Trnka, Mirek	Mendel University in Brno, Czech Republic
	Global Change Research Centre, CAS, Czech Republic
Tříska, Jan	Global Change Research Centre, CAS, Czech Republic
Urban, Otmar	Global Change Research Centre, CAS, Czech Republic
Vačkář, David	Global Change Research Centre, CAS, Czech Republic
Zemek, František	Global Change Research Centre, CAS, Czech Republic
Žalud, Zdeněk	Mendel University in Brno, Czech Republic
	Global Change Research Centre, CAS, Czech Republic

Attribution of European temperature variability during 1882–2010: A statistical perspective

Mikšovský, J.[1, 2,*], Pišoft, P.[2]

[1] *Global Change Research Centre, Bělidla 986/4a, 603 00 Brno, Czech Republic*

[2] *Charles University, Faculty of Mathematics and Physics, Department of Atmospheric Physics, V Holešovičkách 2, 180 00 Prague, Czech Republic*

** author for correspondence; email: jiri@miksovsky.info*

ABSTRACT

Gridded monthly temperature data (GISTEMP and Berkeley Earth) covering the European region were investigated for the presence of components attributable to climate forcings, both anthropogenic and natural, and to major modes of internal climate variability. Effects of individual predictors were separated by multiple linear regression applied to time series over 1882–2010. It was shown that the presence of a warming trend correlated with greenhouse gases concentration was generally strong in European temperatures and typically combined with mild cooling ascribable to anthropogenic aerosols. Components attributable to variations in solar activity were rather weak and not statistically significant in most locations, as were the imprints of large volcanic eruptions. A strong association between North Atlantic Oscillation phase and temperature was confirmed for much of Europe, while temperature oscillations synchronized with the El Niño Southern Oscillation were quite limited in magnitude and displayed low levels of statistical significance. The influence of the Atlantic Multidecadal Oscillation was noticeable particularly in the western-most parts of Europe, whereas the Pacific Decadal Oscillation's significant impact extended to Scandinavia.

INTRODUCTION

The evolution of Earth's climate results from a complex interaction of numerous external influences and internal processes active at a wide range of spatial and temporal scales. Due to the multifaceted nature of the climate system, as well as nonlinear and chaotic features in some of its components, separating the effects of various exogenous and endogenous factors is a nontrivial task and the problem of attributing observed variability patterns to individual climate-forming agents is one of contemporary climatology's prime focal points.

While previous research has brought much insight into the issue of attribution, many questions still remain even for such basic climate descriptors as temperature (see Stocker et al. 2013, Chapter 10, and references therein). Increasing concentrations of greenhouse gases (GHGs) are now considered to be the primary driver of the near-surface warming observed during the industrial era. More uncertain is the influence of anthropogenic aerosols, thought to contribute both to cooling (e.g., sulfates) and warming (e.g., black carbon) tendencies, but also displaying substantial indirect effects. The impact of solar activity variations is also still discussed, although most studies suggest only a mild effect on near-surface temperature that is dwarfed by contributions from GHGs. Temporary cooling following major volcanic eruptions is quite distinct in global temperatures, but less so locally. An important, but regionally varied role is also played by internal climate oscillations: the North Atlantic Oscillation (NAO) is the dominant mode of variability in Europe, but potential contributions to temperature also come from links to the Atlantic Multidecadal Oscillation (AMO) and from teleconnections to the El Niño Southern Oscillation (ENSO) and Pacific Decadal Oscillation (PDO). This

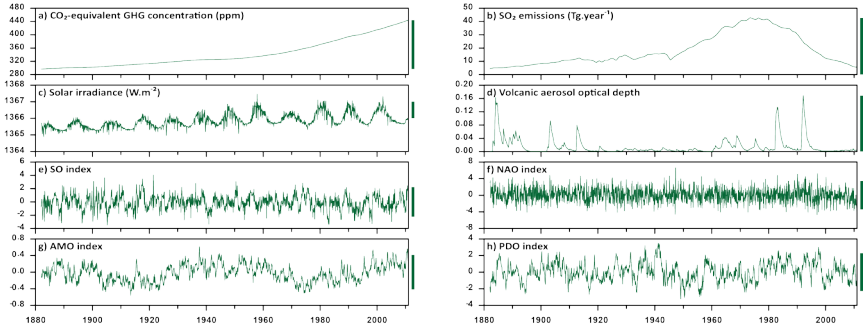

Fig. 1: *Time series of explanatory variables. Bars to the right show magnitudes of the characteristic variations, used to calculate responses in Fig. 2: increase in CO_2-equivalent GHG concentration between 1882 and 2010 (+148 ppm); peak value of European SO_2 emissions (43 Tg year^{-1}); increase in solar irradiance by 1 W m^{-2}; Mt. Pinatubo-sized volcanic event; increases in SO, NAO, AMO, and PDO indices by four times their standard deviations.*

presentation will show a sample of results from regression-based statistical attribution analysis focused on identifying sources of temporal variability in local European temperatures.

MATERIAL AND METHODS

Analysis outcomes are shown for two publicly available datasets of monthly temperature anomalies: GISTEMP from NASA's Goddard Institute for Space Studies (available at http://data.giss.nasa.gov/gistemp/; Hansen et al. 2010) and a combination of land temperature analysis and re-interpolated HadSST data from the Berkeley Earth group (available at http://berkeleyearth.org/data; Rohde et al. 2013).

Eight explanatory variables (predictors) were employed representing anthropogenic and natural forcings as well as major climatic oscillations (Fig. 1): CO_2-equivalent concentration of GHGs controlled by the Kyoto protocol (http://www.pik-potsdam.de/~mmalte/rcps/); European SO_2 emissions adapted from data by Smith et al. (2011) as a proxy for amounts of anthropogenic sulfate aerosols; monthly solar irradiance from KNMI Climate Explorer (http://climexp.knmi.nl/data/itsi_wls_mon.dat); volcanic aerosol optical depth from NASA (http://data.giss.nasa.gov/modelforce/strataer/); the ENSO (SOI) and NAO (NAOI) indices from Climatic Research Unit (http://www.cru.uea.ac.uk/cru/data/pci.htm); the AMO index (AMOI) from NOAA (http://www.esrl.noaa.gov/psd/data/timeseries/AMO/); and the PDO index (PDOI) from KNMI Climate Explorer (http://climexp.knmi.nl/data/ipdo_erssta.txt).

Contributions of individual predictors to local temperature anomalies were approximated by the multiple linear regression model. Regression coefficients were estimated using the least squares method independently for each grid point and their statistical significance was evaluated by moving-block bootstrap. Monthly data were analyzed for 1882–2010. The results are presented in the form of temperature responses to characteristic variations of individual explanatory variables, specified in Fig. 1.

RESULTS

The response patterns in Fig. 2 demonstrate that even across a geographically limited area such as Europe, the local character and magnitude of the effects of external and internal forcings may vary substantially. A relatively prominent example is the component attributed to GHG concentration: strong, statistically significant links throughout the analyzed region imply a close resemblance between the long-term temperature trend

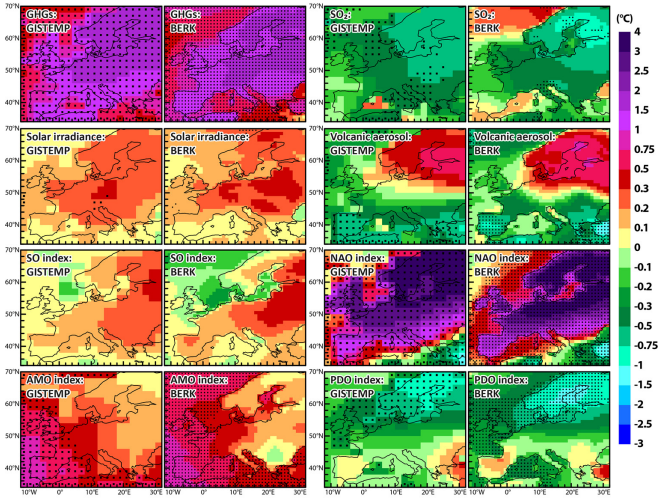

Fig. 2: *Temperature response (°C) associated with individual explanatory variables, calculated as a product of the local regression coefficient and the characteristic variation of the respective predictor (Fig. 1) for GISTEMP and Berkeley Earth (BERK) datasets. Black dots mark grid points with responses statistically significant at the 99% confidence level.*

and GHG forcing, with GHG-ascribed temperature increases between 1882 and 2010 ranging mostly between 1°C and 1.8°C over land. In accordance with conventional knowledge about their negative contribution to radiative forcing, sulfate aerosols provided cooling over land, though the effect was mostly not statistically significant. A warming tendency from increased solar irradiance was indicated for most of Europe, but it was mild and mostly not significant at the 99% confidence level. Responses to volcanic forcing were more varied, with cooling over southern parts of the continent contrasting with warming in the northeast, possibly due to dynamic responses inducing a post-volcanic positive phase of the Arctic Oscillation (Stenchikov et al. 2006). NAO's strong influence on European temperatures appeared as expected, but significant links could also be traced to other internal climate variability modes. Of particular interest is the effect of AMO: this oscillation with a main period of about 70 years has been suggested as a factor explaining the accelerated global temperature growth during the last decades of the 20th century (Zhou & Tung 2013) and its impacts can be seen not just over the northern Atlantic itself, but also over adjacent land. AMO's imprint on European temperatures wanes with increasing distance from the Atlantic Ocean – although a positive correlation was indicated for almost all areas, the links were statistically significant only in the western part of the continent.

Both Pacific-related variability modes, ENSO and PDO, projected a certain amount of influence on the European area, but only PDO manifested through teleconnections statistically significant at the 99% level, over the northern part of the continent. The SOI-attributed component in the temperature series confirms a tendency for colder anomalies during the El Niño phase of ENSO, but the link was not statistically significant at the 99% level. It should be noted that due to the inclusion of both the SOI and PDOI as explanatory variables as well as their mutual relationship (e.g., Newman et al. 2003, Brönnimann et al. 2007), these predictors partly competed for the same variability component in the temperature series. When SOI alone was used as predictor, its approximated apparent influence became stronger and more significant.

DISCUSSION

Our analysis highlighted a strong formal association between long-term trends in European temperatures and GHG amounts as well as a rather ambiguous cooling tendency from sulfate aerosols. Contributions from solar irradiance variations were substantially weaker than was the sum of anthropogenic effects and were largely not significant. Another influential predictor with potential impacts on temperature variability was identified in the AMOI: provided that AMO is stable and well characterized by the scalar index employed (a matter still under intense discussion – see, e.g., Mann et al. 2014 and Zhou & Tung 2013), a sizable part of the warming during the last decades of the 20th century could be ascribed to the increasing AMO phase between the 1970s and 2000s. Effects of teleconnections from the Pacific area are detectable as well, particularly in northern and eastern Europe, although statistically significant links appear only between PDO and temperatures over Scandinavia.

While our results offer some insight into the issue of responses within the climate system, it is important to remember that they are the outcome of a purely statistical analysis. The links revealed therefore represent an indication of a formal match between the temporal variability of the predictors and predictands rather than proof of their physically founded associations and should be interpreted as such. This particularly applies to the effects of GHGs and sulfate aerosols, which are somewhat collinear both with one another and with other potential anthropogenic predictors. Additional uncertainties may also stem from the choice of predictor series – for instance, our representation of anthropogenic aerosols through a single SO_2-based series may be overly simplifying. Issues related to predictor interdependence, nonlinearity, seasonality, and temporal stability also deserve more attention in the future, as does a combination of the results of statistical and general circulation model-based attribution analyses.

Acknowledgement

Supported by the Czech Science Foundation through project No. P209/11/0956 and by the Ministry of Education, Youth and Sports within the National Programme for Sustainability I, project No. LO1415.

References

Brönnimann S, Xoplaki E, Casty C et al. (2007) Clim. Dyn. 28, 181–197.

Hansen J, Ruedy R, Sato M et al. (2010) Rev. Geophys. 48, RG4004.

Mann ME, Steinman BA, Miller SK (2014) Geophys. Res. Lett. 41, 3211–3219.

Newman M, Compo GP, Alexander MA (2003) J. Clim. 16, 3853–3857.

Rohde R, Muller RA, Jacobsen R et al. (2013) Geoinform. Geostat. Overv. 1, 1–7.

Smith SJ, van Aardenne J, Klimont Z et al. (2011) Atmos. Chem. Phys. 11, 1101–1116.

Stenchikov G, Hamilton K, Stouffer RJ et al. (2006) J. Geophys. Res. Atmos. 111, D07107.

Stocker TF, Qin D, Plattner GK et al. (eds.) (2013) Climate Change 2013: The Physical Science Basis. Cambridge University Press, Cambridge.

Zhou J, Tung KK (2013) J. Atmos. Sci. 70, 3–8.

Heat waves over Central Europe in ALADIN-Climate/CZ regional climate model: evaluation and future projections

Lhotka, O. [1, 2, 3, *], Farda, A. [1, 4], Kyselý, J. [1, 2]

[1] *Global Change Research Centre, Czech Academy of Sciences, Bělidla 986/4a, 603 00 Brno, Czech Republic*
[2] *Institute of Atmospheric Physics, Czech Academy of Sciences, Boční II 1401, 141 31 Prague, Czech Republic*
[3] *Faculty of Science, Charles University, Albertov 6, 128 43 Prague, Czech Republic*
[4] *Czech Hydrometeorological Institute, Na Šabatce 17, 143 06 Prague, Czech Republic*
[*] *author for correspondence; email: lhotka.o@czechglobe.cz*

ABSTRACT

We evaluated a simulation of Central European heat waves and analysed possible changes of their characteristics in the future climate using the ALADIN-Climate/CZ regional climate model with 25 km horizontal grid spacing. Lateral boundary conditions were provided by the ARPEGE global climate model, using historical forcing and the SRES A1B scenario. Observed data were taken from the E-OBS gridded data set. Heat waves were evaluated over 1970–1999 and changes in their characteristics were assessed for 2020–2049. Their definition is based on exceedance of the 90th percentile of summer daily maximum temperature calculated separately for modelled and observed data. ALADIN-Climate/CZ simulates characteristics for the recent climate quite well, especially the overall severity of heat waves. In contrast, temperature amplitude was considerably overestimated. This model projects an increase in overall heat wave severity by a factor of 2 to 3 in the future climate, primarily driven by an increasing number of events. The study shows that ALADIN-Climate/CZ is generally capable of simulating Central European heat waves, which gives more credibility to model projections of future heat waves.

INTRODUCTION

Heat waves have substantial impacts on human society and ecosystems as they cause excess illness and mortality, increased energy demand for cooling, forest fires, spreading of pests, crop failure, and other economic losses (Beniston et al. 2007). Due to a projected rise in global mean air temperature (Kirtman et al. 2013), heat waves are expected to become more severe under ongoing climate change. Using climate model outputs, previous studies (e.g. Fischer & Schär 2010, Lau & Nath 2014) have shown a substantial increase in heat wave severity in the future climate, mainly caused by a shift in temperature distribution (Ballester et al. 2010). However, Vautard et al. (2013) evaluated European heat waves in regional climate models and demonstrated that the models suffered from general biases that affected the heat waves' simulated characteristics. The aim of the present study is to analyse the characteristics of Central European heat waves in the ALADIN-Climate/CZ regional climate model for both the recent and future climates.

MATERIALS AND METHODS

Simulated data were obtained from the ALADIN-Climate/CZ regional climate model with 25 km horizontal grid spacing (Farda et al. 2010). This model version was developed at the Czech Hydrometeorological Institute and is based on a numerical weather prediction model built into the frame of the ALADIN consortium. It utilizes a new formulation of cloudiness, radiation code, and semi-Lagrangian horizontal diffusion scheme. Modelled data are available for 1961–2050; we used the 1970–1999 period for model evaluation and the 2020–2049 period for assessing projected changes in heat wave characteristics. Observed data for model evaluation were taken from the E-OBS 10.0 gridded dataset (Haylock et al. 2008). The data have horizontal grid spacing of 25 km (0.22°-rotated grid version). Although the geographic projection differs from the one used in ALADIN-Climate/CZ (Lambert conformal), the study domain was designed in order to minimize the differences.

Heat waves were analysed over Central Europe, which was defined by 1,000 grid points (40 × 25) located approximately between 47–53°N and 8–22°E and covering an area of 625,000 km^2. The definition of a heat wave was based on the persistence of hot days, using daily maximum temperatures (T_{max}) in summer (1 June–31 August). A hot day was recorded when the average of T_{max} deviations in Central Europe from the 90th percentile of the summer T_{max} distribution was positive. Percentiles were calculated separately for observed and modelled data, since our intention was to focus on the characteristics of heat waves rather than on T_{max} bias. In modelled data, the percentile was calculated for the historical period and applied also to the future period. A heat wave was characterized by at least 3 successive hot days.

The severity of individual heat waves was described by the heat wave extremity index (Lhotka & Kyselý 2014), which takes into account events' temperature, length, and spatial extent. This index is calculated as the sum of daily T_{max} excesses above the 90th percentile of the summer T_{max} distribution over the entire heat wave, scaled by the total number of grid points in Central Europe (1,000). Temperature amplitude represents the largest T_{max} excess above the 90th percentile of the summer T_{max} distribution on any day and grid point during the heat wave. Length is the duration of the individual heat wave in days. Area is given by the region where T_{max} deviations from the 90th percentile of the summer T_{max} distribution were positive for at least 3 successive days.

RESULTS

During 1970–1999, E-OBS contained records of 199 hot days forming 23 heat waves with a total duration of 104 days (Table 1). The clustering index (the ratio between the total duration of heat waves and the number of hot days) was 0.52, indicating that about one-half of hot days were involved in heat waves. ALADIN-Climate/CZ simulated these characteristics quite well, but the clustering index was slightly overestimated while the number of hot days and heat waves was underestimated. Since the 90th percentiles were calculated separately for observed and modelled data, this underestimation is probably linked to a smaller spatial autocorrelation of T_{max} in the simulated data. The model simulates the total heat wave extremity index properly, but this originates from a compensatory effect from the overestimated mean extremity index and underestimated number of heat waves.

Regarding the scenario for the future period (2020–2049), ALADIN-Climate/CZ projected an increase in all characteristics. Although the model simulates a less than twofold increase in hot days, the total heat wave extremity index should increase by a factor of 2 to 3 in the future climate.

Table 1: *Characteristics of heat waves in observed and modelled data. HD: number of hot days, HW dur.: total duration of heat waves, I_{cl}: clustering index, HW: number of heat waves, ΣI_{hw}: total heat wave extremity index, I_{hw}: mean heat wave extremity index, T_{amp}: mean temperature amplitude, L: mean length of heat waves, A: mean area of heat waves.*

	HD	HW dur.	I_{cl}	HW	ΣI_{hw}	I_{hw}	T_{amp}	L	A
	no.	*days*		*no.*	*℃*	*℃*	*℃*	*days*	
E-OBS (1970–1999)	199	104	0.52	23	223.0	9.7	6.4	4.5	0.64
Historical (1970–1999)	169	98	0.58	21	232.0	11.0	8.2	4.7	0.66
Scenario (2020–2049)	289	200	0.69	37	569.1	15.4	9.6	5.4	0.68

Fig. 1 shows the statistical distributions of the heat wave extremity index, temperature amplitude, length, and area for all heat waves. The characteristics are expressed by a combination of box plots and violin plots, which provide additional density estimates using probability density functions. For 1970−1999, ALADIN-Climate/CZ reproduced heat wave characteristics reasonably well, except for temperature amplitude. Its distribution was considerably shifted, although the 90th percentile of T_{max} was calculated individually for the model. This resulted in a small overestimation of the heat wave extremity index in the upper tail of its distribution. For 2020−2049, ALADIN-Climate/CZ projects a substantial increase in temperature amplitude combined with an increased heat wave extremity index. Its maximum value reached 150°C, which is about three times larger than the most severe Central European heat wave observed in 1994.

DISCUSSION

We have shown that ALADIN-Climate/CZ is able to simulate Central European heat waves reasonably well. The largest drawback was found in the substantial overestimation of temperature amplitude, but this issue is present in the majority of current regional climate models (Vautard et al. 2013, Lhotka & Kyselý 2015). According to ALADIN-Climate/CZ, heat waves in the future climate (2020−2049) are projected to be almost twice as frequent as they have been in the recent climate (1970−1999) as well as being longer and with higher peak temperatures. The total heat wave extremity index should increase by a factor of 2 to 3 in the future climate. The threat of severe heat waves in the near future emphasizes the need for suitable adaptation strategies to prevent health issues among the population as well as such other related hazards as droughts and wildfires.

Acknowledgement

Funded by projects No. CZ.1.07/2.3.00/20.0248 "Building up a multidisciplinary scientific team focused on drought" and No. GAP209/11/0956 "Global and regional climate model simulations in Central Europe in the 18th–20th centuries in comparison with observed and reconstructed climate". Also supported by Charles University Grant Agency, student project No. 250215, and the Ministry of Education, Youth and Sports, project No. 7AMB15AR001 ("Climate change effects on heat waves and their recurrence probabilities"). We acknowledge the E-OBS data set from the EU-FP6 project ENSEMBLES (http://ensembles-eu.metoffice.com).

References

Ballester J, Rodó X, Giorgi F (2010) Clim. Dyn. 35, 1191–1205.

Beniston M, Stephenson DB, Christensen OB et al. (2007) Clim. Change 81, 71–95.

Farda A, Déqué M, Somot S et al. (2010) Stud. Geophys. Geod. 54, 313–332.

Fischer EM, Schär C (2010): Nat. Geosci. 3, 398-403.

Haylock MR, Hofstra N, Klein Tank AMG et al. (2008) J. Geophys. Res. Atmos. 113, D20119.

Kirtman B, Power SB, Adedoyin AJ et al. (2013) Near-term climate change: projections and predictability. Climate Change 2013: The Physical Science Basis (eds TF Stocker, D Qin, GK Plattner et al.), pp. 953–1028. Cambridge University Press, Cambridge.

Lau NC, Nath MJ (2014) J. Climate 27, 3713–3730.

Lhotka O, Kyselý J (2014) Int. J. Climatol., doi: 10.1002/joc.4050.

Lhotka O, Kyselý J (2015) Clim. Dyn., doi: 10.1007/s00382-015-2475-7.

Vautard R, Gobiet A, Jacob D et al. (2013) Clim. Dyn. 41, 2555–2575.

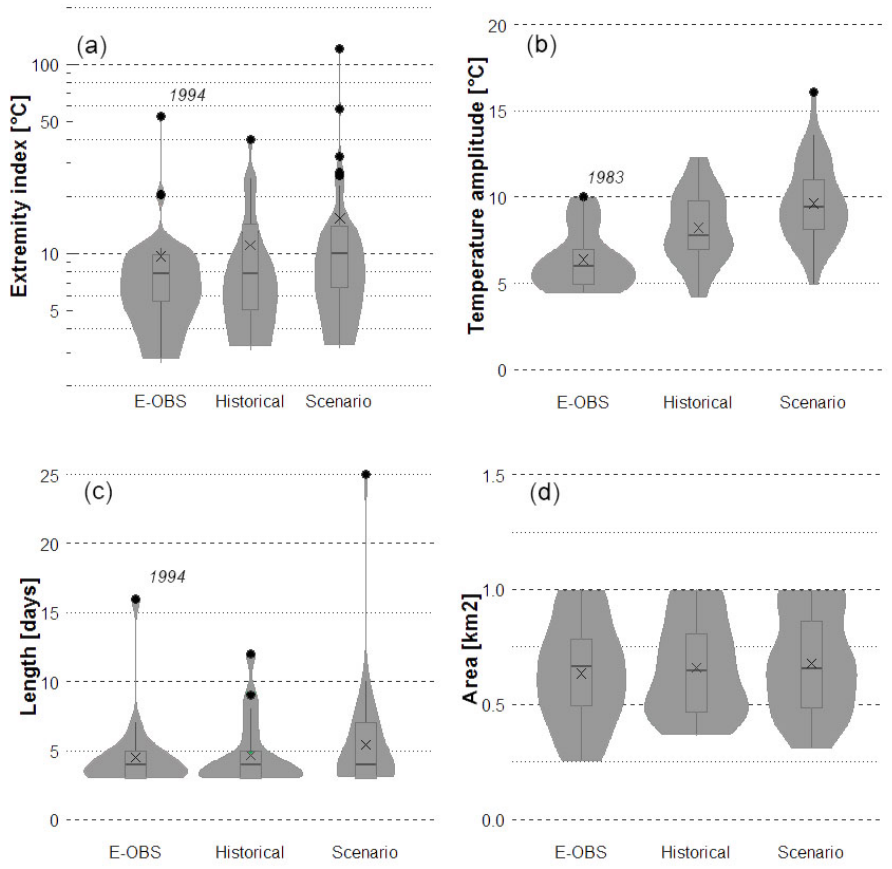

Fig. 1: *Box-violin plots of heat wave characteristics. Crosses indicate mean values, dots depict outliers. Note that y-axis for the extremity index is in a logarithmic scale.*

Köppen–Geiger climate classification by different regional climate models according to the SRES A1B scenario in the 21st century

Szabó-Takács, B.[1,*], Farda, A.[1,3], Zahradníček, P.[1,2], Štěpánek, P.[1,2]

[1]*Global Change Research Centre, Bělidla 986/4a, 60300 Brno, Czech Republic*
[2]*Czech Hydrometeorological Institute, Brno Regional Office, Kroftova 43, 61600 Brno, Czech Republic*
[3]*Czech Hydrometeorological Institute, Na Šabatce 17, 14306, Prague, Czech Republic*
**author for correspondence; email: szabo.b@czechglobe.cz*

ABSTRACT

We investigate future climate conditions projected by six regional climate model (RCM) simulations driven by the SRES A1B emission scenario. As a diagnostic tool of climate change, we used the Köppen–Geiger climate classification as it is suitable for assessing climate change impacts on ecosystems. The analysis is based on a comparison of Köppen–Geiger climate subtypes during two future time slices (2021–2050 and 2070–2100) with climate subtypes observed during 1961–2000. All RCMs showed expansion of the area covered by warmer climate types in the future, but the magnitude of the growth varied among RCMs. The differences stemmed from several sources, mainly boundary forcing provided by the driving global circulation models (GCMs) as well as different physical packages, resolution, and natural variability representation in individual GCMs. In general, RCMs driven by the ECHAM5-r3 GCM projected cooler climate conditions than did RCMs driven by the ARPÈGE GCM. This can be explained by two factors related to ECHAM5-r3: i) exaggerated transport of cool and moist air from the North Atlantic to Europe in summer, and ii) winter advection of cold air from the Artic owing to North Atlantic Oscillation blocking pattern alteration during solar minima as well as higher natural variability. RCM-related properties, such as physical package and spatial resolution, may also significantly affect climate predictions, although they do so to a smaller extent than does the driving GCM data.

INTRODUCTION

Regional climate models (RCMs) and global circulation models (GCMs) are state-of-the-art tools employed for climate change research. They are designed to capture climate evolution based on direct physical modeling of the atmosphere, ocean, and other components of the climate system on both global and regional scales.

Climate classifications are convenient tools for the description of climate and studying its change. The Köppen classification (1923), later adapted by Geiger (1961), divides climate into five types based on annual and monthly mean values of temperature and precipitation. Köppen–Geiger climate zone boundaries seem to correspond with certain prevalent vegetation species (Bonan 2002, Kottek et al. 2006). The main climate types are subdivided into several subtypes. Three vegetation groups (Köppen–Geiger climate classification types) are typical for Europe: the warm temperate zone (C), the snow zone (D), and the polar zone (E). Subtypes are named by adding two additional indices (letters) to the main type. The second index (letter) added to the types C and D indicates the precipitation pattern. An addition of "S" indicates dry summers (mean precipitation in the driest summer month is less than one-third of mean precipitation in the wettest winter month) while "F" means there is significant precipitation in all seasons. The third index (added after

Table 1: *Selected regional climate models (RCMs), their spatial horizontal resolution, and driving global circulation models (GCMs).*

	GCM	RCM	Horizontal Resolution
1	ARPÈGE	–	50 km
2	ARPÈGE	ALADIN	25 km
3	ARPÈGE	HIRHAM	25 km
4	ECHAM5-r3	RACMO	25 km
5	ECHAM5-r3	RCA	25 km
6	ECHAM5-r3	RegCM	25 km

the second letter) indicates the degree of summer heat. An addition of "A" means that the mean temperature of the warmest month is above 22°C with at least 4 months having mean temperature above 10°C. An addition of "B" means that the mean temperature of the warmest month is below 22°C with at least 4 months having mean temperature above 10°C. Finally, "C" means that there are fewer than 4 months having mean temperature above 10°C.

De Castro et al. (2007) and Gallardo et al. (2013) used the Köppen–Trewartha classification (Trewartha 1968) to estimate climate change in Europe with the ensemble means of RCM simulations by incorporating the uncertainty related to their driving GCMs. Using the ensemble mean may reduce the influence of bias in simulated temperature but not in precipitation, and this may consequently affect the quality of future climate projection.

In our work, we investigated the shift of Köppen–Geiger climate zones in Europe using six individual GCM/RCM simulations originally prepared within the EC FP6 project ENSEMBLES (van der Linden & Mitchell 2009). RCMs were driven by two different GCMs following the SRES A1B emission scenario in the 21st century. A bias correction technique was implemented to eliminate the systematic errors of ENSEMBLES RCMs using the observed data as a reference field. The spread among individual simulations was then related to the driving GCMs, properties of RCMs and their setup, downscaling technique, and natural variability (Déqué et al. 2012).

MATERIALS AND METHODS

Table 1 summarizes the selected ENSEMBLES RCMs. The analysis of climate types was carried out for two future periods: 2021–2050 and 2071–2100. Since all models are affected by bias, it is necessary to correct their outputs before further processing. An important point in bias correction is the availability of suitable reference data (e.g. observations or re-analyses). For bias correction, we chose the E-OBS gridded dataset of daily station observations. E-OBS (Haylock et al. 2008) is currently perhaps the best pan-European gridded dataset with spatial resolution of 0.25° in longitude and latitude (or 0.22° on the rotated pole grid typical for many RCMs) covering the period since 1950. The applied methodology of bias correction is described in Déqué (2007) and was performed using the ProClimDB database software (www.climahom.eu).

RESULTS

Fig. 1 summarizes the proportions of Europe covered by different climate zones based on EOBS observed data and RCM simulations in the near and distant future. According to all RCMs, the relative share of climate

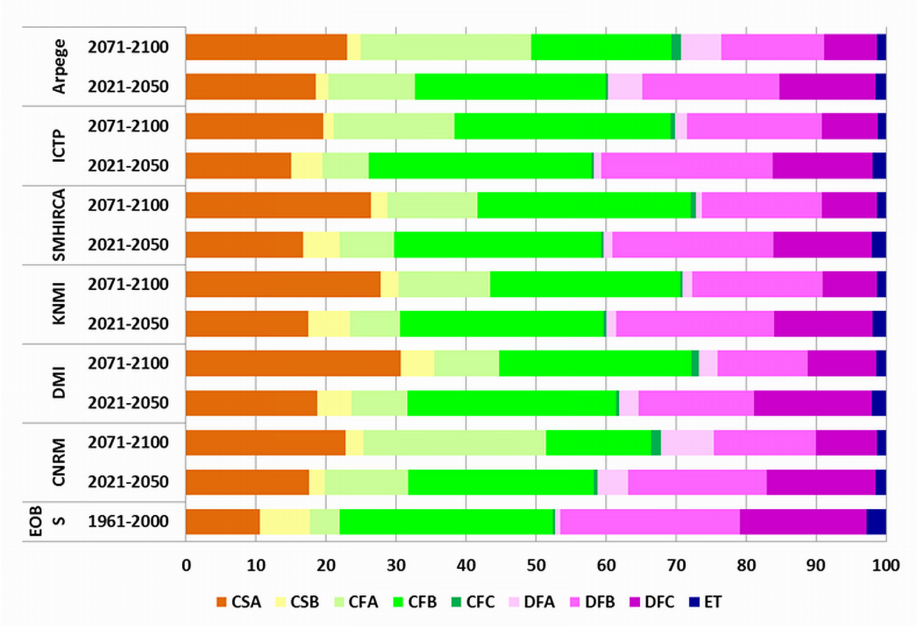

Fig. 1: *The proportions of Europe covered by different climate subtypes based on observations during 1961–2000 (bottom line) and RCM simulations in near and distant future.*

zones CSA, CFA, DFA, and CFC will increase in the future. In contrast, climate zones CSB, CFB, DFB, DFC, and ET will have reduced coverage compared with their current extents. These results are consistent with global warming trends in the future. The extension of climate zones CFA, DFA, and CSA was larger in RCMs driven by ARPÈGE than it was in those driven by ECHAM5-r3.

DISCUSSION

ARPÈGE-driven RCMs predicted the largest differences between observed and simulated results among the models (Fig. 1). The predicted higher mean temperature of the warmest month may be the result of positive snow–albedo feedback over Eastern Europe and high mountains in the ARPÈGE GCM (Gibelin & Déqué 2003). Large-scale circulation in ECHAM5-r3 is too zonal and transports cool and moist air from the North Atlantic to the European continent in summer (Kjellström 2011). Furthermore, several studies have noted the possible influence of solar output variability on the Earth's climate and atmospheric dynamics (Barriopedro et al. 2008, Lockwood 2012, Brugnara et al. 2013). According to these studies, enhanced solar irradiance during the 11-year solar cycle leads to increased ultraviolet absorption by ozone and warming in the stratosphere; this warming then alters the circulation patterns in the atmosphere below. Based on the relationship between the 11-year solar cycle and frequency of blockings, they found a higher likelihood of cold days over Europe during solar minima due to an eastward shift in the mean position of blockings in the North Atlantic. According to Sukhodolov et al. (2014), the radiation code of ECHAM5 GCM takes into account the 11-year solar cycle, which can correlate with the northeastward shift of the blocking pattern in the European

Block region and also contribute to cooler climate predictions by ECHAM5. In addition, natural variability also plays a significant role in temperature tendency. In the ECHAM GCM, natural variability is denoted by "-r1," "-r2," and "-r3," representing low, medium, and high natural variability, respectively. According to Kjellström et al. (2011), the higher natural variability in ECHAM5 (ECHAM5-r3) shows less warming in much of Europe than does the medium variability (ECHAM5-r2). HIRHAM has only one soil moisture layer compared to other RCMs, which results in reduced water holding capacity and a dryer climate. This could explain why HIRHAM gives the largest predicted proportion of Mediterranean climate in Europe.

The overall direction of change of climate zones corresponds with previous studies (Gallardo et al. 2013), but the magnitude of the change varies among RCMs. This spread predominantly stems from the differences in the GCMs chosen.

Acknowledgement

Supported by the Czech Science Foundation within project No. GAP209/11/0956 "Global and regional climate model simulations in Central Europe in the18th–20th centuries in comparison with observed and reconstructed climate." P. Zahradníček was supported by project No. CZ.1.07/2.3.00/20.0248 "InterSucho".

References

Barriopedro D, García-Herrera R, Huth R (2008) J. Geophys. Res. Atmos. 113, D14118.

Bonan GB (2002) Ecological Climatology: Concepts and Applications. Cambridge University Press, Cambridge.

Brugnara Y, Brönnimann S, Luterbacheret J et al. (2013) Atmos. Chem. Phys. 13, 6275–6288.

de Castro M, Gallardo C, Jylha K et al. (2007) Clim. Change 81, 329–341.

Déqué M (2007) Glob. Planet. Change 57, 16–26.

Déqué M, Somot S, Sanchez-Gomez E et al. (2012) Clim. Dyn. 38, 951–964.

Gallardo C, Gil V, Hagel E et al. (2013) Int. J. Climatol. 33, 2157–2166.

Geiger R (1961) Köppen–Geiger / Klima der Erde. (Wandkarte 1:16 Mill.). Klett-Perthes, Gotha.

Gibelin AL, Déqué M (2003) Clim. Dyn. 20, 327–339.

Haylock MR, Hofstra N, Klein Tank AMG et al. (2008) J. Geophys. Res. Atmos. 113, D20119.

Kjellström E, Nikulin G, Hansson U et al. (2011) Tellus A 63, 24–40.

Köppen WP (1923) Die Klimate der Erde: Grundriss der Klimakunde. Walter de Gruyter, Berlin.

Kottek M, Grieser J, Beck C et al. (2006) Meteorol. Z. 15, 259–263.

Lockwood M (2012) Surv. Geophys. 33, 503–534.

Sukhodolov T, Rozanov E, Shapiro AI et al. (2014) Geosci. Model Dev. Discuss. 7, 1337–1356.

Trewartha GT (1968) An Introduction to Climate. McGraw-Hill, New York.

van der Linden P, Mitchell JFB (eds) (2009) ENSEMBLES: Climate Change and Its Impacts: Summary of Research and Results from the ENSEMBLES Project. Met Office Hadley Centre, Exeter, UK.

Documentary evidence in the study of past hydrometeorological extremes in South Moravia

Chromá, K.[1,*], Brázdil, R.[1,2], Valášek, H.[2,3], Dolák, L.[1,2], Řezníčková, L.[1,2]

[1]*Global Change Research Centre, Bělidla 986/4a, 60300 Brno, Czech Republic*
[2]*Institute of Geography, Faculty of Science, Masaryk University, Kotlářská 2, 61137 Brno, Czech Republic*
[3]*Moravian Land Archives, Palachovo náměstí 1, 62500 Brno, Czech Republic*
[*]*author for correspondence; email: chroma.k@czechglobe.cz*

ABSTRACT

Information about hydrological and meteorological extremes (HMEs) in the instrumental period can be extended back into pre-instrumental times using documentary evidence from a variety of data sources. Financial and economic records, particularly those related to taxation data, are among the most important such sources. For the region of South Moravia, they are held by the Moravian Land Archives in the provincial capital of Brno and in certain equivalent state district archives that contain collections of estate accounts and family archives. Exploration of these sources provides information about HMEs in terms of dates and places of occurrence, courses, and impacts. Data of this kind from South Moravia were interpreted and included in a dedicated database, bringing the number of records of past HMEs to 2,010. This contribution demonstrates the high potential of this type of data.

INTRODUCTION

Hydrological and meteorological extremes (HMEs), events with a low probability of occurrence, are destructive natural phenomena that may often result in great material damage or even loss of human life. The study of past HMEs can aid in understanding their equivalents in recent times, especially in terms of frequency, severity, seasonality, and impacts. Insight may also be provided into recent climate change, which can also have a significant influence on certain aspects of HMEs (Stocker et al. 2013). In the Czech Republic (with South Moravia in its south-eastern part), systematic instrumental meteorological and hydrological observations began on a broader scale in the 19th century, particularly in its second half. Documentary data significantly extends knowledge about HMEs further into the past. Documentary evidence has recently been employed in several studies on HMEs (Brázdil et al. 2012b) and selected HME types (floods – Brázdil et al. 2014a, hailstorms – Brázdil et al. 2014b). This contribution summarizes the potential of documentary evidence to investigate past HMEs in South Moravia.

MATERIALS AND METHODS

Data

From the latter half of the 17th century onwards, the taxation system in Moravia enabled farmers and landowners to apply for tax relief if their crops, buildings, or land (fields, meadows, pastures, or gardens) had been affected by HMEs. The alleviation process was divided into a number of stages. At first, the landowners, settlement representatives, or individual farmers provided the regional administrative office with basic information regarding the extreme event, including a description of the damage done. Commissioners nominated by this body then inspected the damaged site in person and drew up their own account. The regional office summarized all this information and prepared a final report for the highest land office (the Gubernium in Brno) which made final decisions about granting

or rejecting tax relief (for more details, see Brázdil et al. 2012b). Documents related to this bureaucratic process, largely written in German, were preserved at several levels (affected communities, regional offices, the Moravian Land Office) and can be found in estate and family archives deposited in the Moravian Land Archives in Brno and some state district archives. Unfortunately, for various reasons, not all the relevant documents for particular estates have survived. Family archives contain a wide variety of records on various topics, including taxation data from estates they administered as well as other documents related to HMEs, such as requests for aid to stricken regions, thanks for such help, requests for loans to repair damage, and other documents. Estate documents contain more than merely taxation data. Great use may also be made of other finance-related records: correspondence between the estate holder and its administrator about as damage to forests, game stocks, bridges, mills, roads, and so on and documents related to aid for dispossessed people, particularly public collections of money.

The main types of HMEs mentioned in such documents are hailstorms, torrential rains, floods, flash floods, windstorms, droughts, and late frosts, all of which caused damage to harvest, agricultural land, and other property. In addition to detailed information about damage directly relevant for taxation purposes, data related to corresponding HMEs also include dates and places of occurrence and course development.

Based on critical analysis of data derived from such estate and family archives, a database of HMEs in South Moravia has been created for the 17th–20th centuries. In the process of analysis, it is essential to distinguish between extreme events and types of extremes. Extreme events are considered as those cases in which the damage caused by weather occurred during a single day. Each event may be then classified into several types of extremes, for example thunderstorm with hailstorm, and torrential rain leading to a flash flood or inundation. This enables studying the frequency of all HMEs together or individual types of extremes separately.

RESULTS

Potential of HME database for South Moravia

To date, a total of 2,010 records of past HMEs have been included in the database, covering 1544–1942. Of these, 1,945 records were extracted from estate archives and 65 from family archives (data extraction from family archives is still in progress and this number will increase). Fig. 1 illustrates the decadal frequency of 1,995 records covering 1641–1950. In addition to these, 12 records have not been dated precisely to a single year and three additional records were found for 1544, 1623, and 1626. Due to information about collections of money for people affected by HMEs, this database also includes several records for the Czech Lands outside of South Moravia and even for other countries within the Hapsburg Empire.

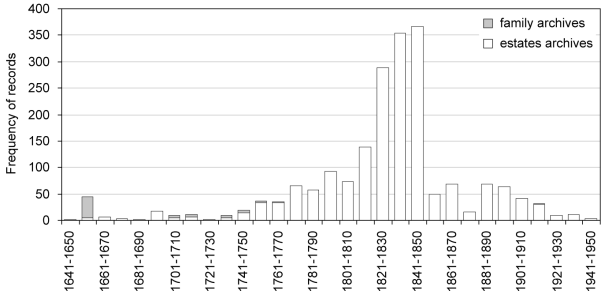

Fig. 1: *Decadal frequency of HME records in South Moravia extracted from estate and family archives and included in a database for 1641–1950.*

As seen in Fig. 1, the highest frequencies were recorded for the decades 1841–1850 (366 records), 1831–1840 (353), and 1821–1830 (288). These three decades (1821–1850) together comprise 50.1% of all records. It is important to note that this largely reflects the availability of existing documents and the concentration of taxation records within the 19th century. Such a distribution of sources also influences frequency analyses based on the data. For example, Brázdil et al. (2014a) analysed floods, flash floods, and inundations in South Moravia and found the highest frequencies of available records during 1821–1850, constituting 45.2% of all records. Brázdil et al. (2014b) found an even more significant predominance within the same period in an analysis of damaging hailstorms (58.9% of all records).

In terms of individual HME types (Fig. 2), flowing water (floods, flash floods, and inundations) comprises the majority with 884 records, followed by hailstorms (809) and torrential rains (488). At a lower level are windstorms (176 records), late frosts (78), and droughts (60). Windstorm records include 12 reports of tornadoes (proven or probable), extending the existing tornado chronology of the Czech Lands (for more details, see Brázdil et al. 2012a). In addition to such specific HMEs, the database also contains 121 records of other information related to negative effects on crops and human property, such as reports of bad harvests without actual causes given, rainy harvest times, wet spring seasons, heavy snow, rime, and, in the earlier times, even locust outbreaks (for more details, see Brázdil et al. 2014c). Besides those records included in Fig. 2, there are also 51 records describing extremes which occurred outside the borders of the Czech Lands (gathered largely from requests for public collections for afflicted communities).

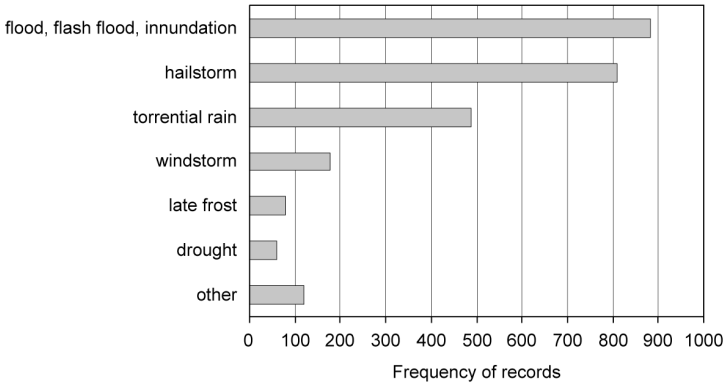

Fig. 2: *Frequency of records of individual HME types in South Moravia extracted from estate and family archives and included in the database for 1641–1950.*

HME data included in the database not only facilitate the study of temporal aspects (frequency distribution, seasonality), they also enable the derivation of the extremes' spatial structures and impacts. For example, Brázdil et al. (2014b) presented four outstanding cases of damaging hailstorms in South Moravia and indicated their territorial extent.

DISCUSSION

Documentary evidence, especially taxation records, enable the identification of damaging HMEs, including their dates and places of occurrence and type and extent of damage. However, the results are influenced

by various uncertainties and limitations (for more details, see Brázdil et al. 2012b, Brázdil et al. 2014b), including:

(1) The spatial and temporal density of records largely reflects the number of surviving documents.

(2) The most important part of taxation records is related to damage to agricultural crops and is thus dependent to a considerable extent on crop phenophases. The information is therefore prevailingly restricted to the period of agricultural work during the height of the vegetation period (May–August).

(3) Details related to HMEs in reports are dependent on their authors' observational talent and literacy.

(4) HME data were often secondary and may have been partly suppressed with respect to the reports' main goal, which was to document and specify the extent of damage for tax relief.

(5) Only events with damage severe enough for entitlement to tax relief, or requests for other help, are recorded, i.e. derived frequencies are lower than would be those obtained from systematic meteorological or hydrological observations.

Documentary evidence significantly extends knowledge of HMEs in the period before systematic observations and has the potential to complement standard hydrological and meteorological observations in the period of overlap. The importance of taxation records was clearly demonstrated by Brázdil et al. (2014a) in the creation of flood chronologies for four selected rivers in South Moravia (the Dyje, Jihlava, Morava, and Svratka rivers), which combined information from the aforementioned database with other documentary and instrumental data.

In the next stage, information from estate and family archives will be supplemented by other types of documentary evidence (chronicles, newspapers) and systematic observations and then used for further studies of HMEs, including their intensities and impacts. The aforementioned HME data extracted from estate and family archives constitutes an important source of documentary evidence for use in historical climatology and historical hydrology (for more details, see Brázdil et al. 2005, Brázdil et al. 2006). Finally, the great potential of this type of documentary evidence in the study of HMEs on a broader European scale cannot be overemphasized.

Acknowledgements

K. Chromá, R. Brázdil, and H. Valášek supported by the Czech Science Foundation under project No. GA13-19831S "Hydrometeorological extremes in Southern Moravia derived from documentary evidence" and L. Dolák and L. Řezníčková by the Ministry of Education, Youth and Sports under project No. CZ.1.07/2.3.00/20.0248 "Building up a multidisciplinary scientific team focused on drought". Our thanks to Tony Long for help with the English.

References

Brázdil R, Chromá K, Dobrovolný P et al. (2012a) Atmos. Res. 118, 193–204.

Brázdil R, Chromá K, Řezníčková L et al. (2014a) Hydrol. Earth Syst. Sci. 18, 3873–3889.

Brázdil R, Chromá K, Valášek H et al. (2012b) Clim. Past 8, 467–481.

Brázdil R, Chromá K, Valášek H et al. (2014b) Theor. Appl. Climatol. online, doi: 10.1007/s00704-014-1338-1.

Brázdil R, Kundzewicz ZW, Benito G (2006) Hydrol. Sci. J. 51, 739–764.

Brázdil R, Pfister C, Wanner H et al. (2005) Clim. Change 70, 363–430.

Brázdil R, Řezníčková L, Valášek H et al. (2014c) Theor. Appl. Climatol. 116, 343–357.

Stocker TF, Qin D, Plattner G-K et al. (eds.) (2013) Climate Change 2013: The Physical Science Basis. Cambridge University Press, Cambridge and New York.

Documentary evidence as a source of data for studying droughts in the Czech Lands

Řezníčková, L.[1, 2,*], Brázdil, R.[1, 2], Kotyza, O[3], Valášek, H.[2, 4]

[1] *Global Change Research Centre, Bělidla 986/4a, 603 00 Brno, Czech Republic*

[2] *Institute of Geography, Masaryk University, Kotlářská 2, 611 37 Brno, Czech Republic*

[3] *Regional Museum, Dlouhá 17, 412 01 Litoměřice, Czech Republic*

[4] *Moravian Land Archives, Palachovo nám. 1, 325 00 Brno, Czech Republic*

* *author for correspondence; email: ladkar@sci.muni.cz*

ABSTRACT

Information about past droughts may be derived from the various kinds of documentary evidence. Documentary data are particularly applicable to the pre-instrumental period but may also be used for the overlapping period with instrumental records. They are extracted from written narrative sources, weather diaries, personal and official letters, newspapers, religious records, epigraphic sources, and other sources. Direct descriptions of weather facilitate identification of meteorological droughts, while descriptions of drought impacts are used to identify agricultural and hydrological droughts. Documentary evidence enabled the creation of series of precipitation indices which classify dry months on a scale of –1 (dry), –2 (very dry), and –3 (extremely dry). In this way, it is possible to study the frequency, seasonality, severity, and impacts of drought episodes in the pre-instrumental period.

INTRODUCTION

Documentary evidence constitutes the basic data source for historical climatology addressing the reconstruction of climate and hydrometeorological extremes (HMEs) as well as their impacts on human society. Documentary sources arising from society's intellectual and material pursuits may be categorized with respect to available data into: (i) direct and proxy data expressing weather information, (ii) individual and institutional data recorded by individuals or bureaucratic bodies, and (iii) primary and secondary data depending on whether the author witnessed the weather described or it was recorded at some distance from the event in time or place or even transferred from other sources (Brázdil et al. 2005). Many documentary sources include data about drought and its impacts. This contribution presents the kinds of documentary data containing drought information and demonstrates their use in the study of droughts' spatio-temporal variability within the Czech Lands.

MATERIALS AND METHODS

A number of types of documentary sources contain information about drought and related phenomena within the Czech Lands (Brázdil et al. 2005).

Narrative sources

This group includes weather reports in annals, chronicles, memoirs, diaries, historical calendars, official "books of memory", and other sources. They usually include descriptions of anomalous weather and HMEs and their impacts on human activity. The earliest credible drought report in the Czech Lands relates to the winter of 1090–1091 and comes from the Old Prague Annals, now lost but quoted by several later sources: "*Et in hieme neque nix neque pluvia fuit*" [And in winter there was neither snow nor rain] (Emler 1874).

Daily weather records

These consist of more-or-less regular daily visual observations of the weather and related phenomena recorded by their authors into ephemerides, calendars, and official or personal diaries. For example, extensive weather records appear in the diaries of the Hradisko Monastery and Svatý Kopeček Priory in Olomouc, preserved for a total of 52 years during 1693–1783; drought is explicitly mentioned in 17 of these years (Brázdil et al. 2011).

Official and personal letters

Those who administered estates and domains reported regularly in writing to their superiors and such correspondence comprises a valuable source as do responses to it as well as lists drawn up for bureaucratic purposes. In addition to personal information, personal letters often feature comments on the weather. An example may be found in a letter from Josef Volek to his wife Rozálii dated 10 June 1863 and written in Luhačovice: "since the Lord has given constant dry weather this year, leave the grain well spread when you cut" (Dobeš 1945).

Shopkeepers' and market songs

Catastrophic events often entered the realm of folk and art production, usually devoted to floods and their impacts. Songs related to drought are scarcer, but "*Klíč od deště aneb Nová píseň v čas sucha*" [A Key from the Rain, or a New Song in Time of Drought] by Rambek, a citizen of Prague New Town, ran to a second edition (Novotný 1940). It was inspired by a severe drought in 1678.

Newspapers

Descriptions of HMEs and their impacts featured in occasionally published newssheets and later in more regularly published newspapers. For example, *Moravské noviny* reported on 17 June 1885 that in Pozořice and its surroundings "dry weather reached such heights that nearly everything became dry. [...] Everything calls upon, everything beseeches, Heaven to irrigate the parched earth."

Financial – economic records

Finance and business have always generated copious paperwork and the influence of weather, especially in an agriculturally based society, is readily traced. In particular, quite extensive records survive of the beginnings of food crop and grape harvests, wine quality and quantity, yields, prices of agricultural products, and compensation for property and assets damaged by HMEs. One very rich source consists of documentation accompanying farmers' applications for tax relief after the negative impacts of drought. For example, tax records from ten estates in south-eastern Moravia have made it possible to recognize eight years with drought during the 18th–19th centuries (Brázdil et al. 2012).

Religious sources

In especially hard times, the church organized processions of religious entreaty, fasts, and prayer vigils to beseech the Lord to relieve adverse weather patterns. For example, fasts and prayers for rain were proclaimed in Prague on 15 July 1503 (Palacký 1941). Surviving sermons may also contain valuable data; the priest Daniel Philomates the Elder mentioned in a sermon at Domaželice in 1616 that such drought and lack of water as afflicted them that year had not been heard of for more than a century (*Philomates 1616*).

Printed sources

Theatrum Europaeum describes various events in Europe between 1633 and 1738. It mentions a hot summer in Austria, Bohemia, and Hungary in 1666 when meadows were dry, watercourses dried out, people needed to travel "6–7 [Austrian] miles" [ca 45–53 km] for water, and fires broke out in villages and woods. Drought-related information can also be found in the annual summaries of agricultural and forestry production

published together with the results of meteorological and phenological observations for the years 1822–1845 by the I. R. Patriotic-Economic Society of Bohemia (Bělínová & Brázdil 2012).

Chronograms

Chronograms are records commemorating a significant event (e.g. a flood). Certain letters within them may be interpreted as Roman numerals and indicate the year of the reported event. A Latin entry in the records of Hieronymus Haura, an Augustinian monk in Brno, recorded the great drought of 1746 thusly: "*Personat he**V**! tu**I**st**I**s Vo**X**: S**V**C**C**I**I**s aret a**D**e**M**pt**I**s / Noster ager s**I**t**I****V**nt fontes, herbaeq**V**e, feraeq**V**e*" [It resounds! Oh, woe betide you, such a voice! Drought has dried up our fields, consumed them; the springs are thirsty [as are] plants and beasts] (Haura s.a.). The year 1746 is then given from a simple sum of the Roman numerals in bold.

Epigraphic records

Symbols or entire reports have been cut or drawn into rocks, stones, bridges, and buildings and chiselled into wood to show extreme water levels or commemorate significant events. Hydrological drought is remembered through what are known as "hunger stones". One example stands on the left bank of the River Elbe in Děčín with indications of low water levels. Its inscription warns of impending drought hardship: "*Wenn du mich siehst, dann weine*" [If you see me, then cry].

Documentary data extracted from the above must be subject to critical interpretation. Some reports make direct mention of a period without rain, indicating a meteorological drought.

A drought may be reported by direct sources, while other sources provide only proxy indicators, often through descriptions of the impacts of droughts (agricultural and hydrological droughts) from which some idea of the severity of the drought may be derived. It is worth mentioning other clear drought indicators that appear in written records: bad harvests of various crops; problems with autumn sowing; lack of drinking water; low water levels in watercourses and standing water; streams and springs drying up completely; large rivers so low that they can be crossed on foot or by cart; watermills out of operation for lack of water; high prices and shortages of flour and bread; religious processions of entreaty, prayers, and fasting; and others.

RESULTS

Series of precipitation indices may be employed for certain quantitative expression of drought in the pre-instrumental period. This involves corresponding documentary data being transformed into an ordinal seven-degree scale (weighted indices) (Brázdil et al. 2005). These are interpreted for individual months (or seasons if data density is low) and express relative deviations of actual precipitation patterns from the normal. The precipitation character of the month is then categorized as follows: –3: extremely dry, –2: very dry, –1: dry, 0: normal, +1: wet, +2: very wet, and +3: extremely wet. Series of seasonal or annual indices are then sums of the corresponding months' indices. Transformation of descriptive reports into series of indices is partly biased by a degree of subjectivity on the part of the interpretation's author. However, this can be minimized through multiple interpretations and cross-checking with similar series and data from countries immediately bordering the Czech Lands.

Such an approach was used by Brázdil et al. (2013) while creating a long-term, 500-year drought chronology for the Czech Lands. While documentary data before AD 1500 are quite scarce and predominantly refer to Bohemia (Brázdil & Kotyza 1995), the density of precipitation/drought documentary records later significantly increases. Using documentary data, Brázdil et al. (2013) considered as drought episodes those cases in which at least two consecutive months were classified as dry (particularly with indices at –2 and –3, but those at –1). From 1805 (instrumental period), such drought data were supplemented by data derived from

analysis of three drought indices (SPEI-1, Z-index, and PDSI) to obtain a drought chronology for 1501–2012 (see Brázdil et al. 2013 for more details).

DISCUSSION

Various types of high-resolution documentary data related to droughts and their impacts facilitate the assembly of an extensive database of such information within the Czech Lands in the pre-instrumental period and the overlapping time within the instrumental period. The character of the documentary data enables the study of the frequency, severity, seasonality, and impacts of droughts as well as discrimination between individual drought types with respect to impacts (meteorological, agricultural, hydrological, and socio-economic). Combining pre-instrumental drought information with that from the instrumental period has enabled the creation of a 500-year drought chronology for the Czech Lands (Brázdil et al. 2013).

Acknowledgement

L. Řezníčková and H. Valášek supported by project No. GA13-19831S of the Czech Science Foundation and R. Brázdil by project No. CZ.1.07/2.3.00/20.0248 of the Ministry of Education, Youth and Sports under. Tony Long helped with the English.

References

Bělínová M, Brázdil R (2012) Meteorol. Bull. 65, 13–22.

Brázdil R, Černušák T, Řezníčková L (2011) The Weather and Climate in the Region of Olomouc, Czech Republic, based on Premonstratensian Diaries Kept by the Hradisko Monastery and Svatý Kopeček Priory, 1693–1783. Masaryk University, Brno.

Brázdil R, Chromá K, Valášek H et al. (2012) Clim. Past 8, 467–481.

Brázdil R, Dobrovolný P, Trnka M et al. (2013) Clim. Past 9, 1985–2002.

Brázdil R, Kotyza O (1995) History of Weather and Climate in the Czech Lands I (Period 1000–1500). Verlag Geographisches Institut ETH, Zürich.

Brázdil R, Pfister C, Wanner H et al. (2005) Clim. Chang. 70, 363–430.

Dobeš F (1945) Kniha o Střítěži (trochu historie, trochu rodopisu). Díl III. Self-published, Valašské Meziříčí.

Emler J (1874) Monachi Sazaviensis Continuatio Cosmae. Fontes rerum Bohemicarum, vol. II. Prague.

Haura H (s.a.) Miscellanea iucundo-curiosa in quibus continentur variae descriptiones, versus, carmina, elogia, epitaphia, vaticinia, illuminationes, declarationes, pugnae, conflictus, notata de bellis et diversis temporibus, casus laeto-fatales, contingentia in monasterio Sancti Thomae, processiones et devotiones ad Thaumaturgam, varii eventus in Moravia, Bohemia, et adjacentibus regionibus, Brunae et aliis civitatibus, ac aliae iucundae, et utiles annotationes et reflexiones ... T. III. Moravian Land Library in Brno, sign. A21.

Novotný M (1940) Špalíček písniček jarmarečních. Evropský literární klub, Prague.

Palacký F (1941) Staří letopisové čeští od roku 1378 do 1527 čili pokračování v kronikách Přibíka Pulkavy a Beneše z Hořovic z rukopisů starých vydané. Dílo Františka Palackého, vol. 2. (ed J Charvát). Nakladatelství L. Mazáč, Prague.

Philomates D (1616) O hrozném a velikém suchu zdržení dešťů a odtud následujícím nedostatku vody, jakéhož sucha žádný z lidí nynějších, ode sta let i výšeji, starých nepamatuje. Kázání učiněné v kostele domaželitském (sic!). Municipal Library of Prague, sign. 35 D 19.

Selected drought impacts in South Moravia in the 18th and 20th centuries based on documentary evidence

Dolák, L.[1,2,*], Brázdil, R.[1,2], Řezníčková, L.[1,2], Valášek, H.[1,3]

[1]*Institute of Geography, Masaryk University, Kotlářská 2, 611 37 Brno, Czech Republic*
[2]*Global Change Research Centre, Bělidla 986/4a, 603 00 Brno, Czech Republic*
[3]*Moravian Land Archives, Brno, Palackého nám. 1, 625 00 Brno, Czech Republic*
[*]*author for correspondence; email: dolak@mail.muni.cz*

ABSTRACT

This contribution addresses the impacts of drought upon human society in South Moravia in the 18th–20th centuries, utilizing documentary evidence (parish and village chronicles, taxation and damage records, and correspondence). The consequences of drought are reviewed with respect to their impacts on agriculture (with special emphasis on crop production), water resources, and socio-economic conditions.

INTRODUCTION

A drought results from a deficiency in precipitation, which drops below the normal or expected amount over a given area. Based on impact type, droughts may be divided into meteorological, agricultural, hydrological, and socio-economic categories (Heim 2002). Such impacts may be assessed by analysing statistical data (e.g. crop yields, discharges) or through descriptions of their impacts as described in documentary sources. This contribution seeks to analyse drought impacts on agriculture, water resources, and overall socio-economic status by means of documentary data available for South Moravia in the 18th–20th centuries (Fig. 1).

MATERIAL AND METHODS

Certain documentary records describe the course of the weather and related phenomena in such a way that it is possible to derive information referring to drought and its impacts. This is especially true of narrative sources, weather diaries, letters, market songs, newspaper items, financial and economic records, church chronicles, printed sources, chronograms, and epigraphic data (see Řezníčková et al. 2015). Parish chronicles, village chronicles, taxation documentation, and official correspondence make up the basic sources of data for this study. Many of these records were hand-written in neo-Gothic italic script, in the deeper past in German and in more recent times also in Czech. The information contained in these records that related to drought was critically analysed and interpreted.

RESULTS

Agricultural drought

For maximum clarity, drought impacts within agriculture are divided into: impacts on fields and crops, impacts on meadows and pastures, and impacts on livestock.

Impacts on fields and crops. Drought has always been a frequent cause of poor harvests of grain, fodder plants, root crops, vegetables, and fruits. If the spring is dry, only some of the seed sown grows at all and the remainder results in only modest yields. For example, in mid-July 1790, the individual municipalities of the Uherský Brod estate reported that a range of spring crops had not grown, while in Suchá Loz 66–75% of fields and winter crops were damaged by drought as well (S1). According to farmers in Nezdenice, "[...] *many cereal seeds*

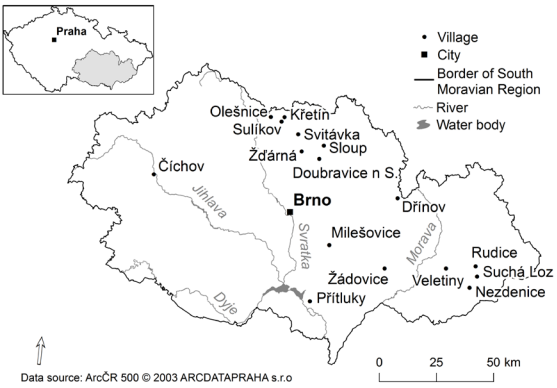

Fig. 1: *Depiction of South Moravia and locations mentioned in text.*

were unable to grow, while other seeds rotted away in the ground [... Those] *cereals that did grow were rendered useless by this drought*", and they estimated the damage to their own fields and those fields they rented at 1440 gulden (S1). For a better understanding of the value of money, in 1771 a reaper earned 15 Kreutzer (Kr.; 1 gulden = 60 Kr.) for mowing one *měřice* (0.192 ha; Hofmann 1984) of rye or wheat and 24 Kr. for a day mowing grass; a labourer earned 12–14 Kr. per day (Brzobohatý 2003).

In spring crops, droughts led to a short growth period, sparse ground cover, limited capacity to form ears, or complete desiccation. In this way, due to drought, winter crops failed to thrive in autumn (e.g. in Sulíkov in 1929; S5). During a long-term drought such as during 1718–1719, both spring and winter crops were affected, as evidenced in the documentary records for Svitávka (S6). Poor cereal harvests lead, quite apart from any direct lack of grain for milling and sale, to seed shortages.

Fruit trees also suffer from lack of water resulting in premature shedding of their products. Drought has especially unfavourable impacts on young or recently-planted trees. For instance, most newly-planted linden trees in Milešovice dried out in the dry summer of 1917 (S13). Root crops, especially potatoes, have lower yields during droughts because the size of their tubers drops, and harvests have been recorded of less than the quantity planted. Dry episodes also help promote the spread of aphids and other crop pests, exacerbating reductions in harvest.

Impacts on meadows and pastures. Droughts have an adverse influence on meadows and pastures in spring and summer. Dry periods often resulted in a lack of hay and aftermath at the beginning of autumn, which would otherwise have served as fodder for livestock and horses over the winter. For instance, a hay shortage in the dry year of 1790 was of acute concern to farmers from Veletiny because they were unable to contribute the regular quarterly quantity of hay dictated by their terms of service to the aristocrat landowner (S1).

Drought also increased vulnerability to fire in meadows and pastures (e.g. on the Doubravice estate in 1822; S2) as well as in timber-yards and forests. The expansion of railways in the second half of the 19th century, with early steam engines in particular throwing sparks in all directions, increased this threat of fires (see burnt pastures in Číchov during the dry period of 1904; S11).

Impacts on livestock. Withered pastures could not provide adequate grazing for livestock, so precious winter fodder or feed substitutes needed to be employed. Thus, an extraordinary yield of acorns served as feed for pigs in Milešovice in the dry year of 1911, and acorns also became a substitute for maize (S13). A lack of winter fodder often resulted in a reduction in livestock numbers, although farmers did their best to maintain at least a minimum of cattle. In critical situations, they prioritized the sale of pigs, often at low prices, using the funds acquired to buy expensive beet scraps to feed their cattle (S13). Lack of cereals, or their stunting, led to shortages of the straw used as bedding for livestock. One response measure, taken in Žďárná during the 1917 drought, was to permit farmers to take foliage from the forest as bedding, enabling modest supplies of straw

to serve as feed instead of fodder and hay (S7). Feed quality also deteriorated during drought; essential nutrients were lost and the feed became less digestible, resulting in, among other health problems, softening of livestock's bones. Again, livestock numbers fell.

Hydrological drought

Dry episodes also have a significant influence on the accessibility of water. Among the immediate historical consequences were a decline in groundwater levels, with subsequent losses of wells, springs and ponds, and decreasing river levels, sometimes to the point of their completely drying out for a while (e.g. the Dyje River near Přítluky in 1718; S8). Such deficits deprived both people and livestock of drinking water and resulted in an acute need to find alternative sources. Since these sources were often pumped, pressure problems emerged. Where fountains could be created, there was sufficient water, which could accumulate in abundant, sometimes excessive, volumes. Elsewhere, however, water needed to be transported from sometimes quite distant springs, as was recorded during dry years in such various locations in South Moravia as Dřínov in 1863 (S10), Sloup in 1893 (S4), and Žďárná in 1921 (S7). Social stress and anxiety frequently increased when water needed to be distributed in times of drought. For example, during the drought in 1863, the Křetín farmstead erupted in disputes and fights among those applying for water (S3). Water mills, in the past often nearly the sole source of mechanical power, required a certain river level and were unable to operate at low water levels. This resulted in both financial losses to the miller himself and increased costs to farmers. The latter were often forced to transport their corn to mills that were still running, which were very often quite distant, e.g. in Křetín in 1863 (S3) and Podolí in 1917 (S12).

Socio-economic impacts of drought

Tax relief was available to those encountering difficulties associated with livestock grazing and increased costs resulting from drought. For example, one decision of the Brno *Gubernium* (the deciding administrative body for such matters), taken on 1 December 1775, granted tax relief to the stock-herder Thomas Zaleschak from Rudice: 30 Kr. for each dairy cow and 15 Kr for each calf (S1). If cattle numbers needed to be reduced owing to lack of fodder, the consequences went beyond the simple loss of the animals themselves. Cattle provided draught power for ploughing and hauling carts as well as milk and meat and any income that might be derived from them. Funds raised by livestock sales served to mitigate drought impacts by enabling the purchase of feed and seeds. However, since drought affected whole regions and livestock was slaughtered on the majority of farms, an excess of pork and later beef on the market soon led to rapid declines in prices. For instance, the price of beef dropped by half for 6 months due to drought in Sloup in 1893 (S4), which meant a significant decrease in farmers' incomes.

Increased prices of scarce commodities, such as cereals, fruits, vegetables, potatoes, and even hay, were a very frequent consequence of drought. In Olešnice, a 50% increase in cereal prices was reported during the dry year of 1911 in comparison to the previous year, which had been very wet (Town of Olešnice 2004).

Drought had a great influence on farm routines, dictating unusual starting and ending times for the year's activities. If drought appeared at the beginning of the year, the soil was parched soon after winter and crops were sown early. The occurrence of warm weather, usually associated with drought, meant that crops in fields and gardens ripened early and the harvest occurred sooner. Moreover, vineyards in many places, from which some quite meticulous records survive, testify to earlier-vintage, high-quality wine, but also to smaller harvests, as in Žádovice in the dry year of 1917 (S9). On the other hand, dry soil is harder to cultivate, leading to

problems with sowing and ploughing in autumn; for example, in Milešovice in the dry year of 1953, farmers postponed ploughing until the first rain on 30 October (S13).

DISCUSSION

The results presented herein demonstrate that droughts have significantly influenced agriculture, agricultural production, and water resources in South Moravia over the past three centuries with significant consequences for its inhabitants' socio-economic conditions. Documentary records thus serve as a source that can convey significant information not only for drought climatology of the past, but also for studying the history of everyday life. This paper demonstrated a model of human behaviour, responses, and adaptations to severe droughts. This knowledge is important for understanding possible impacts on humans from the expected increased frequency and severity of droughts within the Czech Lands in future related to recent global warming.

Acknowledgements

Supported by project No. CZ.1.07/2.3.00/20.0248 "InterDrought" (L. Dolák, L. Řezníčková) and Czech Science Foundation project No. GA13-19831S (R. Brázdil, H. Valášek). Tony Long helped with the English translation.

References

Brzobohatý D (2003) Ceny a mzdy v zemědělství. Slavičín Municipal Museum, Slavičín.

Heim RR (2002) B. Am. Meteorol. Soc. 83, 1149–1165.

Hofmann G (1984) Metrologická příručka pro Čechy, Moravu a Slezsko do zavedení metrické soustavy. State Regional Archive in Pilsen and Šumava Museum in Sušice, Pilsen.

Řezníčková L, Brázdil R, Kotyza O, Valášek H (2015) Documentary evidence as a source of data for studying droughts in the Czech Lands. This volume.

Town of Olešnice (2004) Pamětní kniha městečka Olešnice. Town of Olešnice, Olešnice.

Archival sources

S1 MZA Brno, fonds F 281 Velkostatek Uherský Brod (1351)1580–1945.

S2 State District Archives (SOkA) Blansko, fonds K 19 Doubravice Parish Office, Doubravice Local Protocols 1770–1834.

S3 SOkA Blansko, fonds K 22 Křetín Parish Office, Křetín Local Protocols 1844–1984.

S4 SOkA Blansko, fonds K 37 Sloup Parish Office, Chronicle 1812–1917.

S5 SOkA Blansko, fonds K 38 Sulíkov Parish Office, Chronicle 1786–1991.

S6 SOkA Blansko, fonds K 39 Svitávka Parish Office, Chronicle 1929.

S7 SOkA Blansko, fonds K 44 Žďárná Parish Office, Chronicle 1775–1974.

S8 SOkA Břeclav, fonds Přítluky Municipal Archive, Přítluky Memorial Book 1709–1934.

S9 SOkA Hodonín, fonds Žádovice National School, Žádovice School Chronicle 1880–1940.

S10 SOkA Kroměříž, fonds B-a 21 Dřínov Municipal Archive, Memorial Book for Obec Dřinowskau from 1841, 1841–1874.

S11 SOkA Třebíč, fonds Číchov National School, Číchova School Chronicle 1888–1960.

S12 SOkA Uherské Hradiště, fonds Podolí Municipal Archive, Town Chronicle 1890–1933.

S13 SOkA Vyškov, fonds Milešovice Basic School, Milešovice School Chronicle 1880–1981.

Drivers of soil moisture trends in the Czech Republic between 1961 and 2012

Trnka, M.,[1,2,*], Brázdil, R.[2,3], Balek, J.[1], Semerádová, D.[2], Hlavinka, P.[1,2], Možný, M.[1,4], Štěpánek, P.[2,5], Dobrovolný, P.[2,3], Zahradníček, P.[2,5], Dubrovský, M.[2,6], Eitzinger, J.[2,7], Fuchs, B.[8], Svoboda, M.[8], Hayes, M.[8], Žalud, Z.[1,2]

[1]*Department of Agrosystems and Bioclimatology, Mendel University in Brno, Zemědělská 1/1665, 613 00, Brno, Czech Republic*

[2]*Global Change Research Centre, Bělidla 986/4a, 603 00 Brno, CZ*

[3]*Institute of Geography, Masaryk University, Kotlářská 267/2, 611 37 Brno, Czech Republic*

[4]*Doksany Observatory, Czech Hydrometeorological Institute, 411 82 Doksany, Czech Republic*

[5]*Brno Regional Office, Czech Hydrometeorological Institute, Kroftova 43,616 67 Brno, Czech Republic*

[6]*Institute of Atmospheric Physics, Czech Academy of Sciences, Boční II 1401, 141 31 Prague, Czech Republic*

[7]*Institute of Meteorology, University of Natural Resources and Life Sciences (BOKU), Peter-Jordan-Straße 82, 1190 Vienna, Austria*

[8]*National Drought Mitigation Center, University of Nebraska-Lincoln, 3310 Holdrege Street, 68583 Lincoln, NE, USA*

[*]*author for correspondence; email: mirek_trnka@yahoo.com*

ABSTRACT

Soil moisture dynamics and their temporal trends in the Czech Republic are forced by various drivers. Our analysis of temporal trends indicates that shifts in drought severity between 1961 and 2012 and especially in the April, May, and June period, which displayed such results as a 50% increase in drought probability during 1961–1980 in comparison to 2001–2012. We found that increased global radiation and air temperature together with decreased relative humidity (all statistically significant at $p < 0.05$) led to increases in the reference evapotranspiration in all months of the growing season; this trend was particularly evident in April, May, and August, when more than 80% of the territory displayed an increased demand for soil water. These changes, in combination with the earlier end of snow cover and the earlier start of the growing season (up to 20 days in some regions), led to increased actual evapotranspiration at the start of the growing season that tended to deplete the soil moisture earlier, leaving the soil more exposed to the impacts of rainfall variability. These results support concerns related to the potentially increased severity of drought events in Central Europe. The reported trend patterns are of particular importance with respect to expected climate change, given the robustness and consistency of the trends shown and the fact that they can be aligned with the existing climate model projections.

INTRODUCTION

After floods, droughts represent the next most disastrous natural events in the Czech Republic (Brázdil et al. 2007). A study by Brázdil et al. (2013) analyzed droughts in the Czech lands between 1090 and 2012 based on documentary and instrumental data and concluded that despite great variability since 1501, the frequency of drought occurrence since the 1990s is unusual. There are strong concerns that the increase in drought frequency may neutralize the expected positive effects of a longer growing season, decrease the productivity of ecosystems, or change the conditions for key soil processes. These concerns were strengthened recently by

Trnka et al. (2015), who confirmed significant shifts in drought severity during the 1961–2012 period over the territory of the Czech Republic using newly available high-resolution climate datasets. Although there were no statistically significant trends in precipitation during the 1961–2012 period (Brázdil et al. 2012), statistically significant trends toward lower soil moisture content were present, most notably during the May–June period. The present study explores the causes of the changes in modeled soil moisture content in the Czech Republic during 1961–2012, including how they compare with newly available observations and to what extent these changes agree with larger-scale assessments. The current study utilizes the datasets considered by Trnka et al. (2015) in combination with newly available long-term pan evaporation data.

MATERIALS AND METHODS

The meteorological, soil, land cover, and soil moisture database used in this study was produced as a result of joint projects (listed in the Acknowledgements) by the Czech Hydrometeorological Institute, the Global Change Research Centre, and Mendel University in Brno. The climate data include daily minimum and maximum temperatures, sums of global radiation (combining directly measured shortwave radiation and sunshine duration hours), precipitation totals, and mean wind speed and air humidity. These data were homogenized and assessed for consistency using the AnClim and ProClim software packages (Štěpánek et al. 2009). The study area covers 268 climatological stations and 878 rain gauge stations across the Czech Republic. Finally, the data were interpolated into a 500 m grid.

The principal method used to determine drought (described in detail by Trnka et al. 2015) relies on an analysis of the daily root-zone soil moisture content (up to 1.3 m deep or the maximum rooting depth). This value was calculated for each 500 m grid using the SoilClim model based on the Allen et al. (1998) model, which was partially modified and validated by Hlavinka et al. (2011) and further tested by Trnka et al. (2015). In this study, we first compared trends in the estimated reference evapotranspiration (ET_r; one of the principal driving forces in the overall soil moisture calculation) with observed pan evaporation values. Next, we focused on an analysis of trends in the key predictors of ET_r (i.e., global radiation, air temperature, relative air humidity, and wind speed) as well as snow-cover parameters and dates of key phenophases. In each case, the consistency of the trend toward increasing evapotranspiration (and thus affecting soil water content) was considered. The significance of these trends during 1961–2012 was assessed using Spearman's rank correlation coefficient and was tested by regression analysis using a 0.05 significance level. To avoid the existing autocorrelation that is intrinsic to some of the analyzed data, the trends were separately evaluated for individual months or periods.

RESULTS

Drying trends and key driving factors' contributions are documented in Table 1. The drying trends were strongest in May (44.1% of territory displaying statistically significant trends) followed by June (36.4%). The negative soil moisture trends are most pronounced in grids with grasslands and meadows (results not shown). Overall, the drying trends are strongest during the April–June period. A similar but less pronounced trend was found in the eastern part of the Czech Republic during the July–September period. In summary, as soil water reserves become gradually depleted, actual evapotranspiration (ET_a) values become more dependent on rainfall and no significant trend (or even decrease in ET_a) can be observed. The character of the ET_a trend depends largely on the ratio between the ET_r and precipitation. In regions with relatively ample rain, ET_a has increased significantly (at higher elevations) over a longer period of the growing season in comparison to ET_a

values in regions where precipitation is lower (thus limiting available soil moisture and therefore ET_a). The relationships among the key drivers of May–June drying are qualitatively assessed in Fig. 1.

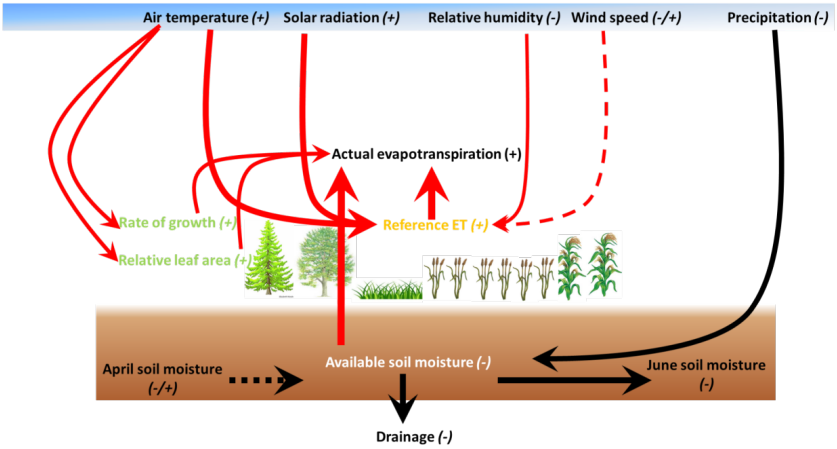

Fig. 1: *Scheme showing the key drivers of soil water content during May in the Czech Republic for the 1961–2012 period. The main climatic and crop parameters are considered in the scheme. Red arrows illustrate increases and black arrows decreases in the respective factors. Line width displays relative importance. Solid lines represent statistically significant trends for a given factor over more than two-thirds of the region studied and broken lines represent inconclusive tendencies.*

Table 1: *Proportion (%) of territory of the Czech Republic with statistically significant ($\alpha = 0.05$) positive (+) and negative (-) trends conducive to* **drier***/wetter conditions in individual months from March to September during 1961–2012. Includes all land uses apart from urban areas and water bodies.*

Month	AWR		AWR1		ET_r		ET_a		SRAD		T_{avg}		Wind		RH		Rain	
	(-)	(+)	(-)	(+)	(+)	(-)	(+)	(-)	(+)	(-)	(+)	(-)	(+)	(-)	(-)	(+)	(-)	(+)
March	**0.3**	32.4	**0.1**	30.2	**26.8**	0.0	**59.4**	0.0	**5.8**	0.4	**20.0**	0.0	**10.5**	34.7	**65.1**	0.3	**0.0**	1.9
April	**5.1**	2.5	**10.7**	1.3	**80.4**	0.0	**43.5**	0.1	**51.3**	0.1	**73.9**	0.0	**8.5**	44.7	**81.5**	0.0	**14.9**	0.0
May	**44.1**	0.4	**55.5**	0.3	**97.5**	0.0	**44.7**	1.5	**83.1**	0.0	**99.1**	0.0	**14.6**	42.7	**86.8**	0.1	**2.1**	0.0
June	**36.3**	0.3	**15.6**	0.4	**12.3**	0.0	**13.1**	3.5	**0.8**	0.9	**82.6**	0.0	**11.0**	47.5	**36.5**	0.6	**3.6**	0.0
July	**2.3**	2.5	**0.0**	13.1	**18.2**	0.0	**27.2**	0.1	**2.2**	0.2	**96.1**	0.0	**20.4**	36.3	**24.4**	1.7	**0.0**	48.3
August	**0.8**	0.7	**0.2**	0.4	**96.3**	0.0	**7.5**	2.1	**63.5**	0.0	**99.2**	0.0	**12.0**	44.9	**46.0**	0.1	**0.1**	0.1
September	**0.7**	1.1	**0.0**	0.4	**0.1**	0.2	**0.2**	13.3	**0.1**	0.8	**0.0**	0.2	**22.4**	32.8	**3.3**	2.7	**0.0**	3.4

AWR: relative saturation of the whole soil profile, AWR1: relative saturation of the topsoil, ET_r: reference evapotranspiration, ET_a: actual evapotranspiration, SRAD: global radiation, T_{avg}: mean air temperature, Wind: wind speed, RH: relative humidity, Rain: precipitation sum.

DISCUSSION

This study offers a detailed analysis of the factors that drive observed drying of the Central European landscape and identifies possible causes and consequences of these trends. These results represent clear progress in comparison to previous analyses (e.g., Brázdil et al. 2007, Potop et al. 2012) that relied on simpler drought indices. Our approach enables us to account for (i) changes in the key driving elements apart from temperature and precipitation, i.e., global radiation, wind speed, and air humidity; (ii) changes in snow cover and snowmelt-based recharge of soil moisture before the start of the growing season; (iii) changes in the rates and timing of phenological development of vegetation cover, including the effect these changes have on evapotranspiration; and (iv) location characteristics (i.e., slope, aspect, soil properties, and the influence of groundwater). Although the reported soil moisture trends are worrisome, one may argue that the presented trends in soil moisture are based on modeled results rather than actual observations. However, our findings agree well with measured soil moisture data (Trnka et al. 2015) and also with the observed trends in evaporation analyzed in this study and independent station-based analyses (Brázdil et al. 2009). We found that soil moisture during the May–June period has decreased on average by 60 mm in the past 50 years, with certain locations reporting reductions of more than 100 mm within the first 1.3 m of their soil profile.

A decrease in soil moisture in May and June in the Czech Republic should be of great concern because these months influence the key period of the growing season for this region. Moreover, the fact that the April–June period of 2001–2012 displayed a 50% increase in drought probability compared with that of 1961–1980 is alarming. The probability of extreme drought was also found to be increasing significantly for the Czech territory, which is further supported (or at least not contradicted) by the results of several large-scale assessments.

Acknowledgement

Analyses supported by project No. CZ.1.07/2.3.00/20.0248 "Building up a multidisciplinary scientific team focused on drought" and project No. LD13030. PH supported by the CzechAdapt project from the EEA Grants. RB, MT, and PD supported by project nos. GAP209/11/0956 and 13-04291S/P209 of the Czech Science Foundation. PS, MM and ZZ supported by project No. QJ1310123 of the National Agency for Agricultural Research. We thank Deborah Wood (National Drought Mitigation Center, University of Nebraska-Lincoln) for editing the final version of the text.

References

Allen RG, Pereira LS, Raes D et al. (1998) Crop Evapotranspiration. Guidelines for Computing Crop Water Requirements. FAO Irrigation and Drainage Paper No. 56. Food and Agriculture Organization of the United Nations, Rome.

Brázdil R, Kirchner K, Březina L et al. (2007) Vybrané přírodní extrémy a jejich dopady na Moravě a ve Slezsku. Masaryk University, Czech Hydrometeorological Institute, and Institute of Geonics, Czech Academy of Sciences, Brno, Prague, Ostrava.

Brázdil R, Chrom K, Dobrovolný P et al. (2009) Int. J. Climatol. 29, 223–242.

Brázdil R, Zahradníček P, Pišoft P et al. (2012) Theor. Appl. Climatol. 110, 17–34.

Brázdil R, Dobrovolný P, Trnka M et al. (2013) Clim. Past 9, 1985–2002.

Hlavinka P, Trnka M, Balek J et al. (2011) Agric. Water Manag. 98, 1249–1261.

Potop V, Možný M, Soukup J (2012) Agric. For. Meteorol. 156, 121–133.

Štěpánek P, Zahradníček P, Skalák P (2009) Adv. Sci. Res. 3, 23–26.

Trnka M, Brázdil J, Balek D et al. (2015) Int. J. Climatol. doi: 10.1002/joc.4242.

Influence of variable weather on incident solar radiation and its spectral composition in the Ostrava region, Czech Republic

Opálková, M.[1,*], Robson, T. M.[2], Navrátil, M.[1], Špunda, V.[1,3]

[1]*Department of Physics, University of Ostrava, Chittussiho 10, 71000 Ostrava, Czech Republic*
[2]*Department of Biosciences, University of Helsinki, Viikinkaari 1, 00790 Helsinki, Finland*
[3]*Global Change Research Centre, Bělidla 986/4a, 60300 Brno, Czech Republic*
[*]*author for correspondence; email: opalkovamarie@seznam.cz*

ABSTRACT

Incident solar radiation is influenced by many factors, including distance from the equator, altitude, time of year, and season. Absorption of radiation and its scattering are connected with the properties of atmospheric compounds. Cloud cover and air pollution are connected with tropospheric properties.

Using our data, the influence of weather changes on the dose of solar irradiance reaching the Earth's surface and its spectral composition are described. Solar radiation components were measured continuously by a system of sensors situated in the Botanical Garden of the University of Ostrava, Czech Republic. Data for 2014 were chosen for analyses. Days were divided into categories of sunny days and cloudy days according to weather conditions and daily radiation patterns. Percent differences in received solar radiation between sunny and cloudy days were calculated for eight months (Jan, Feb, Mar, Jun, Jul, Aug, Sep, and Dec). Differences in received solar radiation between clean and polluted days were calculated for sunny and cloudy days in December 2014. Mean incident solar radiation during cloudy days was reduced by 61% from the value for sunny days (in summer months) and by 64% from the value for sunny days in winter months. The largest influence of clouds on received solar radiation was during September and the smallest was during June. There was a reduction in incident solar radiation caused by the atmospheric pollutant PM_{10} during winter months. This reduction amounted to 10% during sunny days and 21% during cloudy days for December 2014.

Clouds significantly reduced incident solar radiation as did the air pollutant PM_{10}, but there were probably other factors also contributing to the reduction in incident solar radiation.

INTRODUCTION

Solar radiation passing through the atmosphere is mainly influenced by absorption, scattering, and tropospheric conditions. Geographical location, altitude, solar elevation angle, and time of year are other factors influencing incident solar radiation (Paul & Gwynn-Jones 2003). Cloud cover, especially its range and distribution (Oliphant et al. 2011), and air pollution, especially atmospheric turbidity (Jacovides et al. 1997), appreciably affect incident solar radiation. Cloud permeability is the most important and most changeable factor influencing incident radiation (World Meteorological Organization 2011). Atmospheric pollutants not only cause a reduction in total solar irradiance, they also change the proportions of direct and diffuse radiation (Robaa 2009) and affect the spectral composition of radiation (Jacovides et al. 1997). UVB radiation is mainly absorbed by ozone (O_3) and sulphur dioxide (SO_2). In contrast, UVA radiation is absorbed by atmospheric nitrogen dioxide (NO_2), which has no influence on the transmission of UVB. Other chemicals which absorb UV radiation are contained in organic carbon from motor vehicles or biomass burning (World Meteorological Organization 2011).

The Ostrava region is subject to serious air pollution episodes, and for this reason we have studied the spectral

composition of incident radiation in this area. It is useful to determine how much and in what way solar radiation is influenced by weather conditions and air pollution, since in addition to human health this could have an impact on plant photosynthesis and agriculture. In this study, we estimated how much incident solar radiation was decreased during cloudy days in this region during one year and how much it was decreased during those severe air pollution episodes that occurred during the winter months.

MATERIALS AND METHODS

Characteristics of the study area

The Ostrava region is situated in the north-eastern Czech Republic. This area's mean altitude is 244 m a.s.l. and the countryside is flat or slightly undulating (Weissmannová 2004). According to the Köppen–Geiger classification, this area falls within the Dfb climate subtype (Peel et al. 2007). Mean annual air temperature is 8.4°C (mean 18.3°C in July, the warmest month). Mean annual precipitation is about 700 mm (average 95.6 mm in July). This area has been heavily influenced by emissions from industrial factories, but the situation has improved since 1992 (Weissmannová 2004).

Data collection and acquisition

The system of sensors for solar radiation measurement is situated in the Botanical Garden of the University of Ostrava in Slezská Ostrava (49°49.64873'N, 18°19.56197'E). It contains seven sensors which measure radiation at wavelengths of 660 and 730 nm, UVA and UVB radiation (Skye, UK), total energy irradiance of solar radiation within 400–1100 nm (global radiation), and wavelength intervals of: 400–700 nm (photosynthetically active radiation, PAR), 510–700 nm, and 600–700 nm (EMS Brno, Czech Republic). Spectral parts of PAR were calculated from the above mentioned interval measurements: blue 400–510 nm, green 510–600 nm, and red 600–700 nm. Each system contains other sensors to measure air temperature, air humidity (EMS 33R, EMS Brno), and precipitation (type 370C/372C, MetOne Instruments, USA).

Data analyses

Analysis included 1-hour averages of solar irradiance for those hours when solar elevation angles were higher than 5°. Weather and air pollution data were combined with radiation data. Days were divided into the categories of sunny days and cloudy days according to weather conditions and daily radiation patterns. Partly cloudy days were removed from the analyses. In winter months, days were divided into the categories of clear days and polluted days according to the measured value for PM_{10}, with the limit for a clean day of 50 μg m^{-3} (mean per day). Mean daily sum of hourly averages for sunny and cloudy days was calculated for several months during 2014 (Jan, Feb, Mar, Jun, Jul, Aug, Sep, Dec) and for clean and polluted days, both sunny and cloudy, in the winter months of 2014. Percentage differences in received solar radiation between sunny and cloudy days were calculated. Differences in received solar radiation between clean and polluted days, both sunny and cloudy, were also calculated.

RESULTS

During cloudy days, all spectral bands of solar radiation were reduced on average by 65% in March, by 58% in June, by 71% in September, and by 65% in December in comparison to sunny days in those months. Overall mean reduction was by 65%. Spectral irradiance at wavelength 730 nm showed the largest reductions from clouds, except during December when the smallest reduction in 730 nm radiation occurred. The smallest reduction in UVA radiation occurred in June (Fig. 1).

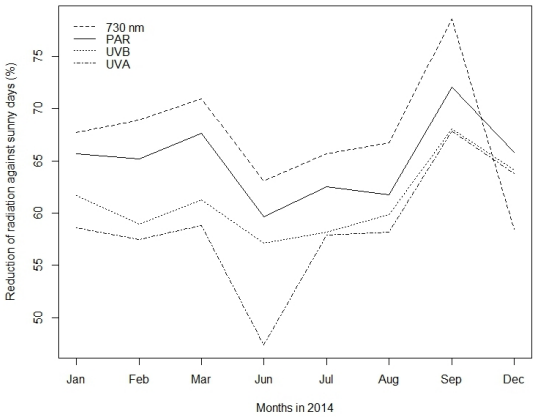

Fig. 1: *Reduction in selected spectral bands of incident solar radiation during cloudy days compared with sunny days in 2014. The smallest reduction occurred in June for UVA. The largest reduction occurred in September for 730 nm.*

There was a reduction in incident solar radiation caused by the atmospheric pollutant PM_{10} during winter months. This reduction amounted to 10% during sunny days and 21% during cloudy days for December 2014. During sunny days, the smallest reduction was in UVA and UVB radiation and the largest reduction was that of global radiation. During cloudy days, the smallest reduction was for 730 nm and the highest reduction was in UVB radiation. There were exceptions, however, such as the reduction in UVA caused by PM_{10} in January 2014 which recorded different values: 30% for sunny days and 24% for cloudy days (Fig. 2).

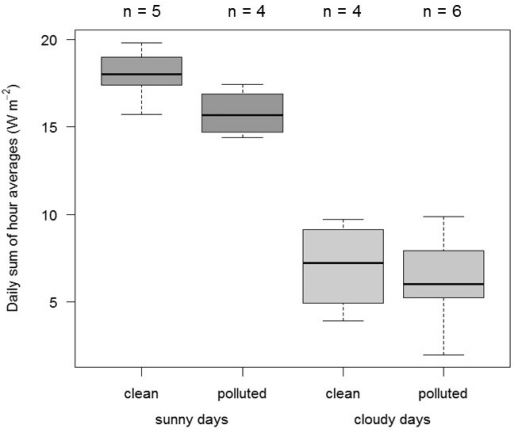

Fig. 2: *Daily sum of hourly averages for UVA radiation on clean and polluted days, both sunny and cloudy, in January 2014. During sunny days, a bigger difference between clean and polluted days was evident. The number of days in each category is given at the top of the figure. Days which were partially cloudy were excluded from the analysis.*

DISCUSSION

Despite the fact that atmospheric pollution is a serious problem in the Ostrava region, there have been no similar studies on the influence of air pollutants on solar radiation in our region. Most research is focused on the effect of pollution on human health, especially among children. It has been known for some time that cases of asthma and other respiratory illnesses occur in children living in Ostrava-Radvanice, which has the highest atmospheric concentration of carcinogenic polycyclic aromatic hydrocarbons of anywhere in the European Union (Sram et al. 2013).

It is generally known that clouds cause a significant reduction in incident solar radiation (Pyrina et al. 2013). The spectral composition of incident PAR has been studied during clear and cloudy days in Bílý Kříž, Beskid Mountains (Navrátil et al. 2007). In the present study, we calculated that mean incident solar radiation was reduced on cloudy days on average by 65% compared with that on sunny days.

Air pollutants also cause substantial reductions in solar radiation (Calinoiu et al. 2013). We found that PM_{10} is able to decrease incident solar radiation but the extent of this reduction was quite variable. This leads us to conclude that there are probably more factors which are related to the reduction in incident radiation. We intend to test this by assessing the contributions of other atmospheric pollutants to this reduction in a more detailed analysis.

In future studies, we would like to create models of solar radiation during clear skies in cooperation with the University of Helsinki and the Finnish Meteorological Institute, which would enable us to compare modelled data with measured data. We also intend to make more detailed analyses of the influence of specific aspects of the weather and atmospheric pollutants on incident solar radiation.

Acknowledgement

Supported by projects No. SGS09/PřF/2015 and COST CZ LD14005. Analysis was performed in the R open source environment, and we thank Pedro Aphalo for his help in using the Photobiology R packages.

References

Calinoiu D, Paulescu M, Ionel I et al. (2013) Energy Convers. Manag. 70, 76–82.

Jacovides CP, Timbios F, Asimakopoulos DN et al. (1997) Agric. For. Meteorol. 87, 91–104.

Navrátil M, Špunda V, Marková I et al. (2007) Trees 21, 311–320.

Oliphant AJ, Dragoni D, Deng B et al. et al. (2011) Agric. For. Meteorol. 151, 781–791.

Paul ND, Gwynn-Jones D (2003) Trends Ecol. Evol. 18, 48–55.

Peel MC, Finlayson BL, McMahon TA (2007): Hydrol. Earth Syst. Sci. Discuss. 4, 439–473.

Pyrina M, Hatzianastassiou N, Matsoukas C et al. (2015) Atmos. Res. 152, 14–28.

Robaa SM (2009) Energy Convers. Manag. 50, 194–202.

Sram RJ, Binkova B, Dostal M et al. (2013) Int. J. Hyg. Environ. Health. 216, 533–540.

Weissmannová H (2004) Ostravsko: Chráněná území ČR, volume X. Nature Conservation Agency of the Czech Republic and EkoCentrum Brno, Prague.

World Meteorological Organization (2011) Scientific Assessment of Ozone Depletion: 2010, Global Ozone Research and Monitoring Project–Report No. 52. Geneva, Switzerland.

LINCOLN – an algorithm for filtering daily NDVI MODIS data and deriving the start of the season

Bohovic, R.[1,2,*], Hlavinka, P.[1,3], Semerádová, D.[1,3], Bálek, J.[1,3], Tadesse, T.[4], Hayes, M.[4], Wardlow, B.[5], Trnka, M.[1,3]

[1]*Global Change Research Centre, Bělidla 986/4a, 603 00 Brno, Czech Republic*

[2]*Institute of Geography, Masaryk University, Kotlářská 2, 611 37 Brno, Czech Republic*

[3]*Institute of Agrosystems and Bioclimatology, Mendel University in Brno, Zemědělská 1, 613 00 Brno, Czech Republic*

[4]*National Drought Mitigation Center, University of Nebraska-Lincoln, 3310 Holdrege Street, 68583 Lincoln, NE, USA*

[5]*Center for Advanced Land Management Information Technologies, School of Natural Resources, University of Nebraska-Lincoln, 3310 Holdrege Street, 68583 Lincoln, NE, USA*

[*]*author for correspondence; email: geo.roman@gmail.com*

ABSTRACT

Monitoring drought has become an important tool for farmers and agriculture decision makers. This has increased efforts to create a monitoring system using satellite data that could provide an independent and current source of real information on vegetation condition. The aim of this study was to develop an algorithm for processing Normalized Difference Vegetation Index (NDVI) data from the Moderate Resolution Imaging Spectroradiometer. A software utility called LINCOLN was developed for this purpose. Its filtering output was further processed to yield a start of the season (SOS) metric. Different settings of the utility were tested and correlated to such phenological ground observations as the emergence of spring barley and the beginning of leaf sheath elongation in winter wheat. There was higher correlation observed in the case of winter wheat, probably due to its weaker dependence on crop sowing date. The matrix of coefficients of determination was applied to determine the optimal settings for the LINCOLN filter. The optimal absolute threshold NDVI value for SOS was set to 4,500.

INTRODUCTION

One of the major current impacts of climate change in the Czech Republic is seen in the occurrence of drought events. These events are of crucial importance in the agricultural sector. In addition to direct measurements of soil water content, drought can be monitored also indirectly through observing vegetation conditions. Satellite data might offer useful information regarding the impact of stress (e.g., drought) on plants even at a large scale. For this purpose, spatial and temporal resolutions of source data are critical factors. The aim of this study was to develop and test a procedure for filtering and processing a daily satellite signal that would otherwise include lots of missing or invalid values as a result of atmospheric conditions (mostly clouds). Our results can be further employed in developing a drought monitoring system with near-real-time vegetation warning signals that would be independent of ground measurements.

MATERIALS AND METHODS

The Normalized Difference Vegetation Index (NDVI) has been computed daily at a 250 × 250 m resolution from red and near infra-red reflectance spectral bands of Moderate Resolution Imaging Spectroradiometer

(MODIS) time series. MODIS is an instrument on board the Terra and Aqua satellites. Its NDVI data of the highest quality flag from 2000–2013 have been processed for vegetation monitoring (Tucker et al. 2005). For the purpose of our calculations, original 250 × 250 m resolution data were masked for arable land and aggregated to a 5 × 5 km grid. A 16-day MODIS NDVI composite product was used for comparison.

Phenology phases of different plants were collected from meteorological stations in the Czech Republic. As defined by their observation methodology, ground phenology metrics are based on individual plant characteristics. For that reason, we selected agricultural crops that are mostly grown as single-crop monocultures, which correspond to ground observation reference. Two early phases of different cereals at the beginning of the year were analyzed: the emergence of spring barley and the onset of leaf sheath elongation in winter wheat. Altogether, we identified 21 sites with consistent observational data with at most 2 missing values for each crop in the 2000 to 2012 time period. These sites are spread all over the agricultural land of the Czech Republic.

To filter daily NDVI data, a three-step algorithm was developed and tested. A software utility was implemented that was named after the city where major design decisions were discussed: LINCOLN. It uses csv files as time-series input. It has the capacity to handle missing data and enables setting different parameters: the threshold for the minimum NDVI value and lower (LowCoef) and upper (UpCoef) buffer coefficients. Fourteen different combinations of input parameters were computed and evaluated in order to determine the optimal settings for the software. Detailed iterative steps of LINCOLN are described in the Results section. An example of filtered NDVI outputs is depicted in Fig. 1.

To evaluate the software's performance, time series were further processed with TIMESAT software (Jönsson & Eklundh 2002, Jönsson & Eklundh 2004). This software served not only as a smoothing tool for output comparison, but also as a means for computing the start of the season (SOS). Out of three filters available, the Savitzky–Golay filter (Chen et al. 2004) was chosen for its ability to adapt to rapid changes in NDVI course, which makes it suitable for monitoring drought events. All data were processed with three different settings of the Savitzky–Golay filter. The first setting (set1) contains LINCOLN outputs without significant changes generated by TIMESAT, which was utilized mainly in order to calculate the SOS metric. Settings set2 and set3 exert additional smoothing on time series, balancing best fit for small changes and rough NDVI course while omitting noise values.

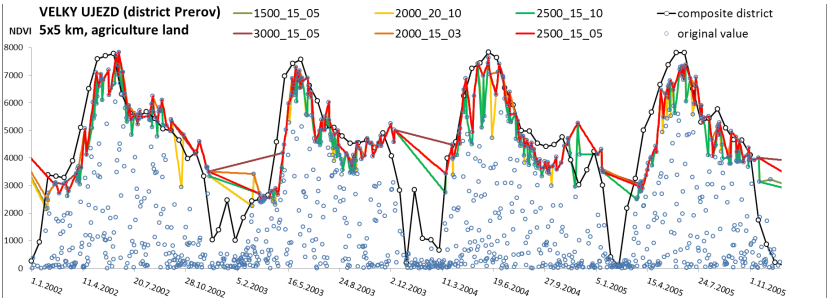

Fig. 1: *Example of NDVI data time series (original and filtered by LINCOLN utility with 6 different settings). 16-day temporal resolution composite data for the district are added.*

To calculate SOS, two approaches were adopted: absolute and relative threshold values. According to the former, SOS is defined as the time of year when the NDVI reaches the NDVI threshold value. Relative threshold is expressed as a certain ratio of the NDVI's seasonal amplitude. SOS was computed for 4 different absolute threshold values (4,000, 4,500, 5,000, and 5,500) and 4 relative threshold values (0.25, 0.35, 0.45, and 0.5).

Coefficients of determination (R^2) of the linear correlation between remotely sensed SOS results and phenological ground observations were calculated in order to evaluate the LINCOLN algorithm's performance, its settings, and SOS derivation parameters. The robust resulting matrix comprises 91,728 possible correlations for both crops separately, containing 14 LINCOLN utility settings in columns and 3 TIMESAT settings and 8 SOS values in 24 rows. Each cell represents mean R^2 for a given setting across the 21 ground observation sites over 13 vegetation seasons. Only reasonable data ranges were taken into account. Subsets of matrices for winter wheat and spring barley are outlined in Table 1.

RESULTS

This work's most important achievement is the development of a filtering algorithm and its implementation as a software utility called LINCOLN. The computation is described and summarized in the following steps:

1. Setting the minimum NDVI value threshold (→ RAW1)
   - Values of original data (RAW) under the threshold level (could be set), which are often influenced by cloud cover, are neglected.
2. Retaining higher values (from RAW1) that better represent a clear signal
   - For each day the 1st, 2nd and 3rd highest values in a +/- 7-day window are selected.
   - Weighted mean according to temporal distance (day = 100%, day ± 7 = 30%) is computed for each day → RAW2.
3. Removing outliers
   - Calculating Delta (normalized difference between RAW & RAW2).
   - Computing standard deviation (STDV) of Delta for each site (pixel).
   - Dismissing days where Delta is out of the buffer zone (-STDV*LowCoef > Delta > STDV*UpCoef).
   - When Delta is in buffer zone RAW1 value is accepted → RAW3
4. Daily linear interpolation of RAW3 → LINCOLN output time series

Table 1: *Mean correlation coefficients of determination (R^2) between ground observations of both spring barley emergence and beginning of leaf sheath elongation in winter wheat at 21 meteorological sites in Czech Republic during 2000–2012 and SOS computed from satellite data processed using LINCOLN in different settings (columns) and TIMESAT and SOS thresholds (rows).*

	Spring barley							*Winter wheat*						
lower env.	*0.5*	*0.3*	*0.5*	*1.0*	*0.5*	*1.0*	*0.5*	*0.5*	*0.3*	*0.5*	*1.0*	*0.5*	*1.0*	*0.5*
upper env.	*1.5*	*1.5*	*1.5*	*1.5*	*1.5*	*2.0*	*1.5*	*1.5*	*1.5*	*1.5*	*1.5*	*1.5*	*2.0*	*1.5*
min. thresh.	*1,500*	*2,000*	*2,500*	*2,500*	*3,000*	*3,000*	*3,500*	*1,500*	*2,000*	*2,500*	*2,500*	*3,000*	*3,000*	*3,500*
set1, 35%	0.12	0.12	0.12	0.12	0.10	0.15	0.11	0.21	0.25	0.32	0.26	0.33	0.29	NA
set1, 45%	0.11	0.12	0.12	0.14	0.12	0.22	0.19	0.25	0.22	0.25	0.22	0.29	0.31	NA
set1, 4,000	0.14	0.17	0.20	0.14	0.15	0.19	0.22	0.25	0.31	0.32	0.26	0.33	0.35	0.17
set1, 4,500	0.13	0.14	0.15	0.11	0.16	0.11	0.15	0.29	0.37	0.38	0.35	0.38	0.38	0.27
set1, 5,000	0.12	0.13	0.15	0.14	0.15	0.14	0.16	0.30	0.32	0.36	0.33	0.35	0.37	0.43
set3, 50%	0.12	0.11	0.11	0.19	0.12	0.21	0.13	0.25	0.22	0.29	0.25	0.32	0.28	0.22
set3, 4,000	0.18	0.23	0.16	0.18	0.22	0.22	0.28	0.26	0.33	0.32	0.31	0.31	0.38	NA
set3, 4,500	0.13	0.15	0.14	0.16	0.18	0.15	0.12	0.30	0.36	0.38	0.30	0.39	0.37	0.27
set3, 5,500	0.08	0.11	0.12	0.15	0.11	0.13	0.14	0.35	0.34	0.37	0.35	0.34	0.37	0.23

Since the development of this algorithm was accompanied by profound testing of different settings of LINCOLN and SOS derivation thresholds, defining a coefficient of determination matrix was crucial for their evaluation. For simplification, only a subset of the matrices is displayed in the table, comprising only lines and columns with the most significant R^2 values.

Using a LINCOLN filter proved to be favorable for noisy daily MODIS NDVI, except for winter-season data, which are often unreliable when vegetation is very limited. In some cases, additional filtering with TIMESAT (set3) yielded slightly higher coefficients of determination than were obtained for LINCOLN alone (set1). In general, LINCOLN itself proved to be sufficient for data filtering, with an optimal minimum threshold of 2,500, upper coefficient of 1.5, and lower coefficient of 0.5.

Correlations for spring barley were generally lower than were correlations for winter wheat. This could have been caused by the unstable winter signal (many missing values or data outside reasonable boundaries) and the strong influence of crop sowing dates on barley growth. Satisfactory results were achieved for winter wheat, where R^2 was 0.38 on average, with values around 0.7 in some sites. Refined results were obtained using the absolute threshold SOS method. Of the values tested, 4,500 gave the best performance.

DISCUSSION

Visual evaluation of filtered time series together with correlation with ground data proved the ability of the LINCOLN filter to yield time series with solid temporal resolution applicable for daily data and surpassing the composite MODIS NDVI product. However, the inaccuracy of the winter signal needs to be addressed in further analysis. Since the testing of LINCOLN showed the redundancy of the TIMESAT filter for additional smoothing, it would be possible to extend the use of our utility alone to process raster data and derive the SOS. In order to bring LINCOLN into operational use for monitoring vegetation conditions, the window size from the second step of the aforementioned algorithm needs to be adapted to backward use only (as future values are not known in real time operation).

Settings considered as optimal for operational monitoring of drought using LINCOLN (minimum threshold 2,500) and SOS (absolute NDVI threshold 4,500) have been chosen with respect to the specific agricultural land. It remains a question whether other land-cover classes would require different optimal settings. This needs to be investigated further.

Acknowledgement

Funded by project No. CZ.1.07/2.3.00/20.0248 of the Ministry of Education, Youth and Sports "Building up a multidisciplinary scientific team focused on drought."

References

Chen J, Jönsson P, Tamura M et al. (2004) Remote Sens. Environ. 91, 332–344.

Jönsson P, Eklundh L (2002) IEEE Trans. Geosci. Remote Sens. 40, 1824–1832.

Jönsson P, Eklundh L (2004) Comput. Geosci. 30, 833–845.

Tucker CJ, Pinzón JE, Brown ME et al. (2005) Int. J. Remote Sens. 26, 4485–4498.

White MA, de Beurs KM, Didan K et al. (2009) Glob. Change Biol. 15, 2335–2359.

Reliability of regional crop yield predictions in the Czech Republic based on remotely sensed data

Hlavinka, P.[1,2,*], Semerádová, D.[1,2], Balek, J.[1,2], Bohovic, R.[1,3], Žalud, Z.[1,2], Trnka, M.[1,2]

[1]*Global Change Research Centre, Bělidla 986/4a, 603 00 Brno, Czech Republic*

[2]*Institute of Agrosystems and Bioclimatology, Mendel University in Brno, Zemědělská 1/1665, 613 00, Brno, Czech Republic*

[3]*Institute of Geography, Masaryk University, Kotlářská 267/2, 611 37 Brno, Czech Republic*

[*]*author for correspondence; email: hlavinka.peta@gmail.com*

ABSTRACT

Vegetation indices sensed by satellite optical sensors are valuable tools for assessing vegetation conditions including field crops. The aim of this study was to assess the reliability of regional yield predictions based on the use of the Normalized Difference Vegetation Index and the Enhanced Vegetation Index derived from the Moderate Resolution Imaging Spectroradiometer aboard the Terra satellite. Data available from the year 2000 were analysed and tested for seasonal yield predictions within selected districts of the Czech Republic. In particular, yields of spring barley, winter wheat, and oilseed winter rape during 2000–2014 were assessed. Observed yields from 14 districts were collected and thus 210 examples (15 years within 14 districts) were included. Selected districts differ considerably in soil fertility and terrain configuration and represent a transect across various agroclimatic conditions (from warm/dry to relatively cool/wet regions). Two approaches were tested: 1) using 16-day temporal composites of remotely sensed data provided by the United States Geological Survey, and 2) using daily remotely sensed data in combination with an originally developed smoothing method. Yields were predicted based on established regression models using remotely sensed data as an independent parameter. In addition to other findings, the impact of severe drought episodes within vegetation was identified and yield reductions at a district level were predicted. As a result, those periods with the best relationship between remotely sensed data and yields were identified. The impact of drought conditions as well as normal or above-normal yields of the tested field crops were predicted using the proposed method within the study region up to 30 days prior to harvest. It could be concluded that remotely sensed vegetation condition assessments could be an important part of early warning systems focused on drought. Such information should be made widely available to various users (decision makers, farmers, etc.) in order to improve planning and business strategies but also target drought relief in case of a major drought event.

INTRODUCTION

Remotely sensed data can be used to assess vegetation conditions for certain landscape points or throughout regions. The possibility for spatial and temporal continuity is a great advantage to this approach. For such purposes, so-called vegetation indices based on surface reflectance can be used. Various tasks such as assessing phenology (e.g. Reed et al. 1994), monitoring vegetation stress including drought stress (e.g. Brown et al. 2008), and estimating and forecasting agricultural yield (e.g. Moriondo et al. 2007, Mkhabela et al. 2011) may be carried out using these indices. The main aim of this study was to compare several approaches using remotely sensed data to forecast regional field crops yields. District yields of spring barley, winter wheat, and winter rape were estimated using the Normalized Difference Vegetation Index (NDVI) and the

Enhanced Vegetation Index (EVI) as 16-day composites derived from the Moderate Resolution Imaging Spectroradiometer (MODIS) aboard the Terra satellite. In addition, the use of daily NDVI and two-band EVI (EVI2) values was tested.

MATERIALS AND METHODS

Analysis was conducted at a district level focused on processing and using remotely sensed data (from the MODIS) to forecast regional yields. For this purpose, average yields from 2000 to 2014 within 14 districts of the Czech Republic were used. The NDVI and EVI (see equations 1 and 2) at 250 m resolution were downloaded as 16-day composites (i.e. using the highest values within consecutive 16-day periods) from https://lpdaac.usgs.gov/ (provided by the United States Geological Survey). Additionally, the necessary bands for the daily NDVI and EVI2 (equation 3) were downloaded at 250 m resolution. For the 16-day composites, values for each time step and district were averaged from grids identified as arable land. For daily NDVI and EVI2 values, an originally developed smoothing procedure (to reduce the effects of atmospheric conditions and cloudiness) was used for data rows within each grid (250 × 250 m) separately. The smoothing procedure consisted of several steps. In the first step, unlikely sudden drops within daily data were excluded as probable errors. For this purpose, daily values observed within preceding 10-day windows were evaluated. Excluded data was the replaced by interpolated values (a linear function) from correct NDVI or EVI2 values. Information about quality flags was not used. Values were then averaged into weekly time steps for grids identified as arable land in each district. Subsequent analysis used data from 5 March to 27 July for composites and from 1 March to 1 August for weekly time steps (originally based on daily values). Due to technical problems (unambiguously unrealistic values), 2003 was not included within the EVI2 analysis.

$$NDVI = \frac{(NIR-RED)}{(NIR+RED)} \quad (1)$$

$$EVI = G \times \frac{(NIR-RED)}{(NIR+C1\times RED-C2\times BLUE+L)} \quad (2)$$

$$EVI2 = G \times \frac{(NIR-RED)}{(NIR+2{,}4\times RED+1)} \quad (3)$$

NIR (near infrared), RED (visible red), and BLUE (visible blue) are surface reflectance; L = 1; C1 = 6; C2 = 7.5; and G = 2.5.

Subsequently, all possible combinations of timing and period lengths of remotely observed data were correlated with reported district yields. In the next step, suggested regression models (linear functions with remotely sensed data as independent variable) were evaluated using mean bias error (MBE) as a parameter of systematic error and root mean square error (RMSE) as a parameter for absolute error (Davies & McKay 1989).

RESULTS

Fig. 1 displays the maximum achieved Pearson correlation coefficients between remotely sensed data and yields. The situations for spring barley, winter wheat, and winter rape are depicted. Results describing the level of correlation are presented for several cases: i) one regression for all districts and years, ii) separate regressions for each district (including all years), and iii) separate regressions for each year (including all districts).

An example yield estimate evaluation (based on daily NDVI data between 18 April and 24 July) for the Vyškov and Brno districts with a combination of spring barley and winter wheat is shown in Fig. 2. In these cases, MBE was 0 and RMSE varied from 0.59 to 0.64 t ha^{-1}.

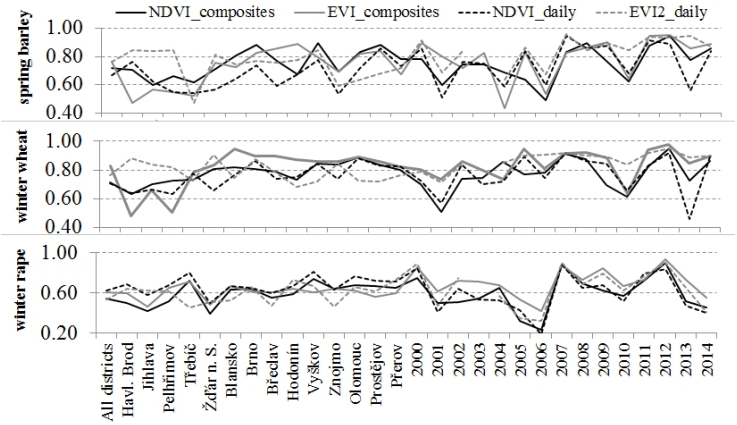

Fig. 1: *Maximum achieved Pearson correlation coefficients between district yields of spring barley, winter wheat, and winter rape and derived values of NDVI and EVI (as 16-day composites) and NDVI and EVI2 (as daily values).*

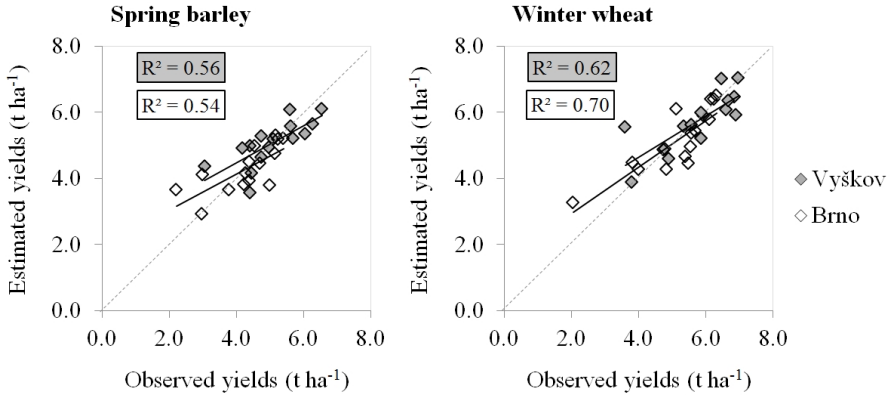

Fig. 2: *Evaluation of spring barley and winter wheat yields estimates. The situation within the Vyškov and Brno districts for 2000–2014 is depicted. Estimates are based on daily NDVI values observed from 18 April to 24 July each year.*

DISCUSSION

Despite the simplicity of the linear regression between remotely sensed data (as independent variable) and yields (as dependent variable), the method resulted in promising accuracy at the district level even in comparison with more sophisticated approaches (e.g. Moriondo et al. 2007). Further improvement would be

achieved if analysis was conducted at sub-district levels, but this is limited by the availability of yield data for such spatial units. Based on the results achieved, it can be concluded that the introduced methods could be used to assess field crops' vegetation conditions and forecast their seasonal yields. It was proven that the smoothing method used within the daily NDVI and EVI2 data did not erase some proportion of the signal. As a result, daily products (e.g. converted into a weekly updated product) could be considered more proper for various applications (e.g. as a part of a drought monitoring system) because they could be updated in an optional time step. Based on a comparison of yields and remotely sensed data, some uncertainty still remains, which is possibly connected with the original MODIS resolution (250 m). Although it is quite challenging to use data with higher spatial resolutions (e.g. from Landsat or Sentinel-2 in future), such use holds great potential for yield forecasting and should be explored in coming years.

Acknowledgement

Supported by project No. CZ.1.07/2.3.00/20.0248 "Building up a multidisciplinary scientific team focused on drought", project No. QJ1310123 of the National Agency for Agricultural Research, and project IGA TP 7/2015.

References

Brown JF, Wardlow BD, Tadesse T et al. (2008) GISci. Remote Sens. 45, 16–46.

Davies JA, McKay DC (1989) Sol. Energy 43, 153–168.

Mkhabela MS, Bullock P, Raj S et al. (2011) Agric. For. Meteorol. 151, 385–393.

Moriondo M, Maselli F, Bindi M (2007) Eur. J. Agron. 26, 266–274.

Reed BC, Brown JF, VanderZee D et al. (1994) J. Veg. Sci. 5, 703–714.

A system for environmental monitoring of the Russian Vostochny spaceport

Mochalov, V.[1], Grigorieva, O.[1], Brovkina, O.[2,*], Potrjasaev, S.[1]

[1]*St. Petersburg Institute for Informatics and Automation of Russian Academy of Sciences, 14 line 39, 199178 St. Petersburg, Russia*

[2]*Global Change Research Centre, Bělidla 986/4a, 603 00 Brno, Czech Republic*

[*]*author for correspondence; email: brovkina.o@czechglobe.cz*

ABSTRACT

The main objective of this study is to obtain a comprehensive assessment of the environment on the Vostochny spaceport's large territory using remote sensing data. Time series satellite and airborne data enabled us to analyze the landscape elements that were under active construction. A methodology for comprehensive environmental assessment was developed and applied to the study area. The methodology included ecological zoning of the territory based on the degree of anthropogenic intensity using original software. The results showed that (1) the level of anthropogenic load increased by 21% from 2013 to 2014, (2) the environmental stability index area decreased by 21%, and (3) the relative tension index of the territory's environmental situation decreased by more than 25%.

INTRODUCTION

The development of new territories is impossible without analysis and environmental monitoring of ecological objects prior to impact and during active operation. The main purpose of environmental monitoring is to minimize potential anthropogenic impacts on the environment. Environmental monitoring includes the monitoring of landscape elements; assessment, prediction, and presentation of current information about the environmental situation for management decisions; and detection of environmental irregularities. Remote sensing data is widely used today for informational support of the environmental monitoring of large territories, because it is a relatively inexpensive and rapid method for acquiring information over large geographical areas and is the only practical way to obtain data from inaccessible regions. Archival and current satellite and airborne data have been employed for environmental monitoring in various studies (Kondratyev 2012, Marconcini et al. 2013), but these works have been limited to identifying negative impact factors without forming a comprehensive environmental assessment.

The environmental monitoring system for the Vostochny spaceport was created prior to the spaceport's construction phase and included a range of ground-based hardware and software technology (Alekseev & Sambros 2012). Descriptions of landscapes and ecological communities of the spaceport's territory have been made only for key areas (Puzanov & Alekseev 2009), and that did not enable presentation of spatial distribution and properties of vegetation and infrastructure objects. Moreover, the system for environmental monitoring of the Vostochny spaceport was presented without remote sensing data, despite the spaceport's large and in places inaccessible area. It should be noted that a map of terrestrial ecosystems developed by the Department of Satellite Monitoring Technologies at the Space Research Institute reflects to some extent the spatial distribution of the main vegetation types, but it is not possible to analyze individual facies due to the map's low (1 km) special resolution (Bartalev et al. 2003). Therefore, it was important to acquire more precise information on species composition and forest frontier in order to assess the self-healing capacity of

the territory under the current and projected anthropogenic loads. The objective of the study was to obtain a comprehensive assessment of the environment of the Vostochny spaceport's large territory using remote sensing data and a developed methodology of ecological zoning in accordance with the degree of anthropogenic intensity.

MATERIALS AND METHODS

Study area. The Vostochny spaceport is located at the 51st parallel north in the Amur Oblast in the Russian Far East and Outer Manchuria (51°49'N 128°15'E). The area of the spaceport and surrounding territory is approximately 440 km^2. The landscape is covered with forest composed of deciduous (mainly birch (*Betula costata* L.) and oak (*Quercus mongolica* L.)) and coniferous (mainly larch (*Larix cajanderi* L.) and pine (*Pinus sylvestris* L.)) trees. Soils are sod-podzolics and waterlogged soils with poor drainage. The hilly surface is at altitude 240–280 m a.s.l.

Data. We used satellite time series Landsat-5 and Landsat-8 data from August of 2004, 2010 and 2014, hyperspectral images from the Resurs-P satellite from 2013 (spectral range 0.4–1 μm, spectral resolution 5–10 nm, spatial resolution 30 m), and multispectral images from the Kanopus-V satellite from 2014 (spectral range 0.45–0.52, 0.51–0.60, 0.61–0.69, 0.75–0.84 μm; spatial resolution 3 m). Airborne data were acquired by the Malahit thermal scanner (8–14 μm, angle of view 1.3 μrad, sensitivity 0.1 K), the Fregat hyperspectral scanner (spectral range 0.4–1 μm, spatial resolution 2 m, spectral resolution 7 nm), and a digital camera (Hasselblad H4D-50, Sweden; RGB, spatial resolution 0.5) in 2013. Field measurements of the spectrometric characteristics of various landscape elements and their negative changes were performed to calibrate and interpret airborne data by a FieldSpec spectroradiometer 3.0 (ASD, USA; 0.35–2.5 μm, spectral range 3–10 nm) and a Termopoint-40 portable pyrometer (8–14 μm).

Software. ENVI 5.0 software and the ArcGIS 10.2 geographic information system (GIS) were used to process multispectral satellite and airborne data and the presentation of the territory's environmental assessment. Original software developed by the St. Petersburg Institute for Informatics and Automation of the Russian Academy of Sciences was used to process hyperspectral and thermal data. The software implemented techniques for recognizing water pollution, solid waste, and hydrocarbons, as well as identifying forest defoliation and the spectral library of objects taking into account vegetation phenology (Grigorieva & Chapursky 2012).

Method of environmental assessment. The ecological characteristics of the study area's main landscape components (forest cover, water bodies, and soil cover) were estimated based on processed satellite, airborne, and field data. Quantitative assessments of the state of these landscape components were the main source of data for comprehensive assessment of the situation regarding the spaceport territory.

The comprehensive environmental assessment was represented as a territorial division based on the degree of anthropogenic intensity (*I*) by means of GIS. *I* is an evaluation of the ecosystem's balance based on the degree of anthropogenic transformation (*R*) and potential stability (*S*): good, satisfactory (destruction of sensitive species), tense (structural changes), crisis, and catastrophic (destruction of the ecosystem). To map *I*, the spaceport territory was covered with a grid of elements of 1 km^2, with each element containing a description of the environmental conditions of vegetation, water areas, and land cover obtained from processed satellite and airborne images. *R* was estimated as a weighted sum of the degree of pollution and negative impacts represented within each grid element depending on the threat to the environment. The threat to the environment factor was developed based on a hierarchy method and enabled the ranking of risk objects and assignment of environmental pollution categories in their position areas. The need to use the weighting factors related to the fact that the spaceport's objects varied greatly as to their effect on the environment and the significance of

these impacts on the landscape. The weighting factors reflect the severity of the infrastructure or the extent of the identified negative impacts or pollution:

$$R = \sum_{i=1}^{m} w_{icp}\left(\frac{S_{io}}{S_c}\right) + \sum_{i=1}^{m}\sum_{j=1}^{n} w_{ij}(s_j/5), \quad (1)$$

where n is the number of natural objects in the grid element; m is the number of infrastructure objects in the grid element; w_{ij} are weighting factors taking into account the maximum impact of the infrastructure object (i) on intensity *j*; w_{ij} is the average impact coefficient of *i*; s_{io} is the area of *i* within the grid element; s_c is the grid element's area; and $s_j/5$ is an inversely proportional value for the degree of the effects on vegetation, water bodies, and soil. The stability of ecosystem S was expressed in the forest, which is an important indicator of the ecological state of the territory and characterizes the ecosystem's adaptive capacity so as to identify projected anthropogenic load. We used vegetation biomass (*B*), ecosystem stability index (*S*), and exergy as indicators of the ecosystem's state. B was estimated based on satellite imagery. The method includes the classification of species composition, parameters of the carbon energy balance, estimation of crown density, tables of growth and productivity of the main tree species' plantations. The stability of the ecosystem was calculated according to the formula:

$$S = (B^{*}\mathrm{NPP}) / R, \quad (2)$$

where *R* is the energy of absorbed radiation and NPP is productivity. The ecosystem's status was determined from the ecosystem's exergy parameter estimation using archival satellite imagery before the spaceport's construction process began. The comprehensive index *I* characterized the relative tension of the environmental situation on the territory (Izrael 1979):

$$I = Sf / Sa, \quad (3)$$

where *Sf* is the area of intact lands and *Sa* is the area of anthropogenically transformed territory. Finally, an interpolation map of the environmental status of the spaceport territory was formed using these *R*, *S*, and *I* indicators.

RESULTS

A map of seven classes of vegetation was created: dense deciduous forest, young leaf forest with an estimated coverage of more than 70%, mixed forest with an estimated coverage of more than 50%, burned forest, mostly

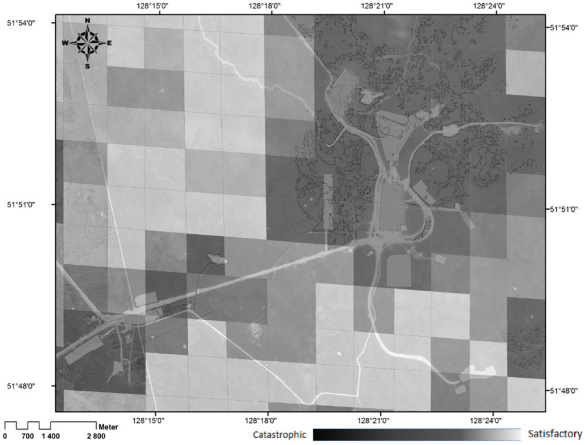

Fig. 1: *A fragment of the map of ecological zoning according to the relative tension index of the environmental situation on the territory (I)*

coniferous mixed forest, mostly deciduous mixed forest, and coniferous forest. The calculated indicators of the degree of anthropogenic load (*R*), the index of ecosystem stability (*S*), and the relative tension index of the environmental situation on the territory (*I*) were represented on the map by means of GIS as separate layers (Fig. 1 shows the *I* layer). Table 1 presents estimates of the indicators.

Table 1: *Indicators of ecological state.*

Indicator	2010	2013	2014
I, relative tension index	0.7	0.72	0.54
R, degree of anthropogenic load	75	80	97
S, ecosystem stability	0.65	0.64	0.50
Assessment of ecological situation	Satisfactory	Satisfactory, close to tense	Tense

DISCUSSION

The proposed methodical approach enabled us to obtain a comprehensive environmental assessment of the spaceport's territory. Analysis of the main indicators characterizing the state of the environment (Table 1) leads to the following conclusion. The level of anthropogenic load (*R*) increased by 21% from 2013 to 2014, which is objectively related to an expansion of the spaceport's construction. However, the environmental stability index area (*S*) decreased by 21%. Uncontrolled decrease in forest area and vegetation biomass due to fire is the main reason for this change. The relative tension index of territory's environmental situation (*I*) decreased by more than 25%. This fact indicates the presence of direct forms of environmental pollution (solid waste dumps and oil spills).

The proposed method of environmental assessment may be adapted and used for areas of approximately 100 km^2 located in areas with strong human impacts. Further research will focus on assessing object-indicators other than forest cover, such as soil cover and wetlands, using remote sensing data. This method of comprehensive environmental assessment can be improved by developing specific algorithms to process remote sensing data and extending the libraries of the landscape elements' spectral features.

Acknowledgement

Supported by project No. LO1415 of the Ministry of Education, Youth and Sports within the National Programme for Sustainability I.

References

Alekseev IA, Sambros VV (2012) The World of Science, Culture and Education 4, 303–307. [In Russian.]

Bartalev SA, Belward AS, Erchov DV et al. (2003) Int. J. Remote Sens. 24, 1977–1982.

Grigorieva OV, Chapursky LI (2012) Modern Problems of Remote Sensing of the Earth from Space 9, 18–25. [In Russian.]

Izrael YA (1979) Ecology and Control of the Natural Environment. Nauka, Moscow. [In Russian.]

Kondratyev DR (2012) Geomatica 4, 40–45. [In Russian.]

Marconcini M, Esch T, Felbier A et al. (2013) Unsupervised high-resolution global monitoring of urban settlements. Proceedings of the 2013 IEEE International Geoscience and Remote Sensing Symposium, pp. 4241–4244. IEEE Geoscience and Remote Sensing Society, Piscataway, NJ.

Puzanov V, Alekseev IA (2009) The World of Science, Culture and Education 7, 29–32. [In Russian.]

Flux footprints in different ecosystems

Macálková, L.[1,2,*], Havránková, K.[1,3], Pavelka, M.[1,3]

[1]*Global Change Research Centre, Bělidla 986/4a, 603 00 Brno, Czech Republic*
[2]*Masaryk University, Faculty of Science, Kotlářská 2, 611 37 Brno, Czech Republic*
[3]*Mendel University in Brno, Zemědělská 3, 613 00 Brno, Czech Republic*
[*]*author for correspondence; email: macalkova.l@czechglobe.cz*

ABSTRACT

Flux footprint is an upwind area where the atmospheric flux measured by an instrument is generated. Footprint size depends on measurement height, surface roughness, and atmospheric thermal stability. Our study focused on the flux footprints of four CzechGlobe ecosystem stations in a wetlands area, an agroecosystem, and young and mature spruce forests. Our aims were to prove that the sites were suitable for eddy covariance measurement and compare flux footprints under various atmospheric thermal conditions: stable, neutral, and unstable. Two computational models were used: the Kormann–Meixner (2001) and Kljun (2004) models. The outputs were processed graphically in site maps.

INTRODUCTION

The eddy covariance technique is the most direct method for measuring turbulent exchanges between ecosystems and the atmosphere. Proper interpretation of flux measurements is essential and depends on good knowledge of the instrumentation and measurement principles. The first thing to know prior to interpreting flux measurements is the study site's footprint. The outreach of the ecosystem cover should be longer than the footprint's extension. If this condition is not fulfilled, the data need to be treated in a special way.

The footprint of a turbulent flux measurement defines the spatial context of the measurement, i.e. the area of surface sources and sinks contributing to the total measured flux.

Every point or area source may potentially contribute to the concentration or flux profile downwind to a degree that varies with the distance from the instrument locations, observation elevation, turbulent boundary layer characteristics, and atmospheric stability (Schuepp et al. 1990).

Many footprint models use a stochastic Lagrangian approach, an analytical approach, or an approach based on large eddy simulation. We chose EddyPro open source software for data processing, including to compute the footprint, to apply the Kljun model (Kljun et al. 2004), which is based on a Lagrangian approach, or the analytical Kormann–Meixner model (Kormann & Meixner 2001).

The aim of our study was to evaluate the flux footprint of four CzechGlobe ecosystem stations in different atmospheric thermal conditions. The sites represent ecosystems common for the Czech Republic: young and mature spruce forests, a wetlands area, and an agroecosystem.

MATERIALS AND METHODS

The four sites analyzed in our study are in ecosystems typical for the Czech Republic: a young spruce forest (Bílý Kříž, Beskid Mounatatins, 49°30'N, 18°32'E, 890 m a.s.l.), a mature spruce forest (Rájec, 49°29''N, 16°43'E, 640 m a.s.l.), a wetlands area (Třeboň, 49°01'N, 14°46'E, 426 m a.s.l.), and an agroecosystem (Křešín u Pacova, 49°35'N, 15°05'E, 534 m a.s.l.). For more details on the sites, see Marek et al. (2011).

The footprint is the fraction of the upwind surface containing effective sources and sinks contributing to a measurement point. Mathematically, it can be defined as follows: Consider the coordinate system such that the x-axis

is pointing against the direction of the wind and the sensors are located at $(0,0,z_m)$, where is z_m measurement height. The footprint function f(x,y,z) describes the flux at (0,0,z) caused by a point source at (x,y,0).

In the cross-wind integrated model used in EddyPro, the footprint function is given by the following equation (Kormann & Meixner 2001)

$$f(x) = \frac{1}{\Gamma(\mu)} \frac{\xi}{x^{1+\mu}} exp\left(\frac{-\xi}{x}\right),$$

where $\xi=\xi(z)$ denotes flux length scale, μ is a model dimensionless constant, and $\Gamma(\mu)$ is the gamma function.

The other model, which uses a stochastic Lagrangian approach (Kljun et al. 2004), computes the footprint function via the equation

$$f(x) = \left(\frac{\sigma_w}{u_*}\right)^{\alpha_2} \left(1 - \frac{z_m}{h}\right)^{-1} z_m \bar{f_y},$$

where σ_w is the standard deviation of vertical velocity, u_* is surface friction velocity, and α_2 is an optimization parameter.

The Monin–Obukhov stability parameter, $\zeta = \frac{z_m - d}{L}$, where d is displacement height and L is Monin–Obukhov length, was used to categorize data into three classes: stable ($0.06 \leq \zeta$), neutral ($-0.06 \leq \zeta < 0.06$), and unstable ($\zeta < -0.06$).

The Kormann–Meixner model was used for extremely stable conditions (the precise value of ζ for extremely stable stratification may be found in the EddyPro manual). For other conditions, the Kljun model was used. The Kormann–Meixner model was not used for unstable and neutral conditions because it is computationally too exacting for these conditions.

The average 70% footprint was used to visualize our results. For each stability class, the wind rose was divided into 5° intervals ([2.5, 7.5), [7.5, 12.5), etc.). The average 70% footprint is the area between the anemometer and the 70% footprint and provides 70% of the total flux.

For the footprint analysis, eddy covariance data from all of 2012 was used.

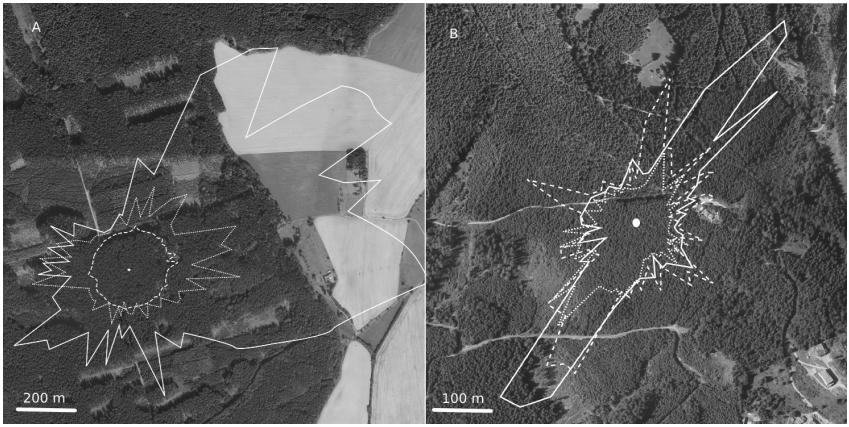

Fig. 1: *Footprint curves for (A) mature spruce forest in Rájec and (B) young spruce forest in Bílý Kříž. Solid lines indicate results for stable conditions, dashed for neutral, and dotted for unstable. The studied ecosystems are dark in color.*

RESULTS

For each site, three footprint curves were computed according to atmospheric stability conditions.

The proportions of stability conditions were as follow: in the mature spruce forest in Rájec – 22% unstable, 52% neutral, and 26% stable; in the young spruce forest in Bílý Kříž – 32% unstable, 30% neutral, and 38% stable; in the agroecosystem in Křešín u Pacova – 28% unstable, 52% neutral, and 20% stable; and in the wetlands in Třeboň – 32% unstable, 30% neutral, and 38% stable. The distribution of stability conditions followed the course of the day, with stable conditions occurring mostly at night and unstable conditions during the day.

For all sites, the footprint curves for neutral and unstable conditions covered mostly only the studied ecosystem (dashed and dotted lines in Figs. 1 and 2). Under stable atmospheric conditions, the footprint curve encroached outside the border of the studied ecosystem in certain wind directions (solid lines in Figs. 1 and 2).

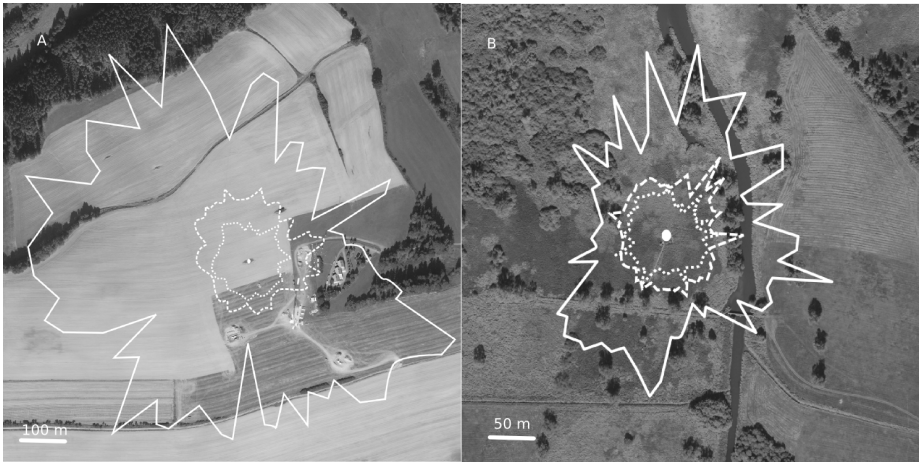

Fig. 2: *Footprint curves for (A) agroecosystem in Křešín u Pacova, and (B) wetlands in Třeboň. Solid lines indicate results for stable conditions, dashed for neutral, and dotted for unstable. The studied ecosystem for (A) is light in color.*

DISCUSSION

Each investigated ecosystem site had different wind and turbulent characteristics (data not shown) connected to footprint features. Křešín u Pacova and Třeboň are situated in plains and the footprints there were more or less circular. In Křešín u Pacova, there was a problematic grassy area in the south, southeast, and east of the footprint under stable conditions. The wind came relatively frequently (15% of stable atmospheric conditions) from this area. Flux data during unstable conditions reached the grass under conditions of southerly winds (8% of unstable conditions). Generally, the south, southeast, and east wind directions should be treated with care while processing flux data.

Třeboň had much lower wind speeds (average 1.5 m s^{-1}) than did Křešín u Pacova (average 4 m s^{-1}) and the footprint was smaller even though the eddy covariance system was placed at the same height above the ground (2.5 m). The most frequent wind directions were from the south–southwest, south, and southeast (30% of all wind). Other prevailing wind directions were northwest (25% of all wind). No data from the unstable and neutral conditions were eliminated from data processing (62% of all atmospheric conditions). This

data represented the studied ecosystem. Although the stable footprint included an area across the river and one must accordingly be attentive in processing flux data, wind from this direction occurred only infrequently (10% of stable conditions).

Although Rájec is situated on a modest slope, and the surrounding landscape is patchy with varying surface roughness, the footprint for unstable and neutral conditions nevertheless covered the studied forest. The footprint under stable conditions (mostly at night) was elongated to the northeast and east. The measured data then included an agricultural field and thus should be excluded from further flux analysis. The amount of such data was not crucial, because the wind infrequently from these directions (14% of stable atmospheric conditions). The unstable and neutral footprints covered the studied ecosystem well.

Bílý Kříž is situated on a slope near the edge of a mountain. Due to flow modification by terrain, south winds prevailed at the locality (40% under all atmospheric conditions) and the south footprint was also preferable, as it covered the young spruce forest and had minimal terrain disturbances. Data from north winds should be treated with care due to the effect of the ridge.

To conclude, all studied ecosystem sites had a source area within the studied ecosystem under unstable and neutral stability conditions (62–80% of yearly 30-min data). Footprints under stable conditions sometimes extended beyond the studied ecosystems (southeastern part in Křešín, eastern part in Rájec) or could be difficult to interpret (north winds at Bílý Kříž). Data from these conditions were generally nighttime data that already were treated with special care due to nighttime CO_2 flux underestimation. These data were typically excluded from flux analysis and gap-filled.

Acknowledgement

Supported by project No. LO1415 of the Ministry of Education, Youth and Sports within the National Programme for Sustainability I as well as projects No. LM2010007 and No. R200871421.

Reference

Kljun N, Calanca P, Rotach MW, Schmid HP (2004) Bound.-Layer Meteorol. 112, 503–523.

Kormann R, Meixner FX (2001) Bound.-Layer Meteorol. 99, 207–224.

Marek MV, Janouš D, Taufarová K et al. (2011) Environ. Pollut. 159, 1035–1039.

Schuepp PH, Leclerc MY, MacPherson JI et al. (1990) Bound.-Layer Meteorol. 50, 355–373.

Automated eddy covariance data quality control for long-term measurements

Šigut, L.[1,2,*], Mauder, M.[3], Sedlák, P.[1,4], Pavelka, M.[1], Špunda, V.[1,2]

[1]*Global Change Research Centre, Bělidla 986/4a, 60300 Brno, Czech Republic*

[2]*University of Ostrava, Chittussiho 10, 71000 Ostrava, Czech Republic*

[3]*Atmospheric Environmental Research, Institute of Meteorology and Climate Research, Karlsruhe Institute of Technology, Kreuzeckbahnstr. 19, 82467 Garmisch-Partenkirchen, Germany*

[4]*Institute of Atmospheric Physics, Boční II 1401, 14131 Prague 4, Czech Republic*

[*]*author for correspondence; email: sigut.l@czechglobe.cz*

ABSTRACT

Estimation of matter and energy exchange using the eddy covariance method is often organized into regional or global networks. To achieve comparability among sites, it is important to standardize and specify the methodology used. Currently, quality control (QC) is one of the most time-demanding steps in data processing within the Czech Carbon Observation System. Although manual QC (MQC) enables consideration of more complex test applications, it is often difficult to document. The aim of this study was to establish an automated QC (AQC) scheme based on available literature and post-processing software and test its effectivity and reliability on sites comprising an agroecosystem and a mature European beech forest. AQC successfully flagged low-quality CO_2 fluxes and provided estimates of net ecosystem productivity similar to estimates based on MQC. The tests' efficiency was particularly high for the agroecosystem, where AQC removed 13% less data than did MQC. We conclude that the adopted AQC displays satisfactory performance, especially for sites with low canopy heights.

INTRODUCTION

The eddy covariance (EC) method enables long-term observations of heat, water, and carbon dioxide (CO_2) exchange between the atmosphere and biosphere under the conditions of a changing climate. EC towers are often organized into networks either on a continental scale, e.g. the Integrated Carbon Observation System (http://www.icos-infrastructure.eu/) and the National Ecosystem Observatory Network (www.neoninc.org), or a national scale, e.g. the Czech Carbon Observation System (http://www.czecos.cz/en.html) and Terrestrial Environmental Observatories (http://teodoor.icg.kfa-juelich.de/overview-en). Achieving intercomparability among sites presents a challenge for unifying data processing methodologies, i.e. raw data post-processing, quality control (QC), and gap-filling of missing data (Aubinet et al. 2012, Foken et al. 2012).

Quality assurance tests proposed by Foken & Wichura (1996) (e.g. a steady-state test and a developed turbulent conditions test) are implemented in all up-to-date post-processing software. However, these are not sufficient to account for unrealistic fluxes. There is not yet any universally accepted set of tests for EC flux QC, but an effective QC scheme for automated QC (AQC) has already been presented (Mauder et al. 2013). It relies on information extracted from measured high-frequency data and their half-hourly products. This is in contrast with the spike detection method proposed by Papale et al. (2006) that looks for outliers in half-hourly data by comparing data points with their neighbours. Manual QC (MQC) generally includes more tests than does AQC but it applies these tests selectively based on visual inspection.

Establishing AQC would improve the reproducibility of EC data post-processing and accelerate its delivery.

In this study, we therefore aimed to assess the effectivity and reliability of an approach adopted to flag low-quality half-hourly CO_2 flux data.

MATERIALS AND METHODS

For the analysis, we selected two site years from ecosystems with contrasting canopy heights, an agroecosystem (a wheat field in Křešín u Pacova, Czech Republic) and a mature European beech forest (Štítná nad Vláří-Popov, Czech Republic). Both datasets were measured during 2013. In the original study, Mauder et al. (2013) applied the tests by using the TK3.1 post-processing software (Mauder & Foken 2011). Although we used EddyPro software (Li-Cor, USA), most of the corresponding tests were applicable. AQC consisted of evaluation of instrument diagnostics, control of plausibility limits (thresholds according to Mauder et al., 2013), evaluation of the percentage of missing high-frequency values within a half-hour (10% allowed), a combination of a steady-state test and a test of integral turbulence characteristics (Foken & Wichura 1996), a test of the mean residual vertical wind component to flag periods with vertical advection, and a test for the interdependence of sensible heat, latent heat, and CO_2 flux flags due to corrections/conversions (summarized in Mauder et al. 2013).

The spike detection method was based on the approach described in Papale et al. (2006). It applies a double-differenced time series using the median of absolute deviation about the median ($z = 7$; threshold value). MQC combined a steady-state test and a test of integral turbulence characteristics (Foken & Wichura 1996), evaluation of instrument diagnostics, control of plausibility limits (based on experience), and a comparison with different meteorological variables and adjacent half-hours.

Net ecosystem productivity (NEP) was estimated using marginal distribution sampling according to Reichstein et al. (2005). u^*-filtering was calculated as described in Papale et al. (2006) and applied only to the mature beech forest site. (Both methods are available online at http://www.bgc-jena.mpg.de/~MDIwork/eddyproc/.)

RESULTS

The AQC scheme removed 13% less data for the agroecosystem than did MQC with a difference in NEP of only 70 kg(C) ha^{-1} $year^{-1}$. Applying the spike detection method removed an additional 2% of data and increased the difference in NEP to 168 kg(C) ha^{-1} $year^{-1}$. To better resolve differences among these three approaches (MQC, AQC, and AQC with spike detection), monthly NEP values were estimated (Fig. 1a). With the exception of May and July, all monthly NEP values were very similar. The most important tests for this site were the evaluation of instrument diagnostics (11.5% of flagged values) and the test of CO_2 flux interdependence (28.2% of flagged values).

In the case of the mature beech forest, AQC discarded 12% more CO_2 flux values than did MQC with a difference in NEP of 502 kg(C) ha^{-1} $year^{-1}$. Utilizing spike detection for the beech forest resulted in only a marginal decrease in available data, but decreased the difference in NEP estimates between the two QC schemes to 169 kg(C) ha^{-1} $year^{-1}$. The monthly resolved NEP for this site showed very similar values for all QC strategies with exception of July (Fig. 1b). In this dataset, evaluation of instrument diagnostics removed 9.7% of flagged values, the test of the mean residual vertical wind component removed 23.4%, and the most important test was again the test of CO_2 flux interdependence which removed 47.3%.

As can be expected from their general application, the steady-state test and test of integral turbulence characteristics played a pivotal role in all QC schemes for both sites. Due to their wide acceptance in the community,

they are not discussed further. It is also important to note that the percentages of flagged values are not cumulative, i.e. a particular half-hour can be flagged by multiple tests.

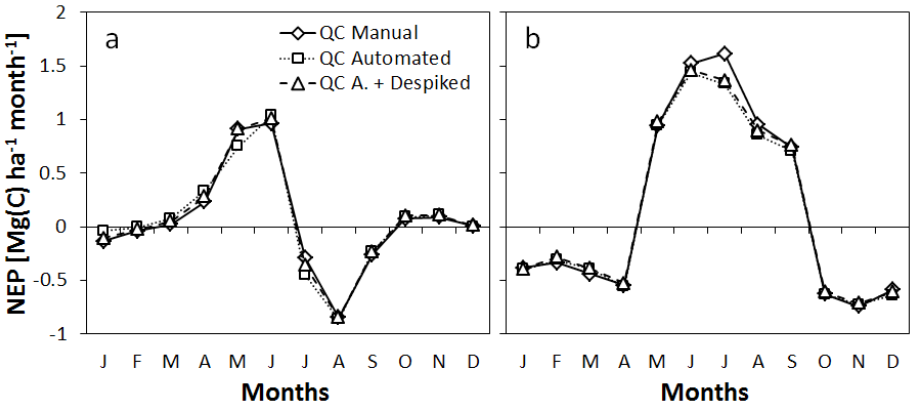

Fig. 1: *Monthly NEP estimates for three QC treatments in (a) an agroecosystem and (b) a beech forest.*

DISCUSSION

Monthly NEP values were in general agreement across individual QC strategies (Fig. 1). This indicates that the number of flagged values was not excessive and was sufficient to compute reliable estimates of monthly NEP. However, the amount of removed data was considerable in the beech forest dataset particularly due to the strict test of the mean residual vertical wind component and the test of CO_2 flux interdependence. Detailed analysis of half-hourly data showed that the biggest differences in NEP estimates between AQC and MQC were due to the presence of extreme values within a month. Although applying the spike detection method after AQC improved the comparison of yearly NEP with MQC for the beech forest, this method should be used with caution because it can remove potentially very interesting data points. Extreme values can have a considerable effect on gap-filling procedures, but they may still represent realistic processes within the ecosystem (Mauder et al. 2013). We conclude that the adopted AQC displays satisfactory performance, particularly for sites with low canopy heights.

Acknowledgement

Supported by project No. LM2010007 "CzeCOS/ICOS"; project No. LO1415 of the Ministry of Education, Youth and Sports of CR within the National Programme for Sustainability I; project No. CZ.1.05/1.1.00/02.0073 "CzechGlobe", and the Helmholtz Research School on Mechanisms and Interactions of Climate Change in Mountain Regions. Manual quality control conducted by Radek Czerný.

References

Aubinet M, Vesala T, Papale D (eds) (2012) Eddy Covariance: A Practical Guide to Measurement and Data Analysis. Springer, Dordrecht.

Foken T, Leuning R, Oncley SR et al. (2012) Corrections and data quality control. Eddy Covariance: A Practical Guide to Measurement and Data Analysis (eds M Aubinet, T Vesala, D Papale), pp. 85–132. Springer, Dordrecht.

Foken T, Wichura B (1996) Agric. For. Meteorol. 78, 83–105.

Mauder M, Cuntz M, Drüe C et al. (2013) Agric. For. Meteorol. 169, 122–135.

Mauder M, Foken T (2011) Documentation and Instruction Manual of the Eddy-Covariance Software Package TK3. Department of Micrometeorology, University of Bayreuth, Bayreuth.

Papale D, Reichstein M, Aubinet M et al. (2006) Biogeosciences 3, 571–583.

Reichstein M, Falge E, Baldocchi D, et al. (2005) Global Change Biol. 11, 1424–1439.

The Bowen Ratio/Energy Balance method and detailed temperature profile measurements to improve data quality control

Pozníková, G.[1,2,*], Fischer, M.[1,3], Orság, M.[1,2], Trnka, M.[1,2], Žalud, Z.[1,2]

[1]*Global Change Research Centre, Bělidla 986/4a, 603 00 Brno, Czech Republic*
[2]*Mendel University in Brno, Zemědělská 1, 613 00 Brno, Czech Republic*
[3]*North Carolina State University, 2820 Faucette Drive, 27695 Raleigh, NC, USA*
[*]*author for correspondence; email: g.poznikova@gmail.com*

ABSTRACT

Water plays a key role in the functionality and sustainability of ecosystems. In light of predicted climate change, research should focus on the water cycle and its individual components. The main component of water balance driving water from ecosystems is evapotranspiration (ET). One standard method for measuring ET is the Bowen Ratio/Energy Balance (BREB) method. It is based on the assumption that water vapour and heat are transported by identical eddies with equal efficiency. When using the BREB method, we assume that the profiles of temperature and air humidity are ideally logarithmic or at least consistent. Since the BREB method is usually based on measurements of temperature and humidity at only two heights, it is difficult to verify whether this assumption has been fulfilled. Potential profile inconsistencies are more likely for temperature because the sensible heat flux changes its sign more often and negative latent heat flux is not physically possible during positive sensible heat flux. We therefore conducted a field experiment using a 4-m-high measurement mast with 20 thermocouples for detailed measurement of air temperature profiles above different covers, e.g. grassland, spring barley, and poplar plantations. Our main objective was to investigate the basic assumptions of the BREB method, i.e. the temperature profile's consistency under various weather conditions. To be more specific, we aimed to investigate whether inflexion points occurred within the temperature profile and if so when.

INTRODUCTION

Water is a key component essential for all ecosystems. In agriculture, evapotranspiration (ET) deserves special attention as it is the main factor driving loss in water balance. There are many different methods for deriving ET. One of the basic methods is the Bowen Ratio/Energy Balance (BREB) method (Bowen 1926), which is based on the assumption of logarithmic profiles of temperature and humidity in the surface layer of the atmosphere. It is described by Monin–Obukhov similarity theory (Foken 2006). In our study, we aimed to test this basic assumption with a 4-m-high measurement mast. The main goal was to find different types of temperature profiles during the day and during the growing season of spring barley (*Hordeum vulgare* L.). We wanted to plot typical nocturnal and diurnal stratifications and situations with an inflexion point, a so-called "kink" (Oke 1987). This happens when the temperature profile does not change consistently with height but instead creates an inflexion point which cannot be captured using the standard BREB method. In situations where the inflexion point occurs between two measuring sensors of a single BREB system, it is impossible to estimate the Bowen ratio correctly and therefore to calculate ET properly. Using measurements recorded during a field campaign in Domanínek, it was possible to determine when inflexion points occurred. In future, measurement error in calculated fluxes will be quantified for the entire season and subsequently minimized. We will also broaden the study to test different cover crops.

MATERIALS AND METHODS

The present study was conducted on an experimental field in Domanínek near Bystřice nad Pernštejnem in the Bohemian–Moravian Highlands. The data used in this study were recorded during the 2013 growing season. During the field experiment, a 4-m-high measurement mast with 20 very fine (0.1 mm), fast response type K thermocouples was used for detailed measurement of the air temperature profile. The thermocouples were connected to a CR1000 data logger (Campbell Scientific, USA) coupled with a thermoelement multiplexer developed and produced by W. Laube from the University of Natural Resources and Life Sciences, Vienna. Measurement took place over different covers, e.g. oat, grassland, spring barley, and poplar plantations. Sampling interval was 5 s and data were then averaged to 30-min values for further processing. In this short paper, several days during measurement over a spring barley field were chosen to examine temperature profiles in detail. An automatic weather station was placed near the measurements in order to record the basic meteorological variables necessary to derive ET using the BREB method (Savage 2010, Todd et al. 2000). In particular, temperature and humidity at two heights above the canopy (0.2 m and 1.0 m) were recorded as were net radiation (W m^{-2}) and soil heat flux (W m^{-2}). Temperature was measured by thermocouples at 5 s intervals and stored as the average every 30 s. These detailed measurements were used to calculate the average between two thermocouple levels and 30 min averages. Further, the correlation coefficient was calculated to describe the relationship between temperature gradients and height. Different times of day were chosen to show the various temperature profiles and stratification of the lower atmosphere.

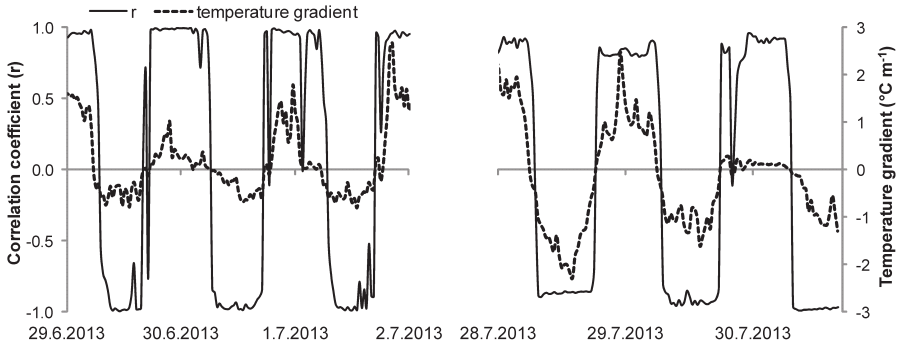

Fig. 1: *The correlation coefficient of temperature gradients (differences between two closest thermocouples for 19 different levels above ground) and the temperature gradient (°C m^{-1}) for sample days (29 June–2 July and 28 July–30 July 2013) on spring barley field in Domanínek.*

RESULTS

Three days at the beginning and three days at the end of July are shown in Fig. 1 to describe green and well watered barley with high ET as well as mature barley lacking water in the soil at the end of the growing period. The dashed line represents the temperature gradient per m height. Taking vegetation height (0.7 m) into account, the gradient was calculated as the difference between the temperature measured by thermocouple 1.8 m above the ground and that 0.8 m above the ground. The gradient displayed the highest positive values at night when temperature increased with height. In contrast, the lowest values were measured around noon

on sunny days when temperature decreased with height and displayed the highest values near the surface. The solid line shows the correlation coefficient course describing the linear relationship between temperature gradients and the logarithm of the measurement height.

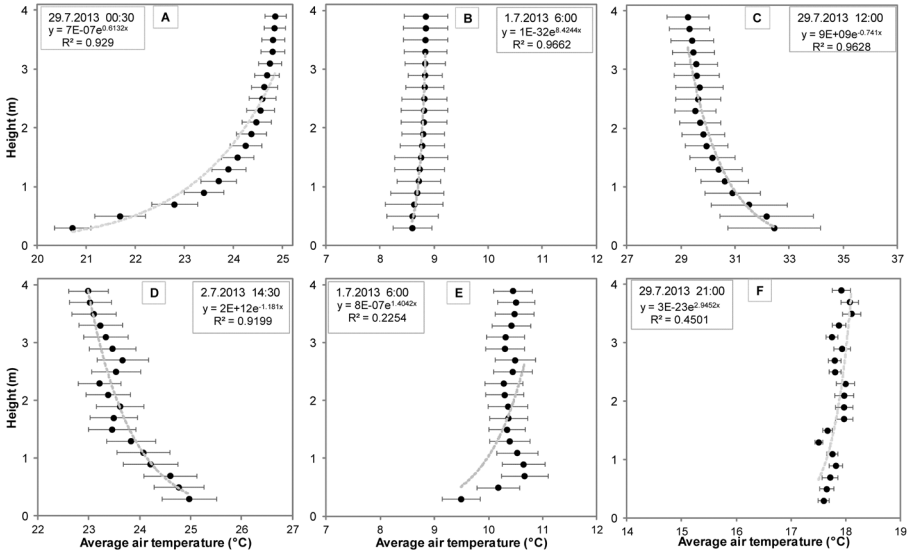

Fig. 2: *Temperature gradients during the day. All figures have the same range (5°C) at the x-axis so as to be graphically comparable. Depicted temperature is the average of two levels and error bars show the standard deviation of temperature differences between these two levels over a 30-min period. A: typical nocturnal conditions with stable stratification, B: near neutral stratification around sunrise, C and D: typical diurnal conditions with unstable stratification, E: morning situation with inflexion point, F: evening situation with inflexion point.*

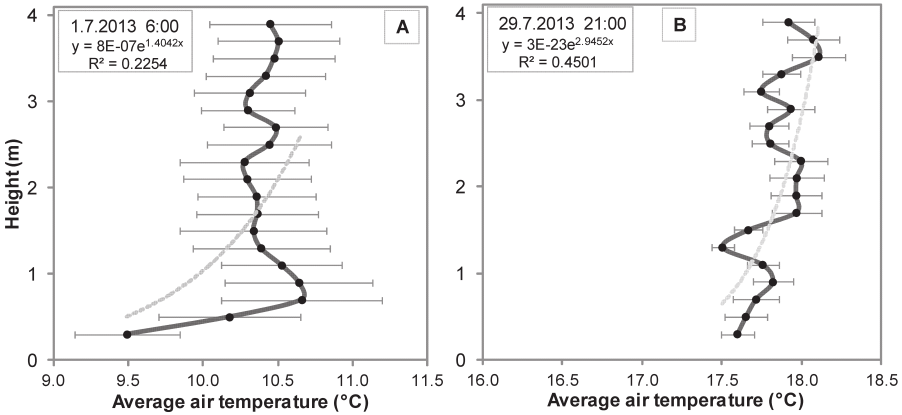

Fig. 3: *Zoomed-in temperature profiles during the change of day and night with the same range (2.5°C) at the x-axis. A typical situation when a "kink" occurs at around 1 m above the surface. A: large standard deviations, B: lower variability in the data.*

The standard deviation of 30 min averages was used for error bars in Figs. 2 and 3. Fig. 2A displays a typical nocturnal temperature gradient where temperature increases with height. In contrast, Figs. 2C and 2D show typical diurnal conditions with higher temperatures closer to the surface. Higher turbulent mixing and more rapid changes in temperature during the day result in high standard deviations, displayed as error bars. Fig. 2B is an example of neutral stratification near sunrise. Figs. 2E and 2F were chosen to demonstrate the situation with an inflexion point when the sensible heat flux changed its sign. For a more detailed look at these gradients, they are zoomed in and displayed in Fig. 3.

DISCUSSION

This short study aimed to use detailed temperature profile measurements to display the importance of such measurements in assessing the basic assumption of the BREB method. Different climatic conditions were chosen for comparison. For example, 28 July 2013 was a day with a clear sky, net radiation up to 550 W m^{-2}, and maximum air temperature at 0.9 m exceeding 35.8°C. Temperature gradients decrease during the day as the surface is heated by the sun. The gradient on 28 July reached the lowest values (−2.3°C). For comparison, on 30 July 2013 the maximum temperature measured at 0.9 m was 26.2°C and the day was cloudy. The temperature gradient recorded a lower minimum value (−1.3°C). At night when temperature rises with height, the gradient has positive values. Similarly, the correlation coefficient is close to 1 at night and close to −1 during the day. Early in the morning and after dusk, the r value is close to 0 and so data quality decreases. These are situations when the temperature profile is changing and a "kink" occurs. Fig. 3 displays two moments of this kind. Fig. 3A shows a profile at 6:00. An inflexion point occurred between 0.4 m and 1.4 m. The standard deviations are high, which emphasizes the averaged data's high variability. In such a situation, we would need extremely accurate sensors (up to +/− 0.1°C) to capture the real profile. In our case, sensor bias may have influenced the result. Fig. 3B captures a situation with a "kink" in the evening at 21:00. The standard deviations were much smaller; the difference between the minimum and maximum temperatures at all heights was only 0.75°C.

A profile's correlation coefficient is a good indicator of the profile's consistency and data quality. Future efforts should focus on classifying it and relating it to flux errors. Further studies will focus on quantifying the error caused by occurrence of an inflexion point in temperature profiles and comparing different crop covers.

Acknowledgement

Supported by project No. CZ.1.07/2.3.00/20.0248 "Building up a multidisciplinary scientific team focused on drought", the KONTAKT II programme under project No. LH12037 "Development of models for assessment of abiotic stresses in selected bio-energy plants", project No. LD130030 supporting COST Action ES1106, and project No. LO1415 of the Ministry of Education, Youth and Sports within the National Programme for Sustainability I.

References

Bowen IS (1926) Phys. Rev. 27, 779–787.

Foken T (2006) Bound.-Layer Meteorol. 119, 431–447.

Oke TR (1987) Boundary Layer Climates. 2nd edition, Methuen, London.

Savage MJ (2010) Sensors 10, 7748–7771.

Todd RW, Evett SR, Howell TA (2000) Agric. For. Meteorol. 103, 335–348.

Selection of a new site for eddy covariance research in Vietnam – Vietnamese and CzechGlobe cooperation

Nguyen, V.X.[1,2,3,*], Pavelka, M.[1], Havránková, K.[1], Hoang, S.N.[3], Lai, Q.T.[3], Dang, S.V.[3], Tran, T.V.[3], Ton, M.T.[4], Truong, C.Q.[4], Pham, N.H.[4], Tran, C.T.[5]

[1]*CAS Global Change Research Centre (CzechGlobe), Bělidla 986/4a, 603 00 Brno, Czech Republic*
[2]*Mendel University, Zemědělská 1, 613 00 Brno, Czech Republic*
[3]*VAST Institute of Tropical Biology, 85 Tran Quoc Toan, District 3, HCMC, Vietnam*
[4]*Bidoup-Nui Ba National Park, Lam Dong Province, Vietnam*
[5]*Southern Region Hydrometeorological Center, 8 Mac Dinh Chi, District 1, HCMC, Vietnam*
**author for correspondence; email: nguyen.v@czechglobe.cz*

ABSTRACT

A montane evergreen broadleaf forest in Bidoup-Nui Ba National Park, Vietnam was selected for a future flux study based on a set of standard selection criteria applied to five protected areas in southern Vietnam. This pristine natural ecosystem within the park is important for its biodiversity conservation, supporting high levels of plant diversity and endemism and representing the Southern Annamites montane rain forests ecoregion. This paper describes general information about the site. Common foggy and calm wind periods can pose a challenge for eddy covariance measurements. Since March 2015, measurement of the horizontal wind regime at the site has begun to provide information on local prevailing wind directions and calm periods to aid in optimizing tower positioning within the site.

INTRODUCTION

To date, estimation of forest carbon stock in Vietnam has mostly been based on campaign measurements for forest biomass inventory within Reducing Emissions from Deforestation and Forest Degradation (REDD+) initiatives. These studies mainly focused on planted forests and offered limited information on forest biomass and carbon stocks in Vietnam's natural forests (Sharma et al. 2013, Vo 2014). Most of the studies used measured data from sample plots to establish length–volume allometric relationships so as to estimate biomass and carbon stocks. Using this approach, it is difficult to capture the continuous exchange of matter and energy between ecosystems and the atmosphere and relate it to changes in microclimate variables so as to understand the dynamics of climate change impacts. The eddy covariance method offers an effective solution to this problem. However, its application is limited in Vietnam, with only one flux study site having been established within a lowland semi-evergreen forest in December 2011 (see http://asiaflux.net/ for details). To fill in this gap, CzechGlobe and the Institute of Tropical Biology have collaborated since 2012 to promote the study of ecosystem carbon flux using eddy covariance methods in Vietnam.

In 2012 and 2013, field surveys were conducted in Cat Tien and Bidoup-Nui Ba national parks within Dong Nai River Basin Conservation Landscape (Pilgrim et al. 2006) as well as in three other protected areas in an adjacent coastal area in southern central Vietnam in order to select a site for a future eddy covariance study. Selection criteria included: 1) representative ecosystem types for Vietnam with typical species composition; 2) a homogeneous area with an appropriate fetch and flat terrain; and 3) an accessible site with access to the electrical grid and the possibility for it to be secured. Major types of natural forest ecosystems considered were: coniferous forest, evergreen (including semi-evergreen) broadleaf forest, mixed broadleaf and

coniferous forest, deciduous forest, bamboo-rich forest, and mangrove forest. A montane evergreen broadleaf forest in Bidoup-Nui Ba National Park which met all the criteria was selected. This forest type covers 30% of the park area and represents a pristine natural habitat of the much larger Southern Annamites montane rain forests ecoregion covering 50,000 km^2 in Laos and Vietnam (Wikramanayake et al. 2002). The ecosystem holds significant importance for biodiversity conservation, watershed protection, and carbon storage in the landscape (detailed information in the Discussion section).

This paper describes the site's forest structure and the initial results of wind condition assessment, within which prevailing wind directions and calm periods were monitored. The site is located in a small valley with surrounding mountainous terrain near an open area of experimental fishponds. The wind condition analysis helped optimize tower positioning within the site in order to avoid possible future problems with flux measurement footprints covering adjacent areas with different land use and land cover types outside of the targeted ecosystem.

MATERIALS AND METHODS

Site description

The evergreen broadleaf forest investigated is located in Central Highlands of Vietnam (12º10'24''N 108º41'51''E) at ca 1,500 m a.s.l. in Bidoup-Nui Ba National Park. Under the tropical monsoon climate, there are two distinct seasons: a rainy season from April to October (with prevailing southwesterly wind) and a dry season from November to March the following year (with prevailing northeasterly wind). Sum of global radiation is 4.8 GJ m^{-2} $year^{-1}$ with a maximum in March, lower values during the rainy season, and a minimum in September (Forest Inventory and Planning Institute 2004). This area has a warm (annual mean air temperature 18ºC) and humid (annual mean relative air humidity 85%) climate with high annual precipitation (>1,800 mm) (Pilgrim et al. 2006).

Table 1: *The forest's five distinct vertical layers. Other species of lianas and vines (e.g., Gnetum montanum, Tetrastigma planicaule) as well as orchids are also common in the forest.*

Layers	Height m	Typical species
Emergent layer	25–30	Pinus krempfii, Quercus spp., Pinus dalatensis, Dacrydium elatum
Canopy layer	18–22	Symplocos spp., Symingtonia populnea, Castanopsis spp., Schima wallichiana, Elaeocarpus bidoupensis, Lithocarpus spp.
Understory tree canopy	7–15	Eurya japonica, Illicium griffithii, Garcinia spp., Cyathea spp.
Understory shrub layer	1–5	Psychotria spp., Allomorphia arborescens, Ardisia spp.
Herbaceous/forest floor layer	0–1	Selaginella spp., Justicia adhatoda, Pentaphragma spp., Chirita spp., Begonia spp., Didissandra evrardii

Method of initial wind regime assessment

Since March 2015, a WindSonic Option 3 2-D wind sonic anemometer (Gill Instruments, UK) with a RailBox V16 data logger (EMS Brno, Czech Republic) was deployed at the site, 1.5 m above the top of the forest canopy, to evaluate local wind conditions to enable proper positioning of a flux tower at the site so that it would not be affected by neighboring ecosystems or infrastructure. Without a proper tower, the sensor was positioned in the roughness sublayer just above the canopy and measured wind speed data in this sublayer tends to be lower than are those at the height where the future eddy sensors will be placed. Underestimated wind speeds

can affect estimation of footprint length. For this reason, we used a common footprint length for forest ecosystems of about 400 m (Burba 2013).

RESULTS

Forest composition and structure. This montane evergreen broadleaf forest is dominated by species in the Fagaceae and Lauraceae families, including *Castanopsis* spp., *Lithocarpus* spp., *Quercus* spp., *Cinnamomum* spp., and *Litsea* spp. (Tordoff et al. 2004). The forest has from four to five distinct vertical layers (Table 1).

Wind conditions

The first wind data measured from the proposed flux tower site in Bidoup-Nui Ba National Park over a 28-day period during 4–31 March 2015 showed a diurnal cycle pattern in the wind regime (Figs. 1 and 2). Calm wind periods, defined by wind speeds less than 1 m s^{-1} where turbulence is not well-developed (Burba 2013), often occurred at night from 21:00 to 03:00. Other times of the day, wind speeds were greater than 1 m s^{-1} and so represented speeds suitable for eddy covariance measurements. Winds were much stronger in the afternoon to evening, with the strongest winds coming from the east and southeast. For this period, prevailing winds blew from the south and southeast.

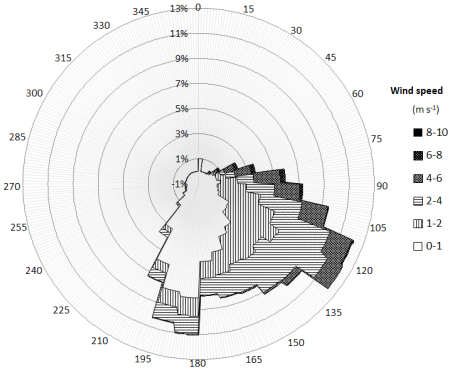

Fig. 1: *A wind rose for a 28-day period in March 2015.*

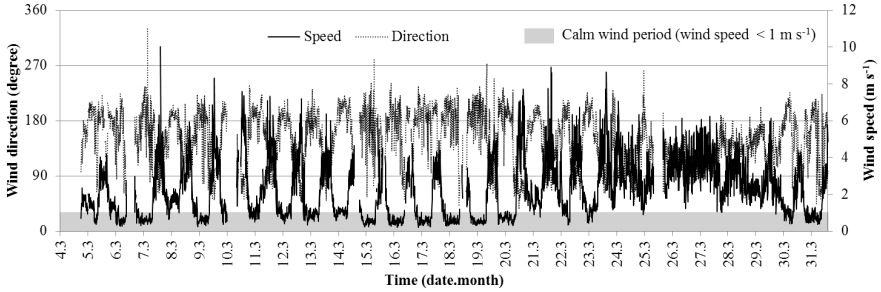

Fig. 2: *The first wind data measured in March 2015 from the selected site in Bidoup-Nui Ba National Park.*

DISCUSSION

Bidoup-Nui Ba National Park is one of four national biodiversity centers in Vietnam and one of 221 Endemic Bird Areas in the world. The park is located in the headwater area of the Dong Nai River, which flows through some of the largest economic centers in Vietnam including Ho Chi Minh City and Biên Hòa. It is a part of a continuous natural forest area of over 200,000 ha and is part of the Southern Annamites montane rain forests ecoregion, which has not yet undergone any flux tower study. To date, the first and only flux tower in Vietnam is in a lowland semi-evergreen forest. The montane evergreen broadleaf forest has faced threats from logging and conversion to other land use types and now from global warming impacts. A flux study of this ecosystem would help in understanding its role in current REDD+ initiatives in Vietnam and improve its management to ensure that this type of forest will be conserved for future generations.

Preliminary data and supplementary information have been gathered to help better understand the site's environment and effectively design the flux study station. The eddy covariance method requires well-developed turbulence such that other mechanisms of transport (e.g., molecular diffusion and advection) are negligibly small (Burba 2013). Wind data measured in March 2015 showed a diurnal cycle pattern with calm wind periods often occurring at night and wind directions gradually shifting from easterly to southerly. April is expected to be the calmest time of year given its period of changing wind directions and the onset of rainy season. Based on the common pattern of the main monsoon wind directions (northeasterly and southwesterly) and their contributions in terms of flux footprints, the wind study site should be moved ca 400 m to the southeast so as to avoid northeasterly winds coming from the fishery area. The small valley has just enough room for such adjustment. The selected location meets all essential requirements for establishing a new eddy covariance site.

Acknowledgement

Supported by project No. LO1415 of the Ministry of Education, Youth and Sports within the National Programme for Sustainability I; and grant No. VAST.HTQT.Sec.02/2012 – 2013 of the Vietnam Academy of Science and Technology.

References

Burba G (2013) Eddy Covariance Method for Scientific, Industrial, Agricultural, and Regulatory Applications. LI-COR Biosciences, Lincoln, NE, USA.

Forest Inventory and Planning Institute (2004) Investment Plan for Bi Dup-Nui Ba National Park, Lam Dong Province. Forest Inventory and Planning Institute, Hanoi. [In Vietnamese.]

Pilgrim JD, Nguyen VX, Nguyen DX et al. (eds) (2006) Biological Assessment of the Dong Nai Conservation Landscape, Vietnam. Asia Regional Biodiversity Conservation Programme, Winrock International, Ho Chi Minh City.

Sharma BD, Phuong VT, Swan SR (2013) Generating Forest Biomass Carbon Stock Estimates for Mapping the Potential of REDD+ to Deliver Biodiversity Conservation in Vietnam. SNV Netherlands Development Organisation, Ho Chi Minh City.

Tordoff AW, Tran QB, Nguyen DT et al. (eds) (2004) Bidoup-Nui Ba National Park. Sourcebook of Existing and Proposed Protected Areas in Vietnam, 2nd ed. Birdlife International in Indochina and the Ministry of Agriculture and Rural Development, Hanoi.

Vo HD (2014) Study Carbon Stock and Its Commercial Value of Some Main Types of Planted Forests in Vietnam. Vietnamese Academy of Forest Sciences, Hanoi. [In Vietnamese.]

Wikramanayake E, Dinerstein E, Loucks CJ et al. (2002) Terrestrial Ecoregions of the Indo-Pacific: A Conservation Assessment. Island Press, Washington, DC.

Orchids of Nepal: phytogeography and economic importance

Timsina, B.[1,2,*], Rokaya, M.B.[2,3], Kindlmann, P.[1,2], Münzbergová, Z.[1,3]

[1]*Institute for Environmental Studies, Department of Botany, Faculty of Science, Charles University, Benátská 2, 12801 Prague, Czech Republic*

[2]*Department of Biodiversity Research, Global Change Research Centre, Czech Academy of Sciences, Bělidla 986/4a, 60300 Brno, Czech Republic*

[3]*Institute of Botany, Czech Academy of Sciences, Zámek 1, CZ-252 43 Průhonice, Czech Republic*

**author for correspondence; email: binu.timsina@gmail.com*

ABSTRACT

Nepal has a biogeographically unique location, which results in a high diversity of vegetation in both north–south and east–west directions. Here we aim to determine the distribution patterns of the largest plant family in Nepal, the Orchidaceae. There are 476 orchid taxa known from Nepal, belonging to 107 genera, 454 species, and 22 infrageneric taxa. We found that out of six floristic regions, the East Asiatic floristic region (EAFR) displays the highest number of species (275 species, 58% of all species and infrageneric taxa) followed by the Indo-Chinese floristic region (ICFR; 261 species, 55%) and the Malesian floristic region (MFR; 78 species, 18%). In total, 118 species (25%) are endemic to the Himalayan region and 21 species are endemic to Nepal. Krober's percentage similarity showed that the EAFR and ICFR have the highest percentage similarity (87%) followed by the MFR and ICFR (62%). In total, 92 species were used for medicinal purposes and 6 as food plants in Nepal. We conclude that Nepal is rich in orchid flora and the highest percentage of orchids originates from the EAFR.

INTRODUCTION

The physiography of Nepal is diverse. The altitude ranges from 60 to 8848 m a.s.l. and there are six bioclimatic zones, ranging from luxuriant tropical forests in the south to alpine scrubs or barren high mountains in the north (Chaudhary 1998). Nepal, which occupies the central part of the Himalayan range, is a transitional zone for many floristic elements. It acts as a bridge facilitating the flux of many taxa (north–south as well as east–west) and as a barrier promoting the endemism of plant species (e.g., Ohba 1988). Thus, there is high plant diversity in Nepal and plant species show affinity for different floristic regions.

The complex biogeography of Nepal is a result of its geological history and its presence at the crossroads of two biogeographic realms (the Palaearctic and Indomalaya realms) and two major phytogeographical kingdoms (the Holarctic division in the north and Palaeotropic division in the south; Takhtajan 1986). The flora of Nepal is influenced by six floristic regions: the East Asiatic floristic region (EAFR) to the east, Irano-Turanian floristic region (ITFR) to the north, Sudano-Zambezian floristic region (SZFR) to the west, Indian floristic region (IFR) to the south, and Indochinese floristic (ICFR) and Malesian floristic (MFR) regions to the southeast (Fig. 1).

The flora of Nepal is well documented (Press et al. 2000). The Orchidaceae, the largest plant family in Nepal, has been well studied due to the presence of unique species and species of great economic importance with both ornamental and medicinal value. This study is aimed at analyzing the distribution of orchid species in order to elucidate the affinities of different species with different regions, and determine their economic importance.

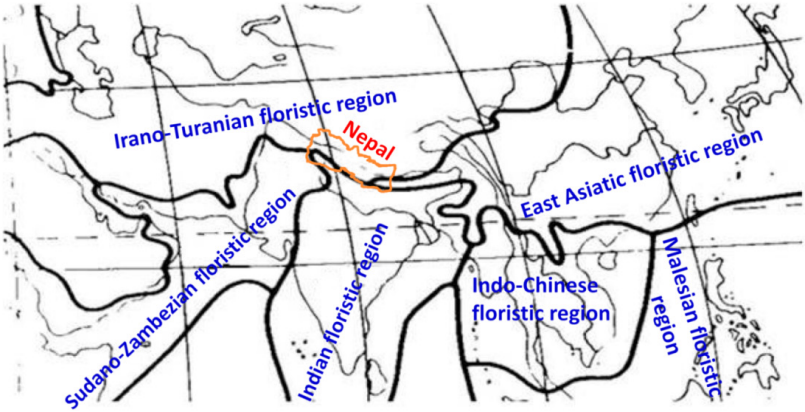

Fig. 1: *Floristic regions influencing flora of Nepal (modified from Takhtajan 1986).*

MATERIALS AND METHODS

Study area

We surveyed all orchid species reported in Nepal. Nepal is a central-Himalayan country with an area of 147,181 km^2. The climate of Nepal is divided into three distinct seasons: (1) a cold winter season from October to February, (2) a hot and dry season from March to mid-June, and (3) a rainy or monsoon season from mid-June to the end of September. Monsoons bring about 90% of total annual rainfall and winter accounts for about 10% of total annual rainfall. The mean annual precipitation of Nepal varies from 1,015 mm to 1,516 mm. The daily maximum temperature rises to 44°C in the south in summer and the daily minimum temperature drops below −18°C in the north in winter (DoHM 2014).

Data collection and analysis

The present research is based on orchid checklists from Nepal (Rokaya et al. 2013, Rajbhandari 2014). Each taxon was allocated to a specific phytogeographical region on the basis of its spatial distribution patterns. The account of phytogeographical regions defined by Takhtajan (1986) (Fig. 1) was followed. The composition of orchid species was compared among floristic regions using Krober's percentage similarity, as previously used for Hong Kong bryophytes (Zhang & Corlett 2003). The advantage of using this formula is that it minimizes the effect of the size difference between the two regions under comparison (Tan 1984). Krober's percentage similarity is defined as: $K = 50 \times C(A + B)/(A \times B)$, where A is the number of taxa occurring in the first region; B is the number of taxa occurring in the second region, and C is the number of taxa shared by both regions.

RESULTS

There are 476 taxa of orchids belonging to 108 genera, 454 species, 17 varieties, 3 subspecies, and 2 forms in Nepal. These orchids grow in a variety of habitats: in tree trunks; in moist places along streams, rivers, and water bodies; in grasslands; on rocks in moist places; or in areas rich in humus. Epiphytic orchids displayed the highest number of species (261 species) followed by terrestrial orchids (219 species), lithophytic orchids (65 species), and saprophytic orchids (21 species). The distribution of different species ranges from 60 m

a.s.l. in the tropical region to 5,200 m a.s.l. in the alpine region and species richness reaches its maximum at 1,500 m a.s.l. where there are 241 species.

With respect to phytogeographical regions, 275 orchid species (58% of all species and infrageneric taxa) have an affinity for the EAFR, 261 species (55%) for the ICFR, 78 species (18%) for the MFR, 40 species (8%) for the IFR, and 32 species (7%) for the ITFR. The least number of orchid species (only 3 species, 1%) have an affinity for the SZFR. Some species are widespread in the wild and are found also in Africa or Europe (18 species, 4%). In total, 118 orchid species (25%) are endemic to the Himalayan region extending from Nanga Parbat in the west to Sikkim, Bhutan, and the Yarlung Zangbo valley in the east. Twenty one (4%) orchid species are endemic to Nepal and are distributed from 100 to 3,800 m a.s.l. Krober's percentage similarity showed that the EAFR and IFR have the highest similarity percentage (87%) followed by the MFR and ICFR (62%) and EAFR and MFR (55%). The lowest similarity was found for the ITFR and MFR (4%) followed by the ITFR and IFR (8%) (Table 1).

Table 1: *Krober's percentage similarity among floristic regions.*

	ITFR	SZFR	IFR	ICFR	MFR
EAFR	45.35	50.55	34.36	87.00	55.13
ITFR		18.23	8.44	15.79	4.41
SZFR			17.92	50.57	51.92
IFR				30.27	34.04
ICFR					62.44

Orchid species can bloom throughout the year, but the highest number of orchid species in our study flowers from April to September with a peak during June, July, and August. More than 80 species of Nepalese orchids have ornamental value, 92 species are used for medicinal purposes, and 6 species are used for food purposes. Out of these, use is mostly made of the whole plant (52 species) followed by the underground parts (roots, rhizome, tubers, pseudobulbs; 42 species) and leaves (9 species).

DISCUSSION

The Orchidaceae, the second largest family of angiosperms, has been well explored in Nepal since the first plant collection began in 1802 when the East India Company sent Francis Buchanan-Hamilton, a Scottish doctor employed by the company, to Kathmandu via Makwanpur as a member of a mission to the Nepalese court (Hara et al. 1978).

Many Nepalese orchid species showed an affinity for the EAFR, a result which is similar to a previous study for angiosperm vascular plants from Nepal (Shakya 1983). It is also notable that Mediterranean and West Asiatic elements (the Western Asiatic Subregion of the ITFR in the present study) are numerous to the west from Sikkim through Nepal to Kashmir and Swat (Mani 1978). Our results also support the fact that a high number of plants typical of the arid regions of west Nepal are close to the Central Asiatic Region, as was also reported in a previous study (Shrestha 1982). Nepal, which occupies the central part of the Himalayan range, is rich in plant diversity. The rich diversity can be explained by the overlap of eastern and western floral elements in Nepal (Stainton 1972). In Nepal, people are good at using plants for such various basic needs as food, fiber, tannin, timber, aroma, and ornamentation. The use of orchid species for economic gain was also

reported previously (Rajbhandari 2014). Our results showing that whole plants or belowground parts are used most frequently was similar to previous findings (e.g., Rokaya et al. 2010). This preference for using belowground parts is supported by the fact that they contain higher concentrations of bioactive compounds than do other plant parts.

Overall, this study indicates that the highest percentage of orchids originates from the EAFR. This region thus represents a biodiversity hotspot for orchids and should be given the greatest protection.

Acknowledgements

B.T. supported by project No. LO1415 of the Ministry of Education, Youth and Sports within the National Programme for Sustainability I; M.R. by postdoc grant No. 13-10850P of the Czech Science Foundation; and P.K. by grant No. 14-36098G of the Czech Science Foundation .

References

Chaudhary RP (1998) Biodiversity in Nepal: Status and Conservation. Tecpress Books, Bangkok.

DoHM (2014) Department of Hydrology and Meteorology. Ministry of Science, Technology & Environment, Kathmandu, Nepal.

Hara H, Stearn WT, Williams LHJ (1978) An Enumeration of Flowering Plants of Nepal. Vol. 1. Trustees of British Museum (Natural History), London.

Mani MS (1978) Ecology and the Phytogeography of High Altitude Plants of the Northwest Himalaya. Oxford and IBH, New Delhi.

Ohba H (1988) The alpine flora of Nepal Himalayas: an introductory note. The Himalayan Plants. Vol. 1. (eds H Ohba & SB Malla). University Museum, University of Tokyo, Tokyo.

Press JR, Shrestha KK, Sutton DA (2000) Annotated Checklist of the Flowering Plants of Nepal. Natural History Museum, London.

Rajbhandari KR (2014) Orchids of Nepal: Status, Threat and Conservation. (eds PK Jha, YB Thapa, U Pun et al.), pp 1–43. Department of Plant Resources, Ministry of Forest and Soil Conservation, Kathmandu, Nepal and Central Department of Botany, Tribhuvan University, Kirtipur, Nepal.

Rokaya MB, Münzbergová Z, Timsina B (2010) J. Ethnopharmacol. 130, 485–504.

Rokaya MB, Raskoti BB, Timsina B et al. (2013) Nordic J. Bot. 31, 511–550.

Shakya PR (1983) Vegetation study in east Nepal. Ecological Studies in the Tamur River Basin, East Nepal, and Mountaineering of Mt. Makalu II (ed M Numata), pp. 123–138. Chiba University, Chiba, Japan.

Shrestha TB (1982) Ecology and Vegetation of North-west Nepal (Karnali Region). Royal Nepal Academy, Kathmandu.

Stainton JDA (1972) Forests of Nepal. John Murray, London.

Takhtajan AL (1986) Floristic Regions of the World. University of California Press, Berkeley.

Tan BC (1984) J. Hattori Bot. Lab. 55, 13–22.

Zhang L, Corlett RT (2003) J. Biogeogr. 30, 1329–1337.

Are there any changes in the beginning of flowering of important allergens in the Czech Republic?

Bartošová, L.[1], Hájková, L.[3,*], Kožnarová, V.[4], Možný, M.[5,2], Trnka, M.[1], Žalud, Z.[2]

[1]*Global Change Research Center, Bělidla 986/4a, 603 00 Brno, Czech Republic*

[2]*Institute of Agrosystems and Bioclimatology, Mendel University of Agriculture and Forestry, Zemědělská 1, 613 00 Brno, Czech Republic*

[3]*Department of Biometeorological Applications, Czech Hydrometeorological Institute, Na Šabatce 17, 143 06 Prague, Czech Republic*

[4]*Faculty of Agrobiology, Food and Natural Resources, Czech University of Life Sciences, Kamycka 129, 160 00 Prague, Czech Republic*

[5]*Agrometeorological Observatory in Doksany, Czech Hydrometeorological Institute, 411 82 Doksany, Czech Republic*

**author for correspondence; email: hajkova@chmi.cz*

ABSTRACT

Phenological observations have a long tradition in the Czech Republic; the first phenological notes were taken in the 18th century. Within the entire phenological observation network of the Czech Hydrometeorological Institute, 45 plant species can be observed. These include perennial herbs, grass, and ground bushes growing wildly. Some observed species are among the group of so-called allergens, e.g. silver birch (*Betula pendula* Roth), cocksfoot (*Dactylis glomerata* L.), and meadow foxtail (*Alopecurus pratensis* L.). In this paper, we evaluated the phenological phase beginning of flowering for two of the aforementioned plants at the Mlýny, Chřibská research site (50°52'N, 14°29'E, 350 m a.s.l.). The aim was to assess which meteorological parameters influence phenological onsets as well as to analyze shifts in phenophase onset dates and temperature trends during 1959–2014. During this period, for *B. pendula* the average date of beginning of flowering was 28 April with a standard deviation of 10 days and for *A. pratensis* it was 20 May with a standard deviation of 8 days. The studied species are allergens and their timing and phenological shifting during the spring and their relationship with climate parameters may provide important information for forecasts as part of a pollen warning service.

INTRODUCTION

Phenology, the description of the developmental stages of wild plants, agricultural fruit and crops, and other organisms (such as insects), has several well-defined applications in addition to its use in simulation models. Phenology also involves an important adaptive trait since it determines the duration and timing of the growing season (e.g., Reich et al. 1992).

Aeropalynology and phenology study different natural phenomena, namely the occurrence of pollen in the air and the dynamics of vegetation's vegetative and generative changes within a year. For pollen to take part in aeroplankton, a plant must begin to bloom and at this stage the two areas of science are interconnected (Edmonds 1980). The presence of pollen of some species may be used to predict the oncoming flowering of other species (Latorre et al. 1997). In order to correctly evaluate the results of aeropalynological studies, we require knowledge of the duration and dates of phenological phases as well as of the distribution of potential sources of pollen (Puppi Branzi & Zanotti 1992).

Over the past 30 years, many studies have developed predictive models of tree phenology using such climate variables as temperature and photoperiod (e.g., Murray et al. 1989, Chuine et al. 1999). The use of degree days

for calculating temperature dependent development of plants is widely accepted as a basis for building phenological and population dynamics models (Roltsch et al. 1999). Similar methods for calculating degree days and temperature thresholds have been published by various authors (e.g., Chmielewski et al. 2013).

The aims of this study were to assess which meteorological parameters influence phenological onsets and to analyze shifts in dates of beginning of flowering, an important phenological phase closely connected with pollen release and aeropalynology. Two important pollen allergens in the Czech Republic, meadow foxtail (*Betula pendula* Roth) and silver birch (*Alopecurus pratensis* L., *Poaceae* family), were analyzed in relation to phenological and meteorological measurements within the Czech Hydrometeorological Institute network during 1959–2014. Temperature trends for this period were also calculated.

MATERIALS AND METHODS

The phenological data of two important pollen allergens, a grass (meadow foxtail) and a tree (silver birch), were used in this study. Phenological data comprised observations from the Czech Hydrometeorological Institute and consisted of a dataset for 1959–2014. The beginning of flowering, closely connected with pollen release as well as aeropalynology, was chosen as the phenological phase for analysis. Long-term time phenological series were used from the Mlýny, Chřibská research site (50°52'N, 14°29'E, 350 m a.s.l.). Basic meteorological data (mean, maximum, and minimum air temperature and total precipitation in daily steps) were used from the Varnsdorf station (48°56'N, 16°35'E, 367 m a.s.l.).

Meteorological and phenological data were processed using PhenoClim software (Bartošová et al. 2011, Černá et al. 2012). This software enabled us to conduct quality control of observed datasets and calculate the climate predictor for the phenological phase. To set up the model, the phenological and meteorological database was split into two parts prior to analysis. The first part of the data was used to calibrate the phenological model and the second part was used for model validation. PhenoClim calculated base temperature (T_{base}) and temperature sums (T_S) using three different methods. The first method was based on a simple thermal time model, where PhenoClim determined T_{base} in a set temperature range (e.g., 0–10°C in 0.1°C steps). The start of the calculation was set by temperature conditions and it was necessary to select available daily air temperatures from the input file (mean, maximum, and minimum) which were used to derive T_S. The second method used a simple sine wave where daily minimum and maximum air temperatures were used to produce sine-wave curves for each 24-h period. Degree days were estimated for each day by calculating the area between the defined temperature thresholds and the area below the curve (e.g., Roltsch et al. 1999). The third method was based on three values: T_{base}, T_S, and "start day" (the day when PhenoClim began calculating T_S). It searched for the best combination of these three parameters to establish the phenophase terms with the lowest errors. Based on the calibration dataset, the software selected the best combination of T_S and T_{base} or combination of T_S, T_{base}, and "start day" for each given species. The calculated statistical variables were mean bias error (MBE), root mean square error (RMSE), and coefficient of determination (R^2).

RESULTS

The average dates of beginning of flowering onset for silver birch were observed at the end of April, while the average start of flowering for meadow foxtail was in the second half of May. Both species flowered earlier in later years, with slightly different rates of change of 1.4 (meadow foxtail) and 2.1 (silver birch) days per decade (Table 1).

At the experimental site in Varnsdorf, mean annual air temperature showed a substantial increase of 0.29°C per decade over 1959–2014. Substantial increasing trends of mean, minimum, and maximum air

temperatures were observed during April and May, as well, increasing by 0.23, 0.45, and 0.49°C per decade, respectively. Total precipitation decreased during April and May, while total annual precipitation increased.

Table 1: *Phenological phase dates and statistical characteristics (** p < 0.01).*

	Average date	Earliest date	Latest date	Standard deviation	Linear trend *days*	
	Day of year	*Day of year*	*Day of year*	*days*	Per decade	1959–2014
Meadow foxtail	19 May	5 May	3 June	6	1.4	7.9**
(Alopecurus pratensis)	*139*	*125*	*154*			
Silver birch	29 April	9 April	18 May	9	2.1	11.8**
(Betula pendula)	*119*	*199*	*138*			

The results showed that for meadow foxtail and silver birch maximum air temperature was the best predictor for the timing of phenological phase BBCH 61 when using PhenoClim. Maximum air temperature and mean air temperature had the lowest error values (RMSE and MBE). The third method with three parameters (T_{base}, T_S, and start day) displayed the best results in predicting phenophase onset (lowest RMSE and MBE values). This method was called the "best combination" model. The results for the meadow foxtail dataset had the error value of 4.9 days (RMSE), while the error value was higher for silver birch at 6.4 days (RMSE). T_{base} using this method was 0.2°C for *A. pratensis* and 4.2°C for *B. pendula*. The thermal time model and the sine wave method had higher error values and lower coefficients of determination (Table 2).

Table 2: *Root mean square error (RMSE) and mean bias error (MBE) for three phenological models (best combination [BS], thermal time [TTM], and sine wave [SW] models) and calculated base temperature (T_{base}) and temperature sums (T_S) for two observed species.*

	Model	RMSE	MBE	R^2	T_{base} °C	T_S °C	Start day
Meadow foxtail *(Alopecurus pratensis)*	BS	4.9	0.7	0.6	0.2	540	67
	TTM	6.1	-1.6	0.6	8.4	411.9	x
	SW	6.2	-1.7	0.6	6.1	264.3	x
Silver birch *(Betula pendula)*	BS	6.4	-0.1	0.4	4.2	301	82
	TTM	7.8	-1.4	0.4	9.3	180.1	x
	SW	7.7	-1.4	0.4	2.7	274.2	x

DISCUSSION

The results of the present study show a trend of increasing air temperature at the experimental site in Varnsdorf as well as an earlier onset of flowering for meadow foxtail and silver birch during the observation period of 1959–2014. PhenoClim calculated the lowest error values (RMSE and MBE) for the best combination model, which is recommended for further phenophase modelling. The thermal time and sine wave models showed higher RMSE and MBE values and are therefore not as useful.

Similar methods for calculating degree days and temperature thresholds have been published by various authors. Chmielewski et al. (2011) used a simple thermal time model for the beginning of apple blossoming. The RMSE between modelled and observed apple blossom data in that study varied from 4.6 to 5.6 days. In a later study, Chmielewski et al. (2013) analyzed phenophases of the great tit (*Parus major*) and selected a

phenological model that was able to calculate the beginning of egg laying. They used four types of thermal time models and finally chose a model with air temperature and photoperiod with a starting date of temperature accumulation on 1 January. Error (RMSE) for this model was 3 days.

Fu et al. (2012) used five types of phenological models (including a thermal time model) to predict bud burst for deciduous trees, including birch. They recommended their sequential model (a model which used a triangular chilling function and a sigmoid forcing function), with RMSE from 3.4 to 4 days, as the most appropriate model for forecasting the terms of bud bursting.

The results of our analysis showed that the best combination model could be used to model phenophase onset as an indicator under both present and future climate conditions. Regarding the question of whether there have been any changes in flowering for the two studied allergens, we can conclude that flowering has shifted to earlier dates. The most probable predictor of these changes is maximum temperature, which could also be used for further modelling. The model could also play an important role in providing information on allergen distribution as well as being useful in predicting the start and end of the pollen season for a public warning service.

Acknowledgement

Supported by project No. CZ.1.07/2.3.00/20.0248 "Building up a multidisciplinary scientific team focused on drought," project No. LD13030 supporting the Czech Republic's participation in COST Action ES1106, and a project of the Ministry of Education, Youth and Sports.

References

Beaubien EG, Freeland HJ (2000) Int. J. Biometorol. 44, 53–59.

Bartošová L, Trnka M, Balek J, Bauer Z, Žalud Z (2011) Various methods of processing long-term phenological series. Bioclimate: Source and Limit of Social Development – International Scientific Conference (eds B Šiška, M Hauptvogl, M Eliašová), Topoľčianky, Slovakia.

Černá H, Bartošová L, Trnka M, Bauer Z, Štěpánek P, Možný M, Dubrovský M, Žalud Z (2012) Acta Univ. Agric. Silvic. Mendelianae Brun. 60, 9–18.

Chmielewski FM, Blümel K, Henniges Y, Blanke M, Weber RWS, Zoth M (2011) Meteorol Z. 20, 487–498.

Chmielewski FM, Blümel K, Scherbaum-Heberer C et al. (2013) Int. J. Biometorol. 57, 287–297.

Chuine I, Cour P, Rousseau DD (1999) Plant Cell Environ. 22, 1–13.

Edmonds RL (1980) Can. J. For. Res. 10, 327–337.

Fu YH, Campioli M, Deckmyn G et al. (2012) PLoS ONE 7, e47324.

Latorre C, Quade J, McIntosh WC (1997) Earth Planet. Sci. Lett. 146, 83–96.

Menzel A (2000) Int. J. Biometorol. 44, 76–81.

Murray MB, Cannell MGR, Smith RI (1989) J. Appl. Ecol. 26, 693–700.

Puppi Branzi G., Zanotti AL (1992) Aerobiol. 8, 69–74.

Reich PB, Walters MB, Ellsworth DS (1992) Ecol. Monogr. 62, 365–392.

Roltsch WJ, Zalom FG, Strawn AJ et al. (1999) Int. J. Biometorol. 42, 169–176.

Tutin TG (1980) Gramineae (*Poaceae*). Flora Europaea. Vol. 5, *Alismataceae* to *Orchidaceae* (eds TG Tutin et al.), pp. 118–267. Cambridge University Press, Cambridge.

Walters SM (1993) *Betula* L. Flora Europaea. Vol. 1, *Psilotaceae* to *Platanaceae* (eds TG Tutin et al.), pp. 68–69. Cambridge University Press, Cambridge.

Summer fluxes of nitrous oxide from boreal forest

Machacova, K.[1,*], Pihlatie, M.[2,3], Halmeenmäki, E.[2], Pavelka, M.[1], Dušek, J.[1], Bäck, J.[2,4], Urban, O.[1]

[1]*Global Change Research Centre, Bělidla 986/4a, 603 00 Brno, Czech Republic*
[2]*Department of Physics, University of Helsinki, P.O. Box 48, 00014 Helsinki, Finland*
[3]*Department of Food and Environmental Sciences, University of Helsinki, P.O. Box 56, 00014 Helsinki, Finland*
[4]*Department of Forest Sciences, University of Helsinki, P.O. Box 27, 00014 Helsinki, Finland*
**author for correspondence; email: machacova.k@czechglobe.cz*

ABSTRACT

Boreal forests cover almost one-third of the global forest area, and results of soil measurements show them to be a natural source of the important greenhouse gas nitrous oxide (N_2O). Nevertheless, N_2O fluxes from boreal tree species have been excluded from calculations of N_2O exchanges from forest ecosystems. Therefore, our objective was to quantify and scale up the N_2O fluxes from stems of mature silver birch (*Betula pendula*), Scots pine (*Pinus sylvestris*), and Norway spruce (*Picea abies*), as well as from the forest floor of a boreal forest in Finland during June and July 2014. This study shows that boreal tree species emit N_2O from their stems under natural field conditions and significantly contribute up to 8% of forest floor fluxes of N_2O. Spruce trees seem to be the strongest N_2O emitter among the studied tree species. Moreover, the N_2O flux rates from both coniferous tree species increased with decreasing soil water content. This study highlights the necessity to include N_2O fluxes from trees within the total greenhouse gas budget of forest ecosystems.

INTRODUCTION

With an area of about 920 million ha, boreal forests represent almost three-fourths of the world's coniferous forests (Kuusela 1992). They are presumed to be a natural source of nitrous oxide (N_2O) (Dalal & Allen 2008), an important greenhouse gas produced in soils. Despite the evidence that trees may be important sources of N_2O (e.g. Rusch & Rennenberg 1998, Pihlatie et al. 2005, Machacova et al. 2013a), they have so far been excluded from calculations of N_2O exchanges from boreal forest ecosystems. Moreover, the ability of boreal tree species to emit N_2O has been characterized only poorly (Machacova et al. 2013b, Machacova et al. 2014) and there is a need for further investigations of the emission capacities of those tree species in the boreal zone. Our main objectives were therefore to quantify and upscale the N_2O fluxes from stems of mature silver birch (*Betula pendula* Roth), Scots pine (*Pinus sylvestris* L.), and Norway spruce (*Picea abies* (L.) Karst.), as well as from the forest floor of a boreal forest in Southern Finland during summer 2014 and to estimate whether soil water content affects forests' N_2O exchange.

MATERIALS AND METHODS

The study was performed in a boreal forest dominated by *P. sylvestris* followed by *P. abies* and *B. pendula* at the SMEAR II station (61°51'N, 24°17'E) in Hyytiälä, Finland, in June and July 2014. All measurements were taken in natural soil moisture conditions, which may be divided into wet (W plot, mean soil volumetric water content [VWC] ± standard error: 0.92 ± 0.01 $m^3 m^{-3}$), moderately wet (MW plot, VWC: 0.37 ± 0.02 $m^3 m^{-3}$), and dry (D plot, VWC: 0.23 ± 0.02 $m^3 m^{-3}$) conditions. Stem N_2O flux rates were investigated from three pine, three spruce, and three birch trees on the W and MW plots and from three pine trees on the D plot, as this plot did not contain birch or spruce trees. Tree and stand characteristics are presented in Table 1. Forest floor fluxes were determined

at three positions on the W and MW plots and at one position on the D plot. Parallel stem and forest floor measurements were conducted in 2-week periods, five times altogether.

N_2O flux rates from the bottom part of stems were determined manually using two different static chamber systems (circumferential and box stem chambers, Machacova et al. 2014). Nine gas samples (20 ml each) were taken from closed chambers at regular intervals of 30–50 min over a period of 5 h. Forest floor N_2O fluxes were measured using six large opaque manual soil chambers (Machacova et al. 2013b) and one opaque automatic chamber (Korhonen et al. 2013). The manual chambers were closed for ca 35 min in June 2014 during which five gas samples (20 ml each) were taken at time intervals of 1, 5, 15, 25, and 35 min. In July 2014, the closure time was changed to ca 75 min with additional uptake intervals of 55 and 75 min. The automatic chamber was closed once per day and gas samples were withdrawn from the headspace at time intervals of 1, 5, 10, 20, 30, and 50 min. The samples were stored in glass vials at 4°C and analysed by a gas chromatograph (electron capture detector). Flux rates, expressed in μg N_2O m^{-2} of stem or soil surface area h^{-1}, were calculated by linear least square fits of the time series of N_2O concentrations. N_2O fluxes were scaled up to the landscape level using stem surface area for each tree calculated as the lateral surface area of a right circular cone, estimated forest density, and stand basal area (Table 1). Due to non-normally distributed data and/or data with unequal variances, the Mann–Whitney rank sum test was applied with statistical significance defined at $p < 0.05$.

Table 1: *Tree and stand characteristics (mean ± SD) from wet (W), moderately wet (MW), and dry (D) plots. Trees were approximately 50 years of age, except for three birches and one spruce on the wet plot, which were unambiguously younger. Stand basal area was measured directly on plots using a rod relascope. DBH – stem diameter at breast height.*

	Tree height	DBH	Stem surface area	Forest density	Stand basal area
	m	*cm*	m^2	*trees* ha^{-1}	m^2 ha^{-1}
Birch *(Betula pendula)*					
W plot	12.3 ± 1.2	9.7 ± 0.4	1.9 ± 0.1	1200	6
MW plot	22.1 ± 0.7	21.3 ± 3.7	7.4 ± 1.2	200	4
Pine *(Pinus sylvestris)*					
W plot	18.2 ± 1.3	19.9 ± 3.3	5.8 ± 1.3	400	20
MW plot	20.6 ± 0.4	18.7 ± 0.2	6.1 ± 0.1	800	21
D plot	18.7 ± 0.7	19.3 ± 1.4	5.7 ± 0.6	1400	27
Spruce *(Picea abies)*					
W plot	14.5 ± 4.4	16.6 ± 6.7	4.2 ± 2.3	400	4
MW plot	21.2 ± 1.0	23.6 ± 2.0	7.9 ± 1.0	400	5

RESULTS

Our study shows that mature *B. pendula*, *P. sylvestris*, and *P. abies* trees have the ability to emit N_2O from their stems (Fig. 1a). The highest up-scaled tree N_2O emissions (i.e. positive fluxes) within the studied forest were determined from spruce stems on both the W and MW plots with median rates of 0.38 and 0.64 mg N_2O ha^{-1} h^{-1}, respectively. Pine was the second largest emitter of N_2O among the selected tree species (0.22, 0.32, and 0.37 mg N_2O ha^{-1} h^{-1} on the W, MW, and D plots, respectively) followed by birch (0.21 and 0.16 mg N_2O ha^{-1} h^{-1} on the W and MW plots, respectively). The stem emission rates of both conifers significantly increased with decreasing soil water content, while the N_2O emissions from birch showed the opposite trend, although the latter was not statistically significant.

The forest floor was either a sink for N_2O (i.e. negative flux or uptake, −4.9 mg N_2O ha^{-1} h^{-1} on the W plot) or a source under lower mean soil water content (15.2 and 7.4 mg N_2O ha^{-1} h^{-1} on the MW and D plots, respectively) (Fig. 1b). The estimated tree stem N_2O emissions accounted for more than 4% of the forest floor uptake for birch and pine trees and almost 8% for spruce trees, thus constituting a positive N_2O source on the W plot (Fig. 1a). With lower soil water content, both stems and the forest floor were sources of N_2O with trees contributing 1–5% of forest floor fluxes.

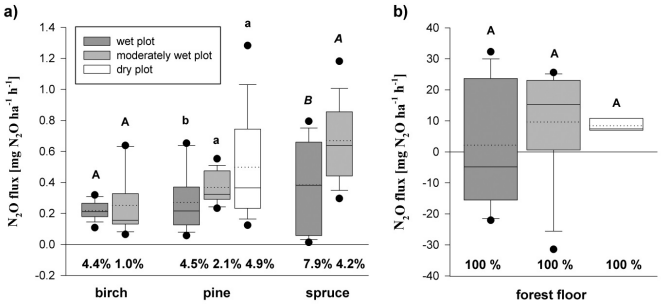

Fig. 1: *N_2O fluxes from (a) stems of birch, pine, and spruce trees, and (b) forest floor in boreal mixed forest. Box plots: solid (dashed) line – median (mean), box boundaries – 25th/75th percentile, whiskers – 10th/90th percentile, dots – outliers. Forest floor fluxes were determined as median/mean of measurements from 3 (W and MW plots) and 1 (D plot) soil chamber(s) with 5 replicates. Stem fluxes were expressed as median/mean of measurements on three trees per tree species and plot, with five replicates. Birch and spruce were not available on the D plot. Statistically significant differences at $p < 0.05$ among plots for each tree species are marked with different letters. Percentage contribution of stems to the N_2O forest exchange is calculated as absolute percentage from the forest floor flux taken as 100%.*

DISCUSSION

Based on our results, it is obvious that the coniferous *P. abies* and *P. sylvestris* and broadleaf *B. pendula* emit N_2O from their stems and that they contribute significantly to the N_2O exchange of boreal forests (Fig. 1a). The highest N_2O emission rates and related contributions to forest floor fluxes (up to 8%) were detected in spruce trees, followed by pine and birch trees. Spruce was also the strongest emitter of N_2O among the selected tree species in a comparison of flux rates per stem area unit (Machacova et al. 2014). We suppose that N_2O is taken up by roots from the soil and transported in xylem via the transpiration stream. This hypothesis is supported by i) the relatively good water solubility of N_2O (Yu et al. 1997), and ii) the detected ability of plants to emit N_2O independently of the formation of an aerenchyma system, which is known as a second possible gas-transport pathway (Machacova et al. 2013a). As spruce trees were characterised by the highest projected leaf area (mean 88 m^2 per tree) among the selected tree species, we expect that spruce have higher transpiration and sap flow rates than do pine and birch (Ge et al. 2011), resulting in higher N_2O flux rates.

The flux rates of N_2O from birch, scaled up to ecosystem level, were unexpectedly lower than were those from pine trees, especially with lower soil water content, even though i) N_2O emission rates per stem area unit were higher for birch than they were for pine trees on the MW plot (Machacova et al. 2014), ii) the projected leaf area of birch trees (54 m^2) exceeded the area of pine trees (28 m^2), and iii) the wood of birch (diffuse-porous type; Arbellay et al. 2010) seems to have a higher gas-diffusion coefficient than do conifers (Sorz & Hietz 2006). The explanation might lie in the scaling up of flux rates, which takes into account different tree and stand characteristics and which enables a comparison of N_2O fluxes between tree stems and the forest floor on the ecosystem level.

Notably, the N_2O emission rates of pine and spruce trees, both conifers, significantly increased with decreasing soil water content. In contrast, the N_2O emissions from stems of broadleaf birch trees indicated the opposite trend. In comparison to conifers, N_2O might be transported by birch trees predominantly via the aerenchyma system, which might be formed by this broadleaf species as a response to high soil water content to supply its roots with O_2. The N_2O emissions from trees were accompanied by relatively low forest floor flux rates (Fig. 1b) typical for the studied forest (Pihlatie et al. 2007). The forest floor was even a sink for N_2O on the W plot. Due to this high soil water content on the W plot, we expect anaerobic conditions in the soil. In these conditions, anaerobic denitrification may result in the reduction of N_2O to dinitrogen (N_2) (Smith et al. 2003), leading to lower N_2O concentrations in the soil and a simultaneous uptake of N_2O from the atmosphere. In contrast, we expect rather aerobic conditions on both MW and D plots supporting greater N_2O production in the soil and therefore also greater N_2O uptake by tree roots.

Stem N_2O emissions on the W plot constituted 4.4%, 4.5%, and 7.9% of the forest floor uptake for birch, pine, and spruce, respectively, thus significantly decreasing forest floor N_2O uptake on the W plot. On the other hand, stem N_2O emissions accounted for 1–5% of the forest floor emissions on the MW and D plots with lower soil water content, thus increasing the N_2O budget of the boreal forest. The shoot fluxes of N_2O were not measured during 2014; however, the shoot-to-stem N_2O flux ratio of 16 for *P. sylvestris* in 2013 (Machacova et al. unpublished data) emphasizes the important role of canopies in the ecosystem's N_2O exchange. We therefore predict a considerably higher contribution from whole trees to forest floor N_2O fluxes compared to the present estimates based only on stem N_2O fluxes.

Acknowledgement

Supported by EU FP7 project ExpeER (No. 262060), Ministry of Education, Youth and Sports projects ENVIMET (No. CZ.1.07/2.3.00/20.0246) and No. LO1415, Emil Aaltonen Foundation, The Academy of Finland Centre of Excellence (project No. 1118615), Academy of Finland Academy Research Fellow project (No. 263858), and ICOS Finland. We thank S. Stellner and J. Mikula for technical support.

References

Arbellay E, Stoffel M, Bollschweiler M (2010) Tree Physiol. 30, 1290–1298.

Dalal RC, Allen DE (2008) Aust. J. Bot. 56, 369–407.

Ge ZM, Kellomäki S, Peltola H et al. (2011) Tree Physiol. 31, 323–338.

Korhonen JFJ, Pihlatie M, Pumpanen J et al. (2013) Biogeosciences 10, 1083–1095.

Kuusela K (1992) Unasylva 43, 3–13.

Machacova K, Papen H, Kreuzwieser J et al. (2013a) Plant Soil 364, 287–301.

Machacova K, Pihlatie M, Vanhatalo A et al. (2013b) Rep. Ser. Aerosol Sci. 142, 362–366.

Machacova K, Halmeenmäki E, Pavelka M et al. (2014) Rep. Ser. Aerosol Sci. 157, 408–412.

Pihlatie M, Ambus P, Rinne J et al. (2005) New Phytol. 168, 93–98.

Pihlatie M, Pumpanen J, Rinne J et al. (2007) Tellus 59B, 458–469.

Rusch H, Rennenberg H (1998) Plant Soil 201, 1–7.

Smith KA, Ball T, Conen F et al. (2003) Eur. J. Soil Sci. 54, 779–791.

Sorz J, Hietz P (2006) Trees 20, 34–41.

Yu KW, Wang ZP, Chen GX (1997) Biol. Fert. Soils 24, 341–343.

The relationships of soil CO_2 flux with selected Norway spruce root parameters and sterol content in the soil

Holub, F.[1,2], Fabiánek, T.[1], Večeřová, K.[1], Moos, M.[1], Oravec, M.[1], Tříska, J.[1], Marková, I.[2], Edwards, M. [1], Cudlín, P.[1,*]

[1]*Global Change Research Centre, Bělidla 986/4a, 603 00 Brno, Czech Republic*

[2]*Institute of Forestry, Faculty of Forestry and Wood Technology, Mendel University in Brno, Zemědělská 3, 613 00 Brno, Czech Republic*

**author for correspondence; email: cudlin.p@czechglobe.cz*

ABSTRACT

The flow of CO_2 from the soil is a very important part of the carbon cycle in an ecosystem. The aim of our work was to determine how roots and rhizospheric fungi contribute to CO_2 flux from the soil. Preliminary results from two years of research are presented. The research on how root biomass as well as ergosterol and phytosterol contents in roots and soil affected CO_2 flux from the soil was conducted in a 108-year-old Norway spruce (*Picea abies* (L.) Karst.) forest in the Drahany Highlands during 2010 and 2011. CO_2 flow was measured using a LI-8100 portable closed gasometric system (Li-Cor, USA). The dry weight and volume of individual root categories (< 1 mm, 1–2 mm, 2–5 mm, > 5 mm), C and N contents in the roots, as well as ergosterol, β-sitosterol, and campesterol contents in the soil and roots were determined from root-containing soil samples located in the circular measurement chamber. In addition, sterol content was determined in the soil only. Our soil respiration results correspond with the findings of Buchman (2000) who found respiration values between 5–7 μmol CO_2 m^{-2} s^{-1} in a 111-year-old spruce forest. A significant influence on soil respiration was proven only for sitosterol content in the soil. The relationships among soil CO_2 flux, root characteristics, and nitrogen and sterol contents in the roots and soil are discussed.

INTRODUCTION

Soil CO_2 flux comprises 60–80% of the carbon cycle in temperate forests escaping from the entire ecosystem into the air (Le Dantec et al. 1999). CO_2 flux from the soil thus significantly contributes to reducing the amount of carbon captured by a forest. Roots create in their surroundings a specific environment inhabited by numerous species of microorganisms depending on the exudate flow from the roots (Smith & Read 1997). Through exudates alone, the roots affect soil biological activity. However, it remains a question how roots influence soil CO_2 flux. Root respiration is usually estimated to be responsible for nearly half of total soil respiration but the amount fluctuates from 10% to 90% in different studies (Hanson et al. 2000). Soil biological activity is connected with the rate of decomposition and mineralization of organic substances. It is therefore important to know the role roots and rhizospheric microorganisms (primarily ectomycorrhizal fungi) play in the release of CO_2 from the soil.

Sterols are one of the most important substances in soil. They indicate the presence and physiological activity of plants (phytosterols), animals (e.g. cholesterol), and fungi (e.g. ergosterol). Ergosterol is a common biomarker for fungi and its occurrence suggests recently metabolically active fungal biomass. Therefore, its quantification in the roots and soils is often used as an indirect measurement of mycorrhizal systems (Nylund & Wallander 1992). The concentration of β-sitosterol, a major plant sterol, in soil may be related to cultivation type and the presence of decomposing plant matter, and it could be considered to be an indicator of

phytomass quantity in the soil (Puglisi et al. 2003). The aim of our paper is to clarify the dependence of soil CO_2 flux on selected parameters of the root system and rhizosphere microflora.

MATERIALS AND METHODS

Research on how root biomass and ergosterol content in roots and soil affect CO_2 flux from the soil was carried out in Rajec nad Svitavou–Němčice in the Drahany Highlands in the Czech Republic during 2010 and 2011. In the two years of observation, samples were processed from 27 measuring locations in a 105-year-old spruce monoculture. Prior to taking measurements, the humus horizons were separated from the mineral horizons by inserting a sharp metal sheet. CO_2 flow was measured using a LI-8100 portable closed gasometric system (Li-Cor, USA). Individual CO_2 flux measurements were performed in triplicate (the average was used) at each location. Each measurement took 2 min. A linear function was applied to calculate soil respiration. To compare individual measurements, R_{10} (the value of soil respiration at 10°C) was used according to Pavelka et al. (2007).

All soil with roots located within the circular measurement chamber over the metal sheet was sampled and analysed. The following parameters were determined: dry weight and volume (using image analysis; Gronský et al. 2008) of individual root categories (< 1 mm, 1–2 mm, 2–5 mm, > 5 mm), C and N contents in the roots, and ergosterol, β-sitosterol, and campesterol contents in the soil and roots. In addition, sterol content was determined in the soil. Obtained data were processed using multiple regression with gradual selection.

RESULTS

Soil respiration in the spruce forest stand ranged between 115 and 445 mg dm^{-3} day^{-1}. Preliminary results obtained in 2010 from 7 independent measurements indicated that samples with higher respiration had lower ergosterol/β-sitosterol and C/N contents in roots and higher ergosterol concentrations in the roots and soils. A significant influence on soil respiration was proven only for the ratio of ergosterol to β-sitosterol.

The results of the second year of experiments from 20 independent measurements are shown in Tables 1 and 2. Of all the root characteristics and sterol content parameters, only N content in fine roots and β-sitosterol content in the soil were significantly correlated with CO_2 flux from the soil (Table 3).

In 2011, we investigated whether inserting a horizontal sheet between soil horizons increased the flow of CO_2. We found that the values of the CO_2 flow were higher when measured prior to insertion than they were after insertion but this difference was not significant. We concluded that sheet insertion did not cause humus horizons disruption and so did not negatively affect the flow of CO_2 from the soil.

DISCUSSION

Our soil respiration results correspond with the findings of Buchman (2000) who found respiration values between 5–7 μmol CO_2 m^{-2} s^{-1} in a 111-year-old spruce forest. Only 7 measurements were successful in the first year of the study. Unfortunately, their results could not be added to the next 20 measurements in 2011 because of different climatic conditions influencing the results. In the first year of observation, only the ratio of ergosterol to β-sitosterol in the soil significantly affected soil respiration. The negative correlation to this ratio could be connected to increased activity of saprophytic microorganisms in the soil.

Table 1: *Respiratory CO_2 flux from the soil and parameter values of the Picea abies root system in 2011. N = 20.*

Sample	Flux CO_2	RDW	RDW	RV	RV	RTN	SRL	SRL
		cat. I	cat. I–IV	cat. I	cat. I–IV	cat. I	cat. I	cat. I–IV
	mg dm^{-3} day^{-1}	*g dm^{-3}*	g dm^{-3}	mm^3 dm^{-3}	mm^3 dm^{-3}	dm^{-3}	mm g^{-1}	mm g^{-1}
Mean	242.799	2.997	7.882	8,999.487	77,640.340	13,546.571	17,053.863	7,929.007
SD	80.893	0.995	3.407	3,997.303	177,184.430	3,648.642	3,034.569	3,601.562

RDW: root dry weight, RV: root volume, RTN: root tip number, SRL: specific root length; cat.: root category, where category I (fine roots) are roots < 1 mm.

Table 2: *Sterol concentrations per dry weight unit of Picea abies roots and per dry weight unit of soil as well as C and N contents in roots in 2011. N = 20.*

Sample	Roots						Soil			
	Erg	**Sit**	**Cam**	**Erg/ Sit**	N	C	**Erg**	**Sit**	**Cam**	**Erg/ Sit**
	µg g^{-1}	µg g^{-1}	µg g^{-1}		%	%	µg g^{-1}	µg g^{-1}	µg g^{-1}	
Mean	91.840	324.174	96.422	0.295	1.548	51.575	132.975	432.494	41.818	0.314
SD	28.489	71.207	17.190	0.105	0.169	0.664	38.725	108.737	10.628	0.075

Erg: Ergosterol, Sit: Sitosterol, Cam: Campesterol.

This corresponds to observations by Kanerva et al. (2007). In the second year of observation, β-sitosterol again correlated with CO_2 flux from the soil. Until now, there has been a lack of data about the role of sitosterol in below ground ecosystem functioning. According to Sinsabaugh & Moorhead (1994) and Puglisi et al. (2003), β-sitosterol content can be considered to be an indicator of increased phytomass in the soil. It is possible that β-sitosterol content in the soil is connected in some manner to fine root and mycorrhiza quantity. The influence of N content in roots on CO_2 flow from the soil might be connected to increased biological activity of the fine roots. Ryan et al. (1995) reported that increased N concentrations in fine roots caused increased respiration.

The other studied parameters were not significantly correlated with soil respiration. This might have been caused also by the small quantity of samples analysed and the huge soil variability across locations.

Determining the complicated interrelationships between the CO_2 flux from soil and roots and rhizospheric and soil microflora will require even more complex experiments and observations in future.

Table 3: *Regression model results.*

Parameter	Coefficient	Standard coefficient	*p*	
β-sitosterol in soil	*0.0050*	*0.459806*	*0.006653*	
Nitrogen in roots	*-10.9782*	*-0.522162*	*0.002603*	
Total model	R^2	*F*	*p*	df
	0.546397	*12.04570*	*0.00369*	*2*

Acknowledgement

Supported by the Ministry of Education, Youth and Sports within the National Programme for Sustainability, project No. LO1415.

References

Buchmann N (2000) Soil Biol. Biochem. 32, 1625–1635.

Gronský R, Cudlín P, Chmelíková E et al. (2005) Bull. Czech Bot. Soc. Materiály 20, 141–145.

Hanson PJ, Edwards NT, Garten CT et al. (2000) Biogeochem. 48, 115–146.

Le Dantec V, Epron D, Dufrêne E (1999) Plant Soil 214, 125–132.

Kanerva S, Kitunen V, Loponen J et al. (2007) Biol. Fert. Soils 44, 547–556.

Nylund J-E, Wallander H (1992) Methods Microbiol. 24, 77–88.

Pavelka M, Acosta M, Marek MV et al. (2007) Plant Soil 292, 171–179.

Puglisi E, Nicelli M, Capri E et al. (2003) J. Environ. Qual. 32, 466–471.

Ryan MG, Hubbard RM, Pongracic S et al. (1995) Tree Physiol. 16, 333–343.

Sinsabaugh RL, Moorhead DL (1994) Soil Biol. Biochem. 26, 1305–1331.

Smith SE, Read DJ (1997) Mycorrhizal Symbiosis. 2nd ed. Academic Press, London.

Convergence of morphological, biochemical, and physiological traits of upper and lower canopy of European beech leaves and Norway spruce needles within altitudinal gradients

Rajsnerová, P.[1,2,*], Klem, K.[1], Večeřová, K.[1], Veselá, B.[1,2], Novotná, K.[1,2], Rajsner, L.[1,2], Holub, P.[1,2], Oravec, M.[1], Urban, O.[1]

1Global Change Research Centre, Bělidla 986/4a, 60300 Brno, Czech Republic
2Mendel University in Brno, Zemědělská 1/1665, 61300 Brno, Czech Republic
**author for correspondence; email: rajsnerova.p@czechglobe.cz*

ABSTRACT

Climatic variation along altitudinal gradients provides an excellent natural experimental set-up for investigating the possible impacts of climate change on terrestrial organisms and ecosystems. The present work has explored for the first time the acclimation of upper versus lower canopy leaves or needles in European beech (*Fagus sylvatica*) and Norway spruce (*Picea abies*) forests along an altitudinal gradient. We tested the hypothesis that restrictive climatic conditions associated with high altitudes reduce within-canopy variations of leaf traits. The investigated beech and spruce forests were located on the southern slope of the Hrubý Jeseník Mountains (Czech Republic). All measurements were taken on leaves from the upper and lower parts of the canopy of mature trees (>60 years old) growing at low (400 m a.s.l.), middle (720 m a.s.l.), and high (1,100 m a.s.l.) altitudes.

Generally, we observed that with increasing altitude, which is associated with adverse microclimatic conditions, a convergence of CO_2 assimilation rate and other physiological, morphological, and biochemical characteristics between the upper and lower canopy occurred. However, differences in altitudinal response among individual traits and species were found. Such plasticity in acclimation of leaves and needles has the potential to cause substantial change in the photosynthesis of individual parts of forest canopies within the vertical profile and their contribution to the overall carbon balance of vegetation.

INTRODUCTION

Altitudinal gradients provide an excellent natural experiment to study such effects of changing microclimatic conditions associated with changing altitude as decreases in partial pressure of gases, reduced temperature and clear-sky turbidity, increased fraction of ultraviolet radiation, and increased precipitation (Körner 2007). In contrast, soil conditions are not directly related to altitude and depend, among other things, on slope orientation, geographical topology, and/or region (reviewed in Becker et al. 2007). Although a number of altitudinal gradient studies have been already conducted on forest tree species, these have not yet sufficiently explored interactions between the effects of altitude and vertical light stratification within the forest canopy.

An exponential attenuation of solar radiation passing through a canopy leads to distinct light intensity across a vertical canopy profile. Leaves can acclimate to their light environments by (i) modulating leaf morphology, anatomy, and chloroplast ultrastructure (e.g. Yano & Terashima 2001); and (ii) changing their chemical composition, including in particular reallocation of N among photosynthetic components associated with light capture, thylakoid membrane composition, and CO_2 assimilation (e.g. Hikosaka 2005).

In our study, we hypothesized that adverse climatic conditions at higher altitudes would reduce photosynthetic light use efficiency in the upper part of the canopy and that lower canopy leaves or needles would replace the functional loss of the upper canopy. The interactions between altitude and light acclimation within a canopy were studied in mature European beech (*Fagus sylvatica* L.) and Norway spruce (*Picea abies* (L.) Karst.) forests.

MATERIALS AND METHODS

Forest stands selected for this study were located on the southern slope of Mravenečník Mountain (Hrubý Jeseník Mountains, Czech Republic, 50°2'N, 17°9'E). Leaf/needle sampling and physiological measurements were made on European beech and Norway spruce trees naturally occurring at low (L; 400 m a.s.l.), middle (M; 720 m a.s.l.), and high (H; 1100 m a.s.l.) altitudes. Individual sites are characterized by gradients in mean annual air temperature (7.59°C for L, 5.94°C for M, and 3.82°C for H) and mean annual sum of precipitation (30-year averages: L 753 mm, M 891 mm, and H 1,083 mm). Stands with mature trees (age > 60 years) and comparable stand density were selected at all altitudes.

We evaluated physiological and biochemical parameters in upper (sun-acclimated) and lower (shade-acclimated) canopy leaves and needles of beech and spruce trees, respectively. Measurements were carried out on 13 representative trees from each altitude and species.

Light-saturated CO_2 assimilation (A_{max}) rates were determined under constant conditions (leaf temperature: 25 ± 1°C, relative air humidity: 55 ± 3%, CO_2 concentration: 385 ± 5 μmol mol^{-1}, and irradiance: 1200 μmol m^{-2} s^{-1}) using a Li-6400XT gas exchange system (Li-Cor, USA). Content of the enzyme Rubisco was determined by sodium dodecyl sulphate polyacrylamide gel electrophoresis using a Mini-PROTEAN 3 system (Bio-Rad, USA). The elemental analyses of C and N were conducted using an automatic analyser (Flash 2000, Thermo Scientific, USA). The leaf mass per area (LMA) ratio was defined as the ratio between leaf dry mass and projected leaf area.

All measurements and samplings were made during the extended noon period (10:00–14:00 LMT) at two stages of the growing season characterized by active growth (June–July) and the end of the season (September) in 2013 and 2014 for beech and spruce respectively.

Two-way ANOVA followed by a multiple range test was used to investigate the effect of altitude on the measured parameters. All statistical tests were done in Statistica 12 (StatSoft, USA).

RESULTS

The upper canopy's A_{max} was highest at altitude M, whereas for lower canopy A_{max} increased with increasing altitude up to altitude H (Fig. 1). Such distribution of A_{max} along the altitudinal gradient led to the convergence of CO_2 assimilation of the upper and lower canopy with increasing altitude, particularly during autumn, in both species studied.

Similarly, convergence of the upper and lower canopy with increasing altitude was observed for LMA, particularly in beech, although the vertical position within the canopy had a major effect on this morphological parameter. Significantly lower LMA values were found in the lower canopy as compared to the upper canopy. Similarly, the convergence of nitrogen content was more pronounced in beech than it was in spruce. In spruce, a significant seasonal change in nitrogen allocation within the vertical canopy profile was observed. While generally higher nitrogen content was observed in the upper canopy for all altitudes in summer, in autumn the opposite nitrogen allocation was found.

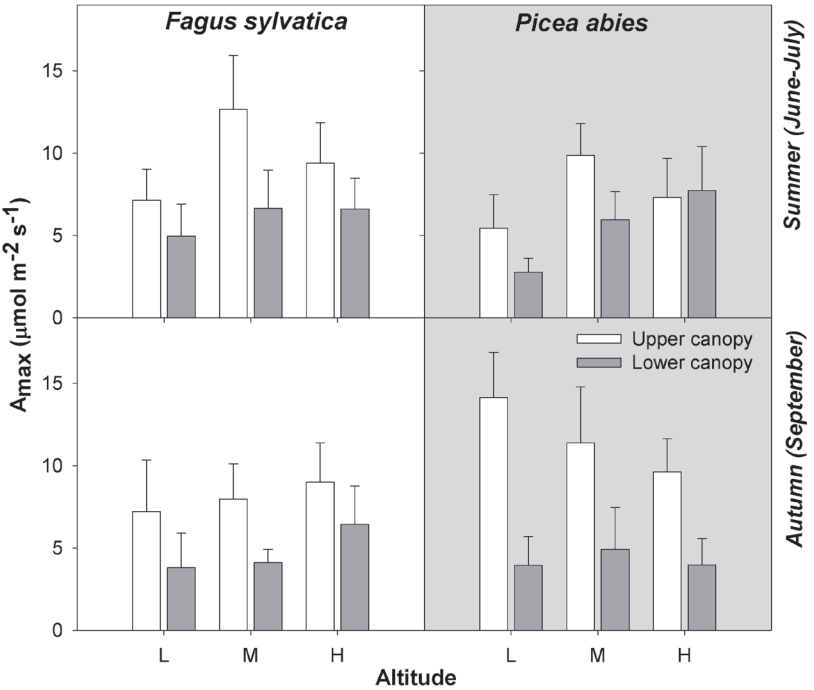

Fig. 1: *Light-saturated (1,200 µmol m^{-2} s^{-1}) CO_2 assimilation (A_{max}) rates in sun (white columns) and shade (grey columns) leaves of European beech (Fagus sylvatica, left) and needles of Norway spruce (Picea abies, right) growing at low (L; 400 m a.s.l.), middle (M; 720 m a.s.l.), and high (H; 1100 m a.s.l.) altitudes. Columns represent means and error bars represent standard deviations. N = 13 (trees).*

Allocation of $Rubisco_{area}$ within the vertical canopy profile was significantly affected by species and altitude. The relationship between N_{area} and $Rubisco_{area}$, analysed for the summer datasets, showed a gradual separation of the relationships for upper and lower canopy with increasing altitude (Fig. 2). This separation was characterized by decrease of slope for the upper canopy with increasing altitude while the relationships for the lower canopy changed only slightly. These altitudinal changes were more pronounced in spruce than they were in beech. This means that with increasing altitude in upper canopy leaves or needles less nitrogen is allocated to Rubisco.

DISCUSSION

Our results show a great capacity in trees to adjust the morphological, physiological, and biochemical traits of the entire canopy. Generally, we observed that with increasing altitude, which is associated with adverse microclimatic conditions, there is a convergence of CO_2 assimilation rate and other physiological, morphological, and biochemical characteristics between the upper and lower canopy. However, differences among individual traits and species were found. Morphological acclimation was more obvious in beech, for example, where the lower canopy leaves tended to increase LMA and converge with the upper canopy. On the other hand, biochemical acclimation was more pronounced in the upper canopy and Norway spruce. This was clearly perceptible from the relationships between N_{area} and $Rubisco_{area}$.

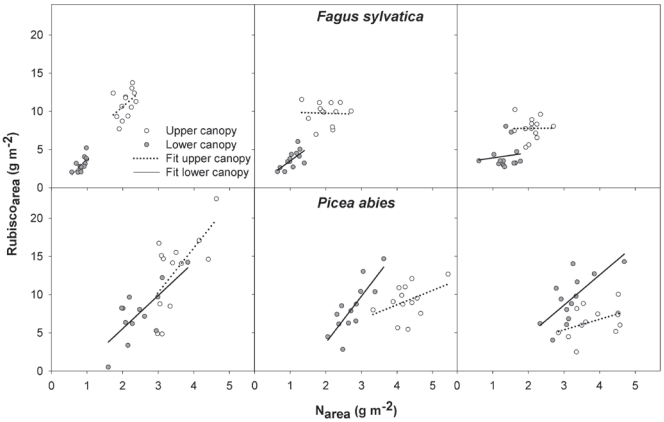

Fig. 2: *Relationship between total nitrogen content per unit leaf area (N_{area}) and total Rubisco content per unit leaf area ($Rubisco_{area}$) in upper (white circles) and lower (grey circles) canopy needles of Norway spruce (Picea abies) growing at low (L; 400 m a.s.l.), middle (M; 720 m a.s.l.), and high (H; 1100 m a.s.l.) altitudes.*

In our previous studies (e.g. Urban et al. 2007), we have shown that the leaves of *F. sylvatica* respond to insufficient light conditions primarily with reduced LMA, which leads to significantly higher A_{max} per leaf weight unit in shade leaves of *F. sylvatica* as compared to sun leaves. Nevertheless, restricted growth conditions associated with high altitudes have the potential to increase the magnitude of biochemical acclimation, represented for example by changes in N_{area}, chlorophyll, and Rubisco contents. Activity of photosynthetic enzymes, in contrast to light absorption, is reduced at low temperatures, which thus leads to an increased risk of photooxidative damage (Tsonev & Hikosaka 2003). The gradually decreased allocation of N to Rubisco in upper canopy leaves with increasing altitude is consistent with previous findings that cold represents an important N sink (Janda et al. 2007).

We can conclude that growth restrictions at higher altitudes, and particularly those caused by low temperatures, lead to apparent functional changes in both sun-acclimated (upper) and shade-acclimated (lower) leaves or needles differently at morphological and biochemical levels. This ultimately leads to convergence in the vertical profile of the canopy and increase in the importance of the lower canopy at higher altitudes.

Acknowledgement

Supported by project No. M200871201 (Czech Academy of Sciences), No. 284443 EPPN (EU, FP7) and the Ministry of Education, Youth and Sports within the National Programme for Sustainability I, project No. LO1415.

References

Becker A, Körner C, Brun J-J et al. (2007) Mt. Res. Dev. 27, 58–65.

Hikosaka K (2005) Plant Cell Physiol. 46, 1283–1290.

Janda T, Szalai G, Leskó K et al. (2007) Phytochemistry 68, 1674–1682.

Körner C (2007) Trends Ecol. Evol. 22, 569–574.

Tsonev TD, Hikosaka K (2003) Plant Cell Physiol. 44, 828–835.

Urban O, Košvancová M, Marek MV et al. (2007) Tree Physiol. 27, 1207–1215.

Yano S, Terashima I (2001) Plant Cell Physiol. 42, 1303–1310.

Leaf area index development and radiation use efficiency of a poplar short rotation coppice culture

Tripathi, A. M.[1,2,3,*], Fischer, M.[1,4], Trnka, M.[1,2], Orság, M.[1,2], Vanbeveren, S. P. P.[5], Marek, M.V.[1]

[1]*Global Change Research Center, Bělidla 986/4a, 603 00 Brno, Czech Republic*

[2]*Institute of Agriculture Systems and Bioclimatology, Faculty of Agronomy, Mendel University in Brno, Zemědělská 1, 613 00 Brno, Czech Republic*

[3]*Institute of Forest Ecology, Faculty of Forestry and Wood Technology, Mendel University in Brno, Zemědělská 1, 613 00 Brno, Czech Republic*

[4]*Department of Forestry and Environmental Resources, North Carolina State University, 2820 Faucette Dr., 27695 Raleigh, NC, USA*

[5]*Department of Biology, University of Antwerp, Universiteitsplein 1, 2610 Wilrijk, Belgium*

[*]*author for correspondence; email: manicfre@gmail.com*

ABSTRACT

Leaf area index (LAI) is the most appropriate parameter for analyzing canopy structure and crop productivity. LAI and radiation use efficiency (RUE) were estimated to evaluate the productivity of a short rotation coppice culture of a poplar clone. RUE was calculated as the ratio between total aboveground woody biomass and available photosynthetic active radiation (PAR) accumulated during one growing season. Prior to coppicing, LAI reached a maximum value of 7.3 (in 2009), whereas the maximum LAI after coppicing was 6.8 (in 2012). The maximum RUE reached prior to coppicing was 0.25 g mol^{-1} (in 2009), while after coppicing it was 0.20 g mol^{-1} (in 2012), which did not represent a significant difference ($p > 0.05$).

INTRODUCTION

Leaf area index (LAI; $m^2_{leaf\ area}\ m^{-2}_{ground\ area}$) is a key parameter for productivity and it is frequently used to describe canopy structure (Watson 1947). LAI and radiation use efficiency (RUE; g mol^{-1}) are used to maximize productivity in a short amount of time and this agricultural technique is applied to forest crops. Biomass production of plants is dependent on available and intercepted radiation by the canopy which is used to convert CO_2 into new biomass (Gifford et al. 1984, Linder 1985). The rate of this production given available photosynthetic active radiation (PAR) is defined as RUE. The aim of this study was to compare differences in LAI and RUE prior to and after coppicing in a culture of poplar clone J-105 (*Populus nigra* L. × *P. maximowiczii* Henry).

MATERIALS AND METHODS

The experimental field site

The study was carried out on an existing short rotation coppice (SRC) culture of poplar clone J-105. The experimental site was located in Domanínek (Bystřice nad Pernštejnem, Bohemian–Moravian Highlands; 49°31'N, 16°14'E; 530 m a.s.l.) and total plantation area was 2.85 ha. Between 1981 and 2012, total annual rainfall was 609 mm and mean annual air temperature was 7.2°C. The experimental site is part of climatic region no. 7 (Havlíčková et al. 2006), which is highly suitable for poplar cultures mainly due to its soil characteristics (Trnka et al. 2008). The plantation was established in April 2002 by planting hardwood cuttings in

a double-row design with spacing of 0.7 m within rows and an inter-row distance of 2.5 m. This resulted in a planting density of 9,216 trees ha^{-1}. The first rotation was 8 years (2002–2009), after which the SRC culture was harvested at 20 cm above ground level.

Field measurements

All measurements were made from 2008 to 2012 and spanned the entire growing season. Meteorological data (air temperature, global radiation, PAR, total annual precipitation) were recorded continuously by an automatic weather station placed at the turf grass next to the plantation. LAI was measured indirectly using a SunScan plant canopy analyzer (type SS1, Delta T, UK). This indirect method was validated using a direct method (litter collection on traps). Litter collection was conducted once prior to coppicing and twice after coppicing. Indirect LAI was measured close to traps where we collected litterfall. Data were obtained on a weekly basis during the growing season on three plots (~80 m^2) close to the center of the plantation. Using a regression equation with cumulative mean daily air temperature, data were interpolated to daily LAI data, whereby winter habits generated an LAI value of 0.

RUE was calculated as the ratio between the difference in stocking biomass at the end of each season (ΔW_s; t ha^{-1} $year^{-1}$), i.e. annual biomass productivity, and the amount of PAR absorbed by the canopy (APAR; mol m^{-2} $year^{-1}$) during the entire growing season (according to Linderson et al. 2007):

$$RUE = \Delta W_s / APAR \quad (1)$$

and

$$APAR = PAR_{above} (1 - e^{-kLAI}), \quad (2)$$

where PAR_{above} is incident PAR above the canopy and k is the extinction coefficient (set to 0.5; Eckersten 1984).

An allometric equation was developed (Fischer 2012) to estimate aboveground stocking woody biomass (annual productivity). We thus determined R^2 values to estimate the yearly aboveground woody biomass prior to and after coppicing. At the end of growing season we performed a stem inventory and repeated the same procedure every year prior to the start of the growing season.

Data analyses were performed using the STATISTICA 9 statistical package (StatSoft, USA), in particular for an analysis of variance with post-hoc Fischer's least significant difference to evaluate the significance of differences between treatments at $p < 0.05$.

RESULTS

Stand woody biomass productivity and productivity rate for poplar hybrid clone J-105 depended on light efficiency or RUE and LAI. Prior to coppicing, the maximum productivity for poplar clone J-105 was 16.5 dry t ha^{-1} $year^{-1}$, LAI_{max} was 7.3, and RUE_{max} was 0.25 g mol^{-1} in 2009 after 8 years of growth. After coppicing, the maximum productivity was 10.31 dry t ha^{-1} $year^{-1}$, LAI_{max} was 6.8, and RUE_{max} was 0.20 g mol^{-1} in 2012 after 3 years of growth. Fig. 1 shows annual stand level woody biomass (dry t ha^{-1} $year^{-1}$) production and RUE both prior to and after coppicing ($p = 0.75$, i.e. the differences were not significant) in a SRC culture of hybrid poplar clone J-105. LAI dynamics are shown in Fig. 2.

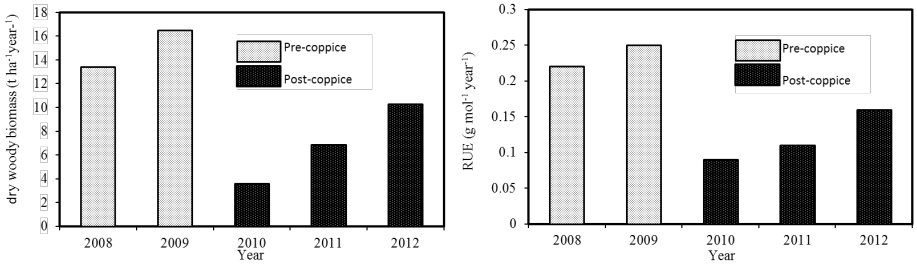

Fig. 1: *Stand level woody biomass production (left) and radiation use efficiency (RUE; right) for each growing season before and after coppicing of poplar clone J-105.*

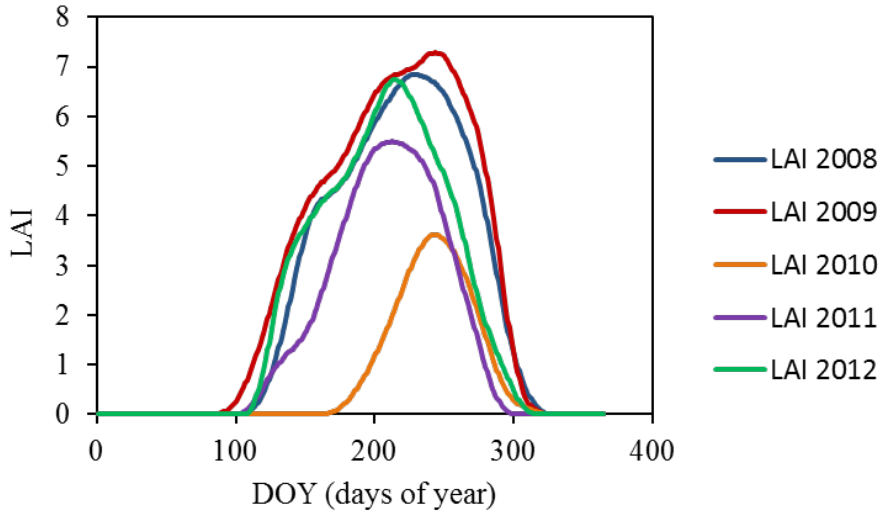

Fig. 2: *Seasonal pattern of leaf area index (LAI; m^2 m^{-2}) in SRC culture prior to (2008 and 2009) and after (2010, 2011, and 2012) coppicing.*

DISCUSSION

The maximum RUE was 0.25 g mol^{-1} prior to coppicing and 0.20 g mol^{-1} after coppicing, which is similar to values reported by Linderson et al. (2007), who estimated 0.31 g mol^{-1} for many clones of willows in southernmost Sweden, as well as Eckersten (1984), who reported RUE of 0.43 g mol^{-1} in western Sweden. Our values were lower than those observed by Bullard et al. (2002), who recorded 0.39–0.53 g mol^{-1} for a similar planting density in the UK. They used extinction coefficients of 0.2–0.5 based on observations in 2-year-old plantations, and so our results are almost similar to these previous results. We used the value reported by Eckersten (1984) of $k = 0.5$. Values ranged from 0.4–0.6. In Pennsylvania and Wisconsin in the US., RUE values were 1.5 for poplar and balsam fir (Pothier et al. 1991).

Acknowledgements

Supported by KONTAKT II project No. LH12037 “PASED,” project No. LD13030 “AGRIWAT,” and project No. CZ.1.07/2.3.00/20.0248 “InterSucho”.

References

Bullard MJ, Mustill SJ, McMillan SD et al. (2002) Biomass Bioenerg. 22, 15–25.

Eckersten H (1984) Light penetration and photosynthesis in a willow stand. Ecology and Management of Forest Biomass Production Systems (ed KL Perttu), pp. 29–45. Department of Ecology and Environmental Research, Swedish University of Agricultural Sciences, Uppsala.

Fischer M (2012) Water balance of short rotation coppice. PhD thesis, Mendel University in Brno, Brno..

Gifford RM, Thorne JH, Witz WD et al. (1984) Science 225, 801–808.

Havlíčková K, Weger J, Havlíčková B et al. (2006) Acta Pruhoniciana 83, 1–96.

Linder S (1985) Potential and actual production in Australian forest stands. Research in Forest Management (eds JJ Landsberg & W Parsons), pp. 11–35. Commonwealth Scientific and Industrial Research Organization, Melbourne.

Linderson ML, Iritz Z, Lindorth A (2007) Biomass Bioenerg. 31, 460–468.

Pothier D, Margolis A (1991) Ann. For. Sci. 48, 123–132.

Trnka M, Fialová J, Koutecký V et al. (2008) Plant Soil Environ. 54, 78–88.

Watson DJ, (1947) Ann. Bot. 11, 41–76

Analysis of poplar water-use efficiency at Domanínek experimental site

Hlaváčová, M.[1,2,*], Fischer, M.[1], Tripathi, A.M.[1,2], Orság, M.[1,2], Trnka, M.[1,2]

[1]*Global Change Research Centre, Bělidla 986/4a, 603 00, Brno, Czech Republic*

[2]*Faculty of Agronomy, Mendel University in Brno, Zemědělská 1, 613 00, Brno, Czech Republic*

**author for correspondence; email: Marci.Hlava.22@gmail.com*

ABSTRACT

The main objective of this study was to test if water-use efficiency (WUE) values are higher for short-rotation poplar coppice than they are for field crops. WUE of woody biomass was determined for 16 trees within a short-rotation poplar coppiced culture (poplar clone J-105) in the Bohemian–Moravian Highlands within the Czech Republic during the 2013 growing season. Total WUE of woody biomass for the 16 measured trees was 4.93 g kg^{-1} when calculated with the data set without a vapour pressure deficit condition and 4.63 g kg^{-1} when calculated with the data set with a vapour pressure deficit condition. Poplar clone J-105 is a tree species with relatively high WUE, but some crops or short-rotation coppice species can reach higher or comparable WUE values.

INTRODUCTION

A site's water availability constitutes one of the main constraints for short-rotation coppice grown on arable land (Fischer 2012). Hellriegel (1883) and Maximov (1923) are among the first researchers to have carried out calculations on the relationship between increases in dry matter and water requirements. By dividing biomass productivity, expressed as organic dry matter, by the water lost by transpiration, water-use efficiency of productivity (WUE_P) or long-term WUE (WUE_L) is obtained (de Wit 1958). This method of determining WUE is usually directly related to forestry practices since it is estimated on the basis of dendrometric measurements. In practice, these measurements can be performed only on the above-ground parts. Therefore, WUE_L is also mostly estimated for above-ground biomass production, expressed either in volume units or as the weight of fresh or dry matter (Cienciala 1994). The present study calculated WUE of woody biomass (WUE_{WB}). Its aim was to test the hypothesis that WUE values are higher for short-rotation poplar coppice than they are for field crops.

MATERIALS AND METHODS

The study was carried out on a short-rotation poplar coppice (J-105, *P. maximowiczii* A. Henry × *P. nigra* L., theoretical density of 9,216 trees ha^{-1}) of the ZEMSERVIS zkušební stanice Domanínek, s.r.o. research company located in Bystřice nad Pernštejnem (530 m a.s.l.) within Bohemian–Moravian Highlands in the Czech Republic. The plantation was established in April 2002 on 2.85 ha of agricultural land. According to long-term (1981–2010) climatic data, the mean annual temperature at the site is 7.2°C and the mean annual precipitation is 609.3 mm. The soil type at the site is deep luvic Cambisol influenced by gleyic processes (Fischer et al. 2013). Measurements were carried out during the 2013 growing season. The study is based on 16 trees where sap flow measuring systems (Granier's thermal dissipation probes [TDPs]) were installed (Granier 1987). Despite the fact that the TDP method involves damage to the wood tissue which consequently changes the wood's thermal properties and wound width of the non-conducting sapwood

due to healing reactions may lead also to underestimating sap flow (Bush et al. 2010, Lu et al. 2004), no conspicuous damage was observed during the present study. Diameter at breast height (DBH; 1.3 m above the ground) was measured once every 7 days (from 24 April 2013 to 15 October 2013) using a digital electronic calliper. The measured trees were divided into three diameter classes according to their DBH values at the beginning of regular measurements. DBH values at the beginning and at the end of regular measurements were calculated as averages of the first three and the final three measurements to increase accuracy. The three diameter classes were as follows: Class 1 49.8–58.5 mm, Class 2 40.7–48.8 mm, and Class 3 26.5–39.1 mm. TDP outputs were expressed as the temperature differences (ΔT) between heated and non-heated probes. Estimation of sap flux density (F_d) using Granier's method relies on the measurement of ΔT. Therefore, data on obtained ΔT (expressed in Kelvins) were first checked for measurement quality and extreme values (< 4 K and > 20 K) were removed. Determining the maximum temperature difference (ΔT_{max}) is essential for F_d calculating. Although ΔT_{max} can be theoretically defined as ΔT at $F_d = 0$, a zero-flow state many be prevented by may factors, such as water loss from the canopy due to a high vapour pressure deficit (VPD) (Lu et al. 2004). Therefore, the VPD condition was established to determine ΔT_{max}. Two ΔT_{max} data sets were established to compare these two approaches: (1) without VPD condition where values were taken every night at 3:00 as this is the time when ΔT should be at its daily maximum, and (2) with VPD condition where ΔT was taken at 3:00 only if mean VPD was less than 0.2 kPa for the 6 previous hours during the night (from 21:00 to 3:00) since this is the supposed time after which the tree has negligible transpiration. Linear interpolation was used to prepare a half-hourly dataset of ΔT_{max}. Subsequently, F_d and Q values were calculated according to Lu et al. (2004) for both variants of ΔT_{max}. F_d and Q data were removed from days where less than 16 h of values were recorded as daily mean F_d values and daily Q totals would be skewed. Missing sap flow data were gap-filled based on the methodology described in Fischer et al. (2013) using regression analysis between reference evapotranspiration (Allen et al. 1998) and sap flow. Allometry was conducted to determine woody biomass. A total of 16 trees with different DBH values (as diameter classes representative of the plantation) were selected and subsequently cut. Stem heights, DBH values (as the average of measurements in 2 directions), and fresh weights of stems and branches (without leaves) were determined separately. These samples were dried to a constant mass (70°C for 4 days) and then dry weights were determined. The relationship between cut trees' dry matter and DBH values was subsequently expressed and used to fit a log-linear allometric equation. Biomass increments were calculated as the difference in dry matter at the end of 2 consecutive months. Finally, WUE_P of above-ground woody biomass was determined by dividing biomass increments by the monthly totals of sap flow for the 16 studied trees (e.g., de Wit 1958, Lindroth et al. 1994). Leaf biomass was not included as we were primarily interested in the WUE of the final harvestable biomass and leaves are not considered as a harvestable product in this type of bioenergy system. Monthly WUE_{WB} values were determined for the period from May to September (due to sap flow values displaying negligible values in April and October).

RESULTS

The graphical depiction of WUE within the Fig. 1 shows the highest WUE in May where all classes produced the largest amount of biomass per consumed water unit (maximum mean WUE values: 14 g kg^{-1} for Class 1, 12 g kg^{-1} for Class 2, and 9 g kg^{-1} for Class 3). While classes 1 and 2 decreased their WUE from May to June, trees in Class 3 displayed the highest WUE in that time. The lowest mean WUE values were recorded in September and ranged from almost 0 to approximately 2 g kg^{-1}.

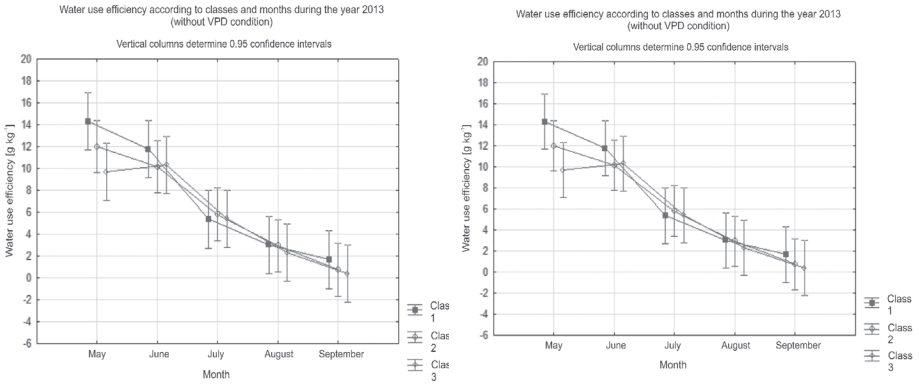

Fig. 1: *WUE for (A) data set without VPD condition and (B) data set with VPD condition.*

The statistical analysis (Table 1) revealed only one statistically significant difference, namely between the WUE of classes 1 and 3 in May. WUE values were very similar for both data sets and also for all 3 classes of trees, which may have been caused by relatively low variation of DBH classes within the measured trees due to the dense spacing that limits radial growth.

Table 1: *Statistical analysis of water-use efficiency. Results of ANOVA and post-hoc Fisher's least significant difference test showing the statistical significance (p-values) of interactions among water-use efficiency values within particular months and classes.*

Without VPD condition					With VPD condition				
Month	**Class**	**Class 1**	**Class 2**	**Class 3**	**Month**	**Class**	**Class 1**	**Class 2**	**Class 3**
May	1		0.199	**0.015**	May	1		0.267	**0.029**
	2	0.199		0.197		2	0.267		
	3	**0.015**	0.197			3	**0.029**	0.227	0.227
June	1		0.372	0.444	June	1		0.416	0.641
	2	0.372		0.925		2	0.416		0.742
	3	0.444	0.925			3	0.641	0.742	
July	1		0.805	0.981	July	1		0.827	0.901
	2	0.805		0.825		2	0.827		0.930
	3	0.981	0.825			3	0.901	0.930	
August	1			0.704	August	1		0.977	0.824
	2	0.964	0.964	0.725		2	0.977		0.839
	3	0.704	0.725			3	0.824	0.839	
September	1		0.609	0.498	September	1		0.653	0.550
	2	0.609		0.844		2	0.653		0.861
	3	0.498	0.844			3	0.550	0.861	

DISCUSSION

Mean WUE_{WB} for all 16 trees was 4.93 g kg^{-1} in the data set without VPD condition and 4.63 g kg^{-1} in the data set with VPD condition with minima of 0 to approximately 2 g kg^{-1} and maxima of 14 g kg^{-1} for Class 1, 12 g kg^{-1} for Class 2,

and 9 g kg^{-1} for Class 3. Schmidt et al. (2014) determined WUE_{WB} ranging from 1.2 to 10 g kg^{-1} for polar clone J-105 and from 4 to 13 g kg^{-1} for willow (*Salix triandra* × *S. viminalis*). Kiniry et al. (2008) determined mean WUE of four switchgrass types ranging from 3 to 5 g kg^{-1}. These authors also presented studies showing mean WUE values for maize (*Zea mays*) in the U.S. of 2.5 g kg^{-1}. Lawes (1850) determined wheat WUE of 4.04 g kg^{-1} when unmanured and 4.50 g kg^{-1} when manured. Later, Condon et al. (1990) determined wheat WUE of 4.06–5.27 g kg^{-1} in well-watered plants and 4.69–5.95 g kg^{-1} in water-stressed plants. When only marketable biomass (yield) WUE (i.e. for crops the grain dry weight per unit water used, WUE_{yield}) is considered (Tallec et al. 2013) instead of above-ground biomass for comparison, mean WUE_{yield} for maize was 1.14 g kg^{-1} (according to the studies presented by Kiniry et al. 2008). Another study presented for two sites in south-west France WUE of 5 g kg^{-1} for maize used for silage, WUE_{yield} of 4.9 g kg^{-1} for maize, and mean WUE_{yield} of 1.7 and 2.1 g kg^{-1} for winter wheat (Tallec et al. 2013). The poplar clone J-105 is a tree species with relatively high WUE, but some crops or short-rotation coppice species can reach higher or comparable WUE values depending especially on the site's water conditions.

Acknowledgement

Supported by project No. CZ.1.07/2.3.00/20.0248 "Building up a multidisciplinary scientific team focused on drought", project No. LD130030 supporting COST Action ES1106, and project No. LO1415 of the Ministry of Education, Youth and Sports within the National Programme for Sustainability I.

References

Allen RG (1996) J. Irrig. Drain. Eng. 122, 97–106.

Allen RG, Pereira LS, Raes D et al. (1998) Crop Evapotranspiration - Guidelines for Computing Crop Water Requirements. FAO Irrigation and Drainage Paper No. 56. Food and Agriculture Organization of the United Nations, Rome.

Bush SE, Hultine KR, Sperry JS et al. (2010) Tree Physiol. 30, 1545–1554.

Cienciala E (1994) Sap flow, transpiration and water use efficiency of spruce and willow in relation to climatic factors. PhD Thesis, Swedish University of Agricultural Sciences, Uppsala.

Condon AG, Farquhar GD, Richards RA (1990) Funct. Plant Biol. 17, 9–22.

de Wit CT (1958) Versl. Landbouwkd. Onderz. 64, 88.

Fischer M (2012) Water balance of short rotation coppice. Ph.D. thesis, Mendel University in Brno, Brno.

Fischer M, Trnka M, Kučera J et al. (2013) Agric. For. Meteorol. 181, 43–60.

Granier A (1987) Tree Physiol. 3, 309–320.

Hellriegel H (1883) Beiträge zu den naturwissenschaftlichen Grundlagen des Ackerbaus mit besonderer Berücksichtigung der agrikultur-chemischen Methode der Sandkultur. Friedrich Vieweg und Sohn, Braunschweig.

Kiniry JR, Lynd L, Greene N et al. (2008) Biofuels and water use: comparison of maize and switchgrass and general perspectives. New Research on Biofuels (eds JH Wright & DA Evans), pp. 17–30. Nova Science Publishers, New York.

Lawes JB (1850) J. Hortic. Soc. Lond. 5, 38–63.

Lindroth A, Verwijst T, Halldin S (1994) J. Hydrol. 156, 1–19.

Lu P, Urban L, Zhao P (2004) Acta Bot. Sin. 46, 631–646.

Maximov NA (1923) Jahrb. wiss. Bot. 62, 128–144.

Schmidt M, Böhme T, Krämer S et al. (2014) Water use and productivity of poplar and willow in SRC plantations in NE Germany along gradients of groundwater depth. 2nd European Agroforestry Conference: Book of Abstracts (eds JHN Palma & A Chalmin), pp. 237–240. Technical University of Lisbon, Lisbon.

Tallec T, Béziat P, Jarosz N et al. (2013) Agric. For. Meteorol. 168, 69–81.

Long-term productivity of short rotation coppice under decreased soil water availability

Orság, M.[1,2,*], Fischer, M.[1,3], Tripathi, A.M.[1,2], Žalud, Z.[1,2], Trnka, M.[1,2]

[1]*Global Change Research Centre, Bělidla 986/4a, 60300 Brno, Czech Republic*

[2]*Department of Agrosystems and Bioclimatology, Mendel University, Zemědělská 1, 61300 Brno, Czech Republic*

[3]*Department of Forestry and Environmental Resources, North Carolina State University, 2820 Faucette Dr., 27695 Raleigh, NC, USA*

[*]*author for correspondence; email: orsag.matej@gmail.com*

ABSTRACT

"Wood, in fact, is the unsung hero of the technological revolution that has brought us from a stone and bone culture to our present age" (Perlin 1991). Given its high-energy content and versatile use, biomass in the form of wood has been used for energy purposes for millennia. The production and use of woody biomass resources has been expanding around the world. The main drivers of its use as a source of energy are diversification and mitigation of energy related greenhouse gas emissions through partial substitution for fossil fuels. An alternative to sourcing wood biomass from natural forests is short rotation woody coppice. Its productivity is largely dependent on the environment in terms of climatic conditions. Especially drought is the main constraint on woody biomass production and involves serious economic consequences. For that reason, our field experiment was designed to evaluate the impact of decreased soil water availability on productivity of a poplar based short rotation coppice plantation over multiple growing seasons during 2011–2014. Aboveground biomass productivity of treatments with and without throughfall exclusion was assessed within this study. Our results show a systematic decline in the productivity of the plots subjected to decreased soil water availability by 30% in 2011, 20% in 2012, 49% in 2013, and 51% in 2014 compared to control plot. Aboveground biomass productivity ranged from 8.8 to 9.9 t dry matter ha^{-1} $year^{-1}$ for the control treatment and 4.5 to 8.0 t dry matter ha^{-1} $year^{-1}$ for the treatment with throughfall exclusion. On average, the throughfall exclusion treatment exhibited 47% less productivity than control treatment had over the entire study period.

INTRODUCTION

Short rotation woody coppice (SRWC) has become the predominant term for biomass productions systems that are cultivated for energy purposes using fast-growing tree species with the ability to re-sprout from stumps after harvest and that are grown over short intervals of 2–6 years (Busch 2009). Species considered for SRWC include willows in northern Europe and poplars in central and western Europe (Mitchell et al. 1999). The productivity of poplar and willow SRWC plantations is largely dependent on the environment in terms of soil characteristics and climatic conditions (Amichev et al. 2010, Broeckx et al. 2013). Especially drought is the main constraint on woody biomass production and involves serious economic consequences. As climate change precedes, the frequency, intensity, and duration of heat waves is increasing across Europe. Higher temperatures increase evaporation and may intensify droughts in the Czech Republic. Increased global radiation and air temperature together with decreased relative humidity have led to higher reference evapotranspiration (ET_o) in all months of the growing season. This trend is particularly evident in April, May, and August, when more than 80% of the territory shows increased demand for

soil water (Trnka et al. 2014). In areas where long-term ET_o exceeds precipitation, biomass productivity may be limited, particularly when the temporal distribution of precipitation is uneven. This also applies to our study site, where total ET_o was 8% higher than was total rainfall over 2008–2014. The main goal of this study is to quantify differences in aboveground biomass yield from a functional SRWC plantation with natural and reduced soil water availability in a throughfall exclusion experiment.

MATERIALS AND METHODS

The study was carried out from June 2011 through November 2014 at the Domanínek research site (49°31'N; 16°14'E, 578 m a.s.l.). The site is located in the eastern part of the Bohemian–Moravian Highlands and is a rain-fed area with mean annual precipitation of 609.3 mm and mean annual temperature of 7.2°C. In April 2002, a high density plantation based on poplar clone J-105 (*Populus nigra* L. × *P. maximowiczii* Henry "Maxfünf") with a total area of 1 ha was established in Domanínek, accommodating a theoretical density of 9,216 trees ha^{-1}. The year 2014 represents the sixth year of the second rotation cycle. The experiment consisted of two adjacent square-shaped plots of 25 m^2 each. The throughfall-exclusion (R) plot was equipped with plastic roof strips intercepting rainfall and a ditch excluding water runoff. The ditch was dug around the perimeter of the R plot in June 2012, down to a depth of 50 cm. The neighboring control (C) plot with natural rainwater income was taken as the reference. Initial throughfall reduction on the R plot was set empirically to 40%, but from June 2013 roof coverage was increased to 70%. Annual aboveground productivity was determined from annual stand inventorying of each plot (R and C treatments). Diameter at breast height (DBH) in mm of all shoots and stems within each treatment was measured at 1.3 m above the ground. Then, the allometric relationship $y = 2.96\ 10^{-4}\ DBH^{2.39}$ ($R^2 = 0.99$) was applied to estimate total standing dry biomass per plot. Total dry biomass production per plot was scaled up to the area of 1 ha according the number of stools per plot and per ha. The C plot contained 20 stools and the R plot 16 stools. Dry biomass production per plot was multiplied by the number of stools per ha divided by the number of stools per plot. In this way, dry biomass production per ha^{-1} was obtained. Volumetric soil moisture was measured at depths of 0–0.3 m using CS 616 time-domain reflectometers (Campbell Scientific, UK).

RESULTS

This field experiment enabled evaluation of the effect of decreased rainwater income on the biomass productivity of a productive SRWC stand. The dry biomass production of contrasting C and R treatments during 2011–2014 is presented in Fig. 1. Mean annual production of the C plot was 9.3 t dry matter (DM) $ha^{-1}\ year^{-1}$, whereas the R plot, which was exposed to drought, displayed mean annual production of 4.9 t DM $ha^{-1}\ year^{-1}$ during the study period of 2011–2014. Annual production of C plot was 8.8 t DM $ha^{-1}\ year^{-1}$ in 2011, 9.9 in 2012, 9.6 in 2013, and 9.2 in 2014, whereas R plots recorded 6.2 t DM $ha^{-1}\ year^{-1}$ in 2011, 8.0 in 2012, 4.9 in 2013, and 4.5 in 2014. Dry biomass production in the R treatment was reduced in comparison to the C plot by 30% in 2011, 20% in 2012, 49% in 2013, and 51% in 2014. The highest yields on both treatments were achieved in 2012, while the lowest yield occurred in 2011 in the C plot and in 2014 in the R plot. The course of volumetric soil moisture of C and R plots during 2011–2014 illustrates the gradual development of drought intensity on the R plot over the study period (Fig. 2). For both treatments, saturation level was around 30%, with a minimum level of 15% for the C plot and 13% for the R plot.

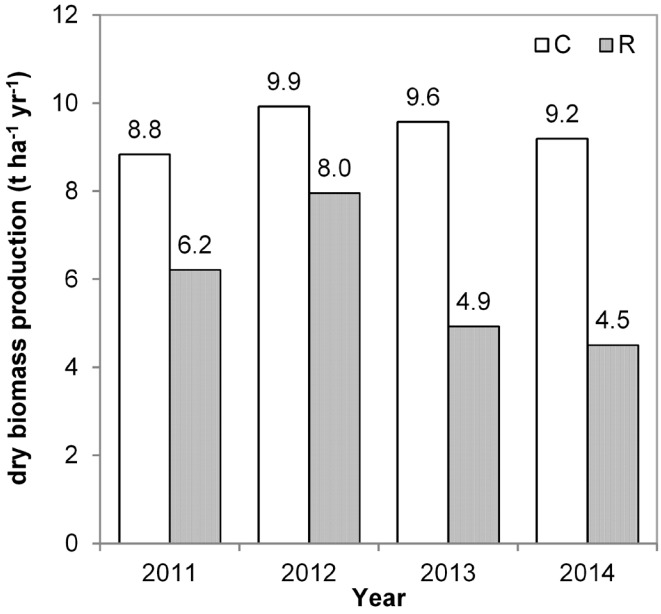

Fig. 1: *Aboveground dry biomass production during 2011–2014 of two contrasting treatments: (C) with natural rainwater income and (R) with reduced rainwater income.*

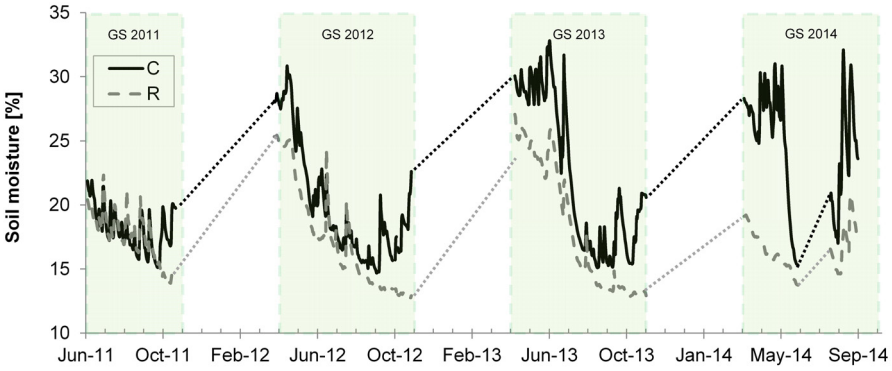

Fig. 2: *Course of volumetric soil moisture (0–0.3m) of two contrasting treatments, (C) natural rainwater income and (R) reduced rainwater income, during the 2011–2014 growing seasons (GS).*

DISCUSSION

Overall biomass production on the C plot was 9.4 t DM ha^{-1} $year^{-1}$, which falls within the range of 5–10 t DM ha^{-1} $year^{-1}$ reported for poplar biomass (Hauk et al. 2014, King et al. 2013, Verlinden et al. 2015). The C plot maintained a more or less consistent yield level across all experimental years. In comparing among years, yield from 2011 should not be considered as a complete seasonal yield because initial stem inventory was carried out as late as mid-June, when seasonal biomass growth had already commenced. The R plot clearly showed reduced productivity (Fig. 1), likely related to a decrease in soil moisture content (Fig. 2). The soil moisture levels of both treatments were almost equal in 2011. In 2012, the insulating ditch was dug around the R plot and the soil moisture difference was more pronounced than it had been in 2011. From mid-June 2013, there was an obvious decrease in soil moisture on the R plot as roof coverage was increased from 40% to 70%. This trend continued in 2014 and most likely caused the decreased productivity on the R plot. Biomass productivity fell from a 20% reduction compared to the C plot in 2012 to a 50% reduction in 2013 and 2014. On average, the R treatment exhibited an overall 47% decrease in productivity compared to the C treatment over the entire study period. Wikberg & Ögren (2007) found that willow clones subjected to 50% rainwater income reduction produced 35–60% less aboveground biomass than did control plants. Souch & Stephens (1998) even reported a 60–75% decrease in productivity for poplar hybrids grown in pots. Our results show the considerable resilience of the poplar clone J-105 as well as its ability to sustain a certain level of productivity even under long-term drought. This study should contribute to understanding the issue of how the changing climate will affect bioenergy production in the Czech Republic, as this country exports much of its bioenergy production abroad (Benetka et al. 2007, Lewandowski et al. 2006).

Acknowledgements

Supported by project No. CZ.1.07/2.3.00/20.0248 "Building up a multidisciplinary scientific team focused on drought," the KONTAKT II program under project No. LH12037 "Development of models for assessment of abiotic stresses in selected bio-energy plants," and project No. LD13030 "AGRIWAT" supporting the Czech Republic's participation in COST Action ES1106.

References

Amichev BY, Johnston M, Van Rees KCJ (2010) Biomass Bioenerg. 34, 687–702.

Benetka V, Vrátný F, Šálková I (2007) Biomass Bioenerg. 31, 367–374.

Broeckx LS, Verlinden MS, Berhongaray G et al. (2013) GCB Bioenergy 6, 473–487.

Busch G (2009) Landbauforsch. vTI Agric. For. Res. 3, 207–222.

Hauk S, Knoke T, Wittkopf S (2014) Renew. Sust. Energ. Rev. 29, 435–448.

King JS, Ceulemans R, Albaugh JM et al. (2013) BioScience 63, 102–117.

Lewandowski I, Weger J, van Hooijdonk et al. (2006) Biomass Bioenerg. 30, 405–421.

Mitchell CP, Stevens EA, Watters MP (1999) For. Ecol. Manag. 121, 123–136.

Perlin J (1991) A Forest Journey: The Role of Wood in the Development of Civilization. Harvard University Press, Boston.

Souch CA, Stephens W (1998) Tree Physiol. 18, 829–835.

Trnka M, Brázdil J, Balek D et al. (2014) Int. J. Climatol. in press. doi: 10.1002/joc.4167

Verlinden M, Broeckx L, Ceulemans R (2015) Biomass Bioenerg. 73, 174–185.

Wikberg J, Ögren E (2007) Tree Physiol. 27, 1339–1346.

Interactive effects of UV radiation and drought on the accumulation of flavonols in selected herbs and grass in a mountain grassland ecosystem

Veselá, B.[1,2,*], Novotná, K.[1,2], Rajsnerová, P.[1,2], Klem, K.[1,2], Holub, P.[1], Urban, O.[1]

[1]*Global Change Research Centre, Bělidla 986/4a, 603 00 Brno, Czech Republic*
[2]*Mendel University in Brno, Zemědělská 1, 613 00 Brno, Czech Republic*
**author for correspondence; email: vesela.b@czechglobe.cz*

ABSTRACT

The main objective of this 4-year experiment conducted in a mountain grassland ecosystem was to investigate the interactive effects of ultraviolet (UV) treatment and drought on changes in accumulation of UV-screening compounds (flavonols) in selected herbs (*Hypericum maculatum* Crantz, *Rumex obtusifolius* L.) and grass (*Agrostis tenuis* Sibth.). Inasmuch as drought and UV radiation induce similar protective mechanisms, we tested the hypothesis that UV radiation and drought elicit synergistic effects on flavonol accumulation.

The experimental plots were manipulated using rainout shelters enabling the exclusion and transmission of incident precipitation and UV radiation. Generally, UV and drought treatments had similar effects on flavonol accumulation. For *R. obtusifolius*, UV exclusion resulted in a substantial reduction of UV-screening compounds, particularly under ambient precipitation conditions, while for *H. maculatum* and *A. tenuis* UV exclusion caused only a slight reduction of flavonol content. Similarly, the drought treatment caused an increase in flavonol accumulation.

INTRODUCTION

Under natural conditions plants are affected by various environmental impacts. In many regions, reduced water availability is frequently accompanied by increased ultraviolet (UV) radiation (Ballaré et al. 2011). Drought stress and UV radiation are the most adverse factors for plant growth and productivity.

An important mechanism of tolerance for water deficits and UV radiation is the production of secondary metabolites (e.g. flavonols) that accumulate in epidermal cells where they effectively screen UV irradiation and reduce its penetration to mesophyll tissue. Flavonols also play a role in water deficit avoidance and tolerance by regulating stomatal closure and improving water use efficiency (Ramanjulu & Bartels 2002).

Some findings attribute the primary role for flavonoid induction to UV (Balakumar et al. 1993) while other results suggest interaction with water stress (Nogués et al. 1998). In addition, accumulation of the osmoregulator proline has been observed in response to a number of environmental factors, including drought and UV (Shetty et al. 2002). UV radiation has been shown to increase proline accumulation and drought tolerance in pea, wheat (Alexieva et al. 2001), and clover (Hofmann et al. 2003). Moreover, exposure of a UV-sensitive Arabidopsis mutant to UV-B radiation increased production of dehydrin proteins, which may have contributed to improved drought tolerance (Schmidt et al. 2000).

Because these protective mechanisms play an adaptive role in both water stress regulation (Gitz & Liu-Gitz 2003) and attenuation of UV-B radiation (Ibañez et al. 2008), interactive effects between UV-B exposure and drought stress in plants are assumed. However, existing data concerning the interaction between UV-B and drought on plant biochemical processes are equivocal.

Since drought and UV radiation induce similar protective mechanisms (e.g. Cechin et al. 2008), we tested the hypothesis that UV radiation and drought elicit synergistic effects on flavonol accumulation.

MATERIALS AND METHODS

Experimental site

The experiment was situated within a grassland ecosystem (association *Molinio-Arrhenatheretea*, alliance *Polygono-Trisetion*) at the Bílý Kříž Ecological Experimental Study Site (49°30'N, 18°32'E) in the Moravian–Silesian Beskid Mountains. The long-term mean annual temperature there is 6.8°C and precipitation is 1,318 mm. The site is located at an altitude of 855 m a.s.l. on an 8.5° slope with south-east exposure. Soil type is Gleyic Luvisol (FAO classification).

Experimental design

The experiment was conducted from 2011 to 2014 (Table 1). The plots (1.5 × 4 m each) were manipulated using six roof constructions covered by acrylic lamellas. The construction either enabled or blocked transmission of incident precipitation. The lamellas were made of two types of acrylic filter (3 mm thick). The first type (UVT Solar, Quinn Plastics, UK) transmitted more than 90% of incident UV-A and UV-B radiation (UV+ treatment) and the second type (Quinn XT, Quinn Plastics, UK) filtered UV-B radiation and most UV-A radiation (UV- treatment). In this way, four treatments were established: UV-dry, UV-wet, UV+dry, UV+wet.

Flavonol measurement

In situ measurements were taken after an induced drought period (Table 1). Flavonol content was determined by the method of epidermal UV screening measured by the chlorophyll fluorescence technique (Dualex 4 Flav, Force-A, FR). All measurements were conducted on dicotyledonous *Hypericum maculatum* (Crantz) and *Rumex obtusifolius* (L.) and monocotyledonous *Agrostis tenuis* (Sibth.) species.

Table 1: *Experimental design. IDP: induced drought period.*

Year	IDP	Length of IDP *days*	Flavonol measurement
2011	5 May–4 Aug	89	4 Aug
2012	10 May–11 Jul	62	10–11 Jul
2013	15 May–2 Jul	48	2–3 Jul
2014	21 May–17 Jul	57	2–3 Jul

RESULTS

Effect of drought stress and UV radiation on flavonol content

Generally, drought and UV treatments had similar effects on flavonol content (Fig. 1), although the effect slightly differed among individual years. Both factors caused an increase in flavonol accumulation. This effect was additive.

The most considerable effect of drought on accumulation of flavonols was observed in 2011 and 2012. The highest impact of UV radiation on flavonol content was observed in 2012 and 2014.

For *A. tenuis*, there was no effect of drought displayed in 2014; only an effect of UV was observed.

Effect of species on flavonol content

UV exclusion resulted in a slight reduction of UV-shielding compounds in all species studied. This reduction was more pronounced under ambient precipitation conditions (wet treatment). As a grass, *A. tenuis* generally had the lowest flavonol content of all monitored species, especially compared to *H. maculatum*. Although *H. maculatum* is a species with high flavonol content, an increase of flavonols was observed under UV exclusion. *Rumex obtusifolius* showed the highest annual variability in flavonol content among the species studied.

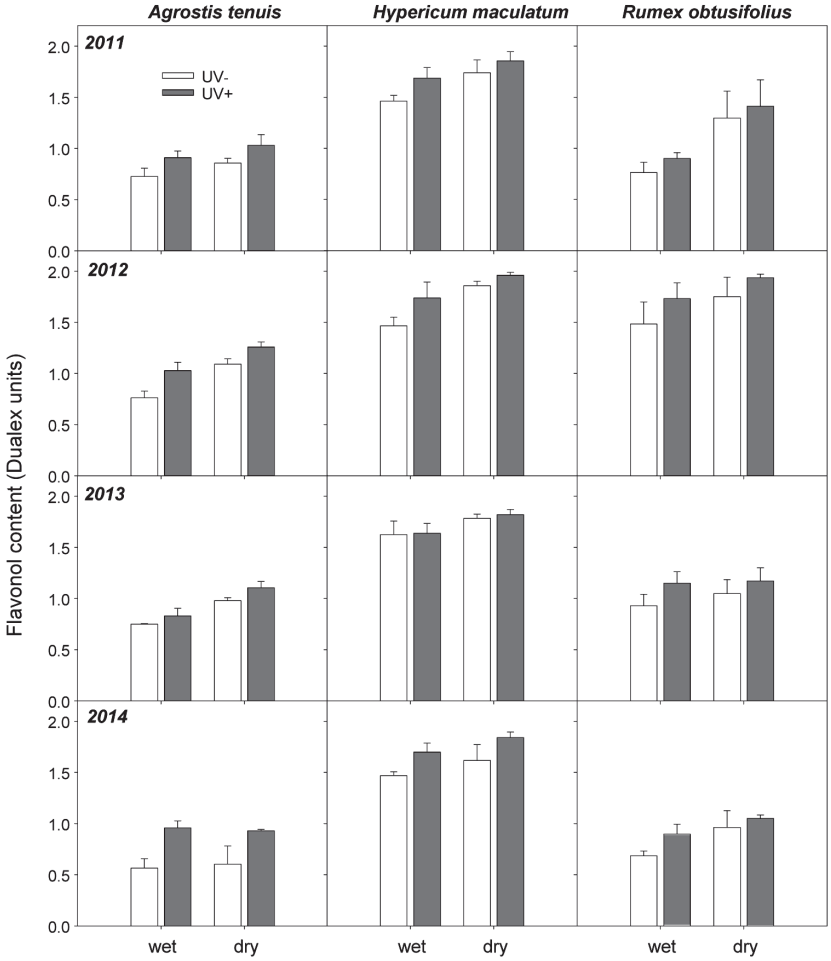

Fig. 1: *Flavonol content measured in vivo using a Dualex 4 Flav. Data are presented for the grass Agrostis tenuis and herbs Hypericum maculatum and Rumex obtusifolius for 4 years of the experiment. Means (columns) and standard deviations (error bars) are presented (N ≥ 10).*

DISCUSSION

In agreement with the tested hypothesis, the highest flavonol contents were observed in UV+dry treated plants, while the lowest contents were found for UV-wet plants. This was observed in all species and years studied. UV radiation thus has the potential to moderate the negative effects of drought on plants via adjusted flavonol content. The initial hypothesis was confirmed in both mono- and dicotyledonous species. Nevertheless, the year-on-year variability is substantial as a result of different precipitation, soil moisture, and solar radiation in particular years.

Generally, accumulation of flavonoids is considered to be the main photoprotective response associated with acclimation to excessive radiation, UV, drought, and so forth (Kataria et al. 2014). Flavonols in particular may serve as epidermal UV-absorbing pigments or as antioxidants scavenging free radicals and reactive oxygen species or contribute to energy dissipation in response to excess light and drought stress (Tattini et al. 2004). It has been shown that increased flavonol accumulation under stress conditions positively correlates with maintenance of both stages (quantum yield of photosystem II and CO_2 assimilation) of photosynthesis (Klem et al. 2015). In addition, it has been reported that when UV irradiation and drought stress were applied simultaneously the flavonol concentration in studied lettuce plants increased in comparison to when there was only a single stress factor (Rajabbeigi et al. 2013).

Acknowledgement

Supported by the Ministry of Education, Youth and Sports (MEYS) of the Czech Republic within the National Programme for Sustainability I, project No. LO1415. The experimental facility is part of project No. LM2010007 the National Infrastructure for Carbon Observations – CzeCOS/ICOS supported by MEYS.

References

Alexieva V, Sergiev I, Mapelli S et al. (2001) Plant Cell Environ. 24, 1337–1344.

Balakumar T, Vincent VHB, Paliwal K (1993) Physiol. Plant. 87, 217–222.

Ballaré CL, Caldwell MM, Flint SD et al. (2011) Photochem. Photobiol. Sci. 10, 226–241.

Cechin I, Corniani N, de Fátima Fumis T et al. (2008) Radiat. Environ. Biophys. 47, 405–413.

Gitz DC, Liu-Gitz L (2003) Photochem. Photobiol. 78, 529–534.

Hofmann RW, Campbell BD, Bloor SJ et al. (2003) Plant Cell Environ. 26, 603–612.

Ibañez S, Rosa M, Hilal M et al. (2008) J. Photochem. Photobiol. B 90, 163–169.

Kataria S, Jajoo A, Guruprasad KN (2014) J. Photochem. Photobiol. B 137, 55–66.

Klem K, Holub P, Štroch M et al. (2015) Plant Physiol. Biochem. doi: 10.1016/j.plaphy.2015.01.001.

Nogués S, Allen DJ, Morison JIL et al. (1998) Plant Physiol. 117, 173–181.

Rajabbeigi E, Eichholz I, Beesk N et al. (2013) J. Appl. Bot. Food Qual. 86, 190–197.

Ramanjulu S, Bartels D (2002) Plant Cell Environ. 25, 141–151.

Schmidt A-M, Ormond DP, Livingstone NJ et al. (2000) Ann. Bot. 85, 571–575.

Shetty P, Atallah MT, Shetty K (2002) Process Biochem. 37, 1285–1295.

Tattini M, Galardi C, Pinelli P et al. (2004) New Phytol. 163, 547–561.

Interactive effects of elevated CO_2 concentration, drought, and nitrogen nutrition on yield and grain quality of spring barley and winter wheat

Novotná, K.[1,2,*], Rajsnerová, P.[1,3], Veselá, B.[1,3], Klem, K.[1]

[1]*Global Change Research Centre, Bělidla 986/4a, 603 00 Brno, Czech Republic*

[2]*Department of Agrosystems and Bioclimatology, Faculty of Agronomy, Mendel University in Brno, Zemědělská 1, 613 00 Brno, Czech Republic*

[3]*Institute of Forest Ecology, Faculty of Forestry and Wood Technology, Mendel University in Brno, Zemědělská 1, 613 00 Brno, Czech Republic*

[*]*author for correspondence; email: novotna.k@czechglobe.cz*

ABSTRACT

The interactive effects of elevated CO_2 concentration (EC; 700 µmol mol^{-1}), drought stress, UV exclusion, and nitrogen nutrition were studied in open-top chambers located in the Bohemian–Moravian highlands (24 in total). Above-ground biomass at the time of harvest, grain yield, and grain quality parameters were studied in winter wheat (variety Bohemia) and spring barley (variety Bojos). The results showed that elevation of CO_2 concentrations increased above-ground biomass and grain yield. Higher levels of nitrogen increased the stimulatory effect of EC on above-ground biomass and grain yield. In addition, UV exclusion stimulated the effect of EC. EC generally led to increased rates of photosynthesis and assimilate formation. Increased storage of starch in the grain led to an unbalanced proportion of proteins and a decrease in their relative content in grain. Similarly to grain yield and above-ground biomass, the decrease in protein content under EC was also more pronounced under UV exclusion. EC led also to reduction of other quality parameters, such as the Zeleny sedimentation test. This effect is more pronounced when nitrogen is not a limiting factor as well as under the effect of drought. The stronger effect under drought stress is probably due to increased water use efficiency.

INTRODUCTION

The global concentration of carbon dioxide (CO_2) has been rising rapidly since the start of the Industrial Revolution in the second half of the 18th century. Current CO_2 concentration is at about 399.39 µmol mol–1 and is increasing by about 2 µmol mol^{-1} per year (Dlugokencky & Tans 2015). This CO_2 concentration is the highest it is has been over the past 15–20 million years (Tripati et al. 2009). Absent any effort to decrease atmospheric CO_2 concentration, it is possible that it may reach a level greater than 1,000 µmol mol–1 by 2100 (Sokolov et al. 2009). Understanding how plants would respond to such increased CO_2 concentration will help us understand how they are now responding and how they have adapted to the increase in CO_2 concentration that already has occurred. Some studies have already shown that doubling atmospheric CO_2 concentration increases total above-ground biomass by approximately 20–110% (Manderscheid et al. 1995). In the short term, C3 plants appear to respond directly to rising CO_2 concentration through Rubisco enzyme acclimation and decreased stomatal opening (Ainsworth & Rogers 2007). These changes, which boost the efficiency of both CO_2 uptake and water use, produce a wide range of secondary responses, most notably large increases in leaf non-structural carbohydrates, improved plant water status including increased leaf water potential, as well as in many cases increases in plant carbon to nitrogen ratio and decreases in leaf Rubisco

activity, stomatal density, and root/shoot mass (Long et al. 2004). This increased potential is rarely realized fully in the long-term, however, due to down-regulation of photosynthetic capacity (Urban 2003). It is obvious that nitrogen nutrition, which is particularly reflected in the amount and activity of the enzyme Rubisco, and water availability for plants, which interacts with the stomatal response to elevated CO_2 concentration, are the main factors that may influence elevated CO_2 concentration's effect on the productivity and qualitative parameters of field crops.

The main objectives of the experiment were to analyse expected global changes' impacts on wheat and barley grain production and quality parameters and study the mutual interactions of several factors simultaneously: elevated CO_2 concentration, exclusion of UV, drought stress, and nitrogen nutrition.

MATERIALS AND METHODS

The open-top chamber (OTC) experimental facility is located at Domanínek near Bystřice nad Pernštejnem in the Bohemian–Moravian Highlands (Czech Republic, 49°31.520'N, 16°13.900'E, 575 m a.s.l.). This region is characterized as a rain-fed area with mean annual precipitation of 610 mm and mean annual temperature of 7.2°C. The soil type is modal cambisol with geological bedrock weathered gneiss at depths of 60–90 cm. Soil texture is sandy loam (45–60% sand and as much as 16% clay) and pH (KCl) is between 4 and 5. The experimental facility consists of 24 OTCs with a hexagonal ground plan with diameter of 4 m. The basic height of a chamber is 2 m and above this construction is placed a roof with rotating lamellas enabling control of chamber ventilation and precipitation. Ventilation (temperature difference), CO_2 concentration, and precipitation were controlled automatically by a control unit based on feedback regulation using data from a set of sensors and analysers.

Each chamber was divided into two halves with one half sown with winter wheat (*Triticum aestivum* L.) and the second half with spring barley (*Hordeum vulgare* L.). Winter wheat variety Bohemia with bread quality A was sown on 10–11 October 2013 at a density of 3.5 million germinable seeds (MGS) per hectare. Spring barley variety Bojos with malting quality was sown on 18 March 2014 at a density of 3.5 MGS ha^{-1}. Each plot was additionally divided into subplots with one half fertilized with nitrogen (calcium nitrate, Ca(NO3)2) and the other half not fertilized at all. Fertilization was done on 14 March 2014 in wheat and 10 April 2014 in wheat and barley always at rate 100 kg N ha^{-1}. Total nitrogen was thus 200 kg ha^{-1} in wheat and 100 kg ha^{-1} in barley. Both crop species were exposed throughout the growing season (May–July) to ambient and elevated (700 µmol mol^{-1}) CO_2 concentrations.

Above-ground biomass was harvested manually at full ripening and weighed. This was followed by grain threshing using a Delta Plot combine small-plot harvester (Wintersteiger AG, Austria). Cleaned grain was used for analysis of protein content on a Flash 2000 elemental analyser (Thermo Scientific, USA). Detailed analyses of grain quality (starch content using the NIRs method, Zeleny sedimentation test, falling number) were performed at an accredited laboratory (Central Institute for Supervising and Testing in Agriculture, Brno, Czech Republic) using certified analytical methods.

Statistical analyses were made using Statistica 12 (StatSoft, USA). Four-way ANOVA followed by Tukey's post-hoc test was used to evaluate the effects of individual treatments.

RESULTS

Assessment of the effects of elevated CO_2 concentration (EC) in interaction with the effects of nitrogen nutrition and drought stress revealed similar results for both above-ground biomass and grain yield in both crop

species studied. EC generally increased above-ground biomass and grain yield (Fig. 1). Nitrogen fertilization strengthened the stimulatory effect of EC on above-ground biomass and grain yield. Similarly, UV exclusion stimulated the effect of EC concentration. The effect of drought on grain yield was more pronounced in spring barley, and the alleviating effect of EC was also more obvious in this crop species. EC also reduced some quality parameters, such as protein content (Fig. 2) and the Zeleny sedimentation test.

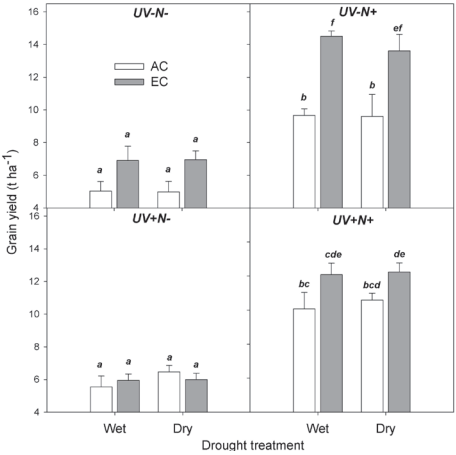

Fig. 1: *Interactive effects of CO_2 concentration (AC: ambient CO_2 concentration, EC: elevated CO_2 concentration – 700 µmol mol^{-1}), UV treatment (UV+: ambient UV radiation, UV–: excluded UV radiation), nitrogen nutrition (N+: 200 kg N ha^{-1}, N–: 0 kg N ha^{-1}) and drought (wet: ambient precipitation; dry: precipitation excluded from the middle of stem elongation) on grain yield of winter wheat (variety Bohemia). Means (columns) and standard deviations (error bars) are presented (N = 3). Different letters denote statistically significant differences among individual treatments using Tukey's post-hoc test ($p \leq 0.05$).*

DISCUSSION

Considering incessant increases in global CO_2 concentration, it is necessary to determine not only how plants will respond to this factor itself but also how these effects will be modified by such other factors expected in future as drought, UV radiation, and nitrogen availability. In our study, we found that the effect of EC is modulated by other growing or environmental factors, particularly nitrogen nutrition and UV radiation and to a lesser extent also drought stress. Nitrogen deficiency is one of the main causes of feedback regulation of photosynthesis under EC and becomes the limiting factor. Therefore, the effect of EC under these conditions is usually low. Reich et al. (2006) showed in a grassland ecosystem that EC stimulated plant biomass much less under ambient than enriched N supply. As these limitations on productivity resulting from insufficient availability of N are widespread in both unmanaged and managed vegetation, those authors concluded that soil N supply is probably an important constraint on global terrestrial responses to EC. In accordance with our results, Teramura et al. (1990) found a reduction or disappearance of EC's stimulatory effect under higher UV radiation intensity on wheat grain yield and biomass. Our study found no interactive effects between EC and drought stress, although some studies have shown modulation of EC by regulation of stomatal closure and thereby increasing water use efficiency. The effect of CO_2 concentration in reducing stomatal conductance and decreasing canopy evapotranspiration was reviewed by Leakey et al. (2009).

Similarly to our results, Wieser et al. (2008) found that EC caused significant reductions in protein content and all protein fractions and types except albumins and globulins. EC effects were more pronounced in wheat samples supplied with larger amounts of N fertilizer, which is in accordance with our results.

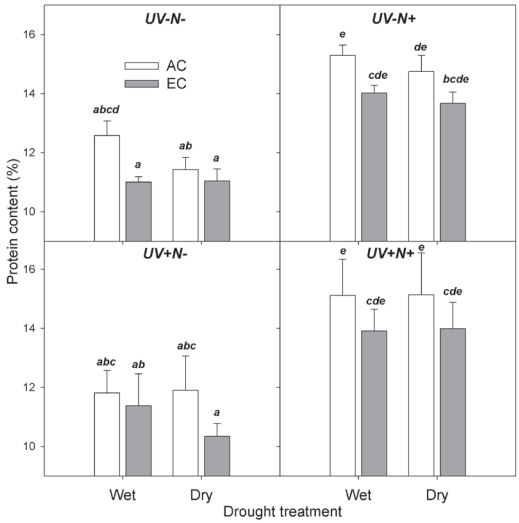

Fig. 2: *Interactive effects of CO_2 concentration (AC: ambient CO_2 concentration, EC: elevated CO_2 concentration – 700 µmol mol^{-1}), UV treatment (UV+: ambient UV radiation, UV–: excluded UV radiation), nitrogen nutrition (N+ 200 kg N ha^{-1}, N–: 0 kg N ha^{-1}) and drought (wet: ambient precipitation, dry: precipitation excluded from the middle of stem elongation) on grain protein content of winter wheat (variety Bohemia). Means (columns) and standard deviations (error bars) are presented (N = 3). Different letters denote statistically significant differences among individual treatments using Tukey's post-hoc test ($p \leq 0.05$).*

Acknowledgement

Supported by National Agency for Agricultural Research projects nos. QJ1310123 and QI111A133.

References

Ainsworth EA, Rogers A (2007) Plant Cell Environ. 30, 258–270.

Leakey ADB, Ainsworth EA, Bernacchi CJ et al. (2009) J. Exp. Bot. 60, 2859–2876.

Long SP, Ainsworth EA, Rogers A et al. (2004) Annu. Rev. Plant Biol. 55, 591–628.

Manderscheid R, Bender J, Jäger H-J et al. (1995) Agric. Ecosyst. Environ. 54, 175–185.

Dlugokencky E, Tans P (2015) Recent global CO_2. Earth System Research Laboratory, National Oceanic and Atmospheric Administration. Available online at http://www.esrl.noaa.gov/gmd/ccgg/trends/global.html.

Reich PB, Hobbie SE, Lee T et al. (2006) Nature 440, 922–925.

Sokolov AP, Stone PH, Forest CE et al. (2009) J. Clim. 22, 5175–5204.

Teramura AH, Sullivan JH, Ziska LH (1990) Plant Physiol. 94, 470–475.

Tripati AK, Roberts CD, Eagle RA (2009) Science 326, 1394–1397.

Urban O. (2003) Photosynthetica 41, 9–20.

Wieser H, Manderscheid R, Erbs M et al. (2008) J. Agric. Food Chem. 56, 6531–6535.

The effect of drought and nitrogen fertilization on the production, morphometry, and spectral characteristics of winter wheat

Trunda, P.[1,2,*], Holub, P.[1], Klem, K.[1]

[1]*Global Change Research Centre, Bělidla 986/4a, 603 00 Brno, Czech Republic*
[2]*Mendel University in Brno, Zemědělská 1, 613 00 Brno, Czech Republic*
[*]*author for correspondence; email: trunda.p@czechglobe.cz*

ABSTRACT

Methods of study based on the spectral reflectance of vegetation are now commonly used in researching both natural ecosystems and field crops (Aparicio et al. 2000). The aims of this experiment were to evaluate the effect of drought and nitrogen (N) fertilization on N use efficiency in winter wheat and use the obtained spectral characteristics to assess stand heterogeneity as a potential consequence of different crop nutrition. Twelve experimental plots of winter wheat were manipulated to drought from 8 May 2013 to 12 June 2013. The effect of drought was observed in two treatments: control without fertilization (N0; 0 kg N ha^{-1}) and N fertilization (N140; 140 kg N ha^{-1}). Plant samples were then taken for determination of above-ground biomass and N content in dry matter. Spectral characteristics of wheat were measured in the earing phase at canopy level. The effect of drought on the morphometric parameters of winter wheat was statistically significant only on N-fertilized plots (N140). Total above-ground biomass decreased by a significant 18% in the N140 treatment as a result of the simulated drought. This decrease was reflected in statistically significant reductions of all individual plant parts (stems, leaves, spikes) in N140. Responses to drought stress were observed in many vegetation indices, particularly in NDVI, GNDVI, and WI/NDVI. The results show that there are significant relationships between N content in the grain and vegetation indices. In particular, a quite marked separation was observed in the relationships between dry and ambient treatments for vegetation indices NRERI, TCARI/OSAVI, VOG2 and GM. Generally, the impact of drought increased at higher levels of N content in the grain, which corresponded with the results of morphometric analysis. Use of reflectance in the study of vegetation and field crops regarding risk assessment of mineral N leaching from soils has considerable potential especially in mapping large areas and monitoring temporal changes relating to N release.

INTRODUCTION

The results of monitoring and research of European soils provide evidence of gradual soil degradation (Van den Akker et al. 2003). Its causes include excessive application of nitrogen (N) fertilizers as well as anthropogenic atmospheric N deposits. It is in the public interest to prevent increases in nitrate content in groundwater. To investigate wheat canopy heterogeneity resulting from different nutrition regimes, we applied non-destructive methods based on spectral reflectance. The basic principle governing canopy reflectance spectra is that specific plant traits are associated with the absorption of specific wavelengths of the spectrum (Reynolds et al. 1999). Statistically significant correlations are often found among spectral characteristics (most frequently vegetation indices) and chlorophyll content per area unit (Houborg et al. 2007), nutritional status of the stand (Jorgensen et al. 2007, Zhao et al. 2005), total above-ground biomass (Starks et al. 2006), and drought effects (Peñuelas et al. 2004).

The aims of this experiment were to assess the impact of drought on N use efficiency in wheat and evaluate

stand heterogeneity as a potential consequence of different nutritional regimes using spectral characteristics. We assumed that a period of drought followed by simulated extreme precipitation would have a decisive influence on wheat primary production (i.e. morphometric characteristics and different accumulation of N in wheat organs), which can be determined by spectral reflectance methods.

MATERIALS AND METHODS

The experiment was conducted at a location near the village of Banín (49°40'N, 16°28'E, 454 m a.s.l.) on experimental plots (10 × 4.5 m) sowed with winter wheat (*Triticum aestivum* L. var. *aestivum*). For the dry treatment, rainout shelters constructed over the experimental plot consisted of a wood frame supporting polycarbonate transparent strips covering experimental plots. The wood frame was anchored by four wooden rods at the corners. The roof had a 20° inclination and on its lowest side a gutter that channelled intercepted water. A 0.2-m wide trench was dug and sheathed with a steel barrier to separate the soil of the roofed plots from the neighbouring soil. Shelter sides and ends remained open to maximize air movement and minimize temperature and relative humidity artefacts. Such rainout shelters with a roof consisting of bands of transparent blocks enable well-replicable experiments with minimal secondary microenvironmental effects. Yahdjian & Sala (2002) had detected only a relatively small edge effect on soil water content. At the beginning of stem extension (8 May 2013), experimental roofs were installed over 12 plots to simulate drought stress. The simulated drought lasted until 12 June 2013 (end of wheat heading). After the drought period, 90 mm of water was applied (in two batches) to simulate extreme rainfall, which amount which equalled the difference by which the areas under roofs had been deprived. Ambient treatment plots without roofs were left to natural precipitation income. During the experiment, soil moisture and temperature were continually monitored by soil sensors installed at a depth of 15 cm. At the end of the drought period, soil moisture had been reduced to 33% as compared with the ambient (100%). The effect of drought was observed in two treatments: a control without fertilization (N0; 0 kg ha^{-1}) and N fertilization (N140; 140 kg ha^{-1}, nitrogen supplied as NH_4, NO_3, and urea in a 1:1:2 ratio) in two doses (25 April and 14 June). All treatments (N0-dry, N0-ambient, N140-dry, and N140-ambient) were carried out in four repetitions. On 13 June 2013, plant samples (stems, leaves, and spikes) were collected to evaluate the impact of the drought period on morphometric characteristics. Three shoots were collected from each plot. Shoot and spike lengths were measured, as were leaf length and width (F, F-1, F-2, and F-3), dry weight of total above-ground biomass, and leaf area. Specific leaf area (SLA) was calculated from the dry weight of leaves and leaf area. Leaf samples (F and F-1) were analysed to determine N and carbon contents in dry mass using a Flash 2000 elemental analyser (Thermo Scientific, USA).

Spectral reflectance measurement at the canopy level was carried out during heading phase using a FieldSpec 4 HiRes spectroradiometer (ASD, USA) in the range of 350–2500 nm. Measurements were made twice for each plot. Subsequently, vegetation and chlorophyll indices were computed from spectral reflectance curves. Data were evaluated by analysis of variance using Statistica 12 (StatSoft, USA).

RESULTS AND DISCUSSION

Drought is a major limiting factor for global agriculture and the limitation is greatly aggravated by N deficiency (Gonzales-Dugo et al. 2010). In the present study, the effect of drought on the morphometric parameters of winter wheat was statistically significant only for the N-fertilized treatment (N140). The total amount of above-ground biomass was reduced by 18% in N140 as a result of simulated drought stress (ambient: 2.8 g

dry weight (DW) per plant; dry: 2.3 g DW per plant). This decrease in dry weight was reflected in statistically significant reductions in all individual plant parts (stems, leaves, spikes) for N140 (Table 1).

Ground-level remote sensing enables rapid evaluation of plant and canopy physiological status in a non-intrusive way. Many high spectral resolution reflectance vegetation indices have been proposed with the aim of monitoring biomass, phenology, and the physiological conditions of plants and canopies (Peñuelas et al. 1998). In the present study, the response to drought stress was monitored in selected vegetation indices, namely NDVI, GNDVI, and WI/NDVI. Because the most significant response to drought stress was recorded in the NDVI index, which is correlated with biomass yield and leaf area index, we can assume that the effect was probably at a biomass level rather than at a biochemical level (e.g. chlorophyll content). Bandyopadhyay et al. (2014) also studied the effects of drought and N fertilization on wheat yield and found that spectral reflectance based on the water indices WI and NWI-1 were significantly and negatively correlated with grain yield and that NWI-1 and NWI-3 were significantly and negatively correlated with biomass yield. In addition, Pradhan et al. (2014) concluded that WI recorded at booting stage can be used successfully to predict in advance grain and above-ground biomass yield of wheat under various water and nitrogen management practices.

Table 1: *Effect of drought on morphometric parameters of winter wheat in control treatment (N0) and fertilized treatment (N140). Δ(%) = percentage differences; shows an increase (+) or decrease (–) in selected parameter in dry treatment in comparison with ambient conditions (n.s.: not significant, *0.01 < p ≤ 0.05, **p ≤ 0.01, ***p ≤ 0.001; n = 4).*

	N0-ambient	N0-dry	Δ(%)	N140-ambient	N140-dry	Δ(%)
Shoot height *(cm)*	54.90	54.20	–1 n.s.	**65.90**	**58.90**	**–11 *****
Spike length *(cm)*	7.70	7.50	–3 n.s.	**7.80**	**8.40**	**+8 ****
Stem (g_{DW})	1.60	1.54	–4 n.s.	**1.95**	**1.57**	**–19 *****
Spike (g_{DW})	0.35	0.35	0 n.s.	**0.40**	**0.35**	**–12 ***
Leaf F (g_{DW})	0.08	0.08	+4 n.s.	**0.14**	**0.12**	**–15 ***
LA F (cm^2)	12.45	11.20	–10 n.s.	**19.54**	**13.39**	**–31 ***
SLA F ($cm^2\ mg^{-1}$)	0.14	0.13	–7 n.s.	0.14	0.12	–19 n.s.
Leaf F1 (g_{DW})	0.10	0.11	+13 n.s.	**0.14**	**0.12**	**–11 ***
LA F1 (cm^2)	17.55	17.60	0 n.s.	21.05	19.36	–8 n.s.
SLA F1 ($cm^2\ mg^{-1}$)	0.17	0.16	–9 n.s.	0.16	0.17	+7 n.s.
Leaf F2 (g_{DW})	0.09	0.09	+3 n.s.	**0.11**	**0.09**	–11 *
LA F2 (cm^2)	16.76	14.39	–14 n.s.	17.19	15.44	–10 n.s.
SLA F2 ($cm2\ mg^{-1}$)	0.17	0.16	–6 n.s.	0.16	0.16	+1 n.s.
Leaf F3 (g_{DW})	0.06	0.06	+3 n.s.	**0.07**	**0.06**	**–15 ****
Total leaves (g_{DW})	0.33	0.35	+6 n.s.	**0.46**	**0.40**	**–13 ****
Total shoot (g_{DW})	2.28	2.25	–1 n.s.	**2.81**	**2.31**	**–18 *****

Vegetation indices measured at canopy level using the FieldSpec were subsequently used to evaluate correlations with N content in grain. The results showed significant correlations of several indices with N content in grain. Some indices (NRERI, TCARI/OSAVI, VOG2, GM) showed clearly evident separation of the correlations between dry and ambient treatments (Fig. 1).

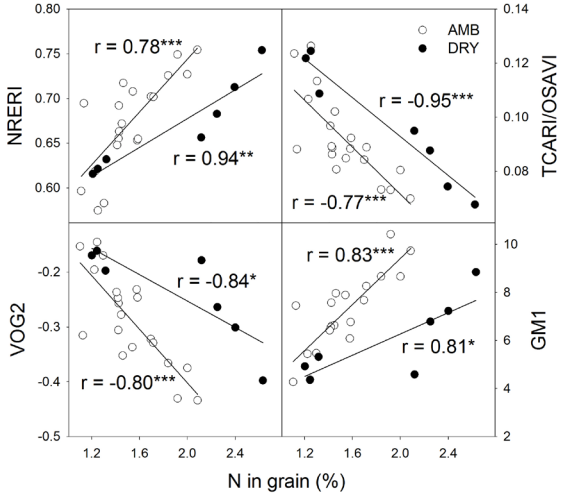

Fig. 1: *Relationships between selected vegetation indices NRERI, TCARI/OSAVI, VOG2, and GM1 and N content in grain. Pearson correlation coefficient and its significance *0.01 < p ≤ 0.05; **p ≤ 0.01; ***p ≤ 0.001.*

Finally, the impact of drought was increased at higher N levels in grain, which corresponded to the results of morphological analyses. Only after converting N uptake per unit of area is it possible to evaluate whether the differences can be attributed indirectly to N use efficiency or whether they are due to the negative drought effect on production caused directly by water deficiency.

Acknowledgement

Supported by project No. QJ1220007 from the Ministry of Agriculture. It is a product of the CzechGlobe Centre, developed within the Operational Programme Research and Development and co-financed from EU funds and the State Budget of the Czech Republic (No. CZ.1.05/1.1.00/02.0073).

References

Aparicio N, Villegas D, Casadesus JL et al. (2000) Crop Sci. 42, 1547–1555.

Bandyopadhyay KK, Pradhan S, Sahoo RN et al. (2014) Agric. Water Manag. 146, 115–123.

Gonzales-Dugo V, Durand J-L, Gastal F (2010) Agron. Sustain. Dev. 30, 529–544.

Houborg R, Soegaard H, Boegh E (2007) Remote Sens. Environ. 106, 39–58.

Jørgensen RN, Christensen LK, Bro R (2007) Int. J. Remote Sens. 28, 943–962.

Peñuelas J, Filella I, Llusià J et al. (1998) J. Exp. Bot. 49, 229–238.

Peñuelas J, Munné-Bosch S, Llusià J et al. (2004) New Phytol. 162, 115–124.

Pradhan S, Bandyopadhyay KK, Sahoo RN et al. (2014) J. Indian Soc. Remote Sens. 42, 711–718.

Reynolds MP, Rajaram S, Sayre KD (1999) Crop Sci. 39, 1611–1621.

Starks PJ, Zhao D, Phillips WA et al. (2006) Crop Sci. 46, 927–934.

Van den Akker JJH, Arvidsson J, Horn R (2003) Soil Till. Res. 73, 1–8.

Yahdjian L, Sala OE (2002) Oecologia 133, 95–101.

Zhao C, Liu L, Wang J et al. (2005) Int. J. Appl. Earth Obs. Geoinf. 7, 1–9.

The influence of reduced precipitation supply on spring barley yields and the ability of crop growth models to simulate drought stress

Pohanková, E.[1,2,*], Orság, M.[1,2], Hlavinka, P.[1,2]

[1]*Global Change Research Centre, Bělidla 986/4a, 603 00 Brno, Czech Republic*
[2]*Mendel University in Brno, Zemědělská 1, 613 00 Brno, Czech Republic*
[*]*author for correspondence; email: Eva.Pohankova@seznam.cz*

ABSTRACT

This paper evaluates the first year (2014) of results from a field experiment with spring barley (cultivar Bojos) under reduced precipitation supply. The field experiment was carried out at an experimental station in the Czech Republic and consisted of small plots in two variants and three repetitions. The first variant was uncovered, and the second was partly covered to exclude rain throughout the entire vegetation season. For plots' partial covering, a material was used to divert rainwater away from 70% of the plots. The main aim was to determine whether there are any differences in soil water content or in grain yield size between uncovered and partly covered plots and to compare the results obtained. Data measured in this field experiment were used to compare simulations of this field experiment in the DAISY crop growth model. Subsequently, the crop growth model's ability to simulate grain yield, which was affected by drought stress, was explored. In reality, differences in phenological development and grain yield size were not evident. Reducing precipitation supply in DAISY by about 70% led to simulations of covered plots with reduced grain yield in accordance with the initial hypothesis. Agreement between observed and simulated grain yield was evaluated using selected statistical indicators: root mean square error (RMSE) as a parameter of average magnitude of error and mean bias error (MBE) as an indicator of systematic error. RMSE of grain yield was 2.6 t ha^{-1}. MBE revealed grain yield undervalued by 2.6 t ha^{-1}.

INTRODUCTION

According to climate prediction models, drought periods can be expected more frequently in future (e.g., Trnka et al. 2011, Dubrovský et al. 2014). Plant growth may be negatively influenced by drought. One possible way to estimate the effects of expected climate conditions, such as drought, on grain yield is to use crop growth models (e.g., Thaler et al. 2012, Eitzinger et al. 2013, Rosenzweig et al. 2013). The hypothesis of the field experiment presented here was that reducing precipitation in the partly covered plot by about 70% would lead to reduced soil moisture and consequently to reduced grain yield in spring barley. The next step was to determine whether the DAISY crop growth model was able to simulate differences in grain yield in spring barley after precipitation reduction of about 70%.

MATERIALS AND METHODS

The experiment was carried out at a field experimental station with the spring barley cultivar Bojos. The experimental station is situated at Domanínek in the Bohemian–Moravian Highlands (Czech Republic; 49°31'42''N, 16°14'13''E; 530 m a.s.l.). The experiment consisted of small plots (3.1 × 8 m) in two variants (a partly covered plot and an uncovered plot) in three repetitions. The first variant was 70% covered, the cover diverting rainwater away from the plot. A clear SUNTUF polycarbonate sheet (Palram, Israel) 0.8 mm thick

was used to cover the plot. The polycarbonate sheet is impermeable to UV radiation. The manufacturer states that this material transmits 90% of solar radiation while excluding UV radiation. The second variant had no cover. For all experimental plots, two time-domain reflectometers (TDRs; CS 616, Campbell Scientific, UK) were placed vertically to monitor soil water content from the surface to a depth of 30 cm. Gypsum blocks, used to measure the soil's water potential, were placed at depths of 20 cm. One gypsum block was placed on each experimental plot. Average values measured by the TDRs and gypsum blocks were stored at 10 min intervals. Daily averages were entered into the analysis. Grain yield harvested in the field experiment was compared with grain yield simulated by the DAISY crop growth model. For the purposes of this paper, DAISY was first calibrated according to phenological phases observed in the 2014 field experiment with the spring barley cultivar Bojos. The next input parameter was meteorological data, where partly covered plots had precipitation reduced by about 70% in comparison to uncovered plots. To statistically evaluate the relationship between the modelled and measured grain yield, the following parameters were used: the mean bias error (MBE) as an indicator of the average systematic error and root mean square error (RMSE), which describes the average of absolute deviation between observed and modelled values (Davies & McKay 1989).

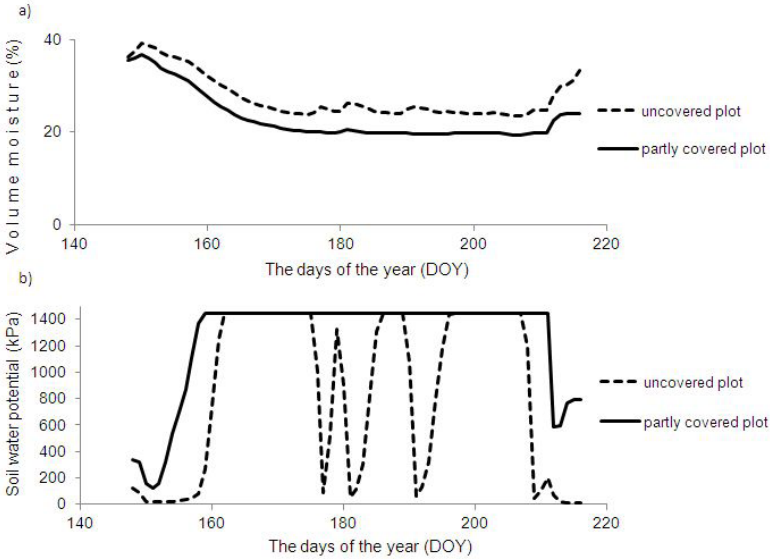

Fig. 1: *(A) Comparisons between uncovered and partly covered plots in soil water content measured by TDR for spring barley cultivar Bojos from 0–30 cm in 2014 (n = 1). (B) Comparisons between uncovered and partly covered plots in soil water potential measured by gypsum block for spring barley cultivar Bojos at 20 cm in 2014 (N = 1).*

RESULTS

Fig. 1 shows the values measured by TDRs in the field experiment. Soil water content (Fig. 1a) was measured by TDR within a range of 20–40% of volumetric soil moisture. Small differences in the curves can be seen where decreased water soil content was measured for the partly covered plot in comparison to that for the

uncovered plot. The curve measured for the uncovered plot shows the times during the year when it rained. This appears four times in the curve. Soil water potential (Fig. 1b) reached 1,400 kPa. This value was valid for the entire measuring time in the soil of the partly covered plot. Based on the four deviations in the curve for the uncovered plot, it can be stated that the gypsum blocks also recorded four significant instances of precipitation which influenced soil moisture. Soil in the uncovered plot was saturated by water for some time. Soil water potential changed considerably over the year. No changes were recorded for the partly covered plot during the rain period.

Table 1 compares actual grain yield and grain yield simulated by the DAISY crop growth model. Real grain yields ranged from 5.18 to 6.00 t ha^{-1}. No differences were detected between uncovered and partly covered plots. Only 30% of precipitation for the uncovered plot was entered into DAISY for the partly covered plot, which resulted in DAISY simulating decreased grain yields in accordance with the initial hypothesis.

Table 1: *Comparison of actual grain yield and grain yield simulated by the DAISY crop growth model.*

	Grain yield (t ha^{-1})					
	Uncovered plot 1	**Partly covered plot 1**	**Uncovered plot 2**	**Partly covered plot 2**	**Uncovered plot 3**	**Partly covered plot 3**
Measured	6.00	5.18	5.20	5.59	5.76	5.38
Simulated	3.13	2.61	3.13	2.61	3.13	2.61

DISCUSSION

The plots in the field experiment did not have trenches dug around them. During precipitation, water could therefore penetrate into a plot from soil adjacent to the plot. No large differences were recorded in soil water content measured by TDR, as can be seen in Fig. 1a. Another possible explanation for this fact is that some TDRs in the partly covered plots may have been placed among stripes and therefore been only partly covered. Precipitation could thus have fallen onto the TDRs. The only recorded potential was measured by gypsum blocks. Soil water potential in partly covered plots increased sooner than it did in uncovered plots (Fig. 1b). When soil water potential rises, plants must expend more effort to obtain necessary water. The less water there is in soil, the more underpressure plants must create to draw water. This is more demanding for the plants and drought stress could become evident. It can be seen in Fig. 1b that water availability under partly covered plots was poorer for plants than it was under uncovered plots. From Table 1, it is clear that no substantial differences in actual grain yield were recorded. The hypothesis was not confirmed in reality. A study by Lawlor et al. (1981) had demonstrated that irrigated spring barley had higher grain yields than did spring barley which suffered from water deficits. The experiment of Morgan & Riggs (1981) also proved that in drought conditions grain yields from spring barley were negatively influenced. After reducing precipitation by about 70%, the DAISY crop growth model simulated decreased grain yield and thus confirmed the hypothesis that decreased yield can be expected at decreased precipitation intake. Generally, simulated grain yield was underestimated in comparison to reality. RMSE was 2.6 t ha^{-1} and MBE revealed grain yield undervalued by 2.6 t ha^{-1}. DAISY was recently calibrated for the conditions of the experimental station in Domanínek and spring barley (Pohanková et al. 2012). This study did not record such a significant underestimation of grain yield. RMSE for grain yield was 1.4 t ha^{-1} and MBE revealed grain yield undervalued by 0.3 t ha^{-1}. The field experiment with covered plots and spring barley will continue in 2015. Based on these results, anticipated recalibration of DAISY as well as discovering the causes for underestimation of the simulated spring barley

grain yield in 2014 can be expected. Due to the fact that in 2014 plots were only 70% covered, no differences were determined in reality. In the following vegetation season, the plots will be 100% covered and so precipitation will be completely diverted.

Acknowledgement

Supported by project No. LO1415 of the Ministry of Education, Youth and Sports within the National Programme for Sustainability I, project No. CZ.1.07/2.3.00/20.0248 "Building up a multidisciplinary scientific team focused on drought", National Agency for Agricultural Research project No. QJ1310123 "Crop modelling as a tool for increasing the production potential and food security of the Czech Republic under Climate Change", and project No. LD13030 supporting COST Action ES1106.

References

Davies JA, McKay DC (1989) Sol. Energy 43,153–168.

Dubrovský M, Hayes M, Duce P et al. (2014) Reg. Environ. Change 14, 1907–1919.

Eitzinger J, Trnka M, Semerádová D et al. (2013) J. Agric. Sci. 151, 787–812.

Lawlor DW, Day W, Johnston AE et al. (1981) J. Agric. Sci. 96, 167–186.

Morgan AG, Riggs TJ (1981) J. Sci. Food Agric. 32, 339–346.

Pohanková E, Trnka M, Hlavinka P et al. (2012) Calibration of the selected crop growth models for spring barley. MendelNet 2012: Proceedings of International Ph.D. Students Conference (eds P Škarpa, P Ryant, R Cerkal et al.), pp. 149–161. Faculty of Agronomy, Mendel University in Brno.

Rosenzweig C, Jones JW, Hatfield JL et al.(2013) Agric. For. Meteorol. 170, 166–182.

Thaler S, Eitzinger J, Trnka M et al. (2012) J. Agric. Sci. 150, 537–555.

Trnka M, Eitzinger J, Semerádová D et al. (2011) Clim. Change 108, 261–289.

Surface water temperature modelling to estimate Czech fishery productivity under climate change

Svobodová, E.[1,2,*], Trnka, M.[1,2], Kopp, R.[3], Mareš, J.[3], Spurný, P.[3], Pechar, L.[4,5], Beděrková, I.[5], Dubrovský, M.[2], Žalud, Z.[1,2]

[1]*Global Change Research Centre, Bělidla 986/4a, 603 00 Brno, Czech Republic*

[2]*Institute for Agrosystems and Bioclimatology, Mendel University in Brno, Zemědělská 1/1665, 613 00, Brno, Czech Republic*

[3]*Department of Zoology, Fisheries, Hydrobiology and Apiculture, Mendel University in Brno, Zemědělská 1/1665, 613 00, Brno, Czech Republic*

[4]*ENKI, o.p.s., Dukelská 145, 379 01 Třeboň, Czech Republic*

[5]*Laboratory of Applied Ecology, University of South Bohemia in České Budějovice, Branišovská 1760, 370 05 České Budějovice, Czech Republic*

[*]*author for correspondence; email: e_svobodova@yahoo.com*

ABSTRACT

Freshwater fish production is significantly correlated with water temperature, which is expected to increase under climate change and affect fish growth, productivity, and survival. This study deals with estimating the change in water temperature in productive ponds and its impact on fishery in the Czech Republic. The target fish species were common carp (*Cyprinus carpio*), maraena whitefish (*Coregonus maraena*), northern whitefish (*Coregonus peled*), and rainbow trout (*Oncorhynchus mykiss)*. It was hypothesized that there would be an increasing risk of high water temperature stress for fish. Water temperature calculations based on 3-day means of air temperature were tested in several ponds in three major fish production areas. The verified model was applied to the climate change conditions determined by standardized scenarios derived from the five global circulation models MPEH5, CSMK3, IPCM4, GFCM21, and HADGEM. The results for changed climate indicated limitations for Czech fish farming in terms of prolonged periods with fish temperature stress as well as the increased number of stress periods and increased number of days within these periods. It is very likely that Czech fishery will have to change the fish species farmed in particular productive areas. In particular, higher altitudes are likely to become less suitable for the *Salmonidae*.

INTRODUCTION

Freshwater aquaculture is an important and integral part of the Czech agricultural sector. Aquaculture production in the Czech Republic is generally characterized by extensive and semi-intensive fish farming in ponds. Temperature heavily influences most physiological processes in fish, including spawning, development, and growth. General relationships have been estimated between temperature, mortality, and growth for most temperate fish species. Given the strong responses of individual freshwater organisms to temperature, anticipated climate warming is likely to have considerable effects on the geographical distributions of freshwater organisms. Rising global temperatures and changing precipitation patterns have altered the thermal and hydrological regimes of many inland waters. Sala et al. (2000) considered lentic (i.e. lakes and ponds) and lotic (i.e. streams and rivers) ecosystems to be most sensitive to land-use change, exotic species, and climate change in a global-scale assessment.

In the present study, the authors consider fish response to rising temperatures linked to climate change. The

main aim of the study is to estimate how the increasing ambient temperature will affect fish persistence in the environment with increasing water temperature and how this experience will alter fish productivity in the Czech Republic under expected climate conditions. For the best expression of climate change impact, the study focuses on a number of productive ponds in various climatic areas with various farming management (e.g. various farmed species).

MATERIALS AND METHODS

Six ponds from three different climatic areas were involved in the study. For studied water bodies, daily surface water temperature was recorded at floating depths of 10–20 cm depending on water level decline/rise during the season. Observed daily surface water temperature data were coupled with supplemented daily meteorological data covering the ambient air temperature for the same period as the observed data. These data were used in the process of verifying the daily surface water temperature equation. The equation was developed based on surface water measurements in two ponds (1985–2003), while the remaining four ponds provided testing datasets. The equation's reliability was verified by comparing observed and calculated surface water temperatures. Following model validation, input meteorological data were modified according to the climate change scenarios MPEH5, CSMK3, IPCM4, GFCM21, and HADGEM (Dubrovsky et al. 2012). The model's final result was an overview summarizing days with surface water temperature exceeding the upper temperature threshold for fish survival in the expected climate. The summary has led to the detection of the number of risks per decade and per year which introduce a limitation on fish farming production in the Czech Republic.

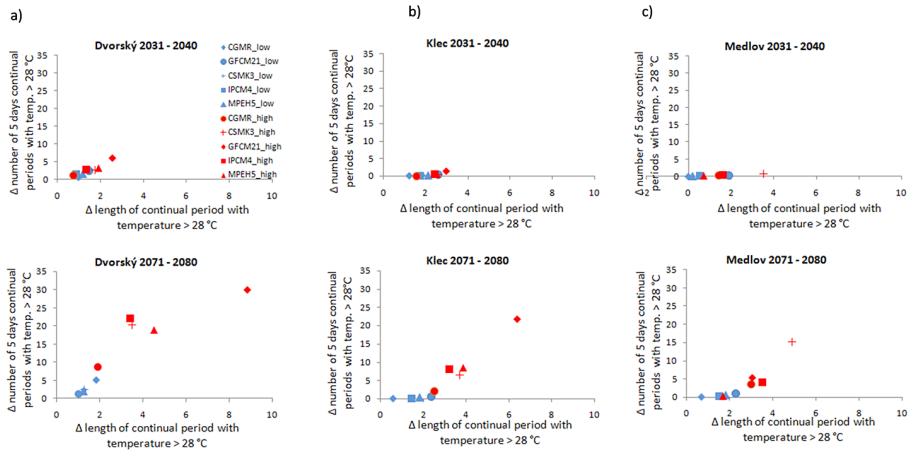

Fig. 1: *Climate change assessment for the two decades 2031–2040 and 2071–2080: change in length of continual periods with surface water temperature above threshold and change in number of continual periods. Threshold surface water temperature 28°C and continual period length 5 days are related to common carp. (a) Dvorský pond, (b) Klec pond, (c) Medlov pond.*

RESULTS

The present study used the following equation expressing surface water temperature:

$t_{sw} = 4.0232 + 0.8877 * t_{3dm}$

where t_{sw} is daily surface water temperature and t_{3dm} is the 3-day mean of air temperature.

A comparison of observed and calculated surface water temperatures revealed that the lower limit of model accuracy is 3°C. Under this threshold temperature, the model loses its predictive ability. In its assessment of surface water temperature above 3°C, the model has demonstrated good consistency between observed and modelled surface water temperatures (Pearson correlation coefficient 0.79–0.96, root mean square error 1.83–2.53, and mean bias error −0.02–0.59). The results of the model using the climate change meteorological dataset estimated progressive conditions for fish development in Czech ponds. The results of overlap among the five climate change models in combination with two emission scenarios (high, low) provided the following estimates for all studied fish species:

an increase in the length of continual periods with surface water temperature above the threshold tolerated by a given fish species (Fig. 1, x-axis),

an increase in the number of continual periods with surface water temperature above the threshold tolerated by a given fish species with a more substantial increase especially during 2071–2080 (Fig.1, y-axis), and

an increase in the overall number of days within a continual period with temperature above the threshold tolerated by a given fish species (Fig. 2).

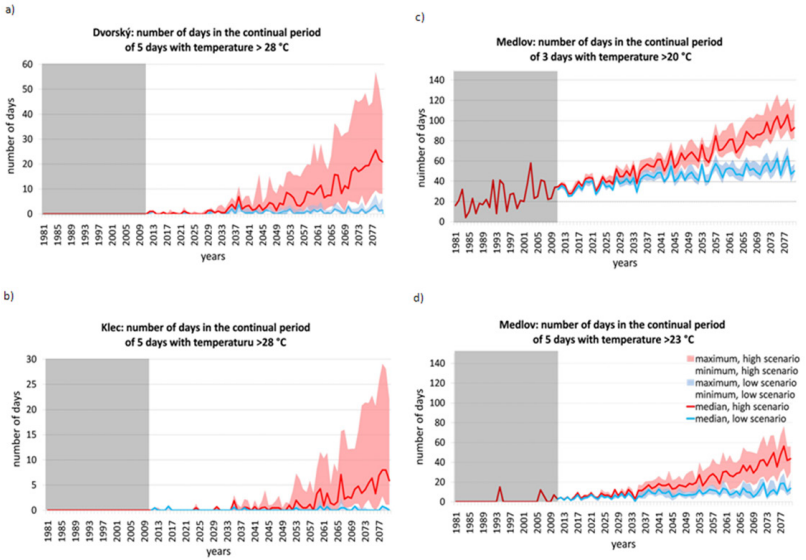

Fig. 2: *Climate change assessment: change in number of days within a continual period for particular ponds regarding the main farmed fish species, (a) Dvorský pond (common carp), (b) Klec pond (common carp), (c) Medlov pond (rainbow trout), and (d) Medlov pond (northern whitefish). Red depicts high-emission scenarios, blue low-emission scenarios. The grey field shows the present climate.*

DISCUSSION

The authors considered it to be meaningful to analyse the summer season (May–October) because, among other reasons, it is the decisive period for fish production. Fish in temperate ecosystems undergo about 90% of their annual growth during the summer months because food availability tends to be highest and water temperatures approach growth optimums. In these cases, a slight increase in water temperature could be beneficial as it would extend the growing season and, moreover, decrease overwintering stress. The general effects of climate change on freshwater systems will likely be increased water temperatures, decreased dissolved oxygen levels, and increased pollutant toxicity (Ficke et al. 2007). Our predictions of water temperature in Czech fishponds based on climate change models show an increase in water temperatures especially after 2030. In the conditions of the Czech Republic, the common carp is the crucial farmed fish species for productive fisheries. A modest water temperature rise at first would lead to an increase in carp productivity due to vegetation season prolongation and faster fish growth in warmer water. In spite of this advantage, the limiting factor for carp production would be the solute oxygen concentration in water. The aerobic metabolic rate of most cold-blooded aquatic organisms increases with temperature, and increases in temperature decrease the dissolved oxygen saturation of water (Kalff 2000). Likewise, increases in summer temperature can also augment the eutrophication of water by increasing cyanobacteria and algal growth, bacterial metabolism, and nutrient cycling rates (Klapper 1991). Along with water pollution, extreme weather events, increased occurrence of toxic substances, and decreased solute oxygen in water, it is likely that there will be a change in the structure and amount of farmed fish species. More significant impacts from climate change are expected in farming cold-water fish (the *Coregoninae*, tainbow trout). As a result of increased water temperature, these species are expected to be farmed in deeper and colder ponds at higher altitudes. Changes will be stronger for stenothermic species (e.g. salmonids, coregonids) than for the eurythermic common carp, which is more adaptable to new temperature conditions. It is also likely that there will be an increase in alien and invasive temperate fish species, parasites, and infections. Such effects are still hard to predict.

Acknowledgement

Supported by project No. CZ.1.07/2.3.00/20.0248 "Building up a multidisciplinary scientific team focused on drought". This work was supported by the Ministry of Education, Youth and Sports within the National Programme for Sustainability Program I, project No. LO1415.

References

Dubrovsky M, Simon K-H, Stuch B et al. (2011) Report on the European Driving Force Database for Use in the Integrated Assessment Platform. Available at http://www.climsave.eu/climsave/doc/Report_on_the_database_of_European_drivers.pdf.

Ficke AD, Myrick CA, Hansen LJ (2007) Rev. Fish Biol. Fisher. 17, 581–613.

Kalff J (2000) Limnology. 2nd edition. Prentice Hall, Upper Saddle River, New Jersey.

Klapper H (1991) Control of Eutrophication in Inland Waters. Ellis Horwood, Chichester, UK.

Sala OE, Chapin FS III, Armesto JJ et al. (2000) Science 287: 1770–1774.

Diurnal changes of monoterpene fluxes in Norway spruce forest

Juráň, S.[1,2,*], Fares, S.[3], Křůmal, K.[4], Večeřa, Z.[4], Urban, O.[1]

[1]*Global Change Research Centre, Bělidla 986/4a, 603 00 Brno, Czech Republic*

[2]*Mendel University, Zemědělská 1665/1, 613 00 Brno, Czech Republic*

[3]*Research Center for the Soil-Plant System, Agricultural Research Council, Via della Navicella, 2-4, 00184 Rome, Italy*

[4]*Institute of Analytical Chemistry, Czech Academy of Sciences, Veveří 97,602 00 Brno, Czech Republic*

[*]*author for correspondence; email: juran.s@czechglobe.cz*

ABSTRACT

Biogenic volatile organic compounds (BVOCs) are important components of biosphere–atmosphere exchange. Their emissions depend on various meteorological parameters and stresses. Diurnal fluxes of different monoterpenes were studied within a Norway spruce (*Picea abies*) mountain forest to investigate their dependence on temperature and global radiation. Fluxes of monoterpenes, the most abundant BVOCs in spruce, were modelled using an inverse Lagrangian transport model, and representative diurnal variation trigged by both temperature and light was observed. This research enables future parametrization and quantification of various factors driving bidirectional fluxes.

INTRODUCTION

Global vegetation is considered to be a sink for CO_2. Some of the carbon assimilated by photosynthesis is afterwards emitted back into the atmosphere in the form of biogenic volatile organic compounds (BVOCs), particularly by trees (Guenther 2002). BVOCs are highly reactive (Atkinson 2000) and their lifetime is therefore limited. Hence, BVOCs play an important role in the chemistry of the atmosphere. Under specific conditions, they are precursors of secondary aerosols (Hoffmann et al. 1997). BVOCs could be oxidized to various compounds and their impact on the bidirectional exchanges of radiative properties and energy balance is significant. Global estimation of BVOC emission from plants ranges from 1,000 to 1,500 Tg C yr^{-1} (Guenther et al. 2012). Even in the later Model of Emissions of Gases and Aerosols from Nature v. 2.1 as well as the Modern-Era Retrospective Analysis for Research and Applications, it was just 760 Tg C yr^{-1}. Global BVOC emissions consist of isoprene (70%), monoterpenes (11%), methanol (6%), acetone (3%), sesquiterpenes (2.5%), and others (Sindelarova et al. 2014). Production of BVOCs can be induced by various factors such as light and temperature, which are the most common stressors occurring in forest ecosystems. Quantification of BVOC emissions is very important, because these compounds react with nitric oxides and/or ozone. Under specific conditions, they form phytotoxic ozone, which subsequently affects forest health. Monoterpene and isoprene emissions are considered to be temperature and light dependent (Dindorf et al. 2006). Norway spruce (*Picea abies* (L.) Karst.) is regarded as a low BVOC emitter. Isoprene emissions are almost negligible, whereas monoterpenes, particularly α–pinene and β–pinene, are major BVOCs emitted (Kesselmeier & Staudt 1999).

Seasonal field campaigns have great value in aiding understanding of the overall dynamics of emission capacities and ambient mixing ratios, which are driven by various meteorological parameters. This study's main goal was to determine diurnal fluxes of monoterpenes in a mountain spruce forest and examine the fluxes' dependence on temperature and global radiation.

MATERIALS AND METHODS

Measurements were conducted at the Bílý Kříž experimental station (Beskid Mountains, 49°33'N, 18°32'E, in the north-east of the Czech Republic, 908 m a.s.l.). This area has a cool (annual mean air temperature 6°C), humid (annual mean relative air humidity 80%) climate with high annual precipitation (mean for 2000–2009 1,374 mm). The investigated forest stand (31 years old) consists of Norway spruce (99%). At the time of the physiological investigations, mean tree height was 15.2 m and mean stem diameter at 1.3 m was 0.18 m.

Air samples were collected on 2 August 2012 using a wet effluent diffusion denuder (WEDD, *n*heptane as absorption liquid) at 5.1 m, 14.3 m, and 25.3 m above the soil surface. Samples were collected at 5 min intervals between 7:00 and 20:00 local time (UTC+2:00). The WEDD was heated to 20°C to maintain identical sampling conditions. See Sklenská et al. (2002) for detailed technical description.

Monoterpenes were quantified using gas chromatography–mass spectrometry (GC–MS, Agilent, 7890A, 5975C, USA). The 2 µl samples were analysed by GC–MS (HP5-MS, 30 m, 1 µm film thickness, 0.32 mm i.d.) in splitless mode at 260°C. Flow of He carrier gas was 4 ml min^{-1}. The programme was started at 50°C for 2 min, a gradient of 5°C min^{-1} was applied up to 160°C, and then a further gradient of 20°C min^{-1} was used up to 240°C. GC–MS was run in electron impact ionization type with energy of 70 eV and in selective ion monitoring mode. Temperatures of the ion source and transfer line were 230°C and 280°C, respectively. Identification of monoterpenes was based on comparison with retention times and mass spectra of analytical standards. After analysis, the mass concentration of components was calculated from the calibration curve of each analytical standard. Concentrations in nmol mol^{-1} were calculated from the volume of air which had passed through the WEDD.

Air temperature was measured (model RHA1, DeltaT, UK) at a height of 15.2 m, corresponding to the tree canopy. Global radiation was recorded at a height of 4.8 m above the tree canopies using a KippZonen CM6B pyranometer (Kipp & Zonen, NL). Both temperature and global radiation were averaged to reach 30 min intervals. Air molar density was calculated based on air temperature and current air pressure. Friction velocity was calculated from multi-horizontal wind speed measured by 2D sonic anemometers (Met One, USA). The 30 min averages of the aforementioned parameters were used to parametrize an inverse Lagrangian transport model (Raupach 1989, Nemitz et al. 2000, Karl et al. 2004). The model enables estimating monoterpene fluxes from their concentrations in the air. Three high concentration levels measured were interpolated to 11 as an input for modelling.

Monoterpene fluxes were computed according to:

$$C - C_{ref} = D \times S,$$

where C is the monoterpene's concentration vector (nmol mol^{-1}) for each level, C_{ref} is the monoterpene's concentration (nmol mol^{-1}) at reference height, D (m) represents the dispersion matrix, and S is the resulting sink/source vector (nmol mol^{-1} m^{-1} m^{-2} h^{-1}). D is expressed as the Lagrangian timescale and profiles of the standard deviations of the vertical wind speed divided by friction velocity. Integrations were performed to reach canopy scale BVOC fluxes (nmol m^{-2} s^{-1}). Fluxes were calculated for 30 min intervals.

RESULTS

Calculated fluxes show diurnal behaviour the dynamics of which are consistent among all monoterpenes measured. The highest fluxes were observed for α–pinene, followed by β–pinene. Camphene, and Δ-3-carene. Limonene fluxes were much lower compared to the aforementioned. Tricyclene is not shown, since its concentration was close to the GC–MS's detection limit. The highest emissions were observed at noon,

when the highest temperature and greatest solar intensity occur. On the other hand, deposition of monoterpenes occurred early in the morning, suggesting that the canopy or soil may act as a sink for certain BVOCs such as α–pinene and limonene. Although temperatures rose in the morning, emissions were delayed since a plant's chemical synthesis of monoterpenes needs to restart. In contrast, evening emissions declined less sharply (Fig. 1B). We cannot conclude whether temperature or radiation was responsible for monoterpene emissions since the two are coupled (Fig. 1A). Evidence in the literature suggests, however, that it is temperature rather than radiation (see Discussion). Temperature triggers emissions in a non-linear manner, which is important especially for future models and accounting for future temperature increases.

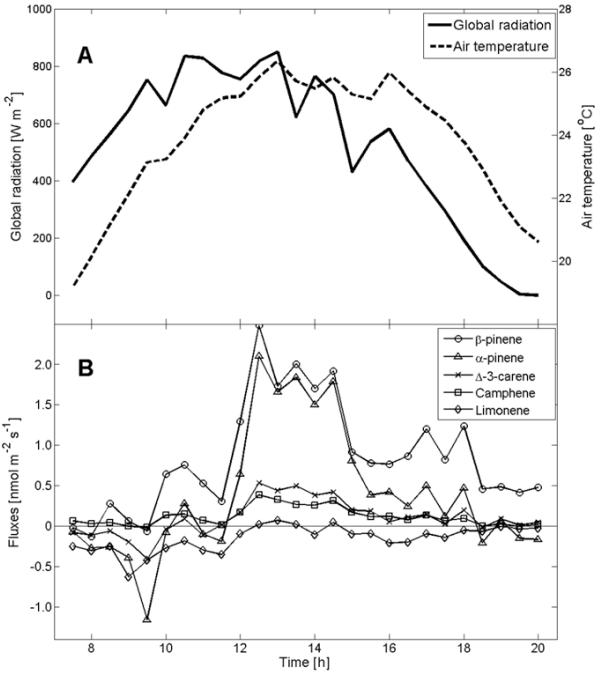

Fig. 1: *Diurnal changes in (A) global radiation and air temperature, and (B) bidirectional fluxes of monoterpenes estimated for Norway spruce stand.*

DISCUSSION

According to Yassaa et al. (2012), monoterpene emissions of Norway spruce are dependent on both temperature and light, since emission rates correlations comparing night and day differed substantially. Similar findings were published by Bourtsoukidis et al. (2014), who showed how monoterpene emissions during the night were about one-sixth those during the day in response to low temperature. They measured emissions at a similar Norway spruce mountain forest in central Germany at a similar altitude as we did. They reported the highest monoterpene fluxes in late afternoon and almost negligible fluxes in the morning. Negative values did not occur since a dynamic branch enclosure system was applied. This strengthens the theory of other sinks

for monoterpenes during the morning. Moreover, limonene is considered a more reactive compound that is reduced by a greater factor (Aumont et al. 2000), highlighting the possible in-canopy sink. In-canopy or soil sinks are only poorly understood. They are reported mainly in grassland ecosystems, where during high volume mixing ratios deposition fluxes were observed (Bamberger et al. 2011). Only a few studies have reported limonene uptake by trees, particularly broadleaf species (Noe et al. 2008). Night deposition of other monoterpenes might be explained by the almost negligible needle emissions and higher ambient mixing ratios due to boundary layer shrink and thus higher cleavage of monoterpenes by ozone, resulting in an early morning canopy or soil sink.

Many European species have been described as light dependent (Dindorf et al. 2006), as have tropical species (Karl et al. 2004). In contrast, only a few species in North America have been categorized as light dependent, mostly indicating only temperature-triggered emissions (Kim et al. 2010). What is responsible for such a difference between continents? Is it the broad spectra of monoterpenes emitted or is it something else, not yet detected? These remain open questions. More comprehensive measurements are thus needed to deeply analyse tree species' chemodiversity and environmental dependencies on BVOC emissions.

To conclude, fluxes of monoterpenes have markedly pronounced diurnal patterns ranging from deposition (limonene, α–pinene) in the early morning hours to emissions in the early afternoon (α– and β–pinene) when the air temperature is highest.

Acknowledgement

Supported by Operational Programme Education for Competitiveness projects CZ.1.07/2.3.00/20.0246 and CZ.1.07/2.3.00/20.0267 and Ministry of Education, Youth and Sports projects nos. LD 13031 and LO1415. Participation of KK and ZV was supported by RVO: 68081715 (Institute of Analytical Chemistry, Czech Academy of Sciences). We thank Prof. Thomas Karl for his valuable support in providing codes functional for our data processing.

References

Atkinson R (2000) Atmos. Environ. 34, 2063–2101.

Aumont B, Madronich S, Bey I et al. (2000) J. Atmos. Chem. 35, 59–75.

Bamberger I, Hőrtnagl L, Ruuskanen TM et al. (2011) J. Geophys. Res. Atmos. 116, D14305.

Bourtsoukidis E, Williams J, Kesselmeier J et al. (2014) Atmos. Chem. Phys. 14, 6495–6510.

Dindorf T, Kuhn U, Ganzeveld L et al. (2006) J. Geophys. Res. Atmos. 111, D16305.

Guenther A (2002) Chemosphere 49, 837–844.

Guenther AB, Jiang X, Heald CL et al. (2012) Geosci. Model Dev. 5, 1471−1492.

Hoffmann T, Odum JR, Bowman F et al. (1997) J. Atmos. Chem. 26, 189–222.

Kim S, Karl T, Guenther A et al. (2010) Atmos. Chem. Phys. 10, 1759–1771.

Nemitz E, Sutton MA, Gut A et al. (2000) Agric. For. Meteorol. 105, 385–404.

Noe SM, Copolovici L, Niinemets Ű et al. (2008) Plant. Biol. 10, 129–137.

Karl T, Potosnak M, Guenther A et al. (2004) J. Geophys. Res. Atmos. 109, D18306.

Kesselmeier J, Staudt M (1999) J. Atmos. Chem. 33, 23–88.

Raupach MR (1989) Agric. For. Meteorol. 47, 85–108.

Sindelarova K, Granier C, Bouarar I et al. (2014) Atmos. Chem. Phys. 14, 9317–9341.

Sklenská J, Broškovičová A, Večeřa Z (2002) J. Chromatogr. A 973, 211–216.

Yassaa N, Song W, Lelieveld J et al. (2012) Atmos. Chem. Phys. 12, 7215–7229.

Comparison of emissions of biogenic volatile organic compounds from leaves of three tree species

Holišová, P.[1,*], Večeřová, K.[1], Pallozzi, E.[2], Guidolloti, G.[2], Esposito, R.[2], Calfapietra, C.[1,2], Urban, O.[1]

[1]*Global Change Research Centre, Bělidla 986/4a, 60300 Brno, Czech Republic*

[2]*Institute of Agro-environmental and Forest Biology, National Research Council, 00015 Monterotondo Scalo, Rome, Italy*

[*]*author for correspondence; email: holisova.p@czechglobe.cz*

ABSTRACT

Biogenic volatile organic compounds (BVOCs) play many roles in plants' ecophysiology and have the potential to affect atmospheric quality due to their chemical reactivity. Rates of BVOC emissions are highly variable depending on plant species and growing condition. Our study evaluated the amounts and spectra of BVOCs emitted from three tree species.

We investigated BVOC emissions from the leaves of mature Norway spruce and sessile oak saplings grown in the field and from 1-year-old cuttings of hybrid poplar grown under laboratory conditions. Emitted BVOCs were sampled on desorption Tenax tubes in parallel with gas-exchange measurements. After subsequent thermal desorption of Tenax tubes, BVOC profiles were estimated by gas chromatography coupled with mass spectrometry.

The tree species showed substantial differences in BVOC emission rates per unit leaf area ranging between 2.33 and 25.67 nmol m^{-2} s^{-1}. Spruce trees had the lowest BVOC emissions and oak had slightly higher BVOC emissions on average than did poplar. Isoprene composed more than 97% of total BVOC emissions from oak and poplar, while no isoprene emissions from spruce needles were detected. Spruce BVOC emissions were mainly composed of such monoterpenes as α-pinene, β-pinene, and limonene.

INTRODUCTION

Plants are able to emit a large range of trace gases known as biogenic volatile organic compounds (BVOCs). These compounds can be released from various above- or belowground parts of the plant, but the largest amount comes from leaves (Laothawornkitkul et al. 2009). BVOCs play different roles in plants' ecophysiology. Some BVOCs serve as signaling molecules in plant–plant and plant–insect communication, including as attractants for pollinators and seed dispersers (Laothawornkitkul et al. 2009). BVOCs play an important role in protection against biotic and abiotic stresses (Niinemets 2010). Due to their high chemical reactivity, BVOCs have large effects on the atmosphere's chemical and physical properties. BVOCs are oxidized and form peroxy radicals that can react with NO_x and lead to O_3 formation in the presence of ultraviolet radiation. In an environment with low NO_x concentration, O_3 can be consumed by BVOC oxidation (Calfapietra et al. 2013). Changes in troposphere oxidative capacity can extend the lifetime of some greenhouse gases, such as methane. Products of BVOC oxidation can also be precursors to secondary organic aerosols that affect climate by scattering solar radiation and act as cloud condensation nuclei (Kavouras et al. 1998).

Precise estimation of BVOC emissions is difficult because of large differences among species, dependence on environmental conditions, and daily and seasonal variability. Isoprene and monoterpenes synthesis in species without terpene storage structures is dependent on light and temperature (Zimmer et al. 2003, Grote et al.

2006). This, however, does not work under severe stress conditions, when electron transport and CO_2 assimilation is reduced (Fortunati et al. 2008). BVOC synthesis requires energy and carbon supply from photosynthesis, but alternative reserved carbon sources can be used under stress conditions (Teuber et al. 2008). The rate of BVOC synthesis is controlled by precursor availability and the activity of synthase enzymes (Niinemets et al. 2004), which are affected also by recent weather conditions and acclimation of emission capacities (Arneth et al. 2008). There remains an insufficiency of information about emission potentials of individual species and our understanding of mechanisms leading to the high variability among species in the BVOCs produced.

The aim of our study was to evaluate the amounts and spectra of BVOCs emitted from the coniferous Norway spruce (*Picea abies* (L.) Karst.), the broadleaf sessile oak (*Quercus petraea* (Matt.) Liebl.), and a hybrid poplar (*Populus nigra* L. × *Populus maximowiczii* A. Henry) used as a fast-growing tree in the Czech Republic.

MATERIALS AND METHODS

We investigated BVOC emissions from two tree species grown in the field, Norway spruce and sessile oak, and from cuttings of hybrid poplar grown under laboratory conditions. All measurements were made in July and August 2014 on sun-exposed and healthy needles or leaves. The current needles of Norway spruce were measured in a 33-year-old spruce stand at the Bílý Kříž research site (Beskid Mountains; 49°30'N, 18°28'E, 900 m a.s.l.). Light intensity of 1,000 μmol m^{-2} s^{-1} and air temperature of 30°C were set in the measurement chamber during sampling. The mature leaves of sessile oak were measured in a 5-year-old oak forest of coppiced origin at the Soběšice research site located in the southeast of the Czech Republic (49°14'N, 16°35'E, 300 m a.s.l.). Light intensity of 1,400 μmol m^{-2} s^{-1} and air temperature of 25°C were set in the measurement chamber. The sixth leaf was taken from the apex of 1-year-old cuttings of hybrid poplar clone J-105 grown in a growth chamber (FS 3400, PSI, CZ) where sunny summer days were simulated. Light intensity of 1,000 μmol m^{-2} s^{-1} and air temperature of 30°C were set in the measurement chamber during sampling.

Emitted BVOCs were sampled on Tenax tubes (35/60 mesh, 200 mg TA, Markes International, UK) suitable for the majority of BVOCs under atmospheric concentrations. These tubes do not trap low molecular weight compounds such as methanol and acetaldehyde. In addition, sesquiterpenes are difficult to detect through standard measuring protocols due to their high reactivity. The gas-exchange measurement of CO_2 assimilation rate (A) and stomatal conductance (G_s) were carried out in parallel with BVOC sampling using an Li-6400 (Li-Cor, USA). Tenax tubes were connected to the outlet of the Li-6400 leaf cuvette by a Teflon tube and the air (at least 4 liters) exiting the cuvette was pumped through the tube. After subsequent thermal desorption of the Tenax tubes in a thermal desorption unit (Markes Unity System 2, Markes International, UK), BVOC profiles were estimated using gas chromatography coupled with mass spectrometry (TSQ Triple Quadrupole Quantum XLS, Thermo Scientific, USA). One-way analysis of variance was performed to evaluate the significance of differences ($p < 0.05$) among species using SigmaPlot 11 software (Systat Software, USA).

RESULTS

Significant differences in BVOC emission rate per unit leaf area were observed between coniferous spruce and the broadleaved species. While the spruce BVOC emission rate was only 2.3 ± 1.7 nmol m^{-2} s^{-1} (mean ± standard deviation), a BVOC emission rate of 25.7 ± 3.3 nmol m^{-2} s^{-1} was observed in oak. Poplar had only a slightly lower BVOC emission rate (21.4 ± 12.4 nmol m^{-2} s^{-1}) than did oak (Fig. 1A). Spruce had also significantly lower mean A and G_S than did the broadleaved species (Fig. 1B). Gas-exchange data did not differ significantly between oak and poplar (Fig. 1B).

Isoprene composed 97% and 99% of BVOC emissions from oak and poplar, respectively. Isoprene emissions from spruce needles were not detected. In contrast, monoterpene emission rates from spruce needles were higher than were those from broadleaved species (Fig. 1A). The main monoterpenes emitted were limonene, α-pinene, and β-pinene in all species studied (Fig. 2). Specifically, carene was the most abundant monoterpene emitted by oak. Spruce BVOC emissions contained 12% of the oxygenated monoterpenoid eucalyptol.

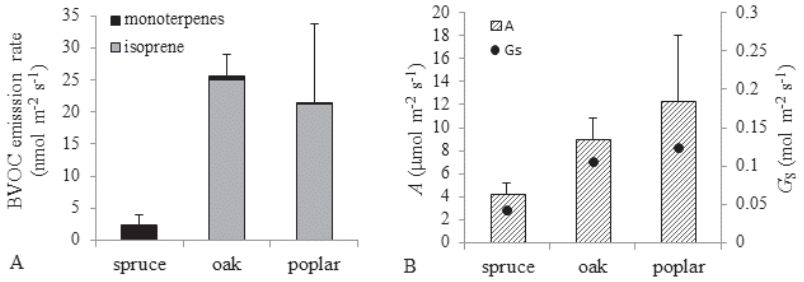

Fig. 1: *Mean values with standard deviation of (A) BVOC emission rates from leaves or needles and (B) CO_2 assimilation rate (A) and stomatal conductance (G_S) of Picea abies (spruce, N = 5), Quercus petraea (oak, N = 5), and the hybrid Populus nigra × Populus maximowiczii (poplar, N = 8).*

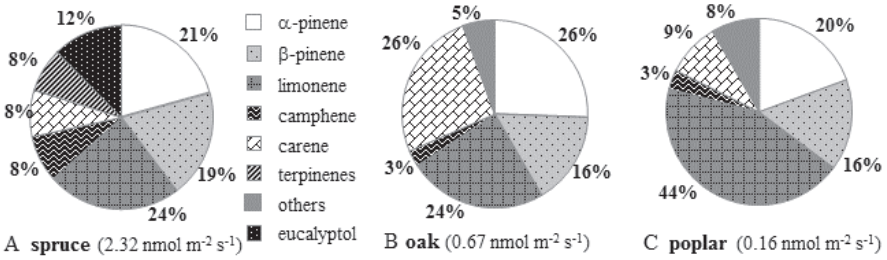

Fig. 2: *Percentages abundance of monoterpenes emitted from leaves or needles of Picea abies (spruce, A), Quercus petraea (oak, B), and the hybrid Populus nigra × Populus maximowiczii (poplar, C). Mean total monoterpene emission rates are in parentheses.*

DISCUSSION

Isoprene is the most abundant biogenic hydrocarbon emitted from plants (Sharkey et al. 2008, Laothawornkitkul et al. 2009). Poplars are known to comprise a large group of isoprene emitters. Isoprene emission from poplar in this study was in the range of isoprene emission reported in the literature, which for different poplar species is from 7 to 45 nmol m^{-2} s^{-1} (Rosenstiel et al. 2004, Loreto et al. 2007, Teuber et al. 2008, Guidolotti et al. 2011). Poplar emits isoprene only from adult leaves while juvenile leaves emit such monoterpenes as α-pinene, β-pinene, and (E)-β-ocimene (Brilli et al. 2014). Monoterpenes comprised less than 1% of total BVOC emissions from poplar leaves in our study and the most abundant monoterpene was limonene (Fig. 2C).

The genus *Quercus* includes some species that emit isoprene and others that do not. Species not emitting isoprene, such as *Q. ilex* and *Q. coccifera*, usually emit monoterpenes to a greater extent than do such isoprene emitters as *Q. petraea* and *Q. pubescens* (Owen et al. 2001, Karl et al. 2009, Keenan et al. 2009). Isoprene emissions from oaks are

recorded with large variability (Keenan et al. 2009). *Q. petraea* is cited in the literature as a weaker isoprene emitter than other isoprene-emitting oaks or poplars (Steinbrecher et al. 1997, Karl et al. 2009). For example, Zimmer et al. (2003) measured isoprene emission rate at 25°C and 1,000 μmol photons m^{-2} s^{-1} in the range 8.1–15.6 nmol m^{-2} s^{-1} depending on isoprene synthase activity in an old *Q. petraea* forest. Our study showed that isoprene emission from young *Q. petraea* can be higher.

Coniferous trees are generally known as monoterpenes emitters. But low isoprene emissions have also been documented in *P. abies* (Grabmer et al. 2006, Karl et al. 2009). In our study, no isoprene emissions were detected from *P. abies* and the most abundant monoterpenes were limonene, α-pinene, and β-pinene. The spectrum of emitted monoterpenes is in accordance with other literature (Yassaa et al. 2012, Kivimäenpää et al. 2013). However, whether the spectrum of emitted monoterpenes changes during the vegetation season remains an open question.

In conclusion, BVOC emission rates were significantly higher among broadleaved trees than in a coniferous tree species. Isoprene was the most abundant compound emitted from those broadleaved species studied, while monoterpenes were the most abundant BVOC in the coniferous spruce.

Acknowledgement

Supported by Ministry of Education, Youth and Sports projects nos. LD13031 and LO1415 and by Operational Programme Education for Competitiveness projects "Coppice" (No. CZ.1.07/2.3.00/20.0267) and "ENVIMET" (No. CZ.1.07/2.3.00/20.0246).

References

Arneth A, Monson RK, Schurgers G et al. (2008) Atmos. Chem. Phys. 8, 4605–4620.

Brilli F, Gioli B, Zona D et al. (2014) Agr. Forest Meteorol. 187, 22–35.

Calfapietra C, Fares S, Manes F et al. (2013) Environ. Pollut. 183, 71–80.

Fortunati A, Barta C, Brilli F et al. (2008) Plant J. 55, 687–697.

Grabmer W, Kreuzwieser J, Wisthaler A et al. (2006) Atmos. Environ. 40, 128–137.

Grote R, Mayrhofer S, Fischbach RJ et al. (2006) Atmos. Environ. 40, 152–165.

Guidolotti G, Calfapietra C, Loreto F (2011) Physiol. Plant. 142, 297–304.

Karl M, Guenther A, Köble R et al. (2009) Biogeosciences, 6, 1059–1087.

Kavouras IG, Mihalopoulos N, Stephanou EG (1998). Nature 395, 683–686.

Keenan T, Niinemets Ü, Sabate S et al. (2009) Atmos. Chem. Phys. 9, 4053–4076.

Kivimäenpää M, Riikonen J, Ahonen V et al. (2013) Environ. Exp. Bot. 90, 32–42.

Laothawornkitkul J, Taylor JE, Paul ND et al. (2009) New Phytol. 183, 27–51.

Loreto F, Centritto M, Barta C et al. (2007) Plant Cell Environ. 30, 662–669.

Niinemets Ü (2010) Trends Plant Sci. 15, 145–153.

Niinemets Ü, Loreto F, Reichstein M (2004) Trends Plant Sci. 9, 180–186.

Owen S M, Boissard C, Hewitt CN (2001) Atmos. Environ. 35, 5393–5409.

Rosenstiel TN, Ebbets AL, Khatri WC et al. (2004) Plant Biol. 6, 12–21.

Sharkey TD, Wiberley AE, Donohue AR (2008) Ann. Bot. 101, 5–18.

Steinbrecher R, Hauff K, Rabong R et al. (1997) Atmos. Environ. 31, 79–88.

Teuber M, Zimmer I, Kreuzwieser J et al. (2008) Plant Biol. 10, 86–96.

Yassaa N, Song W, Lelieveld J et al. (2012) Atmos. Chem. Phys. 12, 7215–7229.

Zimmer W, Steinbrecher R, Körner C et al. (2003) Atmos. Environ. 37, 1665–1671.

Effects of vegetation season and needles' position in spruce canopy on emissions of volatile organic compounds

Večeřová, K.[1,*], Holišová, P.[1], Pallozzi, E.[1], Guidolloti, G.[2], Calfapietra, C.[1,2], Urban, O.[1]

[1]*Global Change Research Centre, Bělidla 986/4a, 603 00 Brno, Czech Republic*
[2]*Institute of Agro-Environmental and Forest Biology, CNR, 00015, Monterotondo Scalo, RM, Italy*
[*]*author for correspondence; email: vecerova.k@czechglobe.cz*

ABSTRACT

The main objective of this study was to investigate seasonal changes and vertical distribution in emissions of biogenic volatile organic compounds (BVOCs) within a Norway spruce canopy profile. Emissions were measured on current-year needles from the upper and lower canopy in early July and late August. Our results show that total BVOC emissions under standardized conditions (light intensity 1,000 μmol m^{-2} s^{-1}, temperature 30°C) are higher in July than they are in August. BVOC emissions from upper canopy needles were approximately 3 times higher than were those from lower canopy needles. This difference was observed in July but not in August. The monoterpenes α-pinene, camphene, and terpinolene showed the most significant differences between emissions from upper and lower canopy needles.

INTRODUCTION

Norway spruce (*Picea abies* (L.) Karsten) is a widely distributed species that is also one of the most economically important conifer species in the boreal zone and mountain areas of central Europe. Biogenic volatile organic compounds (BVOCs) are diverse, are produced by vegetation in different tissues, and impact plants in many ways. In particular, they are thought to defend plants against herbivores and pathogens; attract pollinators, seed dispersers, and other beneficial animals and microorganisms; and serve as signals in plant–plant communication (Dudareva & Pichersky 2008). BVOCs and in particular isoprene might further be involved in protection of plants against such abiotic stresses as high temperature (Loreto et al. 1998) and high ozone concentrations (Calfapietra et al. 2009).

Plants generally re-emit 2–10% of their assimilated carbon back into the atmosphere as a complex of BVOCs, but this figure may increase to as high as 36% under extreme stress conditions (Kesselmeier 2001). BVOCs are very reactive, have lifetimes ranging from mere minutes to hours (Lerdau et al. 1997), and have profound effects on atmospheric chemistry, particularly when abundant together with nitrogen oxides and high radiation.

Many BVOCs, and particularly most monoterpenes and sesquiterpenes, are synthesized and stored in special secretory tissues. In Norway spruce, terpenes are stored in the epithelial cells of the resin ducts and in the mesophyll (Fahn 1988). BVOC emissions from conifers mainly originate from terpene stores in resin ducts. It seems, however, that one-third of terpene emissions originate from original biosynthesis in Norway spruce (Ghirardo et al. 2010) and thus depend fully on the photosynthetic process (Niinemets et al. 2004, Filella et al. 2007). Norway spruce is a low BVOC emitter as compared to such species as poplar or beech, with monoterpenes dominating their emissions followed by oxygenated terpenes, sesquiterpenes, and a minor part of isoprene emission (Bourtsoukidis et al. 2014).

Production of BVOCs is highly variable, depending on the plant species and environmental conditions, especially light intensity and temperature. Most conifers store terpenes in special tissues (resin ducts), and it is assumed

that their diffusion is driven solely by temperature (Kesselmeier & Staudt 1999). In contrast, terpenes synthesized *de novo* are dependent on photosynthesis, analogously to isoprene (Staudt & Seufert 1995). It has been shown that photosynthetic capacity varies along the depth of canopies (Marek et al. 2002), where the light intensity is attenuated. It seems that the upper canopy has higher BVOC emissions and CO_2 assimilation rates than does the lower canopy, but the morphological, physiological, and biochemical traits of upper and lower canopy leaves may converge at high altitudes or in sparse stands (Rajsnerová et al. 2015).
The main objective of this study was to investigate seasonal changes in BVOC emissions and their vertical distribution within the spruce canopy profile under standard conditions.

MATERIALS AND METHODS

Emissions of BVOCs were measured on current-year needles of mature (30 years old) Norway spruce trees at the Bílý Kříž research site (Beskid Mountains, Czech Republic; 49°30'N, 18°28'E; 900 m a.s.l.) in early July 2014 and late August 2013. In this study, samples were measured at two heights above the soil surface: 5 m (lower canopy needles) and 10 m (upper canopy needles). Simultaneously with BVOC sampling, CO_2 assimilation rate and stomatal conductance were automatically measured at 2 min intervals using a Li-6400 open infrared gas analyser (Li-Cor, USA). Emitted BVOCs were sampled on stainless steel TD tubes packed with Tenax TA (35/60 mesh, 200 mg TA, Markes International, UK) under standard conditions (light intensity 1000 µmol m^{-2} s^{-1}; temperature 30°C) for 60 min (flow 200 ml min^{-1}). The tubes were conditioned prior to use for 2 h at 320°C and subsequently for 30 min at 335°C in order to remove any impurities from the sorbent. Absorbed BVOCs were released from desorption tubes using a thermal desorption unit (Markes Unity System 2, Markes International, UK) and subsequently analysed using a gas chromatograph mass spectrometer (TSQ Triple Quadrupole Quantum XLS, Thermo Scientific, USA).
After BVOC measurement, fresh weight and total projection needle area of investigated shoots was determined using a Li-3000A portable leaf area meter (Li-Cor, USA). Rates of CO_2 assimilation and BVOC emissions were recalculated per unit leaf area. Some needles were dried at 60°C and subsequently analysed for total contents of nitrogen (N) and carbon (C) using a Flash-2000 elemental analyser (Thermo Scientific, USA).
The data was statistically analysed using the Statistica 12 program (StatSoft, USA). Data represent 8 repetitions. One-way ANOVA ($p = 0.05$) was used to investigate the effects of season and canopy position on BVOC emissions, C and N contents, CO_2 assimilation rate, and stomatal conductance. Homogeneity of variances was tested using Cochran–Hartley–Bartlett tests, and for normality the Shapiro–Wilk test was used. Differences between treatments were evaluated using Tukey's honest significant difference test.

RESULTS

We found a statistically significant difference between upper and lower canopy needles in C content ($p < 0.05$), while N content was unaffected by canopy position in both July and August. CO_2 assimilation rate and stomatal conductance were unaffected by the position of needles within the canopy in July, but there were significantly ($p < 0.05$) higher values of CO_2 assimilation rate in lower than upper canopy needles in August (Table 1).
The results showed that there were differences in BVOC emissions between those measured during the main vegetation season (July) and those measured at the end of the season (August). Total emissions measured under standard conditions were about eight times higher in July than were those measured in August. In addition, statistically significant differences ($p < 0.05$) in emissions from upper and lower canopy needles were found. BVOC emissions from upper canopy needles were approximately three times higher than were emissions from

lower canopy needles, although this was observed only in July. There was no difference between the upper and lower canopy levels in August (Fig. 1A).

		Assimilation	Conductance	N	C
		µmol m^{-2} s^{-1}	mol m^{-2} s^{-1}	%	%
July					
	UC	4.41 ± 0.89$^{n.s.}$	0.04 ± 0.01$^{n.s.}$	1.27 ± 0.08$^{n.s.}$	47.28 ± 0.51**
	LC	3.84 ± 0.74$^{n.s.}$	0.04 ± 0.01$^{n.s.}$	1.24 ± 0.14$^{n.s.}$	46.28 ± 0.74**
August					
	UC	2.46 ± 0.55*	0.02 ± 0.01*	1.40 ± 0.09$^{n.s.}$	48.8 ± 0.29*
	LC	3.21 ± 0.39*	0.01 ± 0.00*	1.41 ± 0.10$^{n.s.}$	48.2 ± 0.44*

Table 1: *Total C and N contents, light-saturated rate of CO2 assimilation, and stomatal conductance determined in needles from the upper (UC) and lower (LC) canopy in early July and late August. Mean values ± SE are shown for each treatment (N = 8). Statistical significances are shown as: ** $p < 0.01$, * $0.01 < p < 0.05$, n.s. $p \geq 0.05$.*

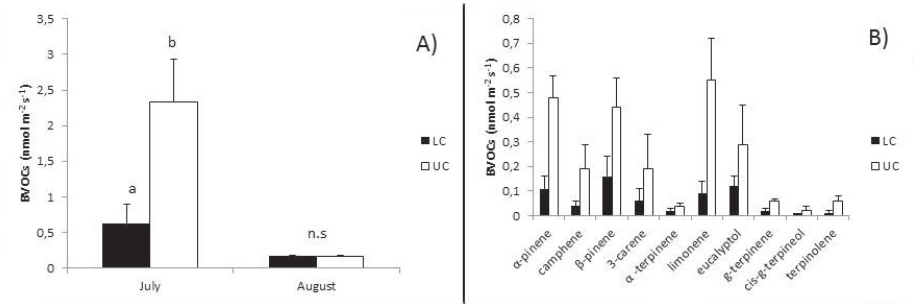

Fig. 1: *A) Total BVOC emissions per unit needle area produced by Norway spruce (Picea abies), differences of emissions in early July (mean daily temperature 23°C) and late August (mean daily temperature 15°C) in upper (UC) and lower canopy (LC) needles are shown. B) Differences between identified BVOCs in UC and LC needles in July. Mean values ± SE are shown for each treatment (n = 8).*

The most abundant terpenes identified in July were α-, β-pinene, and limonene in both upper and lower canopy needles. In particular, α-pinene, limonene, and terpinolene showed the most significant differences ($p < 0.05$) in emissions between upper and lower canopy needles (Fig. 1B). Differences were also observed in the composition of identified terpenes between July and August. In contrast to July, α-, β-pinene, limonene, and myrcene were the most abundant terpenes measured in August.

DISCUSSION

Emissions of BVOCs in conifer species are derived mainly from terpenes synthesized and then stored in resin ducts, and their emission depends on needles temperature (Guenther et al. 1993, Grote & Niinemets 2008). At most one-third of BVOCs are synthesized *de novo* (Ghirardo et al. 2010) and are thus fully dependent on photosynthesis. Due to the fact that BVOC emissions were measured under standard conditions, it is likely that differences in emission rates between upper and lower canopy needles corresponded primarily to *de novo* synthesized BVOCs.

On the other hand, the results of C and N contents, CO_2 assimilation rate, and stomatal conductance indicate relatively small vertical differentiation of the investigated spruce canopy to sun- and shade-acclimated parts. However, it is possible for BVOCs to reflect environmental conditions from hours and even days previously, and this may have had an impact on BVOC emissions.

Studies focusing on vertical profile measurements of BVOC emissions are rare. Wang et al. (2014) reported noticeable differences in emissions measured at different heights within a spruce canopy with emission rates highest at the top of the canopy. Observed changes in emission rates between the main vegetation season (the beginning of July) and the end of the season (the end of the August) are in accordance with data measured by Lappalainen et al. (2009). They reported a seasonal pattern of winter minimum and summer maximum for BVOC emissions in a boreal forest canopy. It is also possible that other abiotic factors common in summer, such as drought and O_3 concentration (Kivimäenpää et al. 2013), had an effect on the increased emission rate of BVOCs.

We conclude that total BVOC emissions from spruce needles decreased at the end of the vegetation season irrespective of their position within the canopy. We have found significantly higher BVOC emissions from upper than from lower canopy needles during the main vegetation season but not at the end of the vegetation season. In addition, the composition of emitted BVOCs changes along the canopy depth.

Acknowledgements

Part of the research supported by projects LD13031 (Ministry of Education, Youth and Sports [MEYS]) and LO1415 (National Programme for Sustainability I; MEYS). The Bílý Kříž experimental site is part of project No. LM2010007 the National Infrastructure of Carbon Observation System – CzeCOS/ICOS.

References

Bourtsoukidis E, Williams J, Kesselmeier J et al. (2014) Atmos. Chem. Phys. 14, 6495–6510.

Calfapietra C, Fares S, Loreto F (2009) Environ. Pollut. 157, 1478–1486.

Dudareva N, Pichersky E (2008) Curr. Opin. Biotech. 19, 181–189.

Fahn A (1988) New Phytol. 108, 229–257.

Filella I, Wilkinson M, Llusià J et al. (2007) Physiol. Plant. 130, 58–66.

Ghirardo A, Koch K, Taipale R et al. (2010) Plant Cell Environ. 33, 781–792.

Grote R, Niinemets Ü (2008) Plant Biol. 10, 8–28.

Guenther AB, Zimmerman PR, Harley PC et al. (1993) J. Geophys. Res. Atmos. 98, 12609–12617.

Kesselmeier J (2001) J. Atmos. Chem. 39, 219–233.

Kesselmeier J, Staudt M (1999) J. Atmos. Chem. 33, 23–88.

Kivimäenpää M, Riikonen J, Ahonen V et al. (2013) Environ. Exp. Bot. 90, 32–42.

Lappalainen HK, Sevanto S, Bäck J et al. (2009) Atmos. Chem. Phys. 9, 5447–5459.

Lerdau M, Guenther AB, Monson R (1997) BioScience 47, 373–383.

Loreto F, Förster A, Dürr M et al. (1998) Plant Cell Environ. 21, 101–107.

Marek MV, Urban O, Šprtová M et al. (2002) Photosynthetica 40, 259–267.

Niinemets Ü, Loreto F, Reichstein M (2004) Trends Plant Sci. 9, 180–186.

Rajsnerová P, Klem K, Holub P et al. (2015) Tree Physiol. 35, 47–60.

Staudt M, Seufert G (1995) Naturwissenschaften 82, 89–92.

Wang M, Schurgers G, Ekberg A et al. (2014) Profile measurements of BVOC in a Swedish boreal forest. Biogenic Hydrocarbons and the Atmosphere Gordon Research Conference (poster).

High night temperature-induced accelerated maturation of rice panicles can be detected by chlorophyll fluorescence

Šebela, D.[1,2,3], Quiñones, C.[3], Olejníčková, J.[1], Jagadish, K.S.V.[3,*]

[1]*Global Change Research Centre, Bělidla 986/4a, 60300 Brno, Czech Republic*
[2]*Faculty of Science, University of South Bohemia, Branišovská 1760, 37005 České Budějovice, Czech Republic*
[3]*International Rice Research Institute, DAPO BOX 7777, 1301 Metro Manila, Philippines*
[*]*author for correspondence: k.jagadish@irri.org*

ABSTRACT

Rice panicle maturation is considered to be highly sensitive to environmental conditions. Since one of the factors accompanying global climate change is increases in minimum night temperatures more pronounced than those in maximum day temperatures, the effect of high night temperature (HNT) on rice panicle maturation was investigated. Two rice genotypes with contrasting HNT responses, N22 (highly tolerant) and Gharib (susceptible), were exposed to control temperatures (ca 23°C) and HNTs (ca 29°C) from flowering until maturity. Loss of photosynthetic activity and/or pigments during rice panicle maturation were evaluated temporally by measuring (i) effective quantum yield of photosystem II efficiency (Φ_{II}), and (ii) steady-state chlorophyll fluorescence level (F_S). To prove the accuracy of the new approach presented in this study, several vegetative indices were calculated from reflectance measurements and correlated with fluorescence parameters. It has been observed that Φ_{II} tracks the accelerated maturation of rice panicles exposed to HNT better than does F_S. Employing a newly identified chlorophyll fluorescence-based parameter could potentially enable larger genetic diversity scans and identification of novel genotypes with longer panicle maturation periods so as to increase rice yields directly under field conditions.

INTRODUCTION

Rice (*Oryza sativa* L.) production worldwide is affected by many environmental factors. As one of the main impacts of global climate change, minimum night temperatures are increasing at a much faster pace than are maximum day temperatures at a global as well as a farm level. Rice panicle maturation, including flowering and the subsequent grain-filling phase, is considered to be highly sensitive to temperature above a critical threshold. Negative effects on rice yield from high night temperatures (HNT) have been proven in controlled-environment studies and more recently by a field experiment (Shi et al. 2013), where reduced yields could potentially be a result of a shortened active grain-filling period. In addition, significantly shorter grain-filling periods under tropical conditions are in contrast to much longer periods under temperate conditions, and they are thus considered to be a key bottleneck for further yield enhancement. The main benefit of breeding programs would thus be in delaying panicle maturation, providing sufficient time for assimilates to fill grains efficiently. However, no progress or even attempt has been made in this direction due to the lack of a standardized phenotyping tool to ascertain and track grain-filling senescence over time.

Rice panicle maturation is accompanied by a change in colour as a consequence of disappearing chlorophyll. Given that based on chlorophyll spikelets' photosynthetic capacity has been found to be similar to that of flag leaves (Imaizumi et al. 1990), such disappearance and/or loss of photosynthetic capacity per unit chlorophyll can be temporally tracked by chlorophyll fluorescence (Chl-F). However, no reports had previoulsy been

published addressing the use of Chl-F measurements to detect rice panicle maturation. Therefore, the objectives of our study were (i) to investigate the temporal Chl-F and reflectance signals of maturing rice panicles, and (ii) to specify a Chl-F parameter suitable for monitoring accelerated maturation of rice panicles exposed to HNT under field conditions.

MATERIALS AND METHODS

The field experiment was carried out during the 2014 dry season at the International Rice Research Institute located in Los Baños, Philippines (14°11'N, 121°15'E).

Plant material. Two rice genotypes with contrasting HNT responses, the highly tolerant N22 cultivar and the susceptible Gharib cultivar, were used in this experiment. Both rice genotypes were sown in seeding trays and then transplanted to field-based temperature controlled tents as 14-day-old seedlings.

HNT experimental set up. To impose HNT with high accuracy, six field-based temperature-controlled tents (three HNT tents and three control tents) each 18 m^2 in size were designed (Shi et al. 2013). Plants were exposed to control temperatures (22.9 ± 0.1°C) or HNTs (28.6 ± 0.5°C) during the nights. To simulate field conditions, the tents were completely open during the day (06:00–18:00) and covered during the nights (18:00–06:00).

Chl-F and reflectance measurements. Both Chl-F and reflectance were measured on identical panicles. Five uniform main tiller panicles of each genotype were selected in each tent and tagged following the procedure detailed in Shi et al. (2013). On each panicle, 10 fluorescence and 5 reflectance measurements were recorded (totalling 150 fluorescence and 75 reflectance measurements for each measurement day).

Chl-F was measured using a FluorPen FP 100 (PSI, Czech Republic). Selected parameters were determined under ambient conditions: (1) effective quantum yield of photosystem II (PSII) photochemistry (Φ_{II}; Genty et al. 1989) and (2) steady-state fluorescence yield in a light-adapted state (F_S; Krause & Weis 1991). Reflectance was measured using a prototype WinePen (SpectraPen platform, PSI, Czech Republic). Vegetative indices (Vis) used to follow the changes in photosynthetic pigment content in rice panicles during maturation (Chen et al. 2006) were calculated as a reference for Chl-F measurements. Both Chl-F and reflectance were measured each day from flowering until maturity in the morning (08:00–10:00) so as to avoid noon photosynthetic depression.

RESULTS

As no reports had previously been published related to using Chl-F on rice panicles, supportive reflectance measurements were carried out. As maturation progressed, reflectance tended to decrease in the green region and increase in the blue and red regions in the bands with strong chlorophyll and carotenoids absorption (data not shown). From the reflectance spectra, particular Vis were calculated and mean values were then correlated with Chl-F measurements (Table 1). Among other indices, the photochemical reflectance index (PRI) tested as the best-fitting Vis to Φ_{II} ($R^2 = 0.71$, $p < 0.001$), while both the PRI and Φ_{II} decreased as panicle maturity progressed, and so Φ_{II} was selected for further investigation.

Given rice's top-down flowering pattern, Chl-F measurements were carried out in the top and bottom sections of panicles. Both genotypes exposed to the control treatment followed a similar pattern in Φ_{II}, remaining constant ($p > 0.5$) after flowering for both the top and bottom panicle sections (Fig. 1). For both genotypes, values remained stable until ca 14 days after flowering (DAF) when they began decreasing to 0.2 for N22 and 0.1 for Gharib.

Table 1: *Coefficients of determination R^2; N = 1650.*
*** significant at $p < 0.001$.

	Φ_{II} (Genty et al. 1989)	F_s (Krause & Weis 1991)
PRI (Gamon et al. 1992; Chen et al. 2006)	0.71***	0.47***
mND_{705} (Sims & Gamon 2002; Chen et al. 2006)	0.62***	0.35***
mSR_{705} (Sims & Gamon 2002; Chen et al. 2006)	0.54***	0.30***

In contrast, genotypes exposed to HNT revealed a time-course of Φ_{II} response until panicle maturation. Values tended to decrease either immediately after flowering (for the top portions of Gharib panicles) or remain constant ($p > 0.5$) for a significantly shorter period compared to the control treatment (ca 4 DAF for N22 and ca 6 DAF for Gharib). For both genotypes in both treatments, the top sections of panicles displayed significantly lower Φ_{II} values than the bottom sections did (Fig. 1).

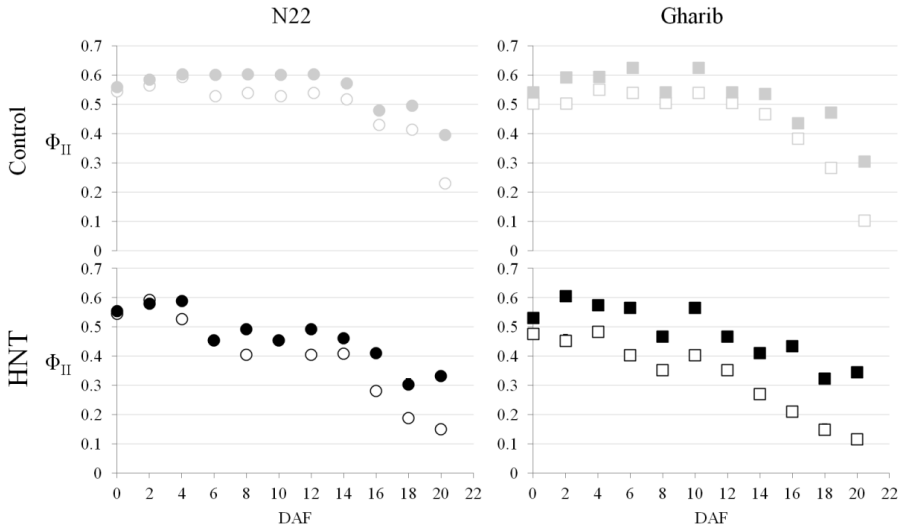

Fig. 1: *Time trend of Φ_{II} for N22 and Gharib rice genotypes in DAF. Open symbols represent the top sections of panicles and closed symbols bottom sections. Grey represents control treatment and black HNT treatment. Each data point represents mean fluorescence value (N = 150).*

DISCUSSION

In addition to flag leaves, chlorophyll-containing rice panicles also have the potential to photosynthesize (Imaizumi et al. 1990, Ishihara et al. 1990). The disappearance of chlorophyll, the main attribute of rice panicle maturation, is related to lower photosynthetic activity and so can be captured through changes in

Chl-F signals. Chl-F has been used as a widely accepted method to reveal the physiological status of senescing plants, as well as to follow the ripening periods of certain fruits. It is generally agreed that changes in Chl-F signals in maturing fruit are connected to either a decrease in chlorophyll content or a loss of chloroplast function. Decreases in Chl-F signals may, however, also be caused by the morphological architecture of the plant material or by object heterogeneity. The small detector area presented in this study and the selected parameter itself limit false readings. Among other Chl-F parameters, the maximum quantum yield of PSII (F_V/F_M) is closely related to the photochemistry of plant tissue. However, its field applications are limited by required dark adaptation prior to each measurement. Numerous studies have presented experimental evidence for a close relationship between F_V/F_M and Φ_{II} across different plant species (e.g. Genty et al. 1989), which makes Φ_{II} a suitable Chl-F parameter for field use. In contrast, F_V/F_M does not have a similarly strong relationship with F_S (Krause & Weis 1991). Moreover, the sensitivity of F_S to drought is a limiting factor as decreasing water content during panicle ripening would confound results. No reports had previously been published regarding using Chl-F measurements in connection with either panicle physiology or changes in Chl-F signals during rice panicle maturation. To support Chl-F measurements, raw spectral characteristics of reflected light from rice panicles were used as a reference for this study. As reported by Chen et al. (2006), 11 Vis were correlated with the pigment content of rice panicles. Of these, the PRI (Gamon et al. 1992) and two modified indices (mND_{705} and mSR_{705}; Sims and Gamon 2002) were selected as having the most potential for monitoring chlorophyll and/or the carotenoid–chlorophyll ratio in maturing rice panicles from milky ripeness to maturity. Moreover, as presented in this study, the PRI significantly correlated with Φ_{II}, suggesting potential applications for Chl-F in rice panicle research.

Even though the study presents an effective tool for detecting rice panicle maturation, the evidence for a close relationship between panicle maturation and the grain-filling period is still missing. Future directions should address this as well as testing the method's robustness across environments (two contrasting seasons) and rice genotypes.

Acknowledgement

First author's visit and stay at the International Rice Research Institute supported by the Federal Ministry for Economic Cooperation and Development of Germany. First and third authors supported by project No. CZ.1.07/2.3.00/20.0246 "ENVIMET" of the Ministry of Education, Youth and Sports (MEYS) within the Operational Programme Education for Competitiveness, project No. LO1415 of the MEYS within the National Programme for Sustainability, and EU FP7 project No. 284443 the European Plant Phenotyping Network.

References

Chen W, Zhou Q, Huang J (2006) Chin. J. Rice Sci. 20, 434–439.

Gamon JA, Peñuelas J, Field CB (1992) Remote Sens. Environ. 41, 35–44.

Genty B, Briantais JM, Baker NR (1989) Biochim. Biophys. Acta 990, 87–92.

Imaizumi N, Usuda H, Nakamoto H et al. (1990) Plant Cell Physiol. 31, 835–844.

Ishihara K, Kiyota E, Imaizumi N (1990) Jap. J. Crop Sci. 59, 321–326.

Krause GH, Weis E (1991) Annu. Rev. Plant Physiol. Plant Mol. Biol. 42, 313–349.

Shi W, Muthurajan R, Rahman H et al. (2013) New Phytol. 197, 825–837.

Sims DA, Gamon JA (2002) Remote Sens. Environ. 81, 337–354.

Elevated temperature stimulates light-induced processes that contribute to protecting photosystem II against oxidative stress

Materová, Z.[1,*], Štroch, M.[1,2], Holubová, I.[1], Sestřenková, J.[1], Oravec, M.[2], Večeřová, K.[2], Špunda, V.[1,2]

[1]*Faculty of Science, University of Ostrava, 30. dubna 22, 701 03 Ostrava, Czech Republic*
[2]*Global Change Research Centre, Bělidla 986/4a, 603 00 Brno, Czech Republic*
[*]*author for correspondence; email: p12183@student.osu.cz*

ABSTRACT

We focused on elucidating the impact of elevated temperature on rapid induction of zeaxanthin (Z)-dependent photoprotection in two different plant species. The dynamics of violaxanthin (V) de-epoxidation under different illumination regimes was studied together with chlorophyll *a* fluorescence transients in *Picea abies* seedlings and *Arabidopsis thaliana* leaves pre-acclimated to temperatures ranging from 20 to 40°C. Whereas for spruce seedlings the rapid phase of V de-epoxidation (induced by either 10 s illumination or 10 light pulses 1 s in duration at 1 min intervals) was gradually stimulated upon increasing temperatures, for *A. thaliana* leaves considerable acceleration of V de-epoxidation occurred only at 40°C. Moreover, only for spruce seedlings was a considerable amount of Z accumulated after 10 × 1 s illumination. Elevated temperatures stimulated rapid formation of Z-dependent non-radiative dissipation of excitation energy within photosystem II (NRD) induced by 1 s light pulses only for spruce seedlings. The possible role of a specific fatty acid composition in spruce thylakoid membrane lipids in facilitated V de-epoxidation and NRD induction at elevated temperatures is discussed.

INTRODUCTION

Upon illumination of dark-adapted plants with saturating light intensities, maximal (steady-state) de-epoxidation state ([Z+A]/[V+A+Z]; DEPS) can be reached usually after ca 30 min (Jahns et al. 2009). Maximal DEPS in higher plants (typically 60–90%) differs among species (Kurasová et al. 2003). In Norway spruce (*Picea abies* [L.] Karst.) acclimated to high light, a rapid induction of maximal NRD and accumulation of zeaxanthin (Z) has been observed (Štroch et al. 2008). Moreover, it has been found that de-epoxidation efficiency depends on the formation of monogalactosyldiacylglycerol (MGDG)-enriched regions in thylakoid membranes that support both binding of violaxanthin de-epoxidase (VDE) to the thylakoid membrane and the availability of V for de-epoxidation (Jahns et al. 2009).

Little is known about the role of Z- and ΔpH-dependent NRD in plants' responses to elevated temperatures and high intensities of photosynthetically active radiation (PAR). Although moderately elevated temperatures are not always associated with enhanced Z accumulation and stimulated NRD levels in illuminated leaves (Štroch et al. 2010), the ΔpH requirement to activate VDE and NRD induction is reduced in plants exposed to heat stress (Zhang et al. 2009).

One of the factors determining the dynamics of NRD induction at elevated temperatures is thylakoid membrane fluidity, which is influenced not only by temperature itself but also by the fatty acid composition of thylakoid membrane lipids. In thylakoid membranes of spruce needles, a considerable amount of

octadecatetraenoic acid (18:4) has been found in MGDG (Wolfenden & Welbrun 1991). That is very rare in higher plants. We suggest that the presence of octadecatetraenoic acid can be engaged in modulation of the temperature dependence of thylakoid membrane fluidity in Norway spruce needles. This in turn can contribute to both facilitated V de-epoxidation and Z-dependent NRD induction at higher temperatures as compared to such typical C3 plants as *Hordeum vulgare* L. and *Arabidopsis thaliana* (L.) Heynh.

To elucidate the presumed impact of elevated temperature on Z-dependent photoprotection, we made a detailed analysis in spruce seedlings and *A. thaliana* leaves of the temperature dependence of the rapid phase of V de-epoxidation under different illumination regimes. For this purpose, an analysis was conducted in both of these species of corresponding chlorophyll *a* (Chl *a*) fluorescence transients (monitoring in particular the inductions of NRD and of cyclic electron transport around photosystem I).

MATERIALS AND METHODS

Spruce and *A. thaliana* seedlings were grown for 17–19 and 60 days, respectively, at 50 µmol m^{-2} s^{-1} PAR in VB 1014 (Vötsch, Germany) and HGC 1014 (Weiss, Germany) growth chambers under 16/8 h (20/20°C) and 8/16 h (20/22°C) light/dark regimes, respectively. After 5 min of acclimation at given temperatures, samples were exposed to different illumination regimes (see Fig. 1 legend for details) at saturating PAR (1,400 µmol m^{-2} s^{-1}) during which Chl *a* fluorescence traces were measured by a chlorophyll fluorescence meter (PAM 101/103; Walz, Germany). Immediately (ca 10 s) after the given PAR regime, samples were placed into liquid nitrogen and used for high-performance liquid chromatography of xanthophyll cycle pigments with an Agilent 1200 (Agilent, USA) (Štroch et al. 2008).

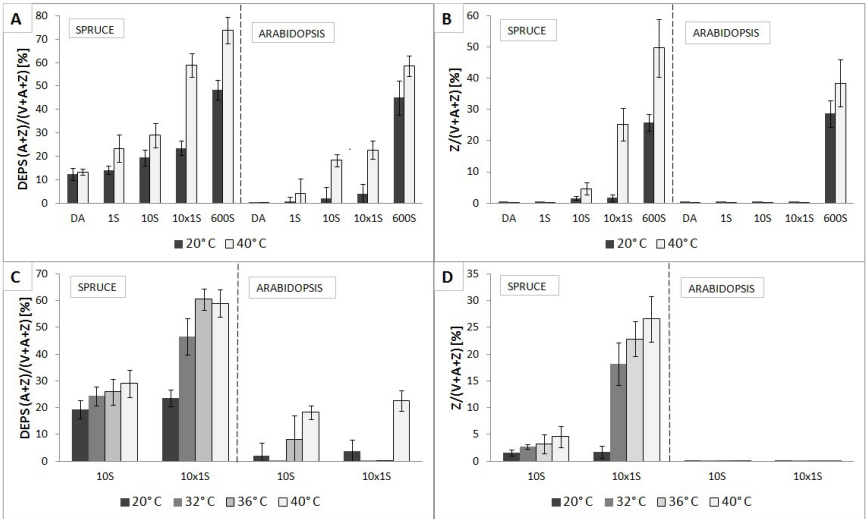

Fig. 1. *Effect of elevated temperature on the dynamics of V de-epoxidation in spruce seedlings and A. thaliana leaves. A, C: de-epoxidation state (DEPS); B, D: amount of converted Z in relation to the pool size of xanthophyll cycle pigments. After 5 min pre-acclimation at the given temperatures, samples were exposed to different illumination regimes at 1,400 µmol m^{-2} s^{-1} PAR. DA: control dark-adapted samples maintained 15 min at the given temperature; 1S: 1 s illumination; 10S: 10 s illumination; 10x1S: 10 light pulses 1 s in duration at 1 min intervals; 600S: continuous illumination for 10 min. N = 5–6 ± SD.*

RESULTS

In both spruce needles and *A. thaliana* leaves, V de-epoxidation at 40ºC was stimulated after 10 s, 10 × 1 s, and 600 s illumination regimes (Fig. 1A). But only in spruce was DEPS significantly enhanced after even a single 1 s pulse and extremely high DEPS was observed after 10 × 1 s illumination at 40ºC which was even higher than after 10 min illumination at 20ºC (Fig. 1A).

Moreover, in *A. thaliana* leaves only A accumulated at 40ºC after both 10 s and 10 × 1 s illumination, whereas in spruce seedlings a considerable amount of Z was converted – and particularly after 10 × 1 s illumination (Fig. 1B). Whereas in spruce seedlings the rapid phase of V de-epoxidation was gradually stimulated at increasing temperatures, in *A. thaliana* leaves considerable acceleration of V de-epoxidation occurred only at 40ºC (Fig. 1C). In addition, accumulation of Z in spruce needles was stimulated already at 32ºC, particularly after 10 × 1 s illumination, whereas no Z was present after that illumination at any temperature in *A. thaliana* leaves (Fig. 1D).

Traces of Chl *a* fluorescence, obtained during 10 × 1 s illumination, were significantly modified by elevated temperatures in spruce needles (Fig. 2A–C). Already at 32ºC (data not shown) and 36ºC, the fluorescence signal after the fourth or fifth light pulse rapidly fell to below the F_0 level and subsequently returned to approximately the same F_0 level as before the pulse (Fig. 2B). At 40ºC, the rapid quenching of fluorescence below the before-pulse level was already observed after the second pulse (Fig. 2C). In *A. thaliana* leaves, by contrast, a typical fluorescence response after light pulse application was observed during the entire sequence of light pulses at temperatures up through 36ºC (Fig. 2D, E). At 40ºC, the fluorescence trace of *A. thaliana* leaves suddenly changed, but instead of a rapid quenching to below the F_0 level the pronounced post-illumination fluorescence rise interrupted the decrease of the fluorescence signal back to the F_0 level (Fig. 2F).

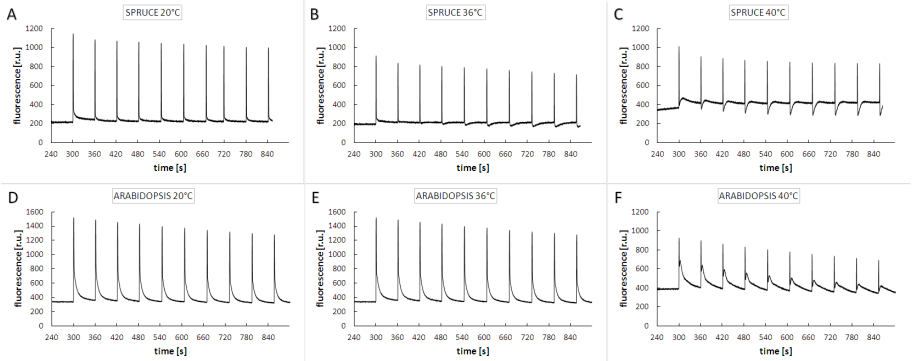

Fig. 2. *Typical traces of Chl a fluorescence obtained during 10 × 1 s illumination in spruce needles (A, B, C) and A. thaliana leaves (D, E, F) at indicated temperatures. Samples were pre-acclimated to given temperatures for 5 min prior to applying illumination regime.*

DISCUSSION

For the first time, V de-epoxidation has been observed after a 1 s light pulse in spruce needles. The high levels of Z accumulation after 10 light pulses 1 s in duration at 1 min intervals and at elevated temperatures clearly demonstrate that the xanthophyll cycle can be accelerated to a higher degree than that which has recently been reported for rapid V de-epoxidation in *Chromera velia* (Kotabová et al. 2011) and *Physcomitrella patens* (Pinnola et al. 2013). Elevated temperatures stimulated V de-epoxidation in both *A. thaliana* leaves and spruce needles, as DEPS after 10 s illumination at 40°C was the same in both species studied. Only in spruce seedlings, however, was the second de-epoxidation step converting A to Z considerably accelerated at elevated temperatures, particularly after 10 × 1 s illumination. As this step requires a flip-flop of A in the MGDG thylakoid membrane domain (Jahns et al. 2009), this result indicates that the fluidity of MGDG domains increased at elevated temperatures to a greater extent in spruce needles.

In agreement with the finding that rapid accumulation of Z at elevated temperatures is specific for spruce needles, the rapid quenching of F_0 fluorescence after the 1 s light pulses in spruce seedlings indicates an extremely rapid induction of Z- and ΔpH-dependent NRD within LHCII. In contrast, the pronounced post-illumination fluorescence rise observed at 40°C in *A. thaliana* supports the notion that in this plant species enhancement of cyclic electron transport at elevated temperatures contributes to rapid ΔpH-dependent NRD induction but not to Z-dependent NRD.

Moreover, stimulation of rapid light-induced V de-epoxidation and NRD at increasing temperatures was gradual for spruce seedlings but rather stepwise at 40°C for *A. thaliana* leaves. This indicates that the temperature dependence of thylakoid membrane fluidity may be different between spruce needles and *A. thaliana* leaves. In agreement with Wolfenden & Welbrun (1991), preliminary analysis of fatty acids in the thylakoid membranes isolated from spruce seedlings revealed the presence of two, yet unidentified, C18 fatty acids with 3 and/or 4 double bonds. These data support the hypothesis that the presence of octadecatetraenoic acid may be engaged in modulation of the temperature dependence of thylakoid membrane fluidity, which in turn may contribute to both facilitated V de-epoxidation and NRD induction at elevated temperatures.

Acknowledgement

Supported by project No. LO1415 of the National Programme for Sustainability I, project No. CZ.1.05/1.1.00/02.0073 of the Global Change Research Centre of the Czech Academy of Sciences, grant No. 13-28093S/P501 from the Czech Science Foundation, and project No. SGS09/PřF/2015 from Ostrava University.

References

Jahns P, Latowski D, Strzalka K (2009) Biochim. Biophys. Acta 1787, 3–14.

Kotabová E, Kaňa R, Jarešová J et al. (2011) FEBS Lett. 585, 1941–1945.

Kurasová I, Kalina J, Urban O et al. (2003) Photosynthetica 41, 513–523.

Pinnola A, Dall'Osto L, Gerotto C et al. (2013) Plant Cell 25, 3519–3534.

Štroch M, Kuldová K, Kalina J et al. (2008) J. Plant Physiol. 165, 612–622.

Štroch M, Vrábl D, Podolinská J et al. (2010) J. Plant Physiol. 167, 597–605.

Wolfenden J, Wellburne AR (1991) New Phytol. 118, 323–329.

Zhang R, Cruz JA, Kramer DM et al. (2009) Plant Cell Environ. 32, 1538–1547.

The thermostability of photosystem II photochemistry is related to maintenance of thylakoid membranes organization

Karlický, V.[1,2,*], Kurasová, I.[1,2], Špunda, V.[1,2]

[1]*Global Change Research Centre, Bělidla 986/4a, 60300 Brno, Czech Republic*
[2]*Department of Physics, Faculty of Science, University of Ostrava, 30. dubna 22, 70103 Ostrava, Czech Republic*
[*]*author for correspondence; email: vaclav.karlicky@osu.cz*

ABSTRACT

For higher plant photosynthetic reactions, responses to the temperature changes are important, particularly if we consider global warming and the increasing frequency of extreme temperature fluctuations. High temperature stress decreases photosynthetic assimilation through the inactivation of photosystem II (PSII), the most heat-sensitive component of the oxygen-evolving complex. We have recently found higher thermostability of spruce PSII photochemistry compared to such control plants as Arabidopsis species and barley. In this work, we have therefore attempted to describe the causes of this effect on the level of the organization of pigment–protein complexes (PPCs) in spruce thylakoid membranes using circular dichroism (CD) spectroscopy. We have confirmed higher maximum efficiency of PSII photochemistry (F_V/F_M) for spruce needles in comparison to barley leaves. Temperature-dependent CD spectra have also demonstrated higher (by about 6°C) PSII thermostability of chiral macro-organization of PPCs in spruce thylakoid membranes compared to those in barley. However, thermal disruption of PPCs did not reveal significant differences. Our results demonstrate that the stability of PSII macro-organization in different plant species correlates with the thermostability of PSII photochemistry in intact needles/leaves and so effective PSII photochemistry is related to the maintenance of PSII macro-organization under high temperature stress.

INTRODUCTION

The response of higher plant photosynthetic reactions to temperature changes is of crucial importance if we take into account both global warming and the increasing frequency of extreme temperature fluctuations. Elevated temperatures may cause direct negative effects on photosynthetic assimilation of carbon dioxide and photosystem II (PSII) is considered the most heat-sensitive component of the oxygen-evolving complex (Lípová et al. 2010, Zhang & Sharkey 2009). In our previous work (Špunda et al., unpublished data), we have found several features of the spruce photosynthetic apparatus that were not observed in such control plants as Arabidopsis species and barley. In particular, these are rapid acceleration of violaxanthin de-epoxidation by short pulses of saturating light at higher temperatures and higher thermostability of PSII photochemistry in spruce than was found in control plants.

In this work, we have focused on studying the macro-organization of pigment–protein complexes (PPCs) in thylakoid membranes from spruce and barley using circular dichroism (CD). CD spectroscopy is a non-invasive method for investigating pigment–pigment interaction even in systems as highly complex as intact cells *in vivo*. Hierarchically organized systems such as thylakoid membranes contain three types of signals of different physical origins. For the study of thylakoid membranes, however, only the excitonic bands from short-range (nanometer scale) excitonic interactions between pigments within PPCs and high-intensity Ψ-type CD bands from the long-range order (hundreds of nanometres) of the chromophores in chirally-organized macroarrays are relevant (Garab & van Amerongen 2009). The main objective of this work is to determine whether the higher thermostability of PSII photochemistry found in spruce is somehow related to the macro-organization of PPCs in the thylakoid membrane.

MATERIALS AND METHODS

Spring barley (*Hordeum vulgare* L. cv. Bonus) and Norway spruce (*Picea abies* L. Karst.) were grown from seeds under controlled environmental conditions inside an HB 1014 growth chamber (Bioline-Heraeus, Germany) at photosynthetic photon flux densities of 50 µmol photons m^{-2} s^{-1}, 20ºC, 65% relative humidity, and 16/8 light/dark regime. The middle segments of dark-adapted primary leaves of 7-day-old barley plants and needles of 3–4-week-old spruce seedlings were used for measurements on intact leaves and isolation of thylakoid membranes. Barley thylakoid membranes were isolated according to Ilík et al. (2002) with modifications described in Karlický et al. (2010), while a special method for conifer needles was used to isolate spruce thylakoid membranes (Holá et al. 2012).

CD spectra were measured on isolated thylakoid membranes between 400 and 800 nm using a J-815 spectropolarimeter (Jasco, Japan). Membranes at chlorophyll (Chl) content of 20 µg ml^{-1} were resuspended in a medium containing 50 mM Tricine (pH = 7.5), 0.4 M sorbitol, 5 mM KCl, and 5 mM $MgCl_2$. Spectra were recorded in steps of 0.5 nm with integration time of 1 s, band-pass of 2 nm, and scanning speed of 100 nm min^{-1}. Optical path length of the cell was 1 cm. Samples were incubated sequentially for 5 min at each temperature starting from 20ºC up to 70ºC. Each experiment was repeated five times. Measured temperature dependences of CD bands and band pairs were fit with a sigmoidal curve that resulted in the estimation of transition temperatures (T_m). These T_m values mark the disassembly of the complexes' chiral macrodomains (Cseh et al. 2000) and are defined as the temperature at which the intensity of the CD band is decreased to 50% of its value at 20ºC.

Temperature responses of Chl *a* fluorescnence parameters were estimated using a PAM 101–103 pulse amplitude-modulated fluorometer (Walz, Germany). Needle and leaf samples were exposed to linear heating in the temperature-controlled measuring chamber equipped with optical lid for PAM fibre-optics and connected to an MC-4 temperature-controlled bath (Julabo, Gemany). The linear heating of the water-bath was set to a speed of 1ºC min^{-1} within 20–48ºC. The sample's surface temperature was continuously monitored during heating using a thermocouple. In order to avoid desiccation during measurement, samples were inserted into the measuring chamber on water-soaked foam and pre-acclimated at 20ºC for 5 min in darkness prior to heating. Saturation pulses (t = 1 s, I = 1,400 µmol photons m^{-2} s^{-1}) applied at 20ºC and then after each 2ºC increase (after ca 2 min), were used to determine maximum fluorescence in dark-adapted states (F_M). Immediately prior to applying the saturation pulse, minimum fluorescence in a dark-adapted state (F_0) was measured and the maximum efficiency of PSII photochemistry (F_V/F_M) was calculated as $(F_M–F_0)/F_M$.

RESULTS

The CD spectra of thylakoid membranes isolated from barley and spruce revealed similar characters. The main CD bands at wavelengths around (+)685, (–)673, and (+)505 nm, which are of Ψ-type origin, and less intensive CD bands of excitonic origin at wavelengths of (–)438, (+)448, (–)459, and (–)650 nm were present in both barley and spruce samples (Fig. 1A, B). Nevertheless, at 20ºC the amplitude of the main Ψ-type CD band for barley membranes was almost double that for spruce membranes (Fig. 1A, B), which indicates a much smaller size of chiral macrodomains or a different macro-organization of PSII-supercomplexes in spruce thylakoid membranes than in those of barley.

In contrast to the similar character of the CD spectra at 20ºC, the thermal stabilities of barley and spruce membranes differed significantly. In barley membranes, chiral macrodomains were affected considerably more by elevating the temperature to 45ºC (Fig. 1A) than were those in spruce membranes (Fig. 1B). This difference in the thermal stability of the macrodomain organization of the PPCs can be seen more clearly in a graph of the temperature dependence

of the Ψ-type CD bands (Fig. 1C), where T_m in spruce membranes is about 6°C higher than is T_m in barley membranes. Temperature dependences of Ψ-type CD bands and band pairs are summarized in Table 1.

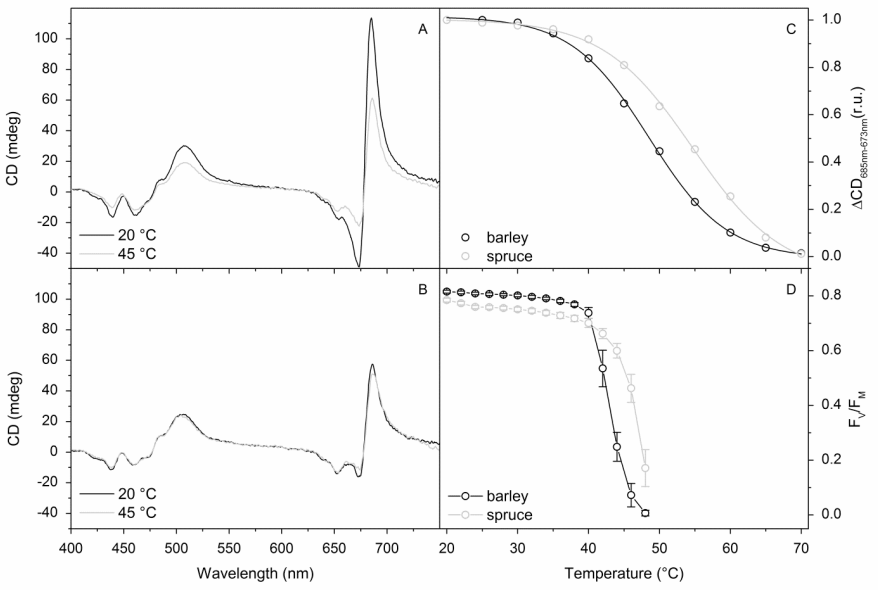

Fig. 1: *CD spectra of isolated thylakoid membranes from (A) barley and (B) spruce measured at 20°C (black) and 45°C (grey). (C) Temperature dependences of the amplitude differences of the main Ψ-type bands, at around (+)685 nm and (–)673 nm, of barley (black) and spruce (grey) thylakoid membranes; data points from one representative series fitted with a sigmoidal curve resulting transition temperatures (T_m) at 48.5°C and 54.7°C, respectively. Experiments were repeated five times and resulted in very similar differences in CD spectra and their thermal behaviour (see Table 1 for complete statistics). (D) Temperature dependences of maximum efficiency of PSII photochemistry (F_V/F_M) measured on overnight dark-adapted barley leaves (black) and spruce needles (gray). Mean values and standard deviation are presented (N = 5–6).*

The thermal destabilization of different PPCs was monitored via the amplitudes of their corresponding excitonic bands. Chl *a* excitonic bands at around 450 nm (Garab et al. 1991), determined either as $CD_{(448–438)}$ or $CD_{(448–459)}$, exhibited similar temperature dependences for barley and spruce and displayed essentially identical T_m values of about 60°C (Table 1). On the other hand, the thermostability of the excitonic band of Chl *b* within the PSII light-harvesting complex (LHCII) at 650 nm (Georgakopoulou et al. 2007) was higher by around 5°C for spruce than it was for barley (Table 1). Nevertheless, the excitonic T_m value especially of the barley thylakoid membrane may be underestimated due to the overlap of excitonic and high-intensity Ψ-type CD bands.

In order to verify the relationship between the structural and functional states of thylakoid membranes at elevated temperatures, we also measured the maximum efficiency of PSII photochemistry (F_V/F_M) on intact leaves/needles. We found that F_V/F_M of control plant leaves steeply decreased at 42°C and almost complete PSII inactivation occurred at 46°C. In contrast, PSII inactivation was more gradual in spruce needles at temperatures above 40°C and F_V/F_M values of about 0.5 were observed at 46°C (Fig. 1D).

CD signal (nm)	Assignment	T_m (barley) (°C)	T_m (spruce) (°C)
685–730	Ψ-type	48.3 ± 2.2	54.1 ± 1.4
685–671	Ψ-type	47.9 ± 1.9	54.3 ± 1.1
505–550	Ψ-type	48.4 ± 1.2	52.4 ± 1.2
448–459	Excitonic (Chl a)	59.9 ± 2.5	61.9 ± 2.4
448–438	Excitonic (Chl a)	60.9 ± 2.3	61.8 ± 2.2
610–650	Excitonic (Chl b, LHCII)	56.0 ± 2.4	61.3 ± 1.6

Table 1: *Transition temperatures (T_m) of selected CD bands and band pairs for barley and spruce thylakoid membranes. Membranes were incubated for 5 min at different temperatures between 20 and 70°C before recording the CD spectra at the given temperature. Amplitudes for individual bands were calculated from differences in intensity at specific wavelengths (see also the text). Mean values and standard deviation are presented (N = 5).*

DISCUSSION

Ψ-type CD bands of spruce thylakoid membranes had significantly higher T_m values than did those of barley membranes, while the T_m values of excitonic bands were not different. Therefore, these results indicate that spruce thylakoid membranes have considerable higher thermal stability of the chiral macro-organization of PPCs, but thermal destabilization of PPCs itself remained unchanged.

Comparing temperature dependences of F_V/F_M and Ψ-type CD bands of both plant species clearly demonstrated that F_V/F_M began decreasing sharply after a decline in Ψ-type amplitude to approximately 80% of its value at 20°C and complete PSII inactivation was caused by a drop in Ψ-type amplitude below roughly 60% of its value at 20°C. Therefore, these results indicate that the stability of PSII macro-organization in different plant species quantitatively correlates with the thermal stability of PSII photochemistry in intact needles/leaves and is therefore related to the maintenance of photochemical activity under high temperature stress.

Acknowledgement

Supported by grant No. 13-28093S/P501 from the Czech Science Foundation, project No. CZ.1.05/1.1.00/02.0073 of the Global Change Research Centre of the Czech Academy of Sciences, and project No. LO1415 of the Ministry of Education, Youth and Sports within the National Programme for Sustainability I. We thank B. Piskořová for technical assistance.

References

Cseh Z, Rajagopal S, Tsonev T et al. (2000) Biochemistry 39, 15250–15257.

Garab G, Kieleczawa J, Sutherland JC et al. (1991) Photochem. Photobiol. 54, 273–281.

Garab G, van Amerongen H (2009) Photosynth. Res. 101, 135–146.

Georgakopoulou S, van der Zwan G, Bassi R et al. (2007) Biochemistry 46, 4745–4754.

Holá D, Kočová M, Rothová O et al. (2012) Photosynthetica 50, 291–304.

Ilík P, Krchňák P, Tomek P et al. (2002) J. Biochem. Bioph. Methods 51, 273–281.

Karlický V, Podolinská J, Nadkanská L et al. (2010) Photosynthetica 48, 475–480.

Lípová L, Krchňák P, Komenda J et al. (2010) Biochim. Biophys. Acta 1797, 63–70.

Zhang R, Sharkey TD (2009) Photosynth. Res. 100, 29–43.

CN-PAGE as a tool for separating pigment–protein complexes and studying their thermal stability in spruce and barley thylakoid membranes

Kurasová, I.[1,2,*], Svrčinová, K.[1], Karlický V.[1,2], Špunda V.[1,2]

[1]*Department of Physics, Faculty of Science, University of Ostrava, Chittussiho 10, 71000 Ostrava, Czech Republic*
[2]*Global Change Research Centre, Bělidla 986/4a, 60300 Brno, Czech Republic*
[*]*author for correspondence; email: Irena.Kurasova@osu.cz*

ABSTRACT

The central aim of our study was to develop a method for solubilization and native electrophoretic (colourless native polyacrylamide gel electrophoresis; CN-PAGE) separation of pigment–protein complexes (PPCs) embedded in thylakoid membranes (tBMs) isolated from spruce. Subsequently, we focused on studying the effect of temperature on the composition and PPC stability of two different species: barley and spruce.

We found that the mild detergent n-dodecyl β-D-maltoside (β-DM) is suitable for PPC solubilization of spruce tBMs, but longer solubilization and a higher ratio of detergent to total chlorophyll are needed for spruce than are needed for barley. We also unified CN-PAGE protocols to optimize the separation of spruce and barley PPCs that resulted in the separation of photosystem I (PSI) and photosystem II (PSII) supercomplexes (SCs), PSI and PSII core dimers, PSII core monomers, trimeric and monomeric light-harvesting complexes of PSII, and bands with free pigments.

Studying the effect of elevated temperature on PPCs using CN-PAGE revealed different thermal stability of PPCs in spruce and barley tBMs. Pronounced PPCs changes were observed at temperatures at or above 40°C. We observed partial disappearance of PSII SCs bands at 44°C in barley and at 52°C in spruce. In addition, spruce PSI SCs exhibited slightly higher thermal stability than did barley PSI SCs. The increased thermal stability of spruce tBMS in comparison to that of barley tBM was also confirmed by the circular dichroism spectra of isolated tBMs at different temperatures (Karlický et al. 2015).

INTRODUCTION

Studying plant responses to changing environments on a molecular level requires, among other matters, biochemical and proteomic methods to isolate cell compartments and to separate, identify, and quantify proteins and protein complexes. Reorganization of pigment–protein complexes (PPCs) within the thylakoid membranes (tBMs) of chloroplasts is one of the adaptation mechanisms by which plants respond to such fluctuating environmental conditions as changing temperature, light quality and quantity, and water and mineral availability. Electrophoretic techniques are useful methods for analysing the arrangement of thylakoid protein complexes and estimating protein composition. Today, colourless native polyacrylamide gel electrophoresis (CN-PAGE) preserving the native state of separated protein complexes plays a considerable role among these methods in the first dimension (Wittig & Schägger 2008). On the other hand, denaturing SDS-PAGE in the second dimension with subsequent western blotting or mass spectroscopy is obviously used to determine the precise polypeptide composition of protein complexes (Ladig et al. 2011). Separation of thylakoid PPCs using various native electrophoretic techniques has been developed and is a widely used method for angiosperms (e.g., Tang et al. 2007, Karlický et al. 2010, Lípová et al. 2010, Järvi et al. 2011). For conifers, however, there are as yet no CN-PAGE protocols, and therefore to date denaturing or mild denaturing SDS-PAGE

electrophoresis has been used (Krivosheeva et al. 1996, Ivanov et al. 2006, Verhoeven et al. 2009). Due to the fibrous character of needles and the presence of waxes, tannins, and phenols (Holá et al. 2012), isolation and solubilization of tBMs from mature needles is more difficult, and using young spruce seedlings (ca 16–26 days old) results in increased quality of isolated tBMs. In contrast to those from older needles, moreover, suspensions of tBMs isolated from spruce seedlings regularly contain sufficient total chlorophyll for CN-PAGE requirements.

In the present contribution, we describe a method for isolating and separating PPCs using non-denaturing CN-PAGE that is suitable for both barley and spruce. Using this method, we were able to separate several tBM SCs and to demonstrate different thermal stabilities of PPCs in spruce and barley tBMs.

MATERIALS AND METHODS

Plant material

Spring barley (*Hordeum vulgare* L. cv. Bonus) seedlings were grown in commercially available soil substrate (Agro CS, Czech Republic) at 20°C in a growth chamber (HB 1014, Bioline-Heraeus, Germany) with 16/8 h photoperiod at 50 µmol photons m^{-2} s^{-1}. The middle parts of 7-day-old primary leaves were used to isolate tBMs. Norway spruce (*Picea abies* (L.) Karst.) seeds were immersed in water for 24 h prior to sowing in perlite (Agro CS, Czech Republic). Seedlings were grown under the same regime as barley and 20-day-old spruce plants were used for tBM isolation.

Isolation, thermal incubation, and solubilization of tBMs

Plant tissue (10 g for barley, 4 g for spruce) was disintegrated (45 s at 18,000 rpm) using an Ultra-Turrax T25-18G blender-type homogenizer (IKA, Germany) in 100 ml of a homogenization medium (400 mM sucrose, 400 mM NaCl, 4 mM $MgCl_2$, 0.2 g BSA, 5 mM ascorbic acid, 35 mM Hepes, pH 7.2). Homogenate was filtrated through 8 layers of polyamide sieve (Uhelon 130T, 42 µm, Silk & Progress, Czech Republic) and centrifuged (3K30, Sigma, UK) for 6 min at 5,000 and centrifuged for 3 min at 200 × *g*. Pellets were resuspended in 15 ml of medium I for disrupting the chloroplast envelope (150 mM NaCl, 8 mM $MgCl_2$, 1 mM Na_2-EDTA, 25 mM Hepes, pH 7.5) and centrifuged for 10 min at 5,000 × *g*. Starch was removed from pellets by resuspending pellets in 10 ml of medium II (400 mM sucrose, 15 mM NaCl, 5 mM $MgCl_2$, 50 mM Hepes, pH 7.2). The resulting supernatant was centrifuged for 5 min at 5,000 × *g* and the resulting pellet containing tBMs was resuspended in medium II to a concentration of 1,000 µg total chlorophylls ml^{-1}. All isolation and centrifugation steps were performed at 0°C according to Nosek (2012).

Suspensions of prepared tBMs were doubly diluted with medium II and placed into water baths pre-heated to 20, 32, 36, 40, 44, 48, 52, 56, and 60°C for 15 min in a dark room. tBMs were then immediately frozen in liquid N_2. Thawed tBMs were solubilized for 5 min (barley) or 10 min (spruce) with 10% (w/v) detergent n-dodecyl-β-D-maltoside (β-DM) to yield a final w/w ratio of detergent to total chlorophylls of 20:1 for barley and 35:1 for spruce. High-speed centrifugation (20,000 × *g* for 10 min) was used to remove unsolubilized tBMs. The supernatant with solubilized tBMs (containing 15 µg of total chlorophylls) was immediately loaded onto polyacrylamide gel.

Native polyacrylamide gel electrophoresis (CN-PAGE)

Separation of PPCs using CN-PAGE was carried out using 4% (w/v) stacking and 4.5–11.5% (w/v) gradient resolving polyacrylamide gel (38:1 acrylamide:bisacrylamide). Prepared gel solutions were loaded between

glass plates (18 × 16 cm) using SG5 gradient maker (Hoefer, USA). A BisTris system of cathode and anode buffers (pH 7.0) was used with the addition of β-DM (0.02% w/v) and anionic detergent sodium deoxycholate (0.05% w/v) to the cathode buffer. Electrophoresis was performed in a chilled (4°C) SE660 running system (Hoefer, USA) in darkness at gradual voltage increase from 75 to 200 V (Järvi et al. 2011) and with total running time of 3.5 h. Gel images containing separated PPCs were captured by a ChemiDoc MP gel imager (BioRad, USA) in transmitting white light with CCD detection.

RESULTS

Our previous experiment (data not shown) had revealed that the mild detergent β-DM is suitable for solubilization of tBMs in both plant species. We tested different durations of tBM solubilization with β-DM (5–20 min) as well as various ratios of detergent to total chlorophyll (5, 10, ... 55:1) to optimize tBM solubilization and subsequent PPC separation. We observed separation of PPCs into PSI SCs and several (4–5) PSII SCs, PSI and PSII core dimers ($PSII_D$), PSII core monomers ($PSII_M$), and trimeric and monomeric light-harvesting complexes of PSII ($LHCII_T$ and $LHCII_M$) in all treatments and both plant species (except for 5:1 and 10:1 ratios of β-DM to chlorophylls for solubilization of barley tBMs, in which cases no or only faint bands with PSII SCs appeared, data not shown). We determined the optimal settings for PPC solubilization were 10 min with a 35:1 ratio of β-DM to chlorophylls for spruce and 5 min with a 20:1 ratio of β-DM to chlorophylls for barley. Fig. 1 shows the effect of elevated temperature on PPC composition and content. As the temperature rises, the bands with PSII and PSI SCs progressively disappear and simultaneously different thermal stabilities of PPCs in spruce and barley tBMs are revealed. Barley exhibits a partial disappearance of PSII SCs bands at 44°C, while for spruce tBMs a pronounced reduction in the corresponding bands was observed at 52°C (Fig. 1). Additionally, PSI SCs exhibited slightly higher thermal stability in spruce tBMs than they did in barley tBMs (the corresponding band was considerably reduced in spruce at 56°C and 60°C while in barley it had almost disappeared at 56°C; Fig. 1).

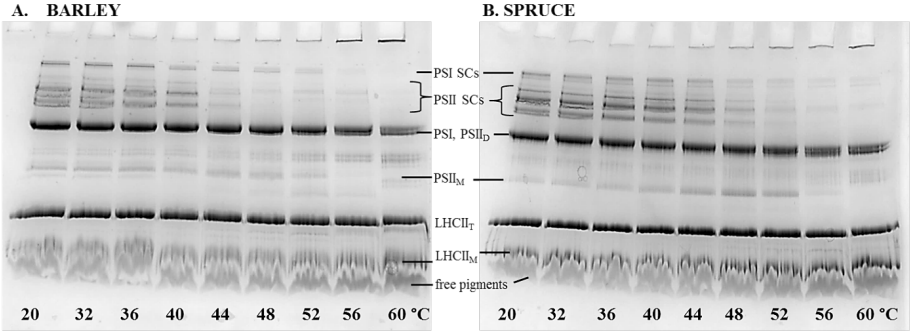

Fig. 1: *CN-PAGE separation of PPCs in tBMs isolated from (A) barley plants and (B) spruce seedlings exposed (for 15 min) to water baths pre-heated to 20–60°C in a dark room. tBMs were solubilized using β-DM with ratios of detergent to total chlorophyll of 20:1 for barley and 35:1 for spruce. Solubilized tBMs (30 µl) containing 15 µg of total chlorophylls were loaded into gel wells.*

The disassociation of SCs is accompanied by increasing formation of PPC aggregates (observed as insolubilized PPCs in gel wells), increased LHCII in monomeric form, and increased free pigment band intensity

in both plant species but more distinctly in barley. Elevated temperatures also caused increased monomerization of $PSII_D$ associated with increased intensity of the $PSII_M$ band (at 48°C and 52°C for spruce and 44°C and 48°C for barley). Complete degradation of $PSII_M$ was observed at 56°C for barley and 60°C for spruce.

DISCUSSION

The main contribution of our work is the development of a tBM solubilization and non-denaturing native-electrophoretic technique for effective and gentle separation of PPCs embedded in tBMs which is suitable for both barley and spruce. The separation of PSI and PSII SCs into several bands indicates the mildness of these techniques compared to those utilizing mild denaturing conditions (with SDS in low concentrations or Deriphat as detergents) to separate PPCs contained in tBMs of conifer species. Our observed PPCs changes under elevated temperatures are in good agreement with previously published results (Lípová et al. 2010, Krumova et al. 2014). The higher thermal stability of PPCs reported from CN-PAGE of heated spruce tBMs was confirmed also by circular dichroism spectroscopy, when the disassembly of chiral macrodomains of PPCs was observed at a higher temperature (by about 5°C) for spruce tBMs than for barley tBMs (Karlický et al. 2015). We assume that the improved thermal stability of spruce tBMs might be associated with a different composition of the lipid phase of spruce tBMs (due to changed unsaturated fatty acids content) than is found in barley. Detailed analysis of the lipid composition of spruce and barley tBMs is an important issue for future research.

Acknowledgement

Supported by project No. LO1415 of the Ministry of Education, Youth and Sports within the National Programme for Sustainability I and grant No. 13-28093S/P501 from the Czech Science Foundation.

References

Holá D, Kočová M, Rothová O et al. (2012) Photosynthetica 50, 291–304.

Ivanov AG, Krol M, Sveshnikov D et al. (2006) Planta 223, 1165–1177.

Järvi S, Suorsa S, Paakkarinen V et al. (2011) Biochem. J. 439, 207–214.

Karlický V, Kurasová I, Špunda V (2015) The thermostability of photosystem II photochemistry is related to maintenance of thylakoid membranes organization. This volume.

Karlický V, Podolinská J, Nadkanská L et al. (2010) Photosynthetica 48, 475–480.

Krivosheeva A, Tao DL, Ottander C et al. (1996) Planta 200, 296–305.

Krumova SB, Várkonyi Z, Lambrev PH et al. (2014) J. Photochem. Photobiol. B 137, 4–12.

Ladig R, Sommer MS, Hahn A et al. (2011) Plant J. 67, 181–194.

Lípová L, Krchňák P, Komenda J et al. (2010) Bichim. Biophys. Acta 1797, 63–70.

Nosek L (2012) Usage of 2D-CN/SDS-PAGE for determination of changes in pigment-protein complexes from thylakoid membranes of stressed plants. Master's thesis, Palacký University, Olomouc.

Tang Y, Wen X, Lu Q et al. (2007) Plant Physiol. 143, 629–638.

Verhoeven A, Osmolak A, Morales P et al. (2009) Tree Physiol. 29, 361–374.

Wittig I, Schägger H (2008) Proteomics 8, 3974–3990.

Development of methods for breeding high-lipid-content algal strain *Chlamydomonas reinhardtii* using fluorescence-activated cell sorting

Fedorko, J.[1,*], Buzová, D.[1], Červený, J.[1]

[1]*Global Change Research Centre, Drásov 470, 664 24, Czech Republic*
[*]*author for correspondence; email: Fedorko.j@czechglobe.cz*

ABSTRACT

Green microalgae are among the most widely distributed microorganisms in the biosphere. They are significant contributors to global photosynthetic productivity and are interesting for biotechnology due to their large variety of high-value compound accumulation and range of applications. To achieve profitable microalgae cultures for biotechnology, one wants to combine antagonistic properties: rapid growth and high accumulation of specific compounds.

Here, we focus on development of advanced cultivation strategies and breeding methods applied to the model algae *Chlamydomonas reinhardtii* for optimized production of lipids. For identification, isolation, and subsequent selection of an optimal subpopulation with high lipid content, we used high-throughput fluorescence-activated cell sorting in combination with imaging flow cytometry on cells stained with lipid-specific fluorescent dye. We observed that post-sort cell viability was not negatively influenced by external parameters used during the sorting procedure (pressure, light quality and quantity, influence of the sorting electromagnetic field, toxic effects of both fluorescent marker and microfluidic system medium composition).

INTRODUCTION

Microalgae are good candidates for fuel production due to their faster growth, higher photosynthetic efficiency, and greater lipid content compared to other energy crops (Bono et al. 2013). One promising microalga is *Chlamydomonas reinhardtii,* a unicellular green alga which has been investigated as a reference organism for studying algal physiology, metabolism, and genetics (Merchant et al. 2010, 2012). It can synthesize intracellular lipid bodies containing triacylglycerol. Lipid-body formation depends on several factors such as nutrient starvation, temperature, salinity, and light intensity (Johnson & Alric 2013). Studies have shown a starchless mutant of *C. reinhardtii* to have heightened lipid synthesis compared to the wild type (Work et al. 2010). We therefore used the starchless mutant for our study.

Fluorescence-activated cell sorting (FACS) is a powerful technique for isolating target cells from a complex population based upon specific fluorescence cell properties. The potential of FACS to enhance feedstock production, specifically to enhance oil-rich strains of microalgae, has been reported in several articles (Doan & Obbard 2012). The background of this method is based on microalgae's unique ability to adapt their metabolism to culture conditions and the opportunity to modify and maximize lipid production (Hyka et al. 2013).

Imaging flow cytometry (IFC) provides multiple high-resolution images of every cell directly in flow, including bright field, dark field, and fluorescent imagery with sensitivity exceeding that of conventional flow cytometers. This enables detailed characterization of cells using a range of criteria and provides a technique combining visual analysis and flow cytometric profiling. We describe a method that combines both flow cytometry techniques, IFC and FACS, using the capacity of specific properties of fluorescent dyes and cultivation under controlled conditions to identify, isolate, and select cells with higher stable lipid production.

MATERIALS AND METHODS

Strains and culturing conditions. The starchless mutant cc4333 (sta6-1) used in this study was kindly provided by Dr. L.G. Valledor, University of Oviedo, Spain. The culture media used in this study were HEPES-Acetate Phosphate (HAP) (Blaby et al. 2013) liquid culture medium, inorganic nitrogen source reduced HAP medium (HAP-N or -60N), and a HAP medium without Na acetate (HAP-A). The HAP-N medium was prepared without HAP 60N and with 60% of the NH_4Cl of the original HAP medium. *C. reinhardtii* culture was cultivated in an FMT-150 bioreactor (PSI, CZ) for 35 days under specific light (45/383 µmol m^{-2} s^{-1} red/cold white light), gassing (1.5% CO_2, 200 ml min^{-1}), and temperature (25 °C) conditions, stirred with a magnetic bar (180 rpm, ø6 × 35 mm). During these 35 days, *C. reinhardtii* was sorted 5 times and after the 35 days cultivated in an Erlenmeyer flask in an AlgaeTron AG230 (PSI, CZ) and shaken on an orbital shaker (125 rpm, 10 mm), under specific light (100 µmol m^{-2} s^{-1} cold white light) and temperature (25°C) conditions and in HAP-A medium for 27 days. Subsequently, the sorted and original *C. reinhardtii* cultures were recultivated for 10 days in HAP-A at approximately the same optical density and then resuspended in HAP-A medium.

Fluorescence staining. Lipid bodies were stained with BODIPY 505/515 according to Cooper et al. (2010) (to 1.5 µg ml^{-1} and incubated for 10 min in darkness at 25°C). BODIPY 505/515 dye has a sharp emission peak at 515 nm with weak emission at higher wavelengths. This dye selectively stains lipids including fatty acids, cholesteryl esters, phospholipids, sphingolipids and their analogues (Chen et al. 2009, Cooper et al. 2010). Cellular activity was determined using fluorescein diacetate (FDA; Sigma–Aldrich, USA) as the marker. FDA is a cell-permeant esterase substrate that can serve as cellular activity probe measuring both enzymatic activity and cell-membrane integrity. Samples were stained with FDA (to 25 µg ml^{-1} and incubated in darkness for 10 min, at 25°C).

Imaging flow cytometry. IFC combines the quantitative power of large sample sizes common to flow cytometry with the information content of microscopy and enables statistical analyses of entire populations with the capability to focus at the single-cell level. This tool was used to study lipid body production and changes in cell viability and chlorophyll (Chl) content. IFC was performed on an ImageStreamX Mark II (Amnis, USA). A sample of 10,000 cells was collected using a 488 nm excitation laser (0.1 mW) for BODIPY excitation and Chl excitation. BODIPY 505/515 fluorescence (alternatively FDA fluorescence) was collected in channel two (505–560 nm), the bright field image in channel three, and Chl fluorescence in channel five (660–740 nm).

Cell sorting. A MoFlo XDP high-speed flow cytometer (Beckman Coulter, USA) was used for cell sorting. The same excitation laser as during IFC measurements was used for the sorting procedure and the BODIPY signal was measured in the 515–545 nm range. Chl fluorescence was measured above 670 nm. As flow cytometry sheath fluid, we used Coulter Isoton II Diluent (Beckman Coulter, USA). Cell sorting was done using purity mode, with a 70 µm nozzle tip. The sorting window was adjusted so that the new subpopulation contained cells with high lipid content quantified by BODIPY 505/515 (Fig. 1). Cells were sorted directly into sterile 50 ml tubes. After the sorting step, the cells were washed and resuspended in HAP medium.

RESULTS AND DISCUSSION

The aim of this study was to apply controlled selective pressure in order to increase the lipid content of *C. reinhardtii*. To obtain healthy growth of *C. reinhardtii*, the cultures were harvested during the early stationary growth phase. The initial cultures for the inoculum were maintained at around 10^7 cells ml^{-1} in HAP-A medium and cultivated in a photobioreactor. When cells reached the early stationary phase, the culture was divided into two samples. One sample was used as the control (compared to non-sorted culture) and the second was used for an additional cell sorting step (sorted culture). Cells for sorting were stained by BODIPY as

described in the "Materials and methods" and sorted using flow cytometry according to the strategy shown in Fig. 1. Cell sorting region (R3) was adjusted to 75 ± 5% of BODIPY fluorescence to sort the subpopulation containing cells with the highest lipid and chlorophyll contents. These conditions assured post-sorting growth performance comparable with original cells from the normal, untreated population.

The sorted subpopulations from each sorting step were used as the inoculum for new cultivation in the bioreactor and later for another sorting step until a final subpopulation with higher lipid productivity was established. Lipid content and cell viability were periodically measured together with growth parameters that were monitored in the photobioreactor.

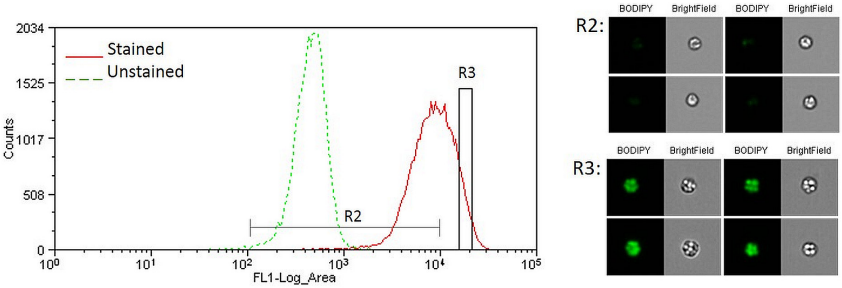

Fig. 1: *Flow cytometry analysis. Selected region R3 (stained cells distribution of BODIPY fluorescence with mean of 75 ± 5%) was gated for cell sorting. Side panel shows an example of BODIPY and bright field (cell morphology) images for subpopulations with low lipid content (R2) and high lipid content selected cells (R3).*

At the end of the first sorting step, we compared the properties of the original and sorted cultures over 13 days. Fig. 2 (left) shows a higher BODIPY fluorescence signal and thus higher lipid content of sorted cells compared to the original cells. These results suggest that the newly developed strategy for sorting and culturing *C. reinhardtii* cells was able to deliver a population with higher lipid content compared to the original culture.

Fig. 2 (right) shows the recorded fluorescence intensity of FDA stain, corresponding to the cells' metabolic activity, monitored over 13 days after the first sorting step. It was observed that sorted cells have weaker mean fluorescence intensity of FDA stain. Based on information collected from the IFC analyses and growth parameters monitored in the photobioreactor, we can conclude that post-sorting cell viability and cell recovery were not reduced. Post-sorting cell viability is an important point to consider for cell recovery and for the quality of subsequent cultivation. It depends on several factors such as the sorted cells' taxonomic group, fluorescent dye used for staining, and properties of the sorter fluidics system. Our sorting strategy shows improvement compared to other works.

To determine the effect of controlled selective pressure on cell lipid content, five sorting steps were performed. Total lipid content and cell viability were determined for each sorting step. We observed improvement in cells' lipid content in the sorted subpopulations. The enhancement of lipid content at the last sorting step was about 24% relative to the initial content. Similar results were described in other recent studies. For example, Doan & Obbard (2012) used FACS to select lineages of *Nannochloropsis* sp. to enhance total lipid content in daughter cells by up to double the lipid content of the wild-type, original strain. The enhanced intracellular lipid content of sorted cells was persistent over subsequent generations and fatty acid profiles did not differ significantly from those of original strains. A sorting-based strategy for rapid isolation of high-lipid *C. reinhardtii* mutants using traditional culturing techniques on plates and in Erlenmeyer flasks was also described previously (Velmurugan et al. 2014, Terashima et al. 2015).

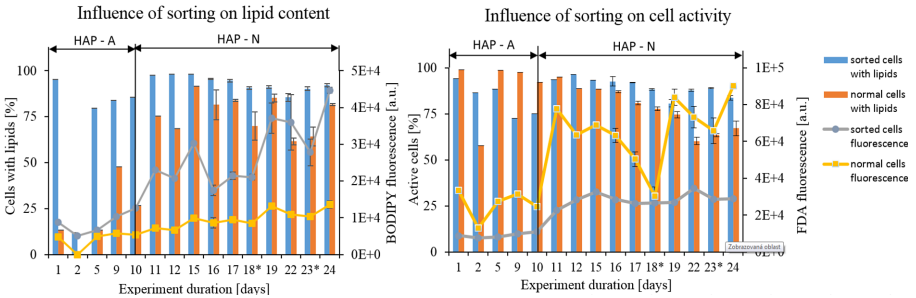

Fig. 2: *(Left) Comparison of lipid production between sorted and normal cultures. Columns show percentages of cells with lipids and lines show mean BODIPY 505/515 fluorescence as a measure of cell lipid content. (Right) Comparison of cell activity between sorted and normal cultures. Columns show percentages of active cells and lines show mean FDA fluorescence as a measure of metabolic activity. The medium was refilled at time points indicated by asterisk (*). The medium was changed from HAP–A (without acetate) to HAP–N (reduced inorganic nitrogen source) on day 10. Medium was refilled or changed only after IFC analysis. These cultures were cultivated in an Erlenmeyer flask in an AlgaeTron AG230. Error bars are calculated as SD from three replicates.*

In correlation with these results, we combined the described FACS strategy with the capacity of IFC and photobioreactor-powered cultivation strategy to maximize lipid production in a highly controlled and reproducible environment focused on developing a long-term stable, high-productivity strain. Using our strategy, we obtained a new substrain of *C. reinhardtii* with higher lipid content. We expect that an additional outcome of the developed methods and cultivation strategies will be to identify a set of genes that contribute to increased lipid accumulation and can be taken as a clue for enhanced artificial genetic manipulation.

Acknowledgement

Supported by the Ministry of Education, Youth and Sports with project No. CZ.1.05/1.1.00/02.0073 484 CzechGlobe, project No. LO1415 within the National Programme for Sustainability I, and project No. CZ.1.07/2.3.00/20.0256 within the Operational Programme Education for Competitiveness.

References

Blaby IK, Glaesener AG, Mettler T et al. (2013) Plant Cell 25, 4305–4323.

Bono MS Jr, Ahner BA, Kirby BJ (2013) Bioresour. Technol. 143, 623–631.

Chen W, Zhanga C, Song L et al. (2009) J. Microbiol. Methods 77, 41–47.

Cooper MS, Hardin WR, Petersen TW et al. (2010) J. Biosci. Bioeng. 109, 198–201.

Doan TTY, Obbard JP (2012) Algal Res. 1, 17–21.

Hyka P, Lickova S, Přibyl P et al. (2013) Biotechnol. Adv. 31, 2–16.

Johnson X, Alric J (2013) Eukaryot. Cell 12, 776–793.

Merchant SS, Kropat J, Liu B et al. (2012) Curr. Opin. Biotechnol. 23, 352–363.

Merchant SS, Prochnik SE, Vallon O et al. (2010) Science, 318, 245–250.

Terashima M, Freeman ES, Jinkerson RE et al. (2015) Plant J. 81, 147–159.

Velmurugan N, Sung M, Yim SS et al. (2014) Biotechnol. Biofuels 7, 117.

Work VH, Radakovits R, Jinkerson RE et al. (2010) Eukaryot. Cell 9, 1251–1261.

Comparative growth characterization of frequently used substrains of the model cyanobacterium *Synechocystis* sp. PCC 6803 under varying culture conditions

Zavřel, T.[1,*], Očenášová, P.[1], Sinetova, M.[2], Červený, J.[1]

[1]*Department of Adaptation Biotechnologies, Global Change Research Centre, Czech Academy of Sciences, Drásov 470, 66424, Czech Republic*

[2]*Laboratory of Intracellular Regulation, Institute of Plant Physiology, Russian Academy of Sciences, Botanicheskaya ulitsa 35, 127276 Moscow, Russia*

[*]*author for correspondence; email: zavrel.t@czechglobe.cz*

ABSTRACT

Cyanobacteria have gained increased attention as ideal candidates for biotechnological applications due to their capacity to produce valuable molecules ranging from therapeutic proteins to biofuels. Their natural phenotypic plasticity in highly dynamic environments enables easy deployment of new biotechnologies as well as opening possibilities for genetic engineering.

This contribution presents a new approach to fast and reliable characterization of cyanobacteria growth in a flat panel photobioreactor that enables examination of changing light, temperature, and nutrient availability. The utilization of semi-continuous automatic cultivation with real-time culture growth monitoring provides a strong experimental basis for both characterization and optimization of cyanobacteria cultures in photobioreactors. We first characterized the autotrophic growth of the substrain of *Synechocystis* sp. PCC 6803 denoted as GT-L. This strain is capable of efficient growth under a wide range of environmental conditions with doubling time as fast as 5 h under favorable conditions. However, differences among *Synechocystis* sp. PCC 6803 substrains have been identified on both the genotype and phenotype levels. We therefore aimed to utilize the experimental platform to characterize multiple commonly used *Synechocystis* sp. PCC 6803 substrains. This method will enable us to identify substrains capable of robust growth and high production yields as reliable biotechnological candidates.

INTRODUCTION

Cyanobacteria can be found in almost all aquatic and terrestrial habitats. Aquatic cyanobacteria have biotechnological potential as they use light as an energy source and can be cultivated in controlled environments. They can be used to produce a wide range of valuable substances (Ducat et al. 2011). The third prokaryote and first photosynthetic organism to have its genome completely sequenced was *Synechocystis* sp. PCC 6803 (hereafter only *Synechocystis*; Kaneko et al. 1996). This strain is the most intensively studied cyanobacterium and we can find derived substrains in many laboratories around the world (Moris et al. 2014). It is important to pay attention to the history and specific cultivation conditions of each *Synechocystis* substrain, especially in the sense of adaptive laboratory evolution(Dragosist & Mattanovich 2013), as differences among individual *Synechocystis* substrains have been identified on both the genotype and phenotype level (Ikeuchi & Tabata 2001, Kanesaki et al. 2012, Trautmann et al. 2012). Phenotypic differences include glucose tolerance, motility, resistance to stress, and basal metabolism. In our study, we aimed to characterize the growth and comparison of various frequently used *Synechocystis* substrains from different laboratories and culture collections. The first experiments were performed on substrain "GT-L" (Zavřel et al. 2015), kindly provided by Prof. D. A. Los (Institute of Plant Physiology, Moscow, Russia). The next substrain known as "GT-K" was kindly provided by Dr. P. Jones (Turku, Finland). This substrain came to Dr.

P. Jones from Prof. A. Kaplan (Jerusalem, Israel) and is derived from the strain "GT Williams" (Morris et al. 2014). We also ordered a reference Pasteur Culture Collection (PCC) *Synechocystis* substrain (Paris, France). All of these substrains have been used in multiple studies as model organisms. *Synechocystis* growth under varying irradiances, temperatures, and nutrient concentrations has been characterized in several studies. However, comparative growth characterization of multiple *Synechocystis* substrains has not yet been published.

MATERIALS AND METHODS

All *Synechocystis* cultures were cultivated in BG-11 medium supplemented with 17 mM HEPES (Sigma-Aldrich, USA). Inoculum cultures were cultivated in 250 ml Erlenmeyer flasks on an orbital shaker (140 rpm, 30 mm) at 31°C and under 110 µmol(photons) m^{-2} s^{-1} of warm white light provided by light emitting diodes (LEDs).

Growth characterization experiments were performed in a laboratory-scale flat panel photobioreactor (Nedbal et al. 2008). The photobioreactor illumination panel was designed as a chessboard configuration of red and blue LEDs. The photobioreactor continuously measured optical density and steady-state pigment fluorescence emission yield. For culture homogenization, we used an inflow gas bubbling system, complemented with rotation of a magnetic stirrer bar. Temperature and pH were measured by an InPro3253 electrode (Mettler-Toledo, USA).

For growth characterization, we used a quasi-continuous cultivation regime using a turbidostat mode. The dilution of actively growing cell suspensions was adjusted to OD_{680} (optical density measured at 680 nm) between 0.52–0.58, corresponding to a cell concentration of approximately 10^7 cells ml^{-1}. Growth rates were calculated for each growth period between dilution steps (Zavřel et al. 2015).

Synechocystis cells were cultivated under red light intensities of 55–660 µmol(photons) m^{-2} s^{-1} supplemented with 25 µmol(photons) m^{-2} s^{-1} of blue light and temperatures of 23–38°C with nutrient concentrations saturated for *Synechocystis* growth. Cultures were cultivated under each specific condition for at least 24 h, a period sufficient for growth stabilization and proper growth rate evaluation.

RESULTS

We focused on *Synechocystis* substrains growth characterization under different temperatures and red light intensities. During light characterization, the temperature was adjusted to 32°C, which was identified as growth-saturating for most *Synechocystis* substrains (see below). Similarly, during temperature characterization, red light intensity was set to a growth-saturating intensity of 220 µmol(photons) m^{-2} s^{-1}.

The best growth performance under varying red light intensities was observed for the PCC substrain. Under 440 µmol(photons) m^{-2} s^{-1} of red light, growth rates were about 0.12 h^{-1}, corresponding to a doubling time of approximately 5.8 h. This light intensity was also saturating for growth of the PCC substrain. For the other two substrains, the saturating red light intensity was 220 µmol(photons) m^{-2} s^{-1}, and the maximum growth rates achieved were about 0.1 h^{-1} for substrain GT-L and 0.08 h^{-1} and for GT-K, corresponding to doubling times of ca 7 h and 9 h, respectively. The growth performance of all three *Synechocystis* substrains under varying red light intensities is depicted in Fig. 1.

Temperature effects on *Synechocystis* growth are shown in Fig. 2. The growth saturating temperature was 32°C for the PCC and GT-L substrains and 35°C for the GT-K substrain. At 38°C, the growth rates of all *Synechocystis* substrains decreased. Also at temperatures bellow growth saturation, all substrains recorded decreased growth rates, but with different temperature coefficients (Q_{10}); 1.69 for the GT-L substrain, 1.76 for PCC, and 2.90 for GT-K. At 35°C, maximum growth rates were in a range of approximately 0.09–0.1 h^{-1} for all substrains, corresponding to doubling times of approximately 7–8 h.

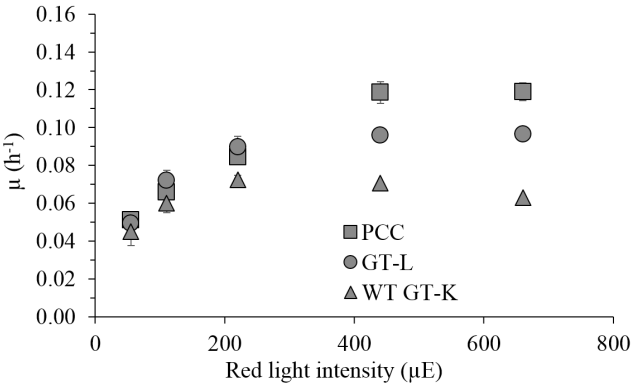

Fig. 1: *Growth characterization of three Synechocystis substrains, PCC (□), GT-L (○), and GT-K (Δ), under red light intensities of 55–660 µmol(photons) m^{-2} s^{-1} with additional 25 µmol(photons) m^{-2} s^{-1} of blue light. Light characterization was performed at 32°C and nutrient concentrations saturated for growth. Each point represents the mean of at least three independent experiments. Error bars represent standard errors. For error bars not visible, standard error was too low for visualization.*

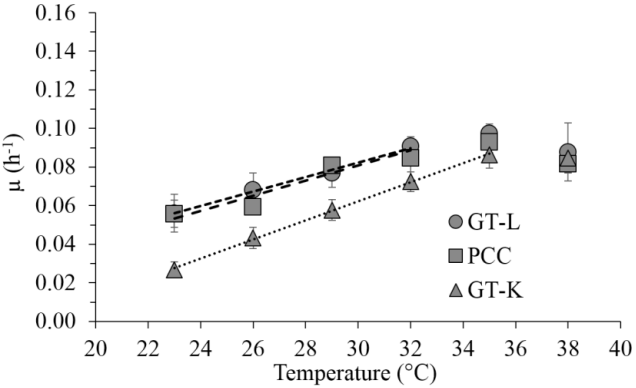

Fig. 2: *Temperature effects on growth of three Synechocystis substrains: PCC (□), GT-L (○), and GT-K (Δ). Temperature characterization was performed under red light intensity of 220 µmol(photons) m^{-2} s^{-1} with additional blue light intensity of 25 µmol(photons) m^{-2} s^{-1} and nutrient concentrations saturated for growth. Linear fits for Q_{10} are depicted for GT-L (- - -) and PCC (– –) at 23–32°C and for GT-K (···) at 23–35°C. Each point represents the mean of at least three independent experiments. Error bars represent standard errors. For error bars not visible, standard error was too low for visualization.*

DISCUSSION

In this work, we systematically characterized the autotrophic growth of several substrains of the model cyanobacterium *Synechocystis* in laboratory-scale photobioreactors and identified conditions for their optimal and suboptimal growth. The characterization focused on irradiance and temperature, environmental factors relevant for both laboratory research and industrial applications.

To monitor growth and determine growth rates, we used optical density measured at 680 nm (OD_{680}). Absorption of light at such a wavelength is influenced by both cell count and morphology as well as cellular

pigment content (mostly chlorophyll *a* in the case of *Synechocystis*). The use of OD_{680} enabled us to detect stabilization of combined cell characteristics based on the linear correlation between OD_{680}, cell count, and chlorophyll *a* content (Nedbal et al. 2008, Zavřel et al. 2015).

One of the most important environmental factors relevant for growth of photosynthetic organisms is light. During photoautotrophic growth, light is the only energy source available for cells. We characterized *Synechocystis* growth under red light of 55–660 μmol(photons) m^{-2} s^{-1} and observed growth inhibition under the highest irradiances only for substrain GT-K. The other two substrains were not inhibited under high light intensities. In general, all substrains displayed significantly different growth under red light intensities above 110 μmol(photons) m^{-2} s^{-1} (light conditions often used in *Synechocystis* related studies).

All strains achieved the highest growth rates at 35°C. In general, GT-K showed the slowest growth rates below 35°C as well as the least efficient adaptation to lower temperatures, as confirmed by the highest temperature coefficient Q_{10}. The specific growth rates of all substrains decreased at 38°C, which is in accordance with previously published studies (Inoue et al. 2001, Zavřel et al. 2015).

In this work, we utilized a growth characterization platform for a comparative growth study of three substrains of the model cyanobacterium *Synechocystis*. We compared growth under varying temperatures and light intensities and identified differences among tested substrains. However, further analysis would be required for detailed understanding of observed differences. Also, additional relevant factors including nutrient availability are of further research interest, similarly as growth characterization of other *Synechocystis* substrains. This study brings the first insight into the growth demands of individual *Synechocystis* substrains and demonstrates the importance of accounting for the adaptive capacities of *Synechocystis* cells under different laboratory environments.

Acknowledgement

TZ, PO, and JČ were supported by project No. CZ.1.05/1.1.00/02.0073 484 CzechGlobe from the Ministry of Education, Youth and Sports; project No. LO1415 within the National Programme for Sustainability; and Operational Programme Education for Competitiveness project No. CZ.1.07/2.3.00/20.0256. MS was supported by grants nos. 14-14-00904 and 14-24-00020 from the Russian Science Foundation.

References

Dragosits M, Mattanovich D (2013) Microb. Cell Fact. 12, 64.

Ducat DC, Way JC, Silver PA (2011) Trends Biotechnol. 29, 95–103.

Ikeuchi, M, Tabata S (2001) Photosynth. Res. 70, 73–83.

Inoue N, Taira Y, Emi T et al. (2001) Plant Cell Physiol. 42, 1140–1148.

Kaneko T, Sato S, Kotani H et al. (1996) DNA Res. 3,109–136.

Kanesaki Y, Shiwa Y, Tajima N et al. (2012) DNA Res. 19, 67–79.

Morris JN, Crawford TS, Jeffs A et al. (2014) New Zeal. J. Bot. 52, 36–47.

Nedbal L, Trtílek M, Červený J et al. (2008) Biotechnol. Bioeng. 100, 902–910.

Trautmann D, Voss B, Wilde A et al. (2012) DNA Res. 19, 435–448.

Zavřel T, Sinetova MA, Búzová D et al. (2015) Eng. Life Sci. 15, 122–132.

The importance of hydromorphological analysis in evaluating floodplain disturbances – an upper Stropnice River case study

Jakubínský, J.[1,*], Pelíšek, I.[2], Cudlín, P.[1]

[1]*Global Change Research Centre, Bělidla 986/4a, 60300 Brno, Czech Republic*
[2]*Research Institute of Soil and Water Conservation, Boženy Němcové 2625, 53002 Pardubice, Czech Republic*
[*]*author for correspondence; email: jakubinsky.j@czechglobe.cz*

ABSTRACT

This contribution deals with a comparative analysis of the hydromorphological state of a river network and the ecological status of a neighbouring floodplain area. The issue has gained great importance especially in addressing the causes and effects of flood events, which are an increasingly frequent manifestation of global environmental change at the local level. The area of interest was the upper part of the Stropnice River basin in Southern Bohemia with an area of about 100 km^2. The basin is characterized by wide variability of natural conditions and human activities. The main objective was to analyse how the river's morphological status affects habitat type naturalness. We endeavoured to determine the extent to which hydromorphological modifications contributed to transforming riparian natural habitats into more human-influenced habitats.

Based on the results, we can conclude that within the area of interest the direct link between rivers and their close surroundings was only minimal. A significant role in shaping this relationship was played by a large anthropogenic modification of the entire floodplain area as well as the actual riverbed, which often causes completely different results. In areas where the floodplain ecosystem displayed relatively favourable environmental values, the relevant channel reach was degraded significantly, and vice versa. These facts point to long-term effects from anthropogenic pressure, which are manifested in the mutually and not well coordinated management of the river network and land-use system within the watershed.

INTRODUCTION

Due to their ideal conditions, flat and often fertile areas along the Stropnice River network encompass a large number of human activities with direct and indirect impacts on the current state of fluvial ecosystems and even streams. This paper analyses the floodplain area in a manner which concentrates in itself four dimensions defined in the concept of Amoros & Petts (1993). Practically, these are considerations of the longitudinal, transverse, vertical (i.e. individual layers of soil horizons and bedrock sequences), and temporal dimensions of the river landscape. According to Štěrba et al. (2008), a river landscape is an area existing in absolute dependence on the river, mostly made up of alluvial deposits that represent the ecosystems created or substantially conditioned by the river. The importance of hydromorphological evaluation is accounted for in European legislation (in particular the Water Framework Directive, 2006/60/EC), where the process, together with evaluation of biological components and selected physicochemical parameters, represents a subpart of the ecological status monitoring of all surface waters. The basic research hypothesis is that the natural river network should be surrounded by nature-friendly habitats, since the individual parts of the river landscape are mutually complementary and evolve jointly. Thus, the main objective was to determine the extent to which the above relationship between the river and floodplain reflects human influences in terms of both negative and positive impacts.

MATERIALS AND METHODS

Morphological assessment of the riverbed status in the area of interest was carried out using two different methods based on similar parameters but somewhat different principles of assessment. These are the national hydroecological monitoring (HEM) method (Langhammer 2013) and a slightly older assessment methodology developed by Šindlar et al. (2008). The Šindlar approach focuses on expressing the differences between a stream's currently identified status and the natural status at the given site. It places greater emphasis on the geomorphological processes affecting the evolution of the riverbed and floodplain, using such indicators as flow and sedimentary regime, riverbed morphology, channel-forming processes, and backwater influence. In contrast, the HEM method only analyses the current status of the stream and floodplain by scoring such basic indicators as channel bottom and banks characteristics, riverbed pattern, and the properties of inundation areas and flow regime, even though it notes that the most positive identified hydromorphological stream quality corresponded to potentially natural conditions. Both methodologies evaluate the watercourse as well as the adjacent floodplain.

Data for hydromorphological analysis using these methods were obtained within a detailed field survey of selected floodplain reaches in the area of interest and also in the form of remote sensing data (especially for floodplain parameters) derived from aerial photographs and other maps. The map in Fig. 1 shows the area of interest including the location of individual segments of the floodplain studied.

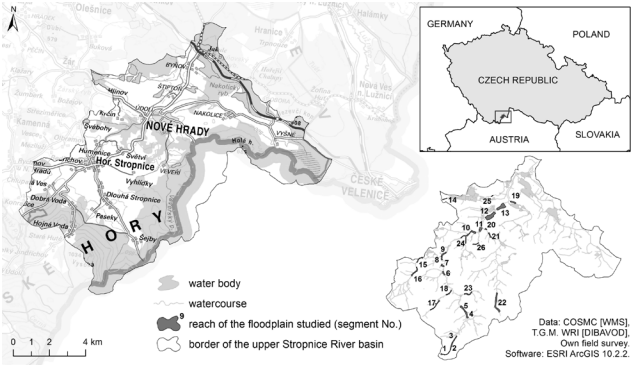

Fig. 1: *Map of study area – upper Stropnice River basin in Southern Bohemia.*

As mentioned above, the hydromorphological status of the river network was further compared with the ecological status of the surrounding floodplain, i.e. its biodiversity. Such diversity was assessed using the biotope valuation method (Seják et al. 2003), where each habitat type has been assessed using a set of characteristics, namely maturity, naturalness, structure diversity, species diversity, habitat type rarity, species rarity, habitat type vulnerability, and threat to habitat type. Based on these characteristics, values indicating their relative ecological importance in relation to other types of habitats in the country were assigned to the various types of habitats in the Czech Republic (including Natura 2000 habitats and groundwater habitats). The total value of habitats for each segment in the studied catchment was calculated as the mean of the values for each habitat in a given floodplain segment weighted by the length of the habitat's boundaries with stream banks. The exact positions of habitats' borders in the studied areas were identified by field mapping and subsequent verification using aerial photos within a GIS analysis.

RESULTS

By comparing the two data sets describing the river network's hydromorphological status and the surrounding fluvial landscape's habitat values, the nature of mutual relationships and the primary factors affecting these relationships have been identified. A key finding is that in the vast majority of reaches the stream and floodplain status do not correspond. In areas where the riverbed displayed positive hydromorphological properties, the floodplain along the river exhibited more degraded values, and vice versa (Table 1). Improved stream status was usually detected in higher-lying areas on the upper stream, in hard-to-reach locations with greatly dissected topography. In these areas, the watercourse displayed values of the first and second degree from the evaluation scale of the HEM method, corresponding to very good or good hydromorphological status within the overall ecological state as required by the Water Framework Directive.

Table 1: *Floodplain ecological status and hydromorphological status of riverbeds in the three areas of the upper Stropnice River basin with different topographic characteristics and runoff conditions.*

Relief character (topography)	**Stream** (basin) area	**Proportion of total stream length** [%]	**Landscape type**	**Floodplain ecological status**[1]	**Riverbed status**[2]
Highly dissected (mountainous area)	Upper	29.8	Forest, forest-agricultural	Degraded, significantly influenced by humans (low species diversity and their rareness)	Very good, good
Less dissected (hilly area)	Middle	33.0	Forest-agricultural, agricultural, urban	Moderate, good (influenced by humans, higher diversity)	Good, moderate, poor
Plain (lowland)	Lower	37.2	Agricultural, urban	Moderate, good, very good (influenced by humans, higher diversity, rareness and naturalness of species)	Poor, destroyed

1According to biotope valuation method (Seják et al. 2003).
2According to HEM method (Langhammer 2013) and the approach according to Šindlar et al. (2008).

Low-lying areas with more developed fertile floodplains frequently contained degraded riverbeds whose state corresponded to the past intensity of use of the surrounding landscape (the unequal current statuses of the river and floodplain points to restoration actions that have taken place in some parts of the catchment). The most common cause of degradation of the river's morphological status is its artificial straightening, unnatural incision against the surrounding terrain and mainly the banks and bottom fortifications which cause the watercourse permanently to lose contact with its surroundings. These interventions often result directly from intensive exploitation of the floodplain as a response to societal demand in the form of an increase in production services of the landscape. In HEM evaluations, this stream status corresponds to category 3, "average condition", while according to the Šindlar approach these sections are classified as "destroyed", reaching a maximum 20% of optimal conditions.

Regarding the ecological status of habitats (i.e. their biodiversity), the most common finding was Norway spruce (*Picea abies* [L.] Karst.) monocultures with low values in the upper part of the study catchment (the habitat value was less than 20% of its maximum possible value according to the biotope valuation method). Conversely, the most positively evaluated floodplain segments (meadows and wetlands close to natural

conditions) occurred in the lower part of the watershed (up to 50% of the maximum possible value), which has recently undergone restoration actions during which there were significant changes in land use.

DISCUSSION

These results suggest that impacts on the river and surrounding floodplain are highly variable and dependent on local conditions. Since the streams in the upper part of the Stropnice River catchment are not primarily perceived as landscape elements with significant potential for society (they are difficult to access without a wider floodplain), they remain at the margin of interest and consequently have a relatively good hydromorphological status. In the middle and lower part of the catchment, however, the surrounding floodplain has significant agricultural potential and the naturally meandering watercourse thus has become an inappropriate landscape element greatly reducing land-use potential. The situation is different in terms of the floodplain's ecological status, which shows anthropogenic influences along almost the entire river length. While the narrow floodplain in the rugged relief near the headwater area of the Stropnice River is degraded in terms of biodiversity by the presence of a uniform commercial forest, the wide floodplain in the catchment's lowland sections was intensively used as arable land until recently. In recent decades, the current states of the floodplain and river have nevertheless been positively affected by landscape restoration programs, which are mainly behind the current non-conforming statuses of the terrestrial and fluvial parts of the river landscape. It could be concluded that the validity of the hypothesis given in the introduction has not been confirmed inasmuch as the functioning of the relationship between the river and floodplain statuses has been improved by restoration projects conducted in the lower part of the watershed and only involving the terrestrial part of the river landscape and not the watercourse itself. Some important factors to consider are financial demands and the character of property relationships, which are very different for floodplain landscape restorations and for watercourse restorations.

Acknowledgement

Supported by the Ministry of Education, Youth and Sports within the National Programme for Sustainability I, project No. LO1415, as well as project No. CZ.1.07/2.3.00/20.0248.

References

Amoros C, Petts GE (1993) Hydrosystemes Fluviaux. Masson, Paris.

Langhammer J (2013) HEM: Hydroekologický monitoring: hodnocení ukazatelů. Charles University, Prague.

Seják J, Dejmal I, Petříček V et al. (2003) Hodnocení a oceňování biotopů České republiky. Český ekologický ústav, Prague.

Šindlar M, Zapletal J, Sucharda M (2008) Metodika monitoringu a vyhodnocení aktuálního stavu hydromorfologie vodních toků včetně návrhů opatření k dosažení dobrého ekologického stavu. Available at: http://pvvc.cz/ckfinder/userfiles/files/Hodnoceni_ hydromorfologie_Sindlar.pdf.

Štěrba O Kubíček F, Měkotová J et al. (2008) Říční krajina a její ekosystémy. Palacký University, Olomouc.

Comparison of forestry reclamation and spontaneous succession from plant diversity, production, and economic perspectives

Cudlín, O.[1,2,*], Faigl, T.[2], Plch, R.[1], Cudlín, P.[1]

[1]*Global Change Research Centre, Lipová 9, 37005 České Budějovice, Czech Republic*

[2]*Faculty of Environmental Sciences, Czech University of Life Sciences Prague, Kamýcká 129, 16521 Prague 6-Suchdol, Czech Republic*

[*]*author for correspondence; email: cudlin.o@czechglobe.cz*

ABSTRACT

The aim of our study was to determine whether the values of plant community diversity, the volume of wood, and the partial economic efficiency of plots left to spontaneous succession have yet reached similar values as those recorded on forestry reclaimed plots. Six forestry reclaimed plots and six plots with spontaneous succession were established at the Great Podkrušnohorská spoil heap and selected tree biometric characteristics were measured. Plots' economic efficiency was calculated as the difference between the costs to level the spoil heap as well as establish and manage the forest reclamation and the theoretical profit from wood. The numbers of tree species, numbers of individuals, wood volume, and Simpson diversity index values did not differ significantly between plots with spontaneous succession and reclaimed plots. The economic efficiencies of both types of plots were too burdened with high initial investments for levelling, which can theoretically be returned within 300 years for reclamation plots and 180 years for succession plots. According to our results and those of some other authors, values for diversity and wood production are similar or higher on plots resulting from spontaneous succession in comparison to values on reclaimed plots. For this reason, both types of management should be used to establish a new suitable mosaic of ecosystems in the post-mining landscape.

INTRODUCTION

Under Czech law, mining companies after mining must expend extremely high costs into restoring the natural landscape (Hendrychová 2008). However, such reclaimed ecosystems have not performed all necessary ecosystem functions for many years (Skaloš et al. 2014). Agricultural, forest, and water reclamations are used most frequently to restore destroyed landscapes. The form most widespread in the Sokolov area is forest reclamation due to its positive impacts on initial soil-forming processes (Filcheva et al. 2000). In recent years, however, another possibility for supporting biodiversity and ecosystem functioning has been emphasized: the use of spontaneous succession (Prach et al. 2011). Frouz et al. (2008) and Mudrák et al. (2010) investigated in the Sokolov area whether spontaneous succession can be successfully used to restore a destroyed area through the development of soil and vegetation. In addition, tree biomass stock on spontaneous succession plots has recorded similar amounts as was found for tree biomass on comparable forest reclamation plots (Dvorščík 2012). In contrast, Frouz et al. (2009) calculated a lower amount of carbon storage in above-ground woody biomass on succession plots than was found on reclaimed plots. The aim of our study was to determine whether the values of plant community diversity, tree volume, and the partial economic efficiency of plots left to spontaneous succession have reached similar values as those recorded on forestry reclaimed plots on the Great Podkrušnohorská spoil heap.

MATERIALS AND METHODS

We conducted our measurements on the Great Podkrušnohorská spoil heap (50°13'52''N, 12°38'29''E),

located near the town of Sokolov. At this spoil heap, 12 permanent research plots (6 forestry reclaimed plots and 6 plots with spontaneous succession) were established; 3 plots in mesophyllous habitats and 3 plots in wet habitats for both reclaimed and succession plots. On each plot of 60 × 25 m, the total number of trees was counted. Plots with different management were compared statistically either in groups of three to compare habitats or groups of six to compare only reclaimed and succession plots. Parent trees were situated approximately 1 km away from succession plots. The following parameters were measured for each species: total height, diameter at breast height (DBH), and tree age measured using a Pressler's borer. Selected parameters were measured for 20 representative individuals (at least 10 individuals in the absence of 20 trees) of each species in young (1–15), middle-aged (16–30), and old (> 30) age classes. The number of trees in each class was selected according to their percentage representation on the plot. Stem volume (hereinafter wood volume) of selected species was calculated based on stem DBH using allometric equations (Zianis et al. 2005) from the following countries: *Acer pseudoplatanus* L. and *Quercus robur* L. (DBH = 7–40 cm) from the Netherlands; *Alnus glutinosa* (L.) Geartn., *Populus tremula* L., *Prunus avium* L., *Picea abies* (L.) Karst. (DBH = 16–60 cm), *Salix caprea* L., and *Sorbus aucuparia* L. from Norway; *Betula pendula* Roth and *Pinus sylvestris* L. from Sweden; *Q. robur* (DBH = 1–7 cm) from Great Britain; *Larix decidua* Mill. from Belgium; and *Picea abies* (DBH = 2–15 cm) from Finland. The Simpson diversity index for the tree layer was computed for each plot from the formula $D = 1 - \Sigma (pi^2)$, where pi is the relative proportion of i-th species. All results were analysed using the non-parametric Kruskal–Wallis ANOVA. The test criterion, level of significance, and number of samples are shown for each tested parameter (degrees of freedom = 1). Means of the measured parameters, weighted by age class representation, were reported for each species. Plots' economic efficiency was calculated as the difference between costs to level the spoil heap as well as to establish and manage the forest reclamation and the theoretical profit from firewood. The cost of spoil heap levelling was calculated from reclamation plans and the cost of forest reclamation from the materials of Sokolovská uhelná (2008). We considered a regular clip of 0.6 × 0.6 m between saplings according to Leitgeb (2005). Wood volume was calculated using allometric equations (Zianis et al. 2005) and wood price was evaluated as the cost of firewood in the Sokolov area in 2013.

RESULTS

The species *Quercus robur* and *Acer pseudoplatanus* occurred on the mesophyllous reclaimed plots and *Betula pendula* dominated on all mesophyllous succession plots. *Alnus glutinosa* dominated on wet reclaimed plots while *Betula pendula* and *Alnus glutinosa* dominated on those wet plots with spontaneous succession. The numbers of tree species ($H = 0.03$, $p = 0.869$, $N = 12$) and individuals ($H = 0.54$, $p = 0.462$, $N = 63$), values of the Simpson diversity index ($H = 1.64$, $p = 0.200$, $N = 12$), and wood volume values ($H = 0.08$, $p = 0.783$, $N = 63$) did not differ significantly between reclaimed plots and plots with spontaneous succession (Table 1). Higher wood volume values were determined on wet plots than were found on mesophyllous plots but this different was not significant ($H = 0.36$, $p = 0.552$, $N = 63$). Higher mean values of wood volume and theoretical profit from the sale of wood were found on plots with mesophyllous spontaneous succession compared to those on mesophyllous reclaimed plots but this difference was slightly outside the range of significance ($H = 0.22$, $p = 0.641$, $N = 35$). On wet reclaimed plots, higher mean values of wood volume and theoretical profit from the sale of wood were determined compared to those on wet succession plots but this difference was not significant ($H = 0.02$, $p = 0.889$, $N = 28$). From an economic perspective, however, both types of plots on the spoil heap were burdened with high initial investments. Theoretically, the time before invested funds can be returned is 300 years on reclamation plots and 180 years on succession plots, assuming that the time required for firewood rotation is only

30 years. For this reason, economic efficiency results were negative (Table 2). Costs for forest reclamation were more than twice as much as were costs for holding the area to spontaneous succession.

Table 1: *Summary of measured data (mean ± standard deviation) from studied plots; mean values were weighted by distributing trees into three age classes.*

Plots	DS	SS	Height	Diameter	Age	WV	N_{ind}	N_{sp}	D
			m	*cm*	*years*	$m^3\ ha^{-1}$	*per ha*	*per ha*	
Rm1	AP	QR	7.0 ± 1.42	16.1 ± 3.73	16.8 ± 4.39	35.9	847	5	0.40
Rm2	QR	AP	5.0 ± 1.46	9.1 ±3.05	21.0 ± 2.29	68.0	1,213	7	0.45
Rm3	QR	BP, PS	4.9 ± 1.42	9.0 ±2.93	23.6 ± 2.28	34.0	1,047	8	0.55
Sm1	BP,PS	PA	9.0 ± 0.73	25.5 ± 1.33	25.5 ± 1.33	86.4	220	5	0.72
Sm2	BP,SC		6.6 ± 1.65	14.3 ± 3.41	26.1 ± 5.00	42.4	713	6	0.46
Sm3	BP		5.8 ± 0.83	9.6 ± 2.55	22.9 ± 2.98	25.4	1,280	5	0.11
Rw4	AG		4.8 ± 1.56	7.7 ± 1.56	17.4 ± 2.43	147.8	1,007	3	0.08
Rw5	AG		5.4 ± 1.30	10.8 ± 3.73	25.5 ± 2.15	132.8	840	3	0.05
Rw6	AG	BP	6.6 ± 1.70	8.6 ± 2.42	19.7 ± 3.75	146.4	1,300	7	0.58
Sw4	AG	BP	6.9 ± 2.50	11.1 ± 4.58	19.7 ± 3.82	219.8	1,107	3	0.17
Sw5	BP	PT, SC	5.9 ± 2.03	12.0 ± 4.45	24.8 ± 3.65	40.0	700	7	0.68
Sw6	BP	PT	6.5 ± 1.94	11.6 ± 4.42	24.8 ± 4.94	44.2	387	7	0.58

Abbreviation of plots: R: reclaimed, S: succession, m: mesophyllous, w: wet; DS: dominant species with at least 25% of occurrence on the plot; SS: subdominant species with at least 10% of occurrence on the plot; WV: wood volume; N_{ind}: number of individuals on the plot; N_{sp}: number of species on the plot; D: Simpson diversity index. Abbreviation of dominant and subdominant plants: AG: Alnus glutinosa, AP: Acer pseudoplatanus, BP: Betula pendula, PA: Picea abies, PS: Pinus sylvestris, PT: Populus tremula, QR: Quercus robur, SC: Salix caprea.

Table 2: *Mean economic efficiency results from reclaimed and spontaneous plots with mesophyllous and wet site conditions.*

Plots	N	Costs		Benefits		Costs – Benefits
		heap lev.	forest rec.	WV	WV	EUR
		EUR	*EUR*	$m^3\ ha^{-1}$	*EUR* ha^{-1}	
R-mesophyllous	3	16,643	18,564	46.3	1,734	–33,473
S-mesophyllous	3	16,643	0	51.4	1,927	–14,715
R-wet	3	16,643	18,564	144.8	5,428	–29,779
S-wet	3	16,643	0	101.3	3,797	–12,845
R-all	6	16,643	18,564	95.5	3,581	–31,626
S-all	6	16,643	0	76.4	2,862	–13,780

Heap lev.: levelling of substrate and treatment of spoil heap, forest rec.: forest reclamation, WV: wood volume.

DISCUSSION

The main reasons for higher wood volume values on the wet plots were probably different site conditions, tree species compositions, and tree ages. This corresponds with the results of Frouz et al. (2009), who ascertained higher

biomass on plots with *Alnus glutinosa* compared to plots with *Quercus robur*. The species *Quercus robur* and *Acer pseudoplatanus* dominated on mesophyllous reclaimed plots, but they grew more slowly than did *Alnus glutionsa* on wet reclaimed plots. Due to its nitrogen fixation ability, *Alnus glutinosa* was able quickly to accumulate C and N in the soil profile within 15 years of reclamation (Mudrák et al. 2010), but this ability decreased in 25-year-old and older reclaimed sites (Šourková et al. 2005). Irregular distances between trees and a higher range of tree ages on our mesophyllous plots with spontaneous succession might have resulted in rapid tree growth and caused the slightly higher wood volume compared to mesophyllous reclaimed plots. The slightly higher number of trees and different tree species composition on wet reclaimed plots probably led to the not significantly higher wood volume compared to that found on mesophyllous reclaimed plots. Values for number of tree species and wood volume were similar on mesophyllous and wet succession plots because *Betula pendula* occurred on all succession plots due to the wide range of environmental conditions (Prach & Pyšek 2001). Reclaimed and spontaneous succession plots displayed similar wood volume values. In addition, Dvorščík (2012) observed similar values for woody biomass of *Alnus glutinosa* stands on reclaimed plots and for biomass of *Salix caprea* stands on spontaneous succession plots. We encountered problems in some cases in precisely distinguishing planted trees on spontaneous succession plots and leaving pioneer trees without thinning on reclaimed plots.

Based on our results and the opinions of some other authors, it is advisable to increase diversity and wood production using spontaneous succession to restore disturbed landscapes (Prach & Pyšek 2001, Mudrák et al. 2010). Because we did not observe statistically significant differences in total height, breast height diameter, or tree age between reclaimed and succession plots, we propose, together with Prach & Pyšek (2001), that spontaneous succession should be used as an inexpensive alternative to forestry reclamation. However, both types of management, supposed as "controlled revegetation", should be used to create a suitable mosaic of ecosystems in the emerging landscape.

Acknowledgement

Supported by project No. LO1415 from the Ministry of Education, Youth and Sports within the National Programme for Sustainability I as well as project No. CZ.1.07/2.3.00/20 "Indicators of trees vitality".

References

Dvorščík P (2012) Plant biomass of reclaimed and unreclaimed heaps of various age. Master's Thesis, Charles University in Prague.

Filcheva E, Noustorova M, Gentcheva-Kostadinova S et al. (2000) Ecol. Eng. 15, 1–15.

Frouz J, Pižl V, Cienciala E et al. (2009) Biogeochem. 94, 111–121.

Frouz J, Prach K, Pižl V et al. (2008) Eur. J. Soil Biol. 44, 109–121.

Hendrychová M (2008) J. Landsc. Stud. 1, 63–78.

Leitgeb J (2005): Reclamation Plans. Sokolovská uhelná, Karlovy Vary.

Mudrák O, Frouz J, Velichová V (2010) Ecol. Eng. 36, 783–790.

Prach K, Pyšek P (2001) Ecol. Eng. 17, 55–62.

Prach K, Řehounková K, Řehounek J et al. (2011) Landsc. Res. 36, 263–268.

Skaloš J, Berchová K, Pokorný J et al. (2014) Ecol. Indic. 36, 80–93.

Sokolovská uhelná (2010) Performance Report for the Year 2010. Sokolovská uhelná, Sokolov.

Šourková M, Frouz J, Šantrůčková H (2004) Geoderma 124, 203–214.

Zianis D, Muukkonen P, Mäkipää R et al. (2005) Silva Fennica Monographs 4.

Forestry operations focusing on different types of felling related to carbon and economic efficiencies

Plch, R.[1,*], Pecháček, O.[2], Vala, V.[2], Pokorný, R.[1,2], Cudlín, P.[1]

[1]*Global Change Research Centre, Bělidla 986/4a, 603 00 Brno, Czech Republic*

[2]*Mendel University in Brno, Zemědělská 3, 613 00 Brno, Czech Republic*

[*]*author for correspondence; email: plch.r@czechglobe.cz*

ABSTRACT

Assessments of carbon and economic efficiencies, completed by an environmental load computation using the Life Cycle Assessment (LCA) method, could be a useful tool for assessing sustainable forest management (e.g. Berg & Lindholm 2005, Michelsen et al. 2008). The purpose of this study was to compare forestry operations focused on manually operated (chainsaw) and fully mechanized (harvester) felling in Norway spruce monocultures and mixed forests within the Novohradské Mts. (Czech Republic) using the methods of carbon efficiency (including LCA) and economic efficiency. In general terms, these methods consist of comparing quantified human inputs (e.g. fossil fuels, electricity, used machinery, and fertilizers, converted into emission units of carbon in t C in CO_2 equivalent or EUR) with quantified ecosystem outputs (biomass production in t C or EUR). Forest operations were modelled for one rotation period. The results showed the main differences in carbon emissions and carbon efficiency related to forest operations with different types of felling. In contrast, the economic efficiency results did not differ much with different types of felling. Differences between Norway spruce monocultures and mixed forests using the same type of felling were relatively small for carbon efficiency but large for economic efficiency (Norway spruce monocultures recorded higher economic efficiency).

INTRODUCTION

In 2012, the total area of forest in the Czech Republic was almost 2.7 million ha (33.8% of total land area) (Czech Statistical Office 2013). Total forest land area is 73.2% covered by coniferous forests (51.4% of forest land area by Norway spruce), 25.6% by broadleaf forests, and 1.2% by unstocked area, compared to the natural composition of forest land area consisting of 34.7% coniferous forests and 65.3% broadleaf forests (Ministry of Agriculture 2012). Norway spruce stands at medium and lower altitudes in the Czech Republic could become more fragile as a result of climate change (Jandl et al. 2007). In the Czech Republic, the proportion of total felling of timber products conducted by harvester increased from 9% in 2002 to 35% in 2011 (Ministry of Agriculture 2011).

The purpose of this study was to compare forestry operations focused on manually operated (chainsaw) and fully mechanized (harvester) felling in Norway spruce monocultures and mixed forests within the Novohradské Mts. by studying carbon efficiency (including Life Cycle Assessment, LCA) and economic efficiency.

MATERIALS AND METHODS

The research area, the upper part of the Stropnice River watershed, is situated in the Novohradské Mts. (Czech Republic). The total research area covers approximately 99 km^2 and the total forest area approximately 49 km^2. With similar forest stands based on similar soil conditions and elevations (Forest Stand

Management Type No. 55 – "high and fertile forest stands"), forest operations with chainsaw and harvester felling in forest stands with different tree species compositions were compared: i) Alternative 1 – Norway spruce monocultures (100% spruce), ii) Alternative 2 – an existing mixed composition of primary tree species (75% spruce, 8% pine, 8% fir, 9% beech), and iii) Alternative 3 – a mixed composition of primary tree species corresponding to potential vegetation under expected climate conditions (spruce 40%, fir 20%, beech 40%) (Cienciala et al. 2011). Forest operations were modelled for one rotation period and were divided into the following stages: seedling production, silviculture, final felling, and timber transport. The average yield class of the tree species was recorded based on forest data from a forest management plan with a "bottom-up approach" (1 for fir, 2 for Norway spruce, and 3 for pine and beech). In general, yield class for tree species is indicated in an interval from 1 (the best) to 9 (the worst). In our study, abiotic and biotic disturbances were not included in the calculation of carbon and economic efficiencies due to not having available all data required.

As applied to forest stands, the carbon and economic efficiency methods consist of comparing quantified human inputs (human activity, fossil fuels, electricity, used machinery, fertilizers, pesticides) with quantified ecosystem outputs (wood production). To compare sustainable management, key indicators of carbon and economic efficiencies (ratio outputs in t C produced t^{-1} emitted C in CO_2 equivalent [CO_2e]; economic benefit/economic costs in %) were used. To quantify C emissions, the LCA method was used within SimaPro software (PRé Consultants, the Netherlands). The functional unit to which all data collected were related was 1 m^3 of harvested timber. The average distance for timber transport was considered to be 70 km (standard for the Czech Republic).

RESULTS

Carbon efficiencies (ecosystem outputs − human inputs in t C) were positive for all tree species alternatives. The highest carbon efficiency was recorded for mixed forests (338–385 t C ha^{-1} with chainsaw felling and 333–381 t C ha^{-1} with harvester felling), whereas the lowest carbon efficiency was recorded in Norway spruce monocultures (332 t C ha^{-1} with chainsaw felling and 328 t C ha^{-1} with harvester felling).

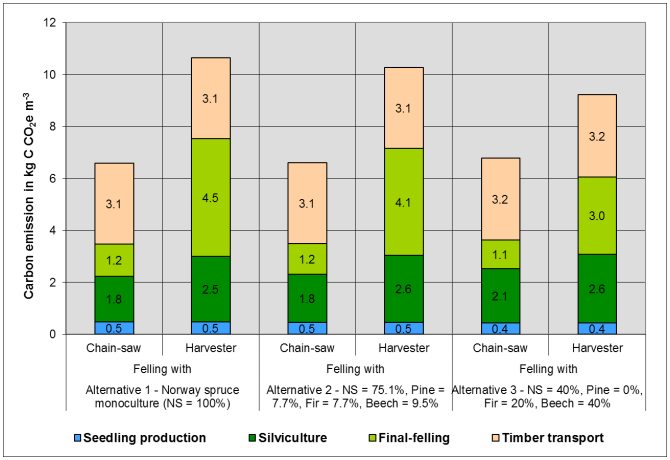

Fig. 1: *Carbon emissions of forest operations with different types of felling in Norway spruce (NS) monocultures and mixed forests.*

Carbon emissions per 1 m^3 from timber harvesting were lower for all tree species alternatives using chainsaw felling than they were for those using harvester felling. Differences between Norway spruce monocultures and mixed forests using the same type of felling were very small. Of the total carbon emissions, silviculture (27–31%) and timber transport (47%) accounted for the most carbon emissions for all tree species alternatives using chainsaw felling, while final felling (32–43%) and timber transport (29–34%) were highest for harvester felling (Fig. 1).

Combining two different indicators (carbon and economic efficiencies) is necessary to obtain a more comprehensive comparison (Fig. 2). With similar forest stands based on similar soil conditions and elevations (Forest Stand Management Type No. 55), the main differences in carbon efficiency related to forest operations with different types of felling. For all tree species alternatives, higher carbon efficiency (45.6–47.3 t C wood production t^{-1} C CO_2e.) was identified in forest operations with chainsaw felling, while lower efficiency was found with harvester felling (28.2–34.8 t C wood production t^{-1} C CO_2e). In contrast, the economic efficiency results did not differ much with different types of felling.

For both types of felling, the lowest carbon efficiencies were achieved in Norway spruce monocultures (45.6 t C wood production t^{-1} C CO_2e for chainsaw felling and 28.2 t C wood production t^{-1} C CO_2e for harvester felling), whereas mixed forest alternatives had higher carbon efficiencies (46.0–47.3 t C wood production t^{-1} C CO_2e and 29.6–34.8 t C wood production t^{-1} C CO_2e). In contrast to economic efficiency, large differences between Norway spruce monocultures and mixed forests using the same type of felling were accounted. Higher economic efficiency was achieved in Norway spruce monocultures (167% and 170%) and lower in mixed forests (78–130%).

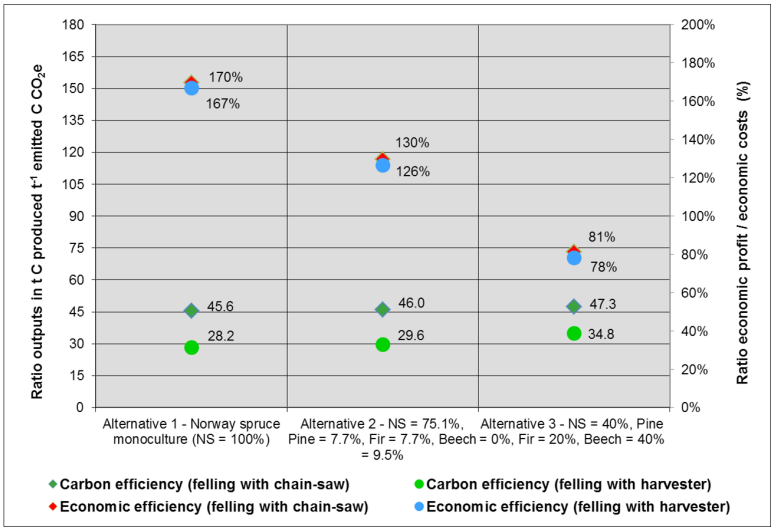

Fig. 2: *Comparison of carbon and economic efficiencies of forest operations with different types of felling and forest stands with Norway spruce (NS) monoculture and mixed forests .*

DISCUSSION

Our results show that total emission of carbon from forest operations for Norway spruce monocultures and mixed forests stands varies between 6.6 and 6.8 kg C CO_2e m^{-3} timber for chainsaw felling and between 9.2

and 10.7 kg C CO_2e m^{-3} timber for harvester felling. Berg & Lindholm (2005) reported higher carbon emissions in Sweden (from 12.5 to 17.1 kg C CO_2e m^{-3} timber) and Michelsen et al. (2008) published higher carbon emissions in Norway (25 kg C CO_2e m^{-3}). In these studies, the largest carbon emissions were caused by timber transport and logging, which is in accordance with our results. Our study identified lower carbon emissions from final chainsaw felling (1.1–1.2 kg C CO_2e m^{-3}) and higher carbon emission from final harvester felling (3.0–4.5 kg C CO_2e m^{-3}). These differences between different types of felling have been confirmed by such authors as Schwaiger & Zimmer (2001).

In general, coniferous forests comprise the most widespread forest area in the Czech Republic (73.2% of total forest area, while 51.4% of total forest area is formed of Norway spruce). The natural composition of forests consists of 34.7% coniferous forest and 65.3% broadleaf forest (Ministry of Agriculture 2012). Forests in Central Europe are particularly sensitive to climate change. The most important effects of climate change will probably be mediated through changes in disturbances (storms, insects, pathogens). Moreover, longer and warmer vegetation periods will especially enhance the development of bark beetles (Lindner et al. 2010). Jandl et al. (2007) concluded that mixtures of beech and Norway spruce are a better forest management option than pure Norway spruce stands. Species occupying different ecological niches can complement each other. For a forest's productivity over its entire rotation period, stability against disturbances is important. In contrast, our results showed that changing tree species composition from Norway spruce monocultures to mixed forests could have a negative impact on economic efficiency. In our case, Norway spruce monocultures showed higher economic efficiency than was found in mixed forests stands, while mixed forests had higher carbon efficiency than did Norway spruce monoculture stands.

Acknowledgement

Supported by the Ministry of Education, Youth and Sports through project No. LO1415 within the National Programme for Sustainability Program I and project No. CZ.1.07/2.3.00/20.0248 within the Operational Programme Education for Competitiveness as well as the Ministry of the Interior through project No. VG20122015091.

References

Berg S, Lindholm EL (2005) J. Clean. Prod. 13, 33–42.

Cienciala E, Apltauer J, Exnerova Z et al. (2011) Les, uhlík a lesnictví ČR v podmínkách měnícího se prostředí. Uhlík v ekosystémech České republiky v měnícím se klimatu (eds MV Marek, A Ač, J Apltauer et al.), pp. 129–177. Academia, Prague.

Czech Statistical Office (2013) Statistical Yearbook of the Czech Republic – 2013. Czech Statistical Office, Prague.

Jandl R, Lindner M, Vesterdal L et al. (2007) Geoderma 137, 253–268.

Lindner M, Maroschek M, Netherer S et al. (2010) For. Ecol. Manag. 259, 698–709.

Michelsen O, Solli C, Strømman AH (2008) J. Ind. Ecol. 12, 69–81.

Ministry of Agriculture (2011) Information on Forests and Forestry in the Czech Republic by 2010. Ministry of Agriculture of the Czech Republic, Prague.

Ministry of Agriculture (2012). Information on Forests and Forestry in the Czech Republic by 2011. Ministry of Agriculture of the Czech Republic, Prague.

Schwaiger H, Zimmer B (2001) A comparison of fuel consumption and greenhouse gas emissions from forest operations in Europe. Energy, Carbon and Other Material Flows in the Life Cycle Assessment of Forestry and Forest Products: Achievements of the Working Group 1 of the COST Action E9 (eds T Karjalainen, B Zimmer, S Berg et al.), 33–52. European Forest Institute, Joensuu, Finland.

The influence of land cover changes and landscape fragmentation on provision of the carbon sequestration ecosystem service

Pechanec, V.[1,*], Purkyt, J.[2,3], Cudlín, P.[2]

[1]*Palacký University in Olomouc, Křížkovského 8, 771 47 Olomouc, Czech Republic*
[2]*Global Change Research Centre, Bělidla 986/4a, 603 00 Brno, Czech Republic*
[3]*University of South Bohemia in České Budějovice, Branišovská 1645, 370 05 České Budějovice, Czech Republic*
[*]*author for correspondence; email: vilem.pechanec@upol.cz*

ABSTRACT

The aim of our contribution is to analyse the influence of land cover changes and landscape fragmentation in two small catchments (Všeminka, Fryštácký potok) within the forest–agricultural landscape of eastern Moravia (Czech Republic) on the carbon sequestration ecosystem service. Fragmentation was analysed using landscape-ecological indices within ArcGIS 10.x software using the Patch Analyst extension. Data about the carbon sequestration ecosystem service were processed in the InVEST model. In the Všeminka catchment, carbon sequestration increased over the entire period of observation of 1953–2012. In the Fryštácký potok catchment, carbon sequestration decreased from 1950 to 2005, but increased from 2005 to 2012. The changes in fragmentation were not significant between 1953 and 2012, and so changes in carbon sequestration were caused mostly by land cover changes. The relationships among land cover change, fragmentation, and carbon sequestration from 1953 to 2012 are discussed.

INTRODUCTION

Ecosystem services (ES) are the benefits humans receive from ecosystems either directly or indirectly. Over the past 50 years, rapid and extensive environmental changes in land cover (LC), climate, and the atmosphere have resulted in substantial losses or degradation of ES, while demand for them has increased (Millennium Ecosystem Assessment 2005). One of the most important ES endangered by human activities is carbon sequestration.

Landscape fragmentation is a process by which biotopes become smaller, more numerous, and more isolated from each other. When fragmentation level decreases the territories of key species substantially below the subsistence area, biodiversity decline can be apparent because it disrupts the entire food web (Porensky & Young 2013).

In addition, many organisms may be endangered by the construction of new transport infrastructure and massive increases in traffic. Changes in the landscape matrix are most apparent within the road-effect zone, which ranges about 20–300 m from roads and sometimes up to several hundred metres (Saunders et al. 2002). Roads have also altered the following physical characteristics of the environment: soil density, temperature, soil water content, light, dust, surface water flow, runoff pattern, and sedimentation (Trombulak & Frissell 2000). Photosynthesis, respiration, and transpiration may be affected by air pollution, especially by dust (Farmer 1993). This may all result in reduced ecosystem function and related ES provision (Frank et al. 2012).

The aim of our contribution is to analyse the influence of LC changes and landscape fragmentation in two small catchments (Všeminka, Fryštácký potok) within the forest–agricultural landscape of East Moravia (Czech Republic) on the carbon sequestration ES. We suppose that not only LC change can decrease provision of the carbon sequestration ES, but also fragmentation of close-to-natural and cultural landscapes.

MATERIALS AND METHODS

LC categories and a set of indices describing structure changes and landscape fragmentation rate were analysed from aerial photographs from 1953, 2005 and 2012 at the scale of 1:10,000. Our LC categories were transformed into CORINE LC categories so as to improve the results' comparability. In addition, LC was verified from aerial photographs (in 2005 and in 2012 based on field research). We used ArcGIS 10.x software with the Patch Analyst extension to calculate: i) edge length and density, ii) patch size changes, iii) patch area to perimeter ratio, and iv) changes in fractal dimension (McGarigal et al. 2002). Based on records from the national traffic census in 2010, transportation intensity and the ratio of road width to the width of the disturbed habitat zone were taken into account (Müller & Berthould 1997). The effect of changes in LC, fragmentation, and disturbed habitat zone area on carbon sequestration for each period was determined. For this purpose, the InVEST model was adapted and sequestration indices and transient zone estimations were assigned in a vector space based on the road-effect zone (Biglin & Dupigny-Giroux 2006). Changes in carbon storage were calculated from four carbon stocks, namely carbon storage in: i) above-ground biomass, ii) below-ground biomass, iii) soil, and iv) dead organic matter.

RESULTS

In the Všeminka catchment, the LC categories pastures and discontinuous urban fabric increased distinctly at the expense of non-irrigated arable land, with the latter category increasing also at the expense of pastures over the entire studied period of 1953 to 2012. In the second studied catchment of Fryštácký potok, pastures and discontinuous urban fabric also increased distinctly but almost exclusively at the expense of non-irrigated arable land (Table 1).

In terms of ecological stability, three coefficients were evaluated for landscape fragmentation and patch shape and one coefficient for landscape quality. According to the indices MPAR (mean perimeter area ratio), ED (edge density), and number of patches per hectare, the fragmentation of all LC categories increased in the Všeminka catchment from 1953 to 2005. During the second period of 2005–2012, the fragmentation of the categories forests and discontinuous urban fabric continued to increase, but in contrast fragmentation of transitional woodland shrub decreased. In the Fryštácký potok catchment, according to the aforementioned indices the fragmentation of all categories except for non-irrigated arable land increased in the first period of 1953 to 2005. The fragmentation of forests, discontinuous urban fabric, and transitional woodland shrub decreased from 2005 to 2012 (Table 2).

Shannon's evenness index, indicating the evenness of LC polygons in the landscape, decreased from 1953 to 2012. In the Fryštácký potok catchment, Shannon's evenness index remained unchanged.

Total carbon storage in the Všeminka catchment increased by 275.65 Mg km^{-2} from 1953 to 2005 and by 289.82 Mg km^{-2} from 2005 to 2012. In the Fryštácký potok catchment, carbon storage decreased by 67.94 Mg km^{-2} from 1953 to 2005 but in contrast increased by 22.52 Mg km^{-2} from 2005 to 2012. The biggest changes in carbon storage in the Všeminka watershed were recorded in the categories non-irrigated arable land and discontinuous urban fabric. In the Fryštácký potok watershed, the biggest changes were found in the categories transitional woodland shrub and discontinuous urban fabric (Table 1).

Landscape fragmentation due to the establishment of new roads and resulting vehicle traffic was influenced in following way. Carbon storage decreased in the Všeminka watershed due to the road-effect zone by 1.88 Mg km^{-2} from 1953 to 2005 and by a further 2.44 Mg km^{-2} from 2005 to 2012. Carbon storage in the Fryštácký potok watershed was less affected, increasing by 1.13 Mg km^{-2} from 1953 to 2005 and by 1.58 Mg km^{-2} from 2005 to 2012.

Table 1: *Changes in land cover category representation and in carbon storage in the Všeminka and Fryštácký potok watersheds.*

	Land cover change			Carbon storage					
	1953–2005	2005–2012	1953–2012	1953	2005	1953–2005	2012	2005–2012	1953–2012
Všeminka	%	%	%	Mg km^{-2}	Mg km^{-2}	%	Mg km^{-2}	%	%
311 Broad-leaved forest, 312 Coniferous forest, 313 Mixed forest	107.37	103.55	111.18	24,500.00	24,498.28	–0.01	24,497.61	0.00	–0.01
324 Transitional woodland shrub	87.03	89.51	77.90	14,300.00	14,288.79	–0.08	14,285.66	–0.02	–0.10
231 Pastures	119.58	130.02	155.47	10,100.00	10,099.27	–0.01	10,099.23	0.00	–0.01
211 Non-irrigated arable land	48.46	23.78	11.52	8,450.00	8,449.69	0.00	8,449.34	0.00	–0.01
112 Discontinuous urban fabric	291.29	132.11	384.84	11.00	11.00	0.00	11.00	0.00	0.00
Total area of all LC categories in the watershed	100.01	100.00	100.01	356,852.55	362,791.27	1.66	369,035.12	1.72	3.41
Fryštácký potok									
311 Broad-leaved forest, 312 Coniferous forest, 313 Mixed forest	101.80	100.70	102.51	24,500.00	24,498.31	–0.01	24,497.44	0.00	–0.01
324 Transitional woodland shrub	61.27	97.61	59.80	14,300.00	14,293.83	–0.04	14,292.75	–0.01	–0.05
231 Pastures	113.18	95.79	108.42	10,100.00	10,099.37	–0.01	10,099.16	0.00	–0.01
211 Non-irrigated arable land	88.36	99.47	87.89	8,450.00	8,449.71	0.00	8,449.68	0.00	0.00
112 Discontinuous urban fabric	151.49	106.12	160.76	11.00	11.00	0.00	11.00	0.00	0.00
Total area of all LC categories in the watershed	100.00	100.00	100.00	687,629.82	684,629.03	–0.44	685,623.69	0.15	–0.29

Mg km^{-2}: megagram of carbon per km^2; land cover change: 1953–2005 (100% in 1953); 2005–2012 (100% in 2005); 1953–2012 (100% in 1953)

Table 2: *Landscape diversity indices in the Všeminka and Fryštácký potok watersheds in periods 1953, 2005, 2012.*

	1953			2005			2012		
Všeminka	NP	ED	MPAR	NP	ED	MPAR	NP	ED	MPAR
311 Broad-leaved forest, 312 Coniferous forest, 313 Mixed forest	1.38	33.61	164.91	2.95	46.44	446.68	5.96	57.64	620.80
324 Transitional woodland shrub	14.20	16.69	290.78	136.24	45.43	1,323.48	142.18	39.63	1,334.95
231 Pastures	8.38	33.38	231.49	26.73	74.71	774.08	23.93	86.05	731.89
211 Non-irrigated arable land	4.65	25.07	182.15	26.03	23.17	819.78	82.58	9.96	876.70
112 Discontinuous urban fabric	39.62	8.72	870.04	77.07	21.09	1,435.86	149.84	29.80	1,419.43
Total area of all LC categories in the watershed	15.09	148.78	2,277.46	39.34	279.51	1,021.65	44.37	291.74	1,548.79
Fryštácký potok									
311 Broad-leaved forest, 312 Coniferous forest, 313 Mixed forest	0.96	15.59	441.45	1.14	18.21	477.56	1.08	18.39	473.17
324 Transitional woodland shrub	30.08	12.22	616.09	106.36	12.96	1,105.54	93.60	11.92	1,143.68
231 Pastures	11.39	11.76	354.62	37.44	19.02	707.67	38.24	18.38	2,014.82
211 Non-irrigated arable land	1.22	30.39	3,166.95	1.69	25.75	557.62	1.58	25.36	544.26
112 Discontinuous urban fabric	18.02	8.54	621.52	31.03	16.71	1,012.13	28.27	17.27	958.51
Total area of all LC categories in the watershed	32.31	104.11	41,655.95	40.96	137.05	28,926.03	41.43	135.50	39,222.84

NP: number of patches per km^2; ED: edge density; MPAR: mean perimeter area ratio

DISCUSSION

One of the most important problems of our recent landscape is LC changing towards less natural habitats, connected with landscape fragmentation (Hofman et al. 2012). In our contribution, we wanted to estimate the role of fragmentation in providing the important ES of carbon sequestration on a landscape scale in two small watersheds (Všeminka, Fryštácký potok) distinguished in agricultural management intensity. The Všeminka watershed is a less-favoured area while the Fryštácký potok watershed is not. This could be one reason for the greater LC changes, including landscape fragmentation, in the Všeminka watershed compared to the more conservative agricultural watershed of Fryštácký potok. Perhaps as a consequence, a higher negative influence on carbon sequestration from the road-effect zone was detected in the Všeminka watershed.

In small watersheds, roads are a major factor in landscape fragmentation. They have unique impacts on the surrounding landscape matrix thanks to their persistence through time (Baker & Dillon 2000). From an historical point of view, the relatively high fragmentation of the cultural landscape in the Czech Republic decreased after 1948 due to fields being consolidated. Since 1990, the fragmentation of all types of LC has been gradually increasing.

In conclusion, it must be admitted we did not confirm our hypothesis that fragmentation can significantly contribute to LC changes in decreasing of carbon sequestration in small watersheds. This result will lead us to test this hypothesis in a broader area with more variable LC categories.

Acknowledgement

Supported by the Ministry of Education, Youth and Sports through project No. LO1415 within the National Programme for Sustainability Program I and project No. CZ.1.07/2.3.00/20.0248 within the Operational Programme Education for Competitiveness as well as the Ministry of the Interior through project No. VG20122015091.

References

Baker WL, Dillon GK (2000) Plant and vegetation responses to edges in the southern Rocky Mountains. Forest Fragmentation in the Southern Rocky Mountains (eds RL Knight, FW Smith, SW Buskirk et al.), pp. 221–245. University Press of Colorado, Boulder.

Biglin K, Dupigny-Giroux LA (2006) J. Conserv. Plan. 2, 1–16.

Braun S, Flueckiger W (1987) Does exhaust from motorway tunnels affect the surrounding vegetation? Air Pollution and Ecosystems (eds P Mathy & D Reidel), pp. 665–670. D. Reidel Publishing Company, Dordrecht.

Farmer AM (1993) Environ. Pollut. 79, 63–75.

Frank S, Fürst C, Koschke L et al. (2012) Ecol. Indic. 21, 30–38.

Hofman J, Trávníčková E, Anděl P (2012) Plant Soil Environ. 58, 282–288.

Müller S, Berthoud G (1997) Fauna/Traffic Safety: Manual for Civil Engineers. École Polytechnique Fédérale de Lausanne (LAVOC), Lausanne.

McGarigal K, Cushman SA, Neel MC et al. (2002) FRAGSTATS v3: Spatial Pattern Analysis Program for Categorical Maps. University of Massachusetts, Amherst. Available from: http://www.umass.edu/landeco/research/fragstats/fragstats.html.

Millennium Ecosystem Assessment (2005) Ecosystems and Human Well-being: Synthesis. Island Press, Washington, DC.

Porensky LM, Young TP (2013) Conserv. Biol. 27, 509–519.

Saunders SC, Mislivets MR, Chen J et al. (2002) Biol. Conserv. 103, 209–225.

Trombulak SC, Frissell CA (2000) Conserv. Biol. 14, 18–30.

Estimating values of urban ecosystem services in Kladno

Frélichová, J.[1,*], Pártl, A.[1], Harmáčková, Z.[1], Vačkář, D.[1]

[1]*Global Change Research Centre, Bělidla 986/4a, 60300 Brno, Czech Republic*
[*]*author for correspondence; email: frelichova.j@czechglobe.cz*

ABSTRACT

The benefits provided by urban nature have a substantial capacity to enhance human well-being. We quantify these benefits in the city of Kladno through the concept of ecosystem services by combining a value transfer method with surveys on citizen satisfaction and ecosystem services recognition. The results provide biophysical values of carbon sequestration and run-off and reveal stronger perception of benefits and higher preferences among citizens of Kladno for recreational services. Therefore, recreation is more suitable as a flagship service to encourage public participation than are such expert indicators as tonnes of carbon sequestered and increased run-off.

INTRODUCTION

The benefits provided by public blue and green spaces in cities are recognized as having a substantial capacity to enhance human well-being (e.g. Bolund & Hunhammar 1999). On the other hand, their role is rarely fully recognized and pressures on green resources continue to increase (Millennium Ecosystem Assessment 2005, European Environment Agency 2013). This trend might be moderated or reversed by quantifying the benefits which make the value of natural spaces in cities distinct. Our study aims to introduce an example of indicators applicable to such quantification. The results of the assessment were combined with results from surveys on citizen's perceptions of the benefits provided by urban nature and satisfaction with their quality of life. This enabled us to reflect on the hypothesis that comprehension of ecosystem services (ESs) differs between experts and the public.

MATERIALS AND METHODS

For the purpose of this paper, we present Kladno as a case study. Kladno is located in the Central Bohemian Region, covers about 37 km^2, and has a population of about 70,000 inhabitants. The city is situated at altitudes from 190 to 500 m a.s.l. The region is located within two climatic regions: moderately warm (unit MT11) and warm (unit T2) (Quitt 1971).

Mapping urban nature and ES assessment

To map urban green areas, the current Spatial Plan of Kladno (from 2012) was used. To estimate ES values, the value transfer method was applied (for more details see e.g. Liu et al. 2010, Frélichová et al. 2014). The present study focused on two particular regulating services: climate regulation indicated by tonnes of carbon sequestered (tC ha^{-1}yr^{-1}) and water cycle regulation in terms of run-off level (mm^{-1}yr^{-1}). We selected these two services as flagship ESs due to their ability to refer to heat waves and floods, key environmental issues in urban ecosystems related to climate change. Mean carbon sequestration values were calculated based on transferred values from relevant studies (e.g. Davies et al. 2011, Strohbach & Haase 2012). To estimate approximate run-off rate in Kladno, we applied altered values from Haase (2009). In particular, values were customized to regional conditions through recalculation based on long-term mean precipitation (for 1961–1990) provided by the Czech Hydrometeorological Institute (www.chmi.cz).

Survey

Benefit recognition by inhabitants was tested by interviewer-administrated questionnaires in July–August 2014. The dataset provided a representative sample of adults in the city (according to such basic population

characteristics as age and sex). The survey was designed to determine citizens' satisfaction with the local community (one of the European Common Indicators) as well as their perceptions of the benefits provided by urban nature. A total of 501 questionnaires were completed. Additional information originated from a survey on people's attitudes towards urban agriculture. Urban agriculture includes agricultural activities producing food and material within and around cities. It can provide an important contribution to sustainable, resilient urban development and multifunctional urban landscapes. As a specific type of green infrastructure in the city, it provides diverse ecosystem services (COST Action Urban Agriculture Europe, http://www.urbanagricultureeurope.la.rwth-aachen.de/). A total of 101 self-administrated online questionnaires (a representative sample of adults in the city) were completed in October 2014.

RESULTS

Climate regulation

Climate regulation services can help to reduce urban heat-island effects, mitigate climate change to some extent, and decrease air pollution (Larondelle & Haase 2013). Carbon sequestration based on land use was calculated and mapped (Fig. 1). It ranged between 0 and 30 tC ha^{-1} yr^{-1} with mean carbon sequestration across the city of 11.5 tC ha^{-1} yr^{-1} This level of carbon sequestration is comparable with mean carbon sequestration in such cites as Leipzig, Germany (12 tC ha^{-1} yr^{-1}) and Chicago, USA (14 tC ha^{-1} yr^{-1}) (Larondelle & Haase 2013). The heterogeneity of urban carbon storage is given by the different capacities of various land use categories to store carbon. In addition, carbon sequestration in Kladno displayed spatial differentiation along an urban-rural gradient, increasing with decreasing urbanization levels.

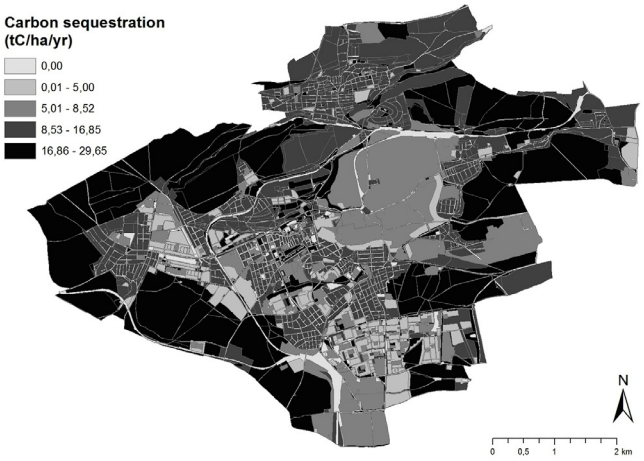

Fig. 1: *Mean above-ground carbon sequestration in Kladno.*

Water retention

Built-up land has a considerable influence on water regime. In contrast to natural conditions, paved surfaces prevent water infiltration, provide an alternate rate of evapotranspiration, and impair ground-water recharge (Haase 2009). With mean annual precipitation in Kladno of about 590 mm, increases in direct run-off have

been estimated as 10–440 mm year^{-1} (depending on land use category) compared to bare soil, for which run-off is considered to be 0 mm year^{-1}. The highest increase in run-off values for industrial and commercial land is equal to almost 75% of total annual precipitation.

Survey Results

The overall satisfaction of citizens living in Kladno was described by the headline indicator "Average satisfaction with the local community". When comparing indicator values between 2008 and 2014, citizens of Kladno are less satisfied in 2014 than they used to be (Table 1). In contrast, the single feature indicator "Satisfaction with the environment" displayed a higher value for the more recent survey.

Table 1: *Overview of citizen satisfaction indicators.*

	2008		2014	
	Satisfied	Dissatisfied	Satisfied	Dissatisfied
Citizen satisfaction indicator* [%]	74.3	25.7	72.9	27.1
Satisfaction with the environment**	5.9		6.2	
Built-up areas [ha]	448.92		442.10 (2013)	

** level of citizen satisfaction in general and in regard to specific features in the municipality,*

*** on a scale of 0 to 10 where 0 is the lowest satisfaction and 10 the highest.*

Given the continual decline in built-up areas during 2001–2014 (Czech Statistical Office 2015), one might explain the stated higher satisfaction with the environment as due to positive changes in area covered by urban nature. In addition, investments in public greenery were approximately 15–20% higher during 2010–2011 (Ministry of Finance 2015a, 2015b). Based on discussion with city representatives (Mrs. Houdková and Mr. Víta, personal communication, February 2015), however, it appears the area has not been enlarged distinctly over 2008–2014. In fact, the Public Database (Czech Statistical Office 2015) shows a decrease in some types of green areas during these years. Additionally, management of urban nature has not noticeably improved (Mrs. Houdková, personal communication, February 2015). Therefore, the reason for higher satisfaction with the environment remains an open question and possible influences from other factors (e.g. air quality) need to be considered. The results of the survey further show that the majority of respondents (almost 82%) believe that the natural environment in the city improves their quality of life. The most strongly perceived benefits provided by urban nature were cultural (especially recreational) services (88% of responses). Regulating services were identified by 53% of respondents and provisioning services by 3%. Similarly, for benefits attributed to urban agricultural areas, the most common response was cultural services (48% of responses), followed by regulating services (27%) and provisioning services (22%). Furthermore, respondents were asked to evaluate the importance of each service. Evaluation was based on a 5-point scale where 1 stood for the most important service and 5 for the least important service. The climate-regulation related services perceived as important were cooling effect (mean of 2.1) and positive moisture regulation (2.3). In contrast, regulation of climate change impacts received a neutral importance score (3.2). Water cycle regulation also seemed to be a nearly neutrally important service (2.8). This might be related to an absence of watercourses in the city and therefore limited risk of floods.

DISCUSSION

This study combined a quantitative assessment of selected ESs with surveys. The results reveal preferences among direct consumers of these benefits. From a methodological point of view, this exercise introduces a guideline for combining two analytical approaches and may alternatively be used for other ESs or other cities. The level of mean carbon sequestration is comparable to some other cities, but the spatial differentiation along the urban-rural gradient might cause a negative effect on residents' comfort in terms of temperature and moisture. The core of the city where the population is concentrated (based on the distribution of urbanized land use categories) also contains higher demand for services. Similarly, it was demonstrated that urbanization importantly modifies run-off levels. To increase the city's resilience, we recommend increasing the proportion of urban nature areas in Kladno and improving their current distribution across the city. We have presented carbon sequestration and regulation of run-off as flagship services because of their key position in relation to cities' vulnerability to climate change. Based on the results of the survey, however, they are only partly perceived as key services, particularly in the case of (micro)climate regulation. Stronger perception of benefits and higher preferences were revealed among Kladno citizens for cultural services (recreation). This outcome confirms the existence of knowledge-based differences between experts and the public and emphasizes the significance of the assessment's purpose. When it comes to participatory urban planning, citizens would probably be more sensitive to indicators directly related to the recreational potential of urban nature and other cultural services. Therefore, recreation is more suitable as a flagship service to encourage public participation than are such expert indicators as tonnes of carbon sequestered and increased run-off.

Acknowledgement

Supported by project No. TD020064 "Analysing the Services of Urban Ecosystems and their Impact on Resident Well-being in the Czech Republic" of the Technology Agency, project No. LD13033 "Challenges of Urban Agriculture Challenge in Europe", and project No. LO1415 of the Ministry of Education, Youth and Sports within the National Programme for Sustainability I.

References

Bolund P, Hunhammar S (1999) Ecol. Econ. 29, 293–301.

Czech Statistical Office (2015) Public Database. Available at: http://vdb.czso.cz/.

Davies ZG, Edmondson JL, Heinemeyer A et al. (2011) J. Appl. Ecol. 48, 1125–1134.

European Environment Agency (2013) Environmental Indicator Report 2013: Natural Resources and Human Well-Being in a Green Economy. Publications Office of the European Union, Luxembourg.

Frélichová J, Vačkář D, Pártl A et al. (2014) Ecosyst. Serv. 8, 110–117.

Haase D (2009) Environ. Impact Assess. Rev. 29, 211–219.

Larondelle N, Haase D (2013) Ecol. Indic. 29, 179–190.

Liu S, Costanza R, Troy A et al. (2010) Environ. Manag. 45, 1271–1285.

Millennium Ecosystem Assessment (2005) Ecosystems and Human Well-being: Synthesis. Island Press, Washington, DC.

Ministry of Finance (2015a) ArisWeb. Available at: http://wwwinfo.mfcr.cz/aris/.

Ministry of Finance (2015b) Monitor. Available at: http://monitor.statnipokladna.cz

Quitt E (1971) Klimatické oblasti Československa. Academia, Geographic Institute of the Czechoslovak Academy of Sciences, Brno.

Strohbach MW, Haase D (2012) Landsc. Urban Plan. 104, 95–104.

Testing a statistical forecasting model of electric energy consumption for two regions in the Czech Republic

Rajdl, K.[1,2,*], Farda, A.[1], Štěpánek, P.[1], Zahradníček, P.[1]

[1]*Global Change Research Centre, Bělidla 986/4a, 603 00 Brno, Czech Republic*

[2]*Department of Mathematics and Statistics, Faculty of Science, MU, Kotlářská 2, 611 37 Brno, Czech Republic*

[*]*author for correspondence; email: rajdl.k@czechglobe.cz*

ABSTRACT

Precise forecasting of electric energy consumption is of great importance for the electric power industry. It helps system operators optimally schedule and control power systems, and even slight improvements in prediction accuracy might yield large savings or profits. For these reasons, many forecasting models based on various principles have been developed and studied. Because of energy consumption's strong dependence on weather conditions, such models often utilize outputs from numerical weather prediction models.

In this study, we present and analyse a statistical model for forecasting hourly electrical energy consumption by customers of E.ON Energie, a.s. in two regions of the Czech Republic. The aim of this model is to create hourly predictions up to several days in advance. The model uses hourly data of consumed energy from 2011–2014 and corresponding predictions of temperature and cloudiness provided by the ALADIN/CZ model. The statistical model is based on a regression analysis applied to appropriate data samples and supplemented by several optional post-processing methods. Specifically, we use a robust linear regression algorithm to identify energy consumption's dependence on temperature, the meteorological variable with the largest influence on consumption. Our post-processing methods focused on removing prediction bias resulting from economic situations (represented by the goss domestic product, GDP) and sudden temperature changes.

We analysed the presented model from the point of view of the hourly predictions' accuracy for 2013 and 2014. Accuracy was primarily measured by mean absolute error. It was evaluated for individual months, and the effects of individual parts of the model on accuracy value are shown.

INTRODUCTION

Electric energy consumption forecasting is very important so that energy system operators can optimally balance produced and consumed energy (Cancelo et al. 2008). Therefore, there are many forecasting models for various situations using various methods (Tso & Yau 2007, Hahn et al. 2009). In this paper, we present and evaluate a statistical model for hourly forecasting electrical energy supplied by E.ON Energie, a.s. in two regions of the Czech Republic: South Bohemia and South Moravia.

The model focuses on reflecting daily, weekly, and yearly consumption cycles as well as utilizing two weather characteristics: air temperature and cloudiness. Air temperature is the main factor influencing consumption through which prediction accuracy can be substantially improved (De Felice et al. 2013). To calculate predictions, we used a selection of appropriate data samples with regression analysis. We also used two post-processing procedures. Prediction accuracy was evaluated using mean absolute error for individual months during July 2013–June 2014. To show the benefit of using temperature, a variant of the model not including temperature was also evaluated.

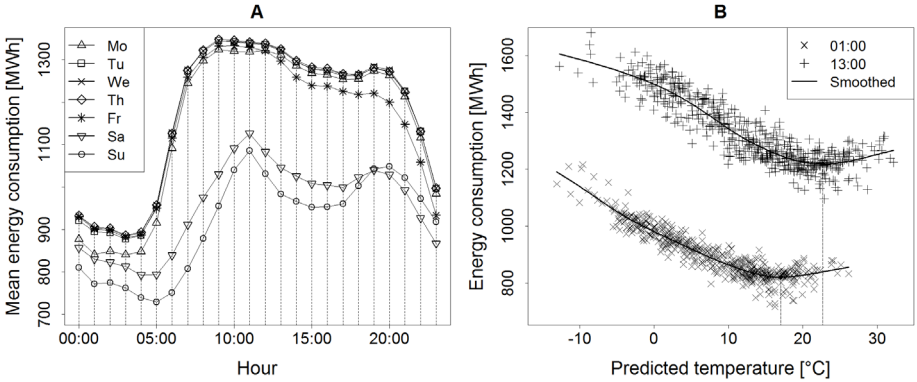

Fig. 1: *Energy consumption in South Moravia. Values strongly affected by holidays are omitted. (A) Mean hourly energy consumption for individual hours and days. (B) Dependence of energy consumption on predicted air temperature. Values shown are from Tuesdays, Wednesdays, and Thursdays at 01:00 and 13:00. Dashed lines show minima of smoothed dependence.*

MATERIALS AND METHODS

The model is based on hourly data energy consumption in the South Bohemian and South Moravian regions during February 2011–June 2014. Each value is the sum of consumption for 1 h denoted by the end time (e.g. the sum of consumption from 12:00 to 13:00 is denoted as 13:00). Corresponding data of predicted temperature and cloudiness was provided in an analogous form by the ALADIN/CZ model (Farda et al. 2010). Instead of sums, however, these data represent hourly and spatial means. Predictions were provided each day at 00:00 for the following several days. To create, calibrate, and evaluate the model in this study, we used predictions up to 24 h ahead. Cloudiness values fall within the range 0–1, representing the proportion of the sky covered by clouds.

Prior to creating the forecasting model, it was necessary to identify those factors having a substantial influence on energy consumption. There are two main types: socio-economic factors and weather factors. The first group includes such factors as the state of the economy and employment as well as the population's personal habits. As a result of these factors, daily, weekly, and yearly cycles can be observed in energy consumption. Daily and weekly cycles are illustrated in Fig. 1A. Within a single day, mainly a rapid increase in the morning and decrease in the evening is apparent. Naturally, there was also a large difference between consumption on weekdays and weekends. Even weekdays are not all equivalent, as considerably different consumption behaviour was recorded on Mondays and Fridays than was found on Tuesdays, Wednesdays, and Thursdays.

The weather factor with the largest influence on consumption is temperature. The temperature–consumption curve has a typical U-shape (see Fig. 1B), with a minimum temperature known as the comfort temperature (Ortiz Beviá et al. 2014). This temperature differs for daytime and night-time hours. Another important weather factor is cloudiness, which affects the need for artificial light, but its effect on consumption is rather mild.

We created a forecasting model so as to reflect the influence of all of the aforementioned factors. To achieve this, we combined a selection of similar data and regression analysis. For each predicted energy value (for a specific hour), a data sample with corresponding consumption was selected, and the influence of temperature

was estimated based on this data using a regression method. Data samples were chosen according to the following criteria. First, the data were restricted to only the same hour and day of the week, except for Tuesdays, Wednesdays, and Thursdays, the data for which were combined. This did not apply to days around public holidays on weekdays, as consumption on these days is very specific and difficult to predict. For these days, we used the following simple rules. Each holiday was treated as a Sunday, each day immediately before as a Friday, and each day immediately after as a Monday. Moreover, predictions for standard days (those not affected by a holiday) did not use data from holidays or the days around them. Next, the yearly cycle was taken into account. According to the day's position within the year, data were selected using a sliding window of 70 days. Finally, a restriction condition was applied to cloudiness and a sliding window was used again, in this case a window of 0.9. Thus, for example, for predicted cloudiness values of 0 data with cloudiness within the range 0–0.45 were selected, for values of 0.5 the range was 0.05–0.95, and so on. This is a relatively large range, but testing revealed it to be a suitable choice for our data.

As mentioned above, the final predictions were calculated using a regression algorithm with predicted temperature as a variable. Ideally, we would have liked to fit a U-shaped curve, as illustrated in Fig. 1B. However, following the described data selection, the data samples had a relatively small range of temperature values with an approximately linear curve. We tested other possibilities, but the most suitable method seems to be linear regression with one linear factor: temperature. We improved the standard algorithm using a procedure providing robustness, in the sense of reducing the harmful influence of outlier data. Regression was performed twice. Following the first fit, data with residuals outside the interquartile range extended to both sides by its width were removed. The dependency obtained from the second regression was used to predict consumption.

In the described method, two factors influencing consumption were not considered: consumption changes over the long term (given by such factors as the state of the economy) and sudden changes in temperature. Both of these factors should be considered, but their effect was not very strong in our data, and so we did not reflect them directly. Instead, we used two post-processing procedures to reduce bias caused by leaving them out. It is not possible to describe these procedures here in detail, but they were also based on regression analysis and used GDP and differences in mean temperature between successive days.

RESULTS

We evaluated the model from the perspective of prediction error. To measure this error, we used the normalized mean absolute error (NMAE). It is defined as

$$\mathrm{NMAE} = \frac{\sum_{i=1}^{n} |\hat{p}_i - p_i|}{\sum_{i=1}^{n} p_i},$$

where $\hat{p}_i$, i=1,...,n, are the predicted energy consumption values for individual hours and p_i, i=1,...,n, are the corresponding real values. By multiplying the total by 100, we obtained the error in terms of the percentage of the total actual production.

We calculated NMAE for the entire period of July 2013–June 2014 as well as for individual months. Predictions were calculated using necessary values from February 2011–June 2014. To obtain NMAE values corresponding to actual applications, only data at least 2 days old were used to calculate each prediction. We tested the main described method (M1), as well as the post-processing procedures based on GDP (M2) and temperature changes (M3). Moreover, to express the benefit of using temperature, we also evaluated a

method which did not utilize temperature and returned consumption means from the selected data sample prior to applying regression (M4).

The NMAE values displayed by individual methods (in both regions combined) are shown in Table 1. Errors in individual months mostly ranged around 2–3%, but they were sometimes considerably higher, mainly due to larger amounts of non-standard days in some months, in particular due to Christmas in December. There are also clear differences among the methods, and we can see such effects as the benefit of using temperature. This benefit was relatively large, except for during the summer, where the effect was negative in August. Both post-processing procedures had overall positive effects. However, improvement was not stable across different months and sometimes error was increased.

Table 1: *Values of NMAE (% of total prediction) for methods M1–M4 during July 2013–June 2014 calculated for the sum of consumption in both South Bohemia and South Moravia.*

Method	2013						2014						Total
	7	8	9	10	11	12	1	2	3	4	5	6	
M1	2.39	3.39	2.48	3.79	1.89	7.39	4.45	2.31	2.25	2.58	4.09	2.81	3.35
M2	2.76	3.29	2.41	3.45	1.89	7.49	4.61	2.04	2.29	2.15	3.53	2.07	3.20
M3	2.57	3.68	2.37	3.66	1.78	7.44	4.34	2.07	2.31	2.19	3.67	2.23	3.22
M4	2.42	3.31	2.50	4.27	2.96	8.63	6.22	2.68	5.37	2.95	4.73	2.81	4.08

DISCUSSION

We have presented a forecasting model for energy consumption. It is clear that it is able to predict consumed energy relatively precisely, although errors were highly variable across individual months. The results also imply some ways to obtain potential improvements which we intend to explore in future. Firstly, holidays, mainly Christmas, cause large increases in errors and thus a more sophisticated method for modelling them could help to improve results. Next, the post-processing procedures were tested separately and thus their combined application might yield higher accuracy. Currently, this variant is problematic because of its relatively low data count. Finally, there seems to be great potential to reduce error through better use of temperature. For example, reflecting thermal inertia, which we are currently studying, seems to be a promising way to decrease errors.

Acknowledgement

Supported by project No. LO1415 of the Ministry of Education, Youth and Sports within the National Programme for Sustainability I.

References

Cancelo JR, Espasa A, Grafe R (2008) Int. J. Forecast. 24, 588–602.

De Felice M, Alessandri A, Ruti PM (2013) Electr. Pow. Syst. Res. 104, 71–79.

Farda A, Déqué M, Somot S et al. (2010) Stud. Geophys. Geod. 54, 313–332.

Hahn H, Meyer-Nieberg S, Pickl S (2009) Eur. J. Oper. Res. 199, 902–907.

Ortiz Beviá MJ, Ruiz de Elvira A, Álvarez García FJ (2014) Energy 76, 850–856.

Tso GKF, Yau KKW (2007) Energy 32, 1761–1768.

Exploring beliefs about climate change and attitudes towards adaptation among Czech citizens

Krkoška Lorencová, E.[1,*], Vačkář, D.[1]

[1]*Global Change Research Centre, Bělidla 986/4a, 603 00 Brno, Czech Republic*

[*]*author for correspondence; email: lorencova.e@czechglobe.cz*

ABSTRACT

Climate change currently represents one of the major global environmental problems. In order to respond to these changes, adaptation actions at all levels, from national to local, need to be undertaken (European Commission 2013). Moreover, perceptions of climate change are an important element affecting actual attitudes towards adaptation actions and influencing policy and communication regarding climate change (Lorenzoni et al. 2005).

This paper presents the results of a survey on perceptions of climate change, including beliefs about climate change and attitudes towards adaptation, conducted among 1,024 Czech citizens in October 2014.

Survey results show that the majority of respondents (78%) agreed with the statement that global climate change is happening. Positive responses about perceptions of climate change were found especially among younger people (18 to 34 years of age). In terms of adaptation measures, 51% of respondents had adopted a variety of individual actions (ranging from water savings to property insurance), discussed in the paper in further detail. Older people (≥ 45 years of age) with higher education preferred rather technical adaptation measures (e.g. flood protection for property, installation of rainwater reservoirs, etc.).

The survey represents unique insights into attitudes towards climate change within the Czech Republic which had not previously been investigated to this extent. The results provided can support decision-making regarding adaptation policy, individual adaptation actions, and communication of climate change issues towards general public.

INTRODUCTION

Climate change, one of the major global environmental problems, poses risks for human and natural systems. To manage the risks of climate change, adaptation and mitigation decisions are essential (IPCC 2014). In order to respond to these changes, adaptation actions at all levels, from national to local, need to be undertaken (European Commission 2013).

Adaptation measures also face difficulties connected with perceptions of risks and adaptation among stakeholders (Otto-Banaszak et al. 2011). In this respect, perceptions of climate change are as an important element affecting actual attitudes towards adaptation actions and influencing policy and communications regarding climate change (Lorenzoni et al. 2005). Additionally, perceptions of climate risks influence the timing and ways now individuals, households, businesses, and communities take adaptation actions (Davidson et al. 2003).

Understanding public perceptions of climate change can support decision-making (Lujala et al. 2015) and ensure social acceptance of adaptation actions (Lorenzoni & Pidgeon 2006).

The performed survey aimed to explore perceptions of climate change among Czech citizens, investigating the extent to which citizens perceive the impacts and risks of climate change, as well as to determine whether they had implemented adaptation measures and if so which particular measures. The study also tested the

relationship between respondents' agreement that the Czech Republic is experiencing effects of global climate change and their actual adoption of individual adaptation measures.

MATERIALS AND METHODS

The survey was conducted in October 2014 in collaboration with Ipsos through a quantitative online survey using computer-assisted self-interviewing technique with Ipsos panel respondents. The online questionnaire covered a representative sample of the population of the Czech Republic with a total of 1,024 respondents. The sample was also representative spatially, across the 14 regions of the Czech Republic. The sample included respondents 18 years of age and older, with nearly equal representation of women (50.5%) and men (49.5%). The questionnaire consisting of 14 questions was developed to provide information on respondents' beliefs about climate change, perceptions of risks and effects associated with climate change, and attitudes toward individual adaptation actions.

RESULTS

Concerning perceptions of climate change, the survey showed that 78% of respondents agreed (35% strongly agree and 43% agree) with the statement that global climate change is happening. In particular, 70% of respondents agreed (23% strongly agree and 47% agree) with the statement that the Czech Republic is experiencing effects of global climate change. Fig. 1 illustrates the distribution of responses to this question according to gender, age, and education and thus the role these characteristics play in perceptions of climate change within the Czech Republic. A higher proportion of women (72%) agreed with the statement than did men (68%). In terms of age, younger respondents (25–34 years of age) more frequently responded positively. Education also played a role in perceptions, as people with higher vocational and university education more frequently agreed with the statement.

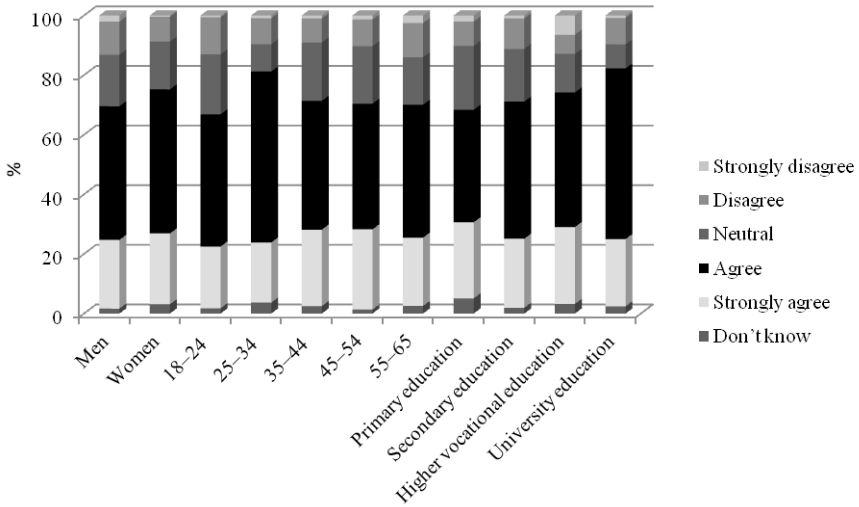

Fig. 1: *Responses to the statement "The Czech Republic is experiencing effects of global climate change" according to gender, age, and education.*

The majority of respondents (51%) had taken measures to adapt to the changing climate. Table 1 provides an overview of individual adaptation measures that citizens undertook. These individual measures varied from rather mitigating measures (e.g. saving energy and water, using solar energy and public transportation, sorting waste, reducing their houses' energy intensity) to so-called soft adaptation measures (e.g. insurance, early warning systems) and technical adaptation measures (e.g. flood protection for property, rainwater harvesting, adjustments in rainwater runoff). Large proportions of respondents had undertaken rainwater harvesting (27%), energy savings (17%), and insurance (17%). Older people (≥ 45 years of age) with higher education preferred technical measures (e.g. flood protection for property, installation of reservoirs to harvest rainwater, etc.).

Table 1: *Overview of individual adaptation measures.*

Individual measures undertaken	Proportion of respondents taking the measure %
Rainwater harvesting	27
Energy savings	17
Insurance (against natural disasters)	17
Water savings	11
Early warning systems (e.g. weather forecast monitoring)	6
Flood protection for property	6
Waste sorting	6
Adjusting rainwater runoff around buildings	5
Reducing houses' energy intensity	2
Solar energy use	2
Measures against storms	1
Public transportation use	1

The results of Pearson's chi-squared test showed a significant relationship between respondent's agreement that the Czech Republic is experiencing effects of global climate change and actual adoption of individual measures to adapt to climate change ($\chi^2 = 64.580$, significant at $p < 0.05$). In summary, respondents who agreed that climate change effects are taking place were more likely to have undertaken individual adaptation measures.

DISCUSSION

The survey represents unique insights into attitudes towards climate change within the Czech Republic which had not previously been investigated to this extent.

The values and perceptions of the general public need to be taken into account when making decisions concerning climate change policies. This is particularly true because climate policies require some degree of buy-in or public acceptance among those who might be affected by the decision (Lorenzoni & Pidgeon 2006).

The present study illustrated the connection between perceptions of climate change and actual adaptation actions. However, the link between concerns about climate change and taking adaptation actions has not yet been fully established in the literature. For instance, such studies as Spence et al. (2011) have proven such a

connection. In contrast, Dessai & Sims (2010) did not confirm that concerns about climate change necessarily led to adaptation measures.

Moreover, the present results can be utilized to support decision-making regarding adaptation policy, individual adaptation actions, and communication of climate change issues towards general public.

Acknowledgement

Supported by project No. LD13032 of the COST programme "Climate Change and Migration as Adaptation" as well as project No. LO1415 of the Ministry of Education, Youth and Sports within the National Programme for Sustainability Program I.

References

Davidson DJ, Williamson T, Parkins JR (2003) Can. J. For. Res. 33, 2252–2261.

Dessai S, Sims C (2010) Environ. Hazards 9, 340–357.

European Commission (2013) An EU Strategy on Adaptation to Climate Change: Strengthening Europe's Resilience to the Impacts of Climate Change. DOI: 10.2834/5599.

IPCC (2014) Summary for policymakers. Climate Change 2014: Impacts, Adaptation, and Vulnerability. Part A: Global and Sectoral Aspects. Contribution of Working Group II to the Fifth Assessment Report of the Intergovernmental Panel on Climate Change (eds CB Field, VR Barros, DJ Dokken et al.), pp. 1–32. Cambridge University Press, Cambridge.

Lorenzoni I, Pidgeon NF, O'Connor RE (2005) Risk Anal. 25, 1387–1398.

Lorenzoni I, Pidgeon NF (2006) Clim. Change 77, 73–95.

Lujala P, Lein H, Rød JK (2015) Local Environ. 20, 489–509.

Otto-Banaszak I, Matczak P, Wesseler J et al. (2011) Reg. Environ. Change 11, 217–228.

Spence A, Poortinga W, Butler C et al. (2011) Nat. Clim. Change 1, 46–49.

Author's index

Title: Global Change: A Complex Challenge
Conference Proceedings
Editors: Otmar Urban, Mirka Šprtová, Karel Klem
Published by: Global Change Research Centre AS CR, v.v.i.
Bělidla 986/4a, 60300 Brno, Czech Republic
First edition
Brno 2015

Contact person: Otmar Urban, M: +420511192250, E: urban.o@czechglobe.cz
ISBN: 978-80-87902-10-3